Cosmological Perturbation Theory and Magnetogenesis

Eleanor Catherine Nalson

A thesis submitted in partial fulfillment of the requirements of the Degree of

Doctor of Philosophy

2014

Declaration

I, Eleanor Nalson, confirm that the research included within this thesis is my own work or that where it has been carried out in collaboration with, or supported by others, that this is duly acknowledged below and my contribution indicated. Previously published material is also acknowledged below.

I attest that I have exercised reasonable care to ensure that the work is original, and does not to the best of my knowledge break any UK law, infringe any third partys copyright or other Intellectual Property Right, or contain any confidential material.

I accept that the College has the right to use plagiarism detection software to check the electronic version of the thesis.

I confirm that this thesis has not been previously submitted for the award of a degree by this or any other university.

Signature: Eleanor Nalson Date: 11/08/14

Details of collaboration and publications: parts of this work have been completed in collaboration with Karim A. Malik, Adam J. Christopherson and Ian Huston, and are published in the following papers:

- E. Nalson, A. J. Christopherson, I. Huston, K. A. Malik:
  Class. Quantum Grav. **30** (2013) 065008 [1]
- E. Nalson, A. J. Christopherson, I. Huston, K. A. Malik:
  13th Marcel Grossmann Proceedings (2013) arXiv:1312.6504 [2]
- E. Nalson, A. J. Christopherson, K. A. Malik:
  JCAP **09** (2014) 023 [3]

Abstract

Cosmological perturbation theory (CPT) is an important tool with which inhomogeneities that seed the observed structure of our universe can be studied. This thesis introduces the subject of CPT and discusses applications of this at both linear and second order.

At linear order the evolution of the curvature perturbation around horizon crossing is examined. We study single field inflation models numerically, and compare the the curvature perturbation at horizon crossing to that at the end of inflation. In addition, linear-order CPT is extended to the case of a multi-fluid system and an approximation for the velocities of the baryons and photons in the early universe as well as the strength of the electric field is found.

We use second order CPT to study magnetogenesis. By using fully relativistic, non-linear CPT we show how magnetic fields are generated. This is done by presenting the first fully analytical calculation of the magnetic field at second order. Our results suggest that magnetic fields with strengths of the order of $10^{27}G$ and with scale dependence $\mathcal{M} \propto k^4$ may be generated - findings which are largely in agreement with previous numerical results.

We end by outlining possible extensions to this work, in particular related to the study of primordial magnetogenesis.

Acknowledgements

Firstly, I would like to thank Karim Malik for all his help and guidance in the past four years. I am also grateful to my collaborators Adam Christopherson and Ian Huston. I would like to thank the rest of the QMUL cosmology group for their support and guidance and for being there when a pint is what's needed, in particular David Mulryne and Tim Clifton. I would like to also thank all my office mates and fellow students at Queen Mary, especially Alex Leithes and Joe Elliston, for making QMUL such a fun place to study.

I would like to thank my flat mates in London, Becs, Pip and Garnet who have been there for me outside of work and made living in London so enjoyable. I am also very grateful to my parents, my other siblings, Alex and Will, and the rest of my family for their encouragement and support over the last few years. Finally, I owe so many thanks to Andrew, I would not have made it through the last four years, especially the last month or two, without the support, love and belief you constantly provide me. Thank you so much!

This thesis is dedicated to my grandad, Robert Ellis.

Contents

List of Figures

Chapter 1

Introduction

It is currently a great time to be a cosmologist. After several decades with very little observational data available, the last two decades have seen not only an influx in data but also a vast improvement in the quality of that data. One of the main observational probes used to study cosmology is the Cosmic Microwave Background (CMB), the radiation that was first emitted during photon decoupling. This is the oldest light in the Universe and allows us to look back to a time when the universe was less than half a million years old. The first discovery of the CMB in 1964 by Penzias and Wilson [4] was a very important test for the standard Big Bang model of cosmology, but it was not until the results of COBE [5], just over 20 years ago, that the tiny anisotropies that would shape the study of cosmology in the following decades were discovered. Since then two satellites, firstly Wmap [6, 7] and more recently Planck [8], have improved upon the data collected by COBE. The evidence we have so far supports the current best theory that the universe started with a phase of rapid expansion known as inflation followed successively by radiation-dominated and matter-dominated eras which are described in the standard Big Bang model. With these detailed observations we are now able to constrain more theoretical models than ever before.

Cosmological perturbation theory (CPT) provides the theoretical framework for the detailed study of the anisotropies in the CMB. For a full review see Ref. [9] and the references therein. CPT is built around the well motivated assumption that our universe is largely isotropic and homogeneous. When working within CPT we use

a smooth background, to which we add inhomogeneous perturbations to describe the small scale detail of our universe. These perturbations are then split order by order and into different types: scalar, vector and tensor. Cosmological perturbation theory has a long history. The very first studies were carried out by by Lifshitz and Bonner [10, 11] and the first covariant study by Hawking [12] and Olsen [13]. The real groundwork though to modern linear CPT, which is still used today came in the 1980's by Bardeen [14], followed by review articles by Sasaki [15] and Mukhanov, Feldman and Brandenberger [16]. An alternative approach is the covariant approach studied by Ellis & collaborators [17–19] and the first paper relating covariant to metric approach was by Bruni [20]. In the last 15 years or so as observations have improved it has been necessary to go beyond linear order to second order and there are many papers on this [21–30]. Recently there have even been attempts to begin to understand third order perturbation theory and any interesting effects which may appear at this order [31].

The main subjects of this thesis are applications of CPT to various problems and questions in modern cosmology. The rest of this chapter gives a brief overview of the standard Big Bang model of cosmology and inflation. Then in Chapter 2 we describe CPT in detail using linear perturbation theory as a starting point. In Chapter 3 we move on to our first application which examines the conservation of the curvature perturbation during inflation. In Chapter 4 we look at perturbation theory in the case where we have multiple species and how one might solve systems of Boltzmann like equations without resorting to numerics. The second half of the thesis is based around an application of CPT to primordial magnetic field generation. Given that the latter is quite a large topic in itself with much history, Chapter 5 contains mainly an introduction to this field as well as a full derivation of the covariant Maxwell equations up to second order. In Chapter 6 we then provide a full analytic derivation of the magnitude and scale dependence of the magnetic fields generated by perturbations, with a comparison to previous numeric work. We end this thesis with our conclusions and future outlook in the final chapter.

1.1 Big Bang cosmology

1.1.1 FLRW metric

Observations [6, 32] suggest that on large scales our universe looks largely homogeneous and isotropic. If we apply the cosmological principle, that is to assume that we do not live in a particularly special part of the universe, then it follows that on large scales, the universe is homogeneous and isotropic everywhere. In addition, observations indicate that our universe is not static but expanding. The simplest description of a homogeneous, isotropic and expanding spacetime is given by the Friedmann-Lemaitre-Robertson-Walker (FLRW) metric, with line element,

$$ds^2 = -dt^2 + a^2(t)d\Omega^2\,, \tag{1.1}$$

where t is coordinate time and a is the scale factor which describes the expansion of the universe. $d\Omega$ is given by,

$$d\Omega^2 = \frac{dr^2}{1-kr^2} + r^2(d\theta^2 + \sin^2\theta d\phi^2)\,, \tag{1.2}$$

where (r, θ, ϕ) are the spherical spatial coordinates. This is the most general spatial geometry which is both homogeneous and isotropic. It allows for a uniform global curvature which is denoted by k, where $k = 0$ denotes a flat universe, $k = -1$ denotes a negatively curved, (i.e. open), universe and $k = 1$ denotes a positively curved, (i.e. closed), universe.

The most recent evidence from Planck [8, 33] suggests that we live in a flat (or close to flat) universe, therefore for the remainder of this thesis we will be considering only a flat metric with $k = 0$. If $k = 0$ we have some freedom in defining the scale factor and therefore can use this to fix $a = 1$ today. The rate of change of the scale factor is denoted by the Hubble parameter

$$H = \frac{\dot{a}}{a}\,, \tag{1.3}$$

where a dot ($\dot{}$) represents differentiation with respect to coordinate time. Due to the homogeneity and isotropy of our universe both a and H are only dependent on time

and not on spatial coordinates. Setting $k = 0$ also allows us to write the FLRW line element in Cartesian coordinates as

$$ds^2 = -dt^2 + a^2(t)\delta_{ij}dx^i dx^j = g_{\mu\nu}dx^\mu dx^\nu \,, \tag{1.4}$$

where the roman indices run from 1 to 3 and (x_1, x_2, x_3) are the Cartesian spatial coordinates. The Greek indices run from 0 to 3 and x_0 is the time coordinate (in this case coordinate time) and $g^{\mu\nu}$ is the FLRW metric.

Alternatively we can also express this metric in terms of conformal time,

$$ds^2 = a^2(\eta)(-d\eta^2 + \delta^{ij}dx_i dx_j) \,, \tag{1.5}$$

where conformal time (η) is defined by

$$\eta(t) = \int_{-\infty}^{t} \frac{1}{a(\tilde{t})} d\tilde{t} \,, \tag{1.6}$$

and the conformal Hubble parameter is

$$\mathcal{H} = \frac{a'}{a} \,, \tag{1.7}$$

and dash ($'$) represents differentiation with respect to conformal time. The conformal Hubble parameter is related to the coordinate Hubble parameter by

$$aH = \mathcal{H} \,. \tag{1.8}$$

In the line element above $(\eta, \mathbf{x})$ are comoving coordinates, the spatial comoving coordinates are related to the physical coordinates, $(\mathbf{d})$, by

$$\mathbf{d} = a(t)\mathbf{x} \,. \tag{1.9}$$

For the remainder of the thesis unless stated otherwise we will present equations in conformal rather than coordinate time.

1.1.2 General Relativity

The language we use to describe the universe we live in is that of General Relativity (GR), we will give a brief overview here for a complete picture see Ref. [34]. The mathematics of GR is defined on differentiable smooth manifolds, so in order to be able to define differentiation of tangent vector fields we must make a choice of affine connection. In the presence of a metric the natural choice is to pick the unique torsion-free metric connection, i.e. the Levi-Civita connection, which is given by the Christoffel symbols, defined in terms of the metric as

$$\Gamma^{\alpha}_{\beta\gamma} = \frac{1}{2} g^{\alpha\delta}(g_{\delta\beta,\gamma} + g_{\delta\gamma,\beta} - g_{\beta\gamma,\delta}) \,, \tag{1.10}$$

which, due to the connection being torsion-free, are necessarily symmetric. The comma (,) in the above equation denotes a partial derivative for example $g_{\alpha\beta,\gamma} = \frac{\partial}{\partial x^{\gamma}} g_{\alpha\beta}$. Using the FLRW metric defined in Eq. (1.5) we find that the non-zero connection coefficients are

$$\Gamma^{0}_{00} = \mathcal{H} \,, \quad \Gamma^{0}_{ij} = \mathcal{H}\delta_{ij} \,, \quad \Gamma^{i}_{0j} = \Gamma^{i}_{j0} = \mathcal{H}\delta^{i}_{j} \,. \tag{1.11}$$

Now that we have picked the affine connection we are able to define covariant differentiation, which we denote using either a ∇ or a semi-colon (;), for instance

$$v^{\mu}{}_{;\nu} = \nabla_{\nu} v^{\mu} = \partial_{\nu} v^{\mu} + \Gamma^{\mu}_{\nu\rho} v^{\rho} \,. \tag{1.12}$$

In order to use GR we will also be interested in the curvature of our spacetime. The Riemann curvature tensor measures the intrinsic curvature of Riemannian manifolds and can be defined in terms of the Christoffel symbols

$$R^{\alpha}_{\beta\gamma\delta} = \Gamma^{\alpha}_{\delta\beta,\gamma} - \Gamma^{\alpha}_{\gamma\beta,\delta} + \Gamma^{\alpha}_{\gamma\lambda}\Gamma^{\lambda}_{\delta\beta} + \Gamma^{\alpha}_{\delta\lambda}\Gamma^{\lambda}_{\gamma\beta} \,. \tag{1.13}$$

We can also define the Ricci tensor as the contraction of the Riemann tensor as

$$R_{\beta\delta} = R^{\alpha}_{\beta\alpha\delta} = \Gamma^{\alpha}_{\delta\beta,\alpha} - \Gamma^{\alpha}_{\alpha\beta,\delta} + \Gamma^{\alpha}_{\alpha\lambda}\Gamma^{\lambda}_{\delta\beta} + \Gamma^{\alpha}_{\delta\lambda}\Gamma^{\lambda}_{\alpha\beta} \,, \tag{1.14}$$

and the Ricci or curvature scalar

$$R = g^{\beta\delta} R_{\beta\delta} \,. \tag{1.15}$$

Einstein's field equations are given by

$$G_{\mu\nu} = 8\pi G T_{\mu\nu} \,, \tag{1.16}$$

where the Einstein tensor, $G_{\mu\nu}$ is defined in terms of the Ricci tensor as

$$G_{\mu\nu} = R_{\mu\nu} - \frac{1}{2} R g_{\mu\nu} \,, \tag{1.17}$$

and $T_{\mu\nu}$ is the stress energy tensor, which describes the matter content of the universe.

1.1.3 Energy-Momentum Tensor and Conservation Equation

To make use of the equations of GR, we need to describe the matter content of the universe. We can describe the 4-momentum's density and flux using the symmetric energy-momentum tensor. For a perfect fluid, that is, one in thermodynamic equilibrium, the energy-momentum tensor is given by

$$T^{\mu\nu} = (\rho + P) u^\mu u^\nu + P g^{\mu\nu} \,. \tag{1.18}$$

Here u^μ is the 4-velocity, which satisfies the constraint $u^\mu u_\mu = -1$ and when using the FLRW metric in Eq. (1.5) is given by

$$u^\mu = \frac{1}{a}(1, 0, 0, 0) \,. \tag{1.19}$$

ρ is the fluid density and P is the fluid pressure. Using the description of the metric in Eq. (1.5) this means that the only non-zero components of the stress-energy tensor for a perfect fluid are

$$T^{00} = \rho \,, \quad T^{ij} = P \delta^{ij} \,. \tag{1.20}$$

The Riemann tensor defined in Eq. (1.13) also satisfies the Bianchi identity

$$\nabla_{[\alpha} R_{\beta\gamma]\delta\epsilon} = 0\,, \tag{1.21}$$

which when combined with Eq. (1.16) gives the following continuity equation

$$T^{\mu\nu}{}_{;\mu} = 0\,, \tag{1.22}$$

and also implies

$$G^{\mu\nu}{}_{;\mu} = 0\,. \tag{1.23}$$

Substituting the energy-momentum tensor from Eq. (1.18) into Eq. (1.22) gives only one non-zero equation, the continuity equation,

$$\rho' + 3\mathcal{H}(\rho + P) = 0\,. \tag{1.24}$$

We also introduce the equation of state

$$P = \omega\rho\,, \tag{1.25}$$

where ω is the equation of state parameter. When the equation of state parameter is a constant, for instance in the case of a perfect fluid, we can solve the continuity equation to find an expression for ρ in terms of the scale factor,

$$\rho = \rho_0 a^{-3(1+\omega)}\,, \tag{1.26}$$

where ρ_0 is the value of the energy density evaluated today.

1.1.4 Friedmann Equations

We now look to combine our knowledge of GR with that of the stress-energy tensor to find equations describing the evolution of the scale factor. Returning to the Einstein field equations and substituting the energy-momentum tensor from Eq. (1.18) and the connection coefficients given in Eq. (1.10) we find two non-zero Einstein

equations. The 00 component gives us the Friedmann equation

$$\mathcal{H}^2 = \frac{8\pi G a^2}{3}\rho\,, \tag{1.27}$$

and the ij components give us the Raychaudhuri equation

$$\mathcal{H}' = -\frac{4\pi G a^2}{3}(\rho + 3P)\,. \tag{1.28}$$

Using the equation of state, Eq. (1.25), and the solution for the density, Eq. (1.26) we find the scale factor and Hubble parameter in terms of conformal time,

$$a = \left(\frac{\eta}{\eta_0}\right)^{2/(1+3\omega)}\,, \quad \mathcal{H} = \frac{2}{1+3\omega}\eta^{-1}\,. \tag{1.29}$$

Assuming that the universe is filled with a single component we can proceed to find exact solutions to the equations above. For dust (m), where we have $\omega = 0$, we find

$$\rho_{\mathrm{m}} = \rho_{0\mathrm{m}} a^{-3}\,, \quad a = \left(\frac{\eta}{\eta_0}\right)^2\,, \tag{1.30}$$

and for radiation (γ), where we have $\omega = 1/3$, we find

$$\rho_\gamma = \rho_{0\gamma} a^{-4}\,, \quad a = \left(\frac{\eta}{\eta_0}\right)\,. \tag{1.31}$$

Finally for a cosmological constant (Λ), where we have $\omega = -1$, we find

$$\rho_\Lambda = \rho_{0\Lambda}\,, \quad a = -\left(\frac{\eta}{\eta_0}\right)^{-1}\,. \tag{1.32}$$

This implies that the radiation density decreases at a faster rate than the matter density, which in turn decreases at a faster rate than the cosmological constant. As the universe is initially dominated by radiation this implies that we will have a radiation dominated period followed by a matter dominated period and finally a dark energy dominated period.

We can also define a density parameter Ω,

$$\Omega - 1 \equiv \frac{k}{\dot{a}^2}\,, \tag{1.33}$$

where $\Omega = 1$ corresponds to a geometrically flat universe. There exists a critical density, defined as the density of the universe that would lead to an exactly flat spatial geometry ($\Omega = 1$). From the Friedmann equation we can see that this density would be,

$$\rho_c = \frac{3H_0^2}{8\pi G}\,, \tag{1.34}$$

where H_0 is the Hubble parameter evaluated today. This means Eq. (1.33) can be written as,

$$\Omega = \frac{\rho}{\rho_c}\,. \tag{1.35}$$

So far we have only considered a universe which contains a single component, either radiation, matter or a cosmological constant: It is of course more realistic to have a mixture of different types of matter. If we have more than one type of matter in our universe each with a different density (ρ_i) and pressure (P_i) then we can define individual density parameters for each type of matter (i)

$$\Omega_i = \frac{\rho_i}{\rho_c}\,. \tag{1.36}$$

The total density, pressure and density parameter are then given by

$$\rho = \sum_i \rho_i\,, \quad P = \sum_i P_i\,, \quad \Omega = \sum_i \Omega_i\,. \tag{1.37}$$

The latest observations by Planck indicate that today our universe is filled with four species: baryonic matter (b), collisionless dark matter (c), radiation (γ) and dark energy (Λ) (or a cosmological constant). The observed values for the density parameters today are, at the 68% confidence level [8],

$$h^2\Omega_b = 0.02207 \pm 0.00033\,, \tag{1.38}$$

$$h^2\Omega_c = 0.1196 \pm 0.0031\,, \tag{1.39}$$

$$\Omega_\Lambda = 0.686 \pm 0.020\,, \tag{1.40}$$

where h is related to the Hubble parameter by $H = 100h\,\mathrm{km\,s^{-1}Mpc^{-1}}$ and was found by PLANCK to be $h = 0.674 \pm 1.4$ (68% confidence level). The curvature density parameter at 95% confidence level including data from PLANCK and Baryon Acoustic Oscillations is given by [8]

$$\Omega_k = -0.0005^{+0.0065}_{-0.0066}\,. \tag{1.41}$$

This implies our universe today is dominated by dark energy and is very close to being flat. A more detailed description of multi-fluid dynamics is given in Chapter 4.

1.2 Inflationary cosmology

1.2.1 Inflation as a solution to the problems of the Big Bang model

Whilst the above description of the standard Big Bang theory of cosmology had long been accepted, it does not allow us to explain everything we observe in the universe. In this section I will highlight some of these problems and explain how inflation may provide an answer. For a detailed overview of the problems of the Big Bang model and motivation for inflation we refer to Ref. [35]. The main problems with the standard Big Bang model can be summarized as follows:

- **Flatness problem:** During the Big Bang since gravity is attractive $\dot{a}$ is necessarily decreasing. This means $\Omega - 1$ is increasing and that the universe is evolving away from flatness, see Eq. (1.33). The latest PLANCK results indicate that Ω is very close to 1, i.e. the universe is close to being flat, see Eq. (1.41). For this to be true in the Big Bang scenario, this requires that at early times the universe must have been extremely flat, for instance, at nucleosynthesis we would require that the density parameter differed from 1 by less than 10^{-16} [35]. This highly fine-tuned initial state is unlikely without some additional explanation.

- **Horizon problem:** The universe appears very smooth, different regions of the sky appear very homogeneous and in fact the temperature across the entire

sky is uniform up to one part in 10^5 [6–8]. However the observable universe today is much bigger than the particle horizon, which means it is made up of causally-disconnected patches. Within the Big Bang model there is no physical reason for this homogeneity. For these patches to be so uniform again requires a high degree of fine tuning.

- **Relic problem:** The breaking of the symmetry of many unified theories in the early universe predicts an abundance of topological relics such as monopoles. However, none of the latter have yet been observed in our universe, something for which, again, there is no physical explanation of within the Big Bang model.

In addition,

- **Structure problem:** There is no explanation in the Big Bang model as to how structure came to form in our universe, i.e. where the initial fluctuations that grew into galaxies today actually came from. Whilst this is not technically a problem with the Big Bang model it is something that would be required for a complete theory of the early universe.

Inflation, which was proposed in the 1980's [36], can provide a solution to all four of the above problems. Inflation itself is the theory that early in its history the universe went through a period of rapid accelerated expansion,

$$\ddot{a} > 0\,. \tag{1.42}$$

There are three other equivalent definitions which allow for a more physical interpretation

$$\frac{d}{dt}\left(\frac{1}{aH}\right) < 0\,, \quad -\frac{\dot{H}}{H^2} < 1\,, \quad \rho + 3P < 0\,. \tag{1.43}$$

The first inequality above is that inflation occurs whilst the comoving Hubble length $(1/aH)$ is decreasing with respect to time, the second is that the H is changing slowly compared to the Hubble timescale and the third states that for inflation to occur the pressure must be negative.

We can also define the number of e-folds of expansion that have occurred between times with scale factor equal to a_{init} and a by

$$\mathcal{N} \equiv \ln \frac{a}{a_{\text{init}}} \,. \tag{1.44}$$

Note that as $\mathcal{N}$ increases monotonically with time (i.e. the universe is always expanding) and therefore we can use $\mathcal{N}$ as an alternative time variable.

This period of rapid expansion solves the problems with the Big Bang model in the following way:

- **Flatness problem:** During inflation the scale factor of the universe is accelerating ($\ddot{a} > 0$) which means that during inflation the density parameter is driven towards 1, i.e. the universe evolves towards flatness, see Eq. (1.33). Including inflation means Ω no longer needs to be so finely tuned - as long as the period of inflation is long enough, we can drive Ω as close as we like to 1.

- **Horizon problem:** So long as the observable universe is inside the horizon at the start of inflation then the entire observable universe will have been in causal contact at some point in the early universe and therefore it is no longer surprising that there is homogeneity across the entire universe that we can see. This notion of scales we observe now being inside the Horizon during inflation is studied in more detail in Section 3.2

- **Relic problem:** The rapid expansion and increase in volume that occurs during inflation will dilute the number density of these relics until they can be considered non-interacting.

- **Structure problem:** It is possible during a period of inflation that the seeds for the structure we see today could be generated by quantum fluctuations. This gives a natural way of sourcing the structure of the universe and is studied in more detail in Section 3.1.1.

While the theory of inflation has many positive aspects, it is also worth noting that inflation itself requires some fine tuning, for instance the small patch which will become our universe needs to be homogeneous and isotropic. We also require a minimum of about 60 e-folds of inflation in order to solve the flatness and horizon

problems (the exact value depends on the details of inflation and reheating) [37,38]. Inflation is only a good solution to the fine tuning problems above if it does not itself need to be very finely tuned.

1.2.2 Scalar field driven inflation

As mentioned above, the type of matter that drives inflation must have negative pressure and the simplest type to consider besides a cosmological constant is a scalar field. There are many possibilities here for both single and multi-inflationary models and they can all be specified by considering their Lagrangian, which is a function of the scalar field and the relativistic kinetic energy. The simplest class of models and the one we will be concentrating on in this thesis is that of canonical single field inflation. Its Lagrangian is given by,

$$\mathcal{L} = \frac{1}{2} g^{\mu\nu} \varphi_{,\mu} \varphi_{,\nu} - U(\varphi)\,, \tag{1.45}$$

where the first term is the relativistic kinetic energy and the second term, U, is the potential. In such a single field model the scalar field is often referred to as the inflaton.

We can define the energy-momentum tensor of the scalar field using the Lagrangian [39]

$$T^{\mu\nu} = -2\frac{\partial \mathcal{L}}{\partial g_{\mu\nu}} + g^{\mu\nu}\mathcal{L}\,. \tag{1.46}$$

Expanding this out gives us [40]

$$T_{\mu\nu} = \varphi_{,\mu}\varphi_{,\nu} - g_{\mu\nu}\left(\frac{1}{2}\varphi_{,}{}^{\alpha}\varphi_{,\alpha} + U(\varphi)\right)\,, \tag{1.47}$$

which, when we consider a FLRW metric and a homogeneous scalar field, has the form of the energy-momentum tensor for a perfect fluid. Comparing to Eq. (1.18) we find that the background pressure and density are given by,

$$\rho_0 = \frac{1}{2a^2}\varphi_0'^{\,2} + U(\varphi)\,, \tag{1.48}$$

$$P_0 = \frac{1}{2a^2}\varphi_0'^{\,2} - U(\varphi)\,. \tag{1.49}$$

We can see from the above equation that we will indeed have a negative pressure if the potential energy dominates over the kinetic energy.

Either by varying the action, using the definition above for the Lagrangian or by directly substituting the expressions for the density and pressure into the equation of motion for a perfect fluid we can determine the governing equations. The continuity equation leads to the following background Klein-Gordon equation [35],

$$\varphi_0'' + 2\mathcal{H}\varphi_0' + a^2 U_{,\varphi} = 0\,, \tag{1.50}$$

and the Einstein field equations give the Friedmann equation

$$\mathcal{H}^2 = \frac{8\pi G}{3}\left(a^2 U_0 + \frac{1}{2}{\varphi_0'}^2\right)\,. \tag{1.51}$$

This description still leads to a multitude of different models with different types of potentials, one of the simplest of which is the original chaotic inflation model. It has the potential

$$U(\varphi) = \frac{1}{2}m^2\varphi^2\,. \tag{1.52}$$

In Section 3.3.3 we will describe some other popular inflaton potentials.

1.2.3 Slow Roll Approximation

A useful simplification can be made if we assume almost exponential inflation, i.e. $|\dot{H}| \ll H^2$. We define a slow roll parameter $\epsilon_{\rm sr}$

$$\epsilon_{\rm sr} = \frac{\dot{\varphi}^2}{4H^2} = -\frac{\dot{H}}{H^2}\,, \tag{1.53}$$

which leads to the following equation

$$\frac{\ddot{a}}{a} = H^2(1 - \epsilon_{\rm sr})\,, \tag{1.54}$$

and implies that we will have an inflationary period for as long as $\epsilon_{\rm sr} < 1$. However in order for our inflationary period to last long enough we must introduce a second

slow roll parameter,

$$\eta_{\rm sr} = -\frac{\ddot{\varphi}}{H\dot{\varphi}}\,. \tag{1.55}$$

Here $\eta_{\rm sr}$ describes the flatness of the potential. While $\eta_{\rm sr} < 1$ the change of $\dot{\varphi}$ and therefore the change of $\epsilon_{\rm sr}$ is slow, leading to an extended period of inflation.

Taking the slow roll approximation amounts to setting $\epsilon_{\rm sr} \ll 1$ and $\eta_{\rm sr} \ll 1$. This implies that the potential energy dominates over the kinetic energy and is equivalent to setting the first term in Eq. (1.50) and the last term in Eq. (1.51) to zero. This leads to the approximate governing equations

$$H^2 \approx \frac{8\pi G}{3}U(\varphi)\,, \tag{1.56}$$

$$\dot{\varphi} \approx -\frac{U_{,\varphi}}{3H}\,, \tag{1.57}$$

and, as we mentioned at the start of this section, exponential expansion (i.e. a quasi-de Sitter spacetime),

$$a(t) \sim e^{Ht}\,. \tag{1.58}$$

While the slow roll approximation holds, inflation will always occur and inflation will end when $\epsilon_{\rm sr} = 1$.

1.3 Time line of events in the early universe

We conclude this introductory section by giving an outline of the key events in the history of our universe. In the table that follows we present the time, scale factor, red shift and energy of these key events [8, 35, 41], some of which are only order of magnitude approximations, for the exact values of those needed in the thesis, see Appendix A.

Event	Time	Scale Factor	Energy	Redshift
Planck Epoch	$< 10^{-43}$s		10^{15} TeV	
String Epoch	$\geq 10^{-43}$s		$\leq 10^{15}$ TeV	
GUT	$\sim 10^{-36}$s		10^{12} TeV	
Inflation	$\geq 10^{-34}$s		$\leq 10^{12}$ TeV	
SUSY breaking	$< 10^{-10}$s		> 1 TeV	
Baryogenesis	$< 10^{-10}$s		> 1 TeV	
EW symmetry breaking	10^{-10}s		246 GeV	
QCD symmetry breaking	10^{-4}s		$200 - 300$ MeV	
Nucleon freeze-out	0.01s	10^{-11}	10 MeV	10^{11}
Neutrino decoupling	1s	10^{-10}	1 MeV	10^{10}
BBN	3 min	10^{-9}	0.1 MeV	10^{9}
Matter-radiation equality	10^{4} yrs	10^{-4}	1 eV	10^{4}
Recombination (CMB)	3.8×10^{5} yrs	9×10^{-4}	0.1 eV	$1,100$
Dark ages	10^{5}- 10^{8} yrs	< 0.038	> 6 meV	> 25
Reionization	10^{8} yrs	$0.06 - 0.14$	$1.7 - 3.9$ meV	$15 - 6$
First galaxies	$\sim 6 \times 10^{8}$yrs	~ 0.09	~ 3 meV	~ 10
Dark energy domination	10^{9} yrs	~ 0.3	~ 0.8 meV	~ 2
Our Solar system	8×10^{9} yrs	0.67	0.35 meV	0.5
Today	13.7×10^{9} yrs	1	0.24 meV	0

1.4 Notation

To finish this chapter we will outline some of the notation conventions we will use throughout this thesis.

- We use the positive metric signature throughout, (-+++).
- We use natural units throughout most of this thesis, which we define as setting $c = \hbar = k_B = 1$. The exception is for two sections (the end of Chapter 4 and most of Chapter 6) where we work in SI units in order to more easily compare with observations. The point at which we switch to SI units is indicated clearly in each case.

- We define the reduced Planck mass as $M_{PL} \equiv (8\pi G)^{1/2} = 2.4 \times 10^{18} GeV$, which we use in some sections of the thesis in place of G.

- We will often use the Fourier component of a function, $f(k^i)$, which is related to the function in real space, $f(x^i)$, by

$$f(\eta, x^i) = \frac{1}{(2\pi)^3} \int d^3k f(\eta, k^i) e^{ik_i x^i} \,. \tag{1.59}$$

- Differentiation with respect to coordinate time, t, will be denoted with an overdot ($\dot{}$), differentiation with respect to conformal time, η, will be denoted by a prime ($'$) and differentiation with respect to the number of e-folds $\mathcal{N}$ will be denoted by a dagger, (†).

- We will be using a comma to denote a partial derivative, $v_{,i} \equiv \frac{\partial}{\partial x^i} v$ and a semi colon to denote a covariant derivative, $v_{\nu;\mu} \equiv \nabla_\mu v_\nu$.

- Greek indices will take values 0 through to 3 and will cover the whole space-time, where as latin indices will take the values 1 through to 3 and will cover the spacial slice.

- When dealing with perturbative expansions we will denote the order by a subscript, this will always be the number closest to the quantity, i.e. $\delta\rho_1$. In Chapter 4, where we consider multiple species, the species type will be indicated by a subscript in brackets. For instance, the first order density perturbation for photons would be given by $\delta\rho_{1(\gamma)}$.

- Background quantities will be denoted by a subscript 0, unless otherwise indicated at the start of a chapter, in particular in Chapter 4 and 6 we will be dropping the subscript 0 and any quantity without a subscript should be considered a background quantity.

Chapter 2

Cosmological Perturbation Theory

In this chapter we will be introducing Cosmological Perturbation Theory (CPT) and briefly outlining some key results. For more details see the review, Ref. [9] and references therein.

2.1 Perturbing Spacetime

As mentioned in the previous chapter, we live in a universe that on large scales is very homogeneous and isotropic, which is why the geometry of our spacetime can be approximated by the FLRW metric. However, we know that on small scales the universe contains structure. This structure can be seen in the CMB, large scale structure surveys and large scale structure simulations. Therefore we need a way to mathematically describe this additional structure. We do this by considering FLRW as a background and then studying perturbations on top of this background, this is known as cosmological perturbation theory (CPT).

2.1.1 Defining perturbed quantities

In general, in FLRW cosmologies[1] all tensor quantities can be decomposed into a time dependent background part and a time and spatially dependent perturbation,

[1] For a non-FLRW example with a background which is both time and spatial dependent, see Leithes & Malik, Ref. [42].

where the background part is homogeneous and isotropic.

$$\mathbf{T}(t,\mathbf{x}) = \mathbf{T}(t) + \epsilon\delta\mathbf{T}(t,\mathbf{x})\,. \tag{2.1}$$

We know that in our universe, on large scales, the perturbations are much smaller than the background values. This is represented by the small parameter ϵ above. Expanding the perturbed part as a Taylor series in powers of ϵ

$$\mathbf{T}(t,\mathbf{x}) = \mathbf{T}_0(t) + \epsilon\delta\mathbf{T}_1(t,\mathbf{x}) + \frac{1}{2}\epsilon^2\delta\mathbf{T}_2(t,\mathbf{x}) + ... \tag{2.2}$$

In this thesis we will follow the literature and not include the ϵ's in our equations. We use subscripts to indicate the order of a particular quantity. First order, or linear, perturbation theory will only consider terms that are first order in ϵ, i.e. terms proportional to ϵ, where as second order perturbation theory considers terms that are second order in ϵ i.e. terms that are proportional to ϵ^2, (including both pure second order terms and terms which are the product of two first order parts). Higher order perturbation theory is defined similarly. Following the example in Eq. (2.2) above we can expand the density of a perfect fluid ρ as

$$\rho = \rho_0(t) + \delta\rho_1(t,\mathbf{x}) + \frac{1}{2}\delta\rho_2(t,\mathbf{x}) + ... \tag{2.3}$$

and similarly for the other quantities introduced in the introduction, such as pressure of a perfect fluid (P) and the inflaton scalar field (φ).

2.1.2 Decomposing perturbations into scalars, vectors and tensors

We split the spacetime into a one-parameter family of spatial hypersurfaces of constant time; this is known as a (3+1) split. Once quantities have been split into temporal and spatial parts they can be further decomposed into scalar, vector and tensor parts depending on their transformation behaviour [14]. This is useful because at linear order the governing equations for these three types of perturbations decouple and can be solved separately. This is no longer true at higher orders where the equations have source terms mixing the different types. The scalar perturba-

tions are constructed from a scalar, its derivatives and/or background quantities, where any 3-vector constructed from a scalar will be curl free. Vector perturbations are divergence free and tensor perturbations are perturbations which can not be constructed from scalar or vector perturbations alone.

For example, starting with 4-vectors, we can decompose any 4-vector into a temporal and spatial part, where the temporal part is necessarily a scalar i.e.

$$u_\mu = (u_0, u_i) \ . \tag{2.4}$$

The spatial part can be further decomposed into the gradient of a scalar and a divergence-free vector part,

$$u_i = u_{,i} + u_i^{\rm vec} \, . \tag{2.5}$$

Note that due to the isotropic nature of the background (FLRW) there will be no vector spatial parts at zeroth order.

Tensors can also be split into temporal and spatial parts but in this case we will also obtain some mixed temporal-spatial parts and again we can then go on to split these parts into scalar, vector and tensor parts due to their transformation properties. For instance, if we consider the metric tensor $g_{\mu\nu}$, which in the background we will take to be the FLRW metric,

$$ds^2 = a^2 \left[-d\eta^2 + \delta_{ij} dx^i dx^j \right] \ , \tag{2.6}$$

then the perturbed metric can be written as

$$g_{00} = -a^2(1+2\phi) \, , \quad g_{0i} = a^2 B_i \, , \quad g_{ij} = a^2(\delta_{ij} + 2C_{ij}) \, . \tag{2.7}$$

We then further split the mixed temporal-spatial and the spatial components into scalar, vector and tensor parts,

$$B_i = B_{,i} - S_i \, , \tag{2.8}$$

$$C_{ij} = -\psi\delta_{ij} + E_{,ij} + F_{(i,j)} + \frac{1}{2} h_{ij} \, . \tag{2.9}$$

The scalar perturbations are given by, ϕ (the lapse function), ψ (the curvature perturbation) and B and E (the scalar parts of the shear), the vector perturbations are given by S_i and F_i (the vector parts of the shear) and h_{ij} is a tensor perturbation which describes gravitational waves. Note that at present we have not yet expanded these metric perturbations as a power series of ϵ and the above quantities should be considered to contain all orders.

As mentioned above the perturbations will satisfy certain constraints, namely, $B_{,i}$ will be curl free i.e. $B_{,[ij]} = 0$ and the vector perturbations will be divergence free i.e. $S_{i,}{}^{i} = 0$ and $F_{i,}{}^{i} = 0$. The symmetric tensor contribution will be both transverse (divergence free) $h_{ij,}{}^{j} = 0$ and trace-free $h^i_i = 0$. These constraints result in the trace of the perturbed spatial metric being given by

$$C^i_i = -3\psi + \nabla^2 E\,. \tag{2.10}$$

Taking all these constraints into account we can see that the 4 scalars contribute 1 degree of freedom each, the 2 divergent-free vectors contribute 2 degrees of freedom each and the tensor also contributes 2 degrees of freedom. This gives us 10 degrees of freedom i.e. the same number as the independent components of the perturbed spatial metric.

Expanding out the perturbations as described we have the complete metric tensor up to second-order,

$$g_{00} = -a^2\left[1 + 2\phi_1 + \phi_2\right]\,, \tag{2.11}$$

$$g_{0i} = a^2\left[B_{1i} + \frac{1}{2}B_{2i}\right]\,, \tag{2.12}$$

$$g_{ij} = a^2\left[\delta_{ij} + 2C_{1ij} + C_{2ij}\right]\,, \tag{2.13}$$

where the perturbations B_{1i}, B_{2i}, C_{1ij} and C_{2ij} can be split into scalar, vector and tensor parts as above. The contravariant metric tensor up to second-order is given

by,

$$g^{00} = -a^{-2}\left[1 - 2\phi_1 - \phi_2 + 4\phi_1^2 - B_{1k}B_1^k\right] , \tag{2.14}$$

$$g^{0i} = a^{-2}\left[B_1^i + \frac{1}{2}B_2^i - 2\phi_1 B_1^i - 2B_{1k}C_1^{ki}\right] , \tag{2.15}$$

$$g^{ij} = a^{-2}\left[\delta^{ij} - 2C_1^{ij} - C_2^{ij} + 4C_1^{ik}C_{1k}^j - B_1^i B_1^j\right] . \tag{2.16}$$

2.2 Gauge transformations

GR is a theory which is covariant under coordinate transformations i.e. it has no preferred coordinate system. When we split a quantity into a background and perturbed part we are considering two objects which live on different 4-dimensional spacetimes (4-manifolds) i.e. a background spacetime, $\mathcal{M}_0$, and a physical spacetime $\mathcal{M}_\epsilon$, both embedded in a higher dimensional manifold ($\mathcal{N}$). We can introduce a mapping or correspondence between these two spacetimes, $p_\epsilon : \mathcal{M}_0 \to \mathcal{M}_\epsilon$, which is often referred to as a gauge. This mapping is generated by a vector field X on $\mathcal{N}$ which identifies points on the same integral curve of X as the same physical point as depicted in Fig. 2.1.

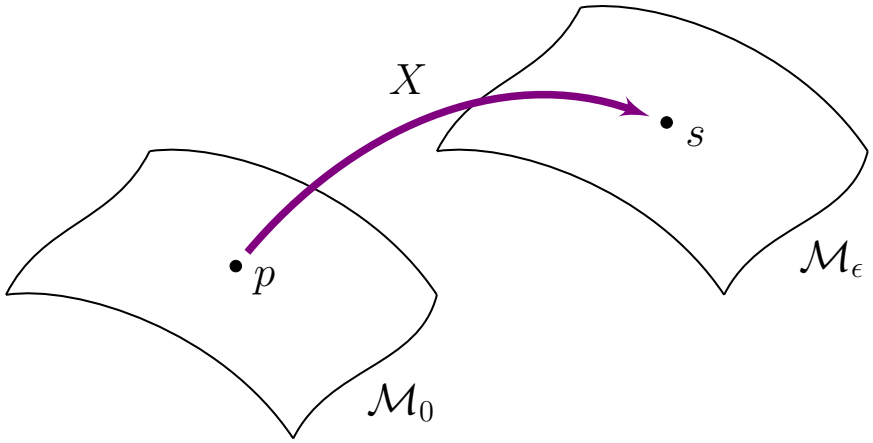

Figure 2.1: This diagram shows a background manifold, $\mathcal{M}_0$ and a physical manifold, $\mathcal{M}_\epsilon$, both embedded in a higher dimensional mainfold, $\mathcal{N}$. The mapping between the manifolds is called a gauge and is generated by a vector field (X).

The choice we make here for both the mapping and the vector field, X is not unique and this specification of a mapping is called a choice of gauge. A gauge transformation describes how we move from one gauge choice to another.

2.2.1 Active and Passive approach

Splitting variables into a background and perturbed part is not a covariant process and therefore this introduces a coordinate dependence which effects the perturbed part. To study this further we need to calculate how perturbations will vary under a small coordinate transformation. There are two approaches to this, the active and passive approaches.

In the passive approach we pick the same physical point in the background spacetime (q) then we make a small change to the coordinate system on $\mathcal{M}_\epsilon$. As, by construction, we require that the background part remains unchanged, this will necessarily mean that the perturbed quantity on $\mathcal{M}_\epsilon$ will have to go through a gauge transformation, see Fig. 2.2.

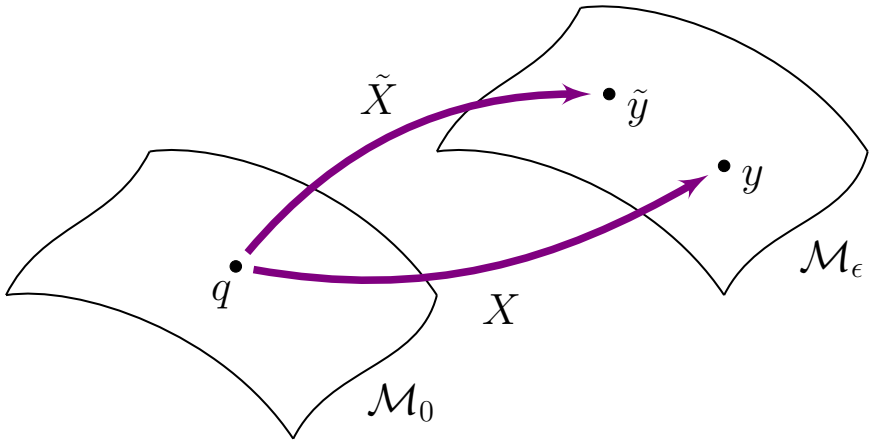

Figure 2.2: Passive Approach: The transformation of the perturbed quantities is evaluated at the same physical point.

In the active approach we pick the same coordinate point in the perturbed spacetime (z) and this time look at a the transformation of the perturbed quantity directly

induced by a mapping. This leads to a gauge transformation on the background spacetime, see Fig. 2.3.

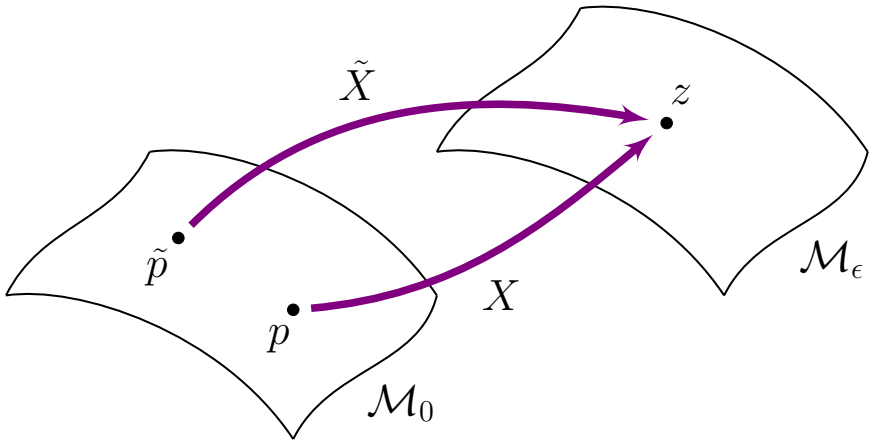

Figure 2.3: Active Approach: The transformation of the perturbed quantities is evaluated at the same coordinate point.

As the two approaches are equivalent for simplicity we will only consider the active approach here. We need to find out how a tensor would transform under a change of coordinates. In other words we would like to find an expression for $\tilde{T}$, an arbitrary tensor evaluated at the physical point $\tilde{p}$ in terms of T, the same tensor evaluated at the physical point p, where the points $\tilde{p}$ and p have the same coordinate value. To proceed we need to define our gauge transformation vector, which at first order is

$$\xi_1{}^{\mu} = (\xi_1{}^{0}, \xi_1{}^{i}) = (\alpha_1, \beta_1,{}^{i} + \gamma_1{}^{i}) \,. \tag{2.17}$$

Under such a coordinate transform our arbitrary tensor will transform via the exponential map [27]

$$\widetilde{\mathbf{T}} = e^{\pounds_\xi} \mathbf{T} \,. \tag{2.18}$$

Where $\pounds_\xi$ is the Lie derivative with respect to the generating vector and we use a tilde to denote a transformed quantity. Expanding out the exponential map as a series we have

$$\widetilde{\mathbf{T}} = \left(1 + \epsilon \pounds_{\xi_1} + \frac{1}{2}\epsilon^2 \pounds^2_{\xi_1} + \frac{1}{2}\epsilon^2 \pounds_{\xi_2} + ...\right) \mathbf{T} \,, \tag{2.19}$$

and then in addition, expanding our tensor order by order leads to the following transformations up to second order,

$$\widetilde{\mathbf{T}_0} = \mathbf{T_0}\,, \tag{2.20}$$

$$\widetilde{\delta\mathbf{T}_1} = \delta\mathbf{T_1} + \pounds_{\xi_1}\mathbf{T_0}\,, \tag{2.21}$$

$$\widetilde{\delta\mathbf{T}_2} = \delta\mathbf{T_2} + \pounds_{\xi_2}\mathbf{T_0} + \pounds^2_{\xi_1}\mathbf{T_0} + 2\pounds_{\xi_i}\delta\mathbf{T_1}\,. \tag{2.22}$$

The Lie derivatives on scalars, vectors and tensors are given by

$$\pounds_\xi X = \xi^\rho X_{,\rho}\,, \tag{2.23}$$

$$\pounds_\xi Y_\mu = \xi^\rho Y_{\mu,\rho} + \xi^\rho{}_{,\mu} Y_\rho\,, \tag{2.24}$$

$$\pounds_\xi Z_{\mu\nu} = \xi^\rho Z_{\mu\nu,\rho} + \xi^\rho{}_{,\mu} Z_{\rho\nu} + \xi^\rho{}_{,\nu} Z_{\mu\rho}\,. \tag{2.25}$$

If we apply the transform above and recall that the background quantities are only time dependent then we find that at first order a perturbed four-scalar transforms as,

$$\widetilde{\delta X_1} = \delta X_1 + X_0'\alpha_1\,. \tag{2.26}$$

In the same way at first order a four-vector transforms as,

$$\widetilde{\delta U_{1\mu}} = \delta U_{1\mu} + U_\mu'\alpha_1 + U_\lambda \xi^\lambda_{1,\mu}\,, \tag{2.27}$$

and at first order a tensor transforms as,

$$\widetilde{\delta T_{1\mu\nu}} = \delta T_{1\mu\nu} + T'_{\mu\nu}\alpha_1 + T_{\lambda\nu}\xi^\lambda_{1,\mu} + T_{\mu\lambda}\xi^\lambda_{1,\nu}\,. \tag{2.28}$$

By applying the above expression to the FLRW metric and comparing the original and transformed quantities we can write down the transformations of the first order metric perturbations. Firstly, the scalars,

$$\widetilde{\phi_1} = \phi_1 + \mathcal{H}\alpha_1 + \alpha_1'\,, \tag{2.29}$$

$$\widetilde{\psi_1} = \psi_1 - \mathcal{H}\alpha_1\,, \tag{2.30}$$

$$\widetilde{B_1} = B_1 - \alpha_1 + \beta_1'\,, \tag{2.31}$$

$$\widetilde{E_1} = E_1 + \beta_1\,, \tag{2.32}$$

and now the vectors,

$$\widetilde{S_1^i} = S_1^i - \gamma_1^{i\prime}\,, \tag{2.33}$$

$$\widetilde{F_1^i} = F_1^i + \gamma_1^i\,. \tag{2.34}$$

The first order tensor perturbation is gauge-invariant.

2.2.2 Gauge-invariant quantities and choosing a gauge

As we have seen above the process of splitting our spacetime into a background part and a perturbed part is not a covariant process. Carrying out a coordinate transformation on our perturbed quantities, as we did above, introduced extra gauge modes, therefore leaving us with variables dependent on our coordinate choice. In order to get physical results which do not depend on coordinate choices we will remove these extra gauge modes. This must be done in a consistent way by specifying the threading and slicing and is also known as making a choice of gauge.

To make this gauge choice we introduce gauge-invariant variables following the method of Bardeen, Ref. [14]. We choose coordinates such that two of the scalar metric perturbations and one of the vector metric perturbations is zero. This removes the additional gauge dependencies introduced by α, β and γ^i in the previous section. The remaining scalar, vector and tensor perturbations will all be gauge-invariant.

There are many ways to specify the mapping between the background and perturbed spacetimes and therefore many different gauge choices you can make. We will go through two such gauge choices below, uniform curvature gauge and Newtonian gauge. For a in-depth look at different gauges and the resulting equations we refer to Ref. [9].

2.2.2.1 Uniform curvature gauge

In the uniform curvature gauge (or flat gauge) the spatial metric is unperturbed at linear order and therefore spatial hypersurfaces are flat. At first order this means

$$\widetilde{E}_1 = \widetilde{\psi}_1 = 0\,, \quad \widetilde{F}_{1i} = 0\,, \tag{2.35}$$

giving the following expressions for the components of the generating vector,

$$\alpha_{1\,\mathrm{flat}} = \frac{\psi_1}{\mathcal{H}}\,, \tag{2.36}$$

$$\beta_{1\,\mathrm{flat}} = -E_1\,, \tag{2.37}$$

$$\gamma^i_{1\,\mathrm{flat}} = -F^i_1\,. \tag{2.38}$$

We then have two gauge-invariant scalars,

$$\widetilde{\phi_{1\,\mathrm{flat}}} = \phi_1 + \psi_1 + \left(\frac{\psi_1}{\mathcal{H}}\right)'\,, \tag{2.39}$$

$$\widetilde{B_{1\,\mathrm{flat}}} = B_1 - \frac{\psi_1}{\mathcal{H}} - E_1'\,, \tag{2.40}$$

and one gauge-invariant vector,

$$\widetilde{S^i_{1\,\mathrm{flat}}} = S^i_1 + F^i_1\,, \tag{2.41}$$

in addition to the original gauge-invariant tensor perturbation.

This also allows us to evaluate how the density perturbation and scalar field perturbation transform in the flat gauge, using Eq. 2.26, as

$$\widetilde{\delta\rho_{1\mathrm{flat}}} = \delta\rho_1 + \rho_0'\frac{\psi_1}{\mathcal{H}}\,, \tag{2.42}$$

$$\widetilde{\delta\varphi_{1\mathrm{flat}}} = \delta\varphi_1 + \varphi_0'\frac{\psi_1}{\mathcal{H}}\,. \tag{2.43}$$

When working in flat gauge in the following chapters we will drop the tilde for convenience. Note that in flat gauge the scalar field fluctuation is also known as the Sasaki-Mukhanov variable [43, 44].

2.2.2.2 Conformal Newtonian Gauge

In the conformal Newtonian gauge the shear, σ is zero. This gauge is also referred to as the Longitudinal or Poisson gauge. In order that $\tilde{\sigma}_1 = 0$ we have

$$\tilde{E}_1 = \tilde{B}_1 = 0\,, \quad \tilde{S}_{1i} = 0\,, \tag{2.44}$$

giving the following expressions for the components of the generating vector,

$$\alpha_{1\,\mathrm{newt}} = -\sigma_1 = -(E_1' - B_1)\,, \tag{2.45}$$

$$\beta_{1\,\mathrm{newt}} = -E_1\,, \tag{2.46}$$

$$\gamma^i_{1\,\mathrm{newt}} = \int S^i_1 d\eta + \mathcal{F}^i_1(x^j)\,, \tag{2.47}$$

where $\mathcal{F}^i_1$ is an arbitrary constant three-vector. The two gauge-invariant scalars are then equivalent to the variables introduced by Bardeen,

$$\widetilde{\phi_{1\,\mathrm{newt}}} = \phi_1 - \mathcal{H}(E_1' - B_1) - (E_1' - B_1)'\,, \tag{2.48}$$

$$\widetilde{\psi_{1\,\mathrm{newt}}} = \psi_1 + \mathcal{H}(E_1' - B_1)\,, \tag{2.49}$$

and the gauge-invariant vector is given by

$$\widetilde{F^i_{1\,\mathrm{newt}}} = F^i_1 + \int S^i_1 d\eta + \mathcal{F}^i_1(x^j)\,. \tag{2.50}$$

Finally, the transformation of the density perturbation and scalar field perturbation in Newtonian gauge are given by,

$$\widetilde{\delta\rho_{1\mathrm{newt}}} = \delta\rho_1 - \rho_0'\sigma_1\,, \tag{2.51}$$

$$\widetilde{\delta\varphi_{1\mathrm{newt}}} = \delta\varphi_1 - \varphi_0'\sigma_1\,. \tag{2.52}$$

2.3 Energy-Momentum Tensor

We now wish to extend our discussion of the matter content of the universe up to linear order in CPT. In Section 1.1.3 we introduced the energy-momentum tensor, which was a function of the fluid's 4-velocity, density and pressure. In order to extend this description to perturbed quantities we will need to look at the 4-velocity in more detail.

The 4-velocity is defined as

$$u^\mu = \frac{dx^\mu}{d\tau}\,, \tag{2.53}$$

where τ is the proper time, i.e. the time between two events as measured by an observer travelling between the events, and is given by $d\tau^2 = ds^2$. As with the pressure and density the 4-velocity can be written as a series expansion,

$$u^\mu = u_0^\mu + \delta u_1^\mu + ... \tag{2.54}$$

As mentioned in Section 1.1.3 the 4-velocity must satisfy the constraint $u^\mu u_\mu = g_{\mu\nu}u^\mu u^\nu = -1$. Using the expression for the metric we are able to write down the full 4-velocity up to first order,

$$u_0 = -a(1+\phi_1)\,, \quad u_i = a(v_{1i} + B_{1i})\,, \tag{2.55}$$

$$u^0 = a^{-1}(1-\phi_1)\,, \quad u^i = a^{-1}v_1^i\,. \tag{2.56}$$

2.3.1 Perfect fluids

To extend the stress-energy tensor for perfect fluids given in Eq. (1.18) to general fluids we include an anisotropic stress term $\pi^{\mu\nu}$ [9],

$$T^\mu_\nu = (\rho + P)u^\mu u_\nu + P\delta^\mu{}_\nu + \pi^\mu{}_\nu\,. \tag{2.57}$$

The above stress-energy tensor is written in a generic inertial frame and u^μ is the fluid 4-velocity. The spatial part of the anisotropic stress can be decomposed into scalar (Π), vector (π^i) and tensor ($\pi^i{}_j$) parts,

$$\pi^i{}_j = \Pi_{,}{}^i{}_j - \frac{1}{3}\nabla^2\Pi\delta^i{}_j + \pi^{(i}{}_{,j)} + \pi^i{}_j\,. \tag{2.58}$$

We can now expand all matter quantities order by order as we did for the density in Eq. (2.3). Substituting in the metric, Eq. (2.7), and 4-velocity, Eq. (2.56), we

have the following expressions up to first order,

$$
\begin{aligned}
T^0{}_0 &= -(\rho_0 + \delta\rho_1)\,, && (2.59)\\
T^0{}_i &= (\rho_0 + P_0)(B_{1i} + v_{1i})\,, && (2.60)\\
T^i{}_0 &= -(\rho_0 + P_0)v_1^i\,, && (2.61)\\
T^i{}_j &= (P_0 + \delta P_1)\delta^i{}_j + \pi^i{}_j\,. && (2.62)
\end{aligned}
$$

2.3.2 Scalar fields

In Eq. (1.47) we wrote down the energy-momentum tensor for a canonical single scalar field as

$$T^\mu_\nu = g^{\mu\lambda}\varphi_{,\mu}\varphi_{,\lambda} - \delta^\mu_\nu\left(U(\varphi) + \frac{1}{2}g^{\alpha\beta}\varphi_{,\alpha}\varphi_{,\beta}\right)\,.$$

Once again expanding the scalar field order by order and substituting in the metric, Eq. (2.7), we have the following expressions up to first order,

$$
\begin{aligned}
T^0{}_0 &= -\frac{\varphi_0'^2}{2a^2}\left(1 - 2\phi_1 + \frac{2\delta\varphi_1'}{\varphi_0'}\right) - U(\varphi_0) - U_{,\varphi}\delta\varphi_1\,, && (2.63)\\
T^0{}_i &= -\frac{\varphi_0'^2}{a^2}\delta\varphi_{1,i}\,, && (2.64)\\
T^i{}_0 &= \frac{\varphi_0'^2}{a^2}\left(B_1^i + \frac{\delta\varphi_,{}^i}{\varphi_0'}\right)\,, && (2.65)\\
T^i{}_j &= -\delta^i{}_j\left[U(\varphi_0) + U_{,\varphi}\delta\varphi_1 - \frac{\varphi_0'^2}{2a^2}\left(1 - 2\phi_1 + \frac{2\delta\varphi_1'}{\varphi_0'}\right)\right]\,. && (2.66)
\end{aligned}
$$

It is worth noting that the scalar field has no anisotropic stress at first order. By comparing the components for the energy-momentum tensor for the scalar field with the energy-momentum tensor for a fluid we can write down effective first order densities and pressures for the scalar field as we did for the background quantities in Eq. (1.48),

$$
\begin{aligned}
\delta\rho_1 &= \frac{1}{a^2}\left(\delta\varphi_1'\varphi_0' - \phi_1\varphi_0'^2\right) + U_{,\varphi}\delta\varphi_1\,, && (2.67)\\
\delta P_1 &= \frac{1}{a^2}\left(\delta\varphi_1'\varphi_0' - \phi_1\varphi_0'^2\right) - U_{,\varphi}\delta\varphi_1\,. && (2.68)
\end{aligned}
$$

As mentioned above, at linear order $\pi^i_j = 0$ for single scalar fields.

2.4 Dynamical equations at first order

We now wish to extend our description of the dynamics of the universe to linear order in CPT.

2.4.1 Einstein Equations

As we saw in Section 1.1.2, Einstein's equations are given by $G_{\mu\nu} = 8\pi G T_{\mu\nu}$. We follow through as we did in that section, evaluating the connection coefficients, Ricci tensor and then Einstein tensor for the perturbed metric and then equating this with the perturbed energy-momentum tensor to get first-order equations. In this section we present the first order Einstein equations for both a fluid and a scalar field. Initially we will not specify a particular gauge. We include the full connection coefficients up to second order in Appendix B.

2.4.1.1 Fluids

The following equations are obtained from the Einstein equations, using the stress-energy tensor for a fluid. The 00 component is given by

$$-\mathcal{H}\nabla^2 B_1 - 3\mathcal{H}\psi_1' + \mathcal{H}\nabla^2 E_1' + \nabla^2\psi_1 - 3\mathcal{H}^2\phi_1 = 4\pi G a^2 \delta\rho_1\,, \tag{2.69}$$

the $0i$ component is given by,

$$\frac{1}{4}\nabla^2(S_{1i} + F_{1i}') + \mathcal{H}\phi_{1,i} + \psi_{1,i}' = -4\pi G a^2(\rho + P)(B_{1,i} - S_{1i} + v_{1i})\,, \tag{2.70}$$

and finally the ij component is given by,

$$\Big(\nabla^2(B_1{}' + 2B_1\mathcal{H} - \psi_1 + \phi_1 - 2\mathcal{H}E_1' - E_1'') + 4\phi_1\mathcal{H}' + 2\psi_1'' + (\psi_1 - \phi_1)_{,ij}\,,$$
$$+2\mathcal{H}(2\psi_1' + \phi_1{}' + \phi_1\mathcal{H})\Big)\delta_{ij} - (2\mathcal{H} + \partial_\eta)(B_{1,ij} - S_{1(j,i)}) - \frac{1}{2}\nabla^2 h_{ij}\,,$$
$$+(2\mathcal{H}\partial_\eta + \partial_\eta^2)(E_{1,ij} + F_{1(i,j)} + \frac{1}{2}h_{1ij}) = 8\pi G a^2(\delta P_1\delta_{ij} + \pi_{ij})\,. \tag{2.71}$$

Recall that at first order the scalar, vector and tensor equations decouple. Eq. (2.69) is already a scalar equation but to see that the other two equations can be separated we act with ∂^i on Eq. (2.70) which gives a scalar equation which we then subtract from Eq. (2.70) to leave a vector equation. In a similar way we can find two scalar equations from the ij equation; firstly, by acting with $\partial^i\partial^j$ on Eq. (2.71) and then by multiplying Eq. (2.71) by δ^{ij}. Again by subtracting the two scalar equations from the original ij equation, Eq. (2.71), we arrive at an equation containing only vectors and tensors which can be separated to give a vector and tensor equation.

In summary we have four scalar equations. Firstly, the energy and momentum constraint equations,

$$-\mathcal{H}\nabla^2 B_1 - 3\mathcal{H}\psi_1' + \mathcal{H}\nabla^2 E_1' + \nabla^2\psi_1 - 3\mathcal{H}^2\phi_1 = 4\pi G a^2\delta\rho_1\,, \tag{2.72}$$
$$\mathcal{H}\phi_1 + \psi_1' = -4\pi G a^2(\rho + P)(B_1 + v_1)\,, \tag{2.73}$$

and secondly two evolution equations,

$$2\phi_1\mathcal{H}' + \psi_1'' + 2\mathcal{H}\psi_1' + \mathcal{H}\phi_1{}' + \phi_1\mathcal{H}^2 = 4\pi G a^2(\delta P_1 + \frac{2}{3}\nabla^2\Pi)\,, \tag{2.74}$$
$$B_1{}' + 2B_1\mathcal{H} - \psi_1 + \phi_1 - 2\mathcal{H}E_1' - E_1'' = 8\pi G a^2\Pi\,, \tag{2.75}$$

We also have two vector equations,

$$\nabla^2(S_{1i} + F_{1i}') = 16\pi G a^2(\rho + P)(S_{1i} - v_{1i})\,, \tag{2.76}$$
$$S_{1i}' + F_{1i}'' + 2\mathcal{H}S_{1i} + 2\mathcal{H}F_{1i}' = 4\pi G a^3\pi_{(i,j)}\,, \tag{2.77}$$

and one tensor equation,

$$h_{ij}'' + 2\mathcal{H}h_{ij}' - \nabla^2 h_{ij} = 16\pi G a^2\pi_{ij}\,. \tag{2.78}$$

2.4.1.2 Scalar fields

For completeness, we consider here the stress-energy tensor for a scalar field and metric expanded out to first order. As above we can use the Einstein field equations to get four scalar, two vector and one tensor equation.

The scalar equations are:

$$\begin{aligned}
&-\mathcal{H}\nabla^2 B_1 - 3\mathcal{H}\psi_1' + \mathcal{H}\nabla^2 E_1' + \nabla^2\psi_1 - 3\mathcal{H}^2\phi_1 = 4\pi G\left(\delta\varphi_1'\varphi_0' - \phi_1{\varphi_0'}^2 + a^2 U_{,\varphi}\delta\varphi_1\right)\,,\\
&\mathcal{H}\phi_1 + \psi_1' = -4\pi G(B_1 + v_1){\varphi_0'}^2\,,\\
&2\phi_1\mathcal{H}' + \psi_1'' + 2\mathcal{H}\psi_1' + \mathcal{H}{\phi_1}' + \phi_1\mathcal{H}^2 = 4\pi G\left(\delta\varphi_1'\varphi_0' - \phi_1{\varphi_0'}^2 - a^2 U_{,\varphi}\delta\varphi_1\right)\,,\\
&{B_1}' + 2B_1\mathcal{H} - \psi_1 + \phi_1 - 2\mathcal{H}E_1' - E_1'' = 0\,,
\end{aligned} \tag{2.79}$$

the vector equations are,

$$\nabla^2(S_{1i} + F_{1i}') = 16\pi G(S_{1i} - v_{1i}){\varphi_0'}^2\,, \tag{2.80}$$

$$S_{1i}' + F_{1i}'' + 2\mathcal{H}S_{1i} + 2\mathcal{H}F_{1i}' = 0\,, \tag{2.81}$$

and the tensor equation is,

$$h_{ij}'' + 2\mathcal{H}h_{ij}' - \nabla^2 h_{ij} = 0\,. \tag{2.82}$$

2.4.2 Conservation Equations

In Section 1.1.3 we saw that by either using the Bianchi identities or by varying the action we arrive at a continuity equation, given in Eq. (1.22). Now that we have expressions for the stress-energy tensor up to first order we can use these in combination with the continuity equations to find first-order conservation equations.

2.4.2.1 Fluids

Using the stress-energy tensor for a fluid given in Eq. (2.59) and expanding the 0 component of the continuity equation gives us the following energy conservation equation at first-order,

$$\delta\rho_1' + 3\mathcal{H}(\delta\rho_1 + \delta P_1) = (\rho + P)(3\psi_1' - \nabla^2(E_1' + v_1))\,. \tag{2.83}$$

Now expanding the i component of the continuity equation we arrive at the following momentum conservation equation at first-order,

$$[(\rho+P)(v_{1i}+B_{1i})]'+(\rho+P)\left[4\mathcal{H}(v_{1i}+B_{1i})+\phi_{1,i}\right]+\delta P_{1,i}+\frac{2}{3}\nabla^2\Pi_{1,i}+\frac{1}{2}\nabla^2\pi_{1i}=0\,. \tag{2.84}$$

This equation, as for the Einstein equations, can be separated into a scalar and vector equation. The scalar equation is,

$$[(\rho+P)(v_1+B_1)]'+(\rho+P)\left[4\mathcal{H}(v_1+B_1)+\phi_1\right]+\delta P_1+\frac{2}{3}\nabla^2\Pi=0\,, \tag{2.85}$$

and the vector equation is,

$$[(\rho+P)(v_{1i}-S_{1i})]'+4\mathcal{H}(\rho+P)(v_{1i}-S_{1i})+\frac{1}{2}\nabla^2\pi_{1i}=0\,. \tag{2.86}$$

2.4.2.2 Scalar fields

Either using the stress-energy tensor for a scalar field given in Eq. (2.63) and expanding the continuity equation, or by substituting the expressions for pressure and density in terms of the scalar field into Eq. (2.83), or indeed by varying the full first order action for a scalar field we arrive at the Klein-Gordon equation at first-order,

$$\delta\varphi_1{}''+2\mathcal{H}\delta\varphi_1{}'-\nabla^2\delta\varphi_1+a^2U_{,\varphi\varphi}\delta\varphi_1+2a^2U_{,\varphi}\phi_1-\phi_0'\phi_1-\phi_0'(3\psi_1'+\nabla^2(B_1-E_1'))=0\,. \tag{2.87}$$

This equation describes the evolution of the scalar field, in terms of the metric perturbations and the scalar field potential.

2.5 Solving for the density perturbation

Under certain conditions we can solve the equations given in Sections 2.4.1.1 and 2.4.2.1 to find out how the density perturbation would evolve in the early universe. In this section we will solve the equations to find the large scale density perturbation for a perfect fluid in the radiation era. Starting with the assumption that the universe is filled with a perfect fluid with equation of state $P=\omega\rho$, we write Eq. (2.83) and

Eq. (2.85) in flat gauge,

$$\delta\rho_1' + 3\mathcal{H}(\delta\rho_1 + \delta P_1) = -\rho(1+\omega)\nabla^2 v_1\,, \tag{2.88}$$

$$\rho(1+\omega)V_1' - 3\mathcal{H}\rho(1+\omega)^2 V_1 + \rho\omega' V_1 + \frac{1}{2}\mathcal{H}\rho(1+\omega)\left(8 - 3(1+\omega)\right)V_1 + \delta P_1 = 0\,, \tag{2.89}$$

where we have written $V_1 = v_1 + B_1$ and used Eq. (2.73) and Eq. (1.24), to substitute for ϕ_1 and ρ'. We can then use Eq. (2.88) and Eq. (2.72), to get an expression for V_1,

$$\rho(1+\omega)\nabla^2 V_1 = \frac{9\mathcal{H}^2}{2}(1+\omega)^2\rho V_1 - \frac{3\mathcal{H}}{2}(\omega+1)\delta\rho_1 - \delta\rho_1' - 3\mathcal{H}(\delta\rho_1 + \delta P_1)\,, \tag{2.90}$$

which if we switch to Fourier space and rearrange becomes

$$V_1 = \frac{3\mathcal{H}(\omega+3)\delta\rho_1 + 2\delta\rho_1' + 6\mathcal{H}\delta P_1}{2\rho(1+\omega)\left(\frac{9}{2}\mathcal{H}^2(1+\omega) + k^2\right)}\,. \tag{2.91}$$

Now differentiating Eq. (2.88) and using Eq. (2.89) and Eq. (2.91) we arrive at the following second order differential equation for the density perturbation [45],

$$\begin{aligned}\delta\rho'' + \left(7\mathcal{H} - \frac{\mathcal{I}'}{\mathcal{I}}\right)\delta\rho' + \frac{3}{2}\mathcal{H}(3+\omega)\left[\frac{\mathcal{H}'}{\mathcal{H}} + \frac{\omega'}{3+\omega} - \frac{\mathcal{I}'}{\mathcal{I}} + \frac{1}{2}\mathcal{H}(5-3\omega)\right]\delta\rho \\ +3\mathcal{H}\delta P' + \left[3\mathcal{H}\left(\frac{\mathcal{H}'}{\mathcal{H}} - \frac{\mathcal{I}'}{\mathcal{I}}\right) + \frac{3}{2}\mathcal{H}^2(5-3\omega) + \mathcal{I}\right]\delta P = 0\,,\end{aligned} \tag{2.92}$$

where $\mathcal{I} = k^2 + \frac{9}{2}\mathcal{H}^2(1+\omega)$. Assuming that we are in radiation domination and the pressure perturbation can be described by $\delta P = c_s^2\delta\rho$, that is, there is no non-adiabatic pressure perturbation, Eq. (2.92) becomes,

$$\delta\rho'' + 4\mathcal{H}\left(2 + \frac{3\mathcal{H}^2}{k^2+6\mathcal{H}^2}\right)\delta\rho' + \left(6\mathcal{H}^2 + \frac{1}{3}(k^2+6\mathcal{H}^2) + \frac{72\mathcal{H}^4}{k^2+6\mathcal{H}^2}\right)\delta\rho = 0\,. \tag{2.93}$$

Finally if we are interested in the large scale result, where $k^2 \ll 6\mathcal{H}^2$ then our second order equation becomes

$$\delta\rho'' + \frac{10}{\eta}\delta\rho' + \frac{20}{\eta^2}\delta\rho = 0\,, \tag{2.94}$$

which can be solved exactly to give,

$$\delta\rho(\eta, \mathbf{k}) = A(\mathbf{k})\eta^{-4} + B(\mathbf{k})\eta^{-5}\,, \tag{2.95}$$

where the functions $A(k)$ and $B(k)$ are set by initial conditions.

Chapter 3

Constraining the Curvature Perturbation

In this chapter we will be introducing the curvature perturbation. We will start by discussing how we can generate seeds for the structure in the universe using quantum fluctuations during inflation. We will then introduce conserved quantities, such as the curvature perturbation. Finally we will solve the evolution equations for the perturbation of the scalar field numerically in order to evaluate the evolution of the curvature perturbation. This will allow us to give a detailed account of the behaviour of the curvature perturbation close to horizon crossing. Large sections of this chapter are published in the papers Ref. [1, 2].

3.1 Producing perturbations during inflation

3.1.1 Quantum produced fluctuations

In Section 1.2 we mentioned that it was possible to generate the seeds for the structure we see today by quantum fluctuation during a period of inflation. In this section we will be formulating this mathematically and explaining how the quantum fluctuations in the very early universe lead to perturbations in the energy density at later times.

Starting from the Klein-Gordon equation, Eq. (2.87) and working in flat gauge we make the change of variables $u = a\delta\varphi_1$ and $z = \frac{a\varphi_0'}{\mathcal{H}}$. If we re-write the resulting

equation in Fourier space then we arrive at the Mukhanov equation,

$$u''(k^i) + \left(k^2 - \frac{z''}{z}\right) u(k^i) = 0\,. \tag{3.1}$$

If we wish to study what happens at a quantum level we will need to quantise this equation; in Minkowski space this is straight forward, we do it by promoting u and u' to operators [46],

$$u(k^i) \to \hat{u}(k^i)\,, \quad u'(k^i) \to \hat{u'}(k^i)\,. \tag{3.2}$$

Working in the Heisenberg picture we can expand the operator $\hat{u}$ in terms of the standard creation and annihilation operators ($\hat{a}$ and $\hat{a}^\dagger$),

$$\hat{u}(k^i) = \omega(k^i)\hat{a}(k^i) + \omega^*(-k^i)\hat{a}^\dagger(-k^i)\,, \tag{3.3}$$

where ω, the mode function, also satisfies the Mukhanov equation,

$$\omega''(k^i) + \left(k^2 - \frac{z''}{z}\right) \omega(k^i) = 0\,. \tag{3.4}$$

In order to solve this equation we require two boundary conditions. The first is given by imposing the canonical commutator on our operators,

$$[\hat{u}, \hat{u}'] = i\,, \tag{3.5}$$

which leads to the following normalisation condition for the mode function [46],

$$\omega^*(k^i)\omega'(k^i) - \omega^{*\prime}(k^i)\omega(k^i) = -i\,. \tag{3.6}$$

The second boundary condition comes from our choice of vacuum. There is not a unique choice for the vacuum state [47–49], so we pick the most natural choice which is the Minkowski vacuum. This is the vacuum state seen by a comoving observer in the far past when $\eta \to -\infty$ and all modes are much smaller than the Hubble radius, and is known as the Bunch-Davies vacuum [47, 49].

In the limit $\eta \to -\infty$ Eq. (3.4) becomes

$$\omega''(k^i) + k^2\omega(k^i) = 0\,, \tag{3.7}$$

which leads to the following solution

$$\omega = Ae^{-ik\eta} + Be^{ik\eta}\,. \tag{3.8}$$

In the limit $\eta \to -\infty$ the first term dominates and the solution becomes

$$\omega = Ae^{-ik\eta}\,. \tag{3.9}$$

Applying the first boundary condition in Eq. (3.6) to the solution in Eq. (3.9) we find that $A = 1/\sqrt{2k}$ so the initial condition for the mode function when $\eta \to -\infty$ is

$$\omega = \frac{1}{\sqrt{2k}}e^{-ik\eta}\,. \tag{3.10}$$

This initial condition holds for all modes as long as it is applied well inside the horizon. This gives us the following initial conditions, see Refs. [50–52]:

$$\begin{aligned} \delta\varphi|_{\rm init} &= \frac{1}{aM_{\rm PL}\sqrt{2k}}e^{-ik\eta}\,, \\ \delta\varphi_{,\mathcal{N}}|_{\rm init} &= -\frac{1}{aM_{\rm PL}\sqrt{2k}}e^{-ik\eta}\left(1 + i\frac{k}{aH}\right)\,, \end{aligned} \tag{3.11}$$

where $\eta = -(aH(1-\epsilon_H))^{-1}$ and $\epsilon_H = -\frac{H_{,\mathcal{N}}}{H}$ and $\mathcal{N}$ is the number of e-folds defined in Eq. (1.44) .

During slow roll inflation we have a quasi-de Sitter spacetime. In the case of a de Sitter spacetime, the Hubble parameter is constant and $z''/z = 2/\eta^2$ which means Eq. (3.4) becomes

$$\omega''(k^i) + \left(k^2 - \frac{2}{\eta^2}\right)\omega(k^i) = 0\,. \tag{3.12}$$

and has solutions,

$$\omega = Ae^{-ik\eta}\left(1 - \frac{i}{k\eta}\right) + Be^{ik\eta}\left(1 + \frac{i}{k\eta}\right)\,. \tag{3.13}$$

When we impose the two boundary conditions given by Eq. (3.6) and the initial solution in the $\eta \to -\infty$ limit, Eq. (3.10), we find that the constants in Eq. (3.13) are given by $A = 1/\sqrt{2k}$ and $B = 0$. So our solution for de Sitter spacetimes is given by

$$\omega = \frac{e^{-ik\eta}}{\sqrt{2k}}\left(1 - \frac{i}{k\eta}\right) . \tag{3.14}$$

In the numerical work that follows, once we have implemented the quantum initial conditions, we only consider the evolution of the scalar field perturbations classically. There are issues concerning how and when the quantum-to-classical transition takes place but we will not attempt to address these here. For further discussion on these issues, see for instance, Refs. [53, 54].

3.1.2 Evolving the field fluctuations

In order to evolve the fluctuations in the scalar field we use the Einstein and conservation equations in flat gauge outlined in Section 2.4. We assume the Klein Gordon equation, Eq. (1.50), and Friedmann equation Eq. (1.51), in the background and consider only single field canonical inflation as described in Section 1.2. We only consider scalar perturbations which, as explained in Section 2.1.2, will decouple at first order. The evolution equation for the fluctuations is then given by the perturbed Klein-Gordon equation, Eq. (2.87), which we gave in Section 2.4.2.2.

We present the equation again here in Fourier space,

$$\delta\varphi'' + 2\mathcal{H}\delta\varphi' + k^2\delta\varphi + a^2\left\{U_{,\varphi\varphi} + \frac{1}{\mathcal{H}M_{\rm PL}^2}\left(2\varphi_0' U_{,\varphi} + {\varphi_0'}^2\frac{1}{\mathcal{H}M_{\rm PL}^2}U_0\right)\right\}\delta\varphi = 0\,, \tag{3.15}$$

where the Fourier component of the field fluctuation, $\delta\varphi(k^i)$, is related to the fluctuation in real space, $\delta\varphi(x^i)$, by

$$\delta\varphi(x^i, \eta) = \frac{1}{(2\pi)^3}\int d^3k\,\delta\varphi(k^i)e^{ik_i x^i} . \tag{3.16}$$

3.2 From field fluctuations to observables

3.2.1 The problem of reheating

Now that we have fluctuations to the inflaton field we need to understand how these fluctuations generate perturbations in the energy density of radiation and matter that we observe today. Unfortunately, the process describing the decay of the inflaton scalar field into radiation, known as reheating, is not fully understood. Currently we do not know what particles were initially created or how the energy was transferred from the inflaton to the radiation.

The simplest scenario is one where the scalar field loses energy through oscillations about its minimum. This corresponds to the decay of particles and can be modelled by the following modified continuity equation,

$$\dot{\rho} + (3H + \Gamma)\rho = 0\,, \tag{3.17}$$

where Γ is the particle decay rate. The decay products are relativistic and the energy quickly thermalizes leaving a species with a blackbody distribution and eventually all energy is in a radiation species at thermal equilibrium. One can simplify this even further by assuming this transition happens instantaneously when $T = T_{\rm reh}$, this is known as instantaneous reheating, and is the model we will be using to evaluate the parameters and initial conditions for our scalar fields below. Even when using this model for reheating we must specify by what process the decay happens and give a decay rate. There are also many other scenarios for how the reheating process happened beyond this simplest example. For many more details on reheating and the various options for decay rates see for instance Refs. [37, 38].

Fortunately there is a method we can use which does not rely on the equations for this unknown process, namely, we can proceed by considering conserved quantities. The relative size of a given field fluctuation compared to the Hubble radius $(1/aH)$ is important. As the fluctuations generated initially are quantum fluctuations, they are necessarily created on very small scales (i.e. $k \gg aH$). We call such fluctuations subhorizon. During inflation, the comoving Hubble rate (aH) increases approximately exponentially so the scales of interest will eventually become larger than the comoving Hubble radius (i.e. $k \ll aH$) and we say the scales have "left the

horizon"; the fluctuations are now superhorizon. During the radiation and matter era the comoving Hubble rate decreases and eventually those same scales will satisfy $k \gg aH$ and will cross back inside the horizon again. As the field fluctuations cross the horizon (i.e. when the size of the fluctuations is similar to the size of the Hubble radius, $k = aH$) they continue to evolve, however there are quantities that under certain conditions remain conserved whilst outside the horizon (in the limit $k \to 0$). It is these quantities we will study in the following sections. By mapping the inflaton fluctuation's power spectrum onto the spectrum of one such conserved quantity, we can connect the fluctuations during inflation to the ones we observe at later times. For instance, the spectrum of the conserved quantity (e.g. the curvature perturbation, see below) can be used to set the initial conditions for standard Boltzmann codes see e.g. Ref. [55], that are used to calculate the CMB anisotropies.

3.2.2 Conserved quantities

We focus here on two quantities which are conserved outside the horizon under certain conditions. Firstly the curvature perturbation on uniform density hypersurfaces ζ [56], and secondly the comoving curvature perturbation $\mathcal{R}$ [57]. The curvature perturbation on uniform density hypersurfaces is defined as

$$-\zeta \equiv \psi + \frac{\mathcal{H}}{\rho_0'}\delta\rho\,, \tag{3.18}$$

which simplifies if we evaluate the right hand side in flat gauge to $-\zeta = \frac{\mathcal{H}}{\rho_0'}\delta\rho_{\rm flat}$, where $\delta\rho_{\rm flat}$ was defined in Eq. (2.42). For ease of use we drop the subscript flat in the following. In terms of the scalar field perturbations this is

$$\zeta = \frac{1}{3{\varphi_0'}^2}\left[\varphi_0'\delta\varphi' + \left(U_{,\varphi}a^2 - 3\mathcal{H}\frac{{\varphi_0'}^3}{{\varphi_0'}^2 + 2Ua^2}\right)\delta\varphi\right]\,, \tag{3.19}$$

The comoving curvature perturbation, that is, the curvature perturbation evaluated on comoving or uniform field slices, is defined by

$$\mathcal{R} \equiv \psi + \frac{\mathcal{H}}{\varphi_0'}\delta\varphi\,, \tag{3.20}$$

which simplifies again if the right hand side is evaluated in flat gauge to $\mathcal{R} = \frac{\mathcal{H}}{\varphi_0'}\delta\varphi$. Note that these two gauge-invariant curvature perturbations, defined in different gauges, are related by the constraint equation,

$$k^2\Psi = -9\frac{\mathcal{H}^2{\varphi_0'}^2}{2a^2\rho_0}(\mathcal{R}+\zeta)\,, \tag{3.21}$$

where $\Psi = \psi + \mathcal{H}\sigma_s$ is the curvature perturbation in longitudinal gauge. As can be seen from Eq. (3.21), $\zeta + \mathcal{R}$ will become small on super-horizon scales.

We can determine what conditions are required for these two quantities to be conserved outside the horizon by considering the evolution equation for the curvature perturbation. Firstly note that ζ will be conserved outside the horizon during inflation driven by a single scalar field. To consider the period after inflation note that for $k \ll aH$ we have,

$$\dot{\zeta} = \frac{\dot{\rho}\delta P - \dot{P}\delta\rho}{3(\rho+P)^2}\,. \tag{3.22}$$

Setting the right hand side of this equation equal to zero is equivalent to the adiabatic condition for a fluid,

$$\frac{\delta P}{\dot{P}} = \frac{\delta\rho}{\dot{\rho}}\,, \tag{3.23}$$

implying that after inflation the curvature perturbation is conserved for an adiabatic fluid. Note also that if the pressure can be given as a function of density only ($P = f(\rho)$) then the right hand side of Eq. (3.22) is also zero, even if the fluctuations are not adiabatic, and the curvature perturbation is also conserved.

If the fluid is not adiabatic then there exists a non-adiabatic pressure perturbation, $\delta P_{\rm nad}$. In general this is not directly observable, but is a source term for the evolution of the curvature perturbations, (see Ref. [58]) and therefore will be a quantity we are interested in.

The total pressure perturbation is split into an adiabatic and non-adiabatic part as seen in Ref. [59],

$$\delta P_{\rm nad} = \delta P - c_{\rm s}^2\delta\rho\,, \tag{3.24}$$

where $c_{\rm s}^2$ is the adiabatic speed of sound and is defined as $c_{\rm s}^2 \equiv {P_0}'/{\rho_0}'$. This gives

us an expression for $\delta P_{\rm nad}$ in terms of the scalar field quantities [60],

$$\delta P_{\rm nad} = \left[\frac{U_{,\varphi}}{3\mathcal{H}^2 M_{\rm PL}^2}\varphi_0'^2 - 2U_{,\varphi}\Big(1 + \frac{U_{,\varphi}a^2}{3\mathcal{H}\varphi_0'}\Big)\right]\delta\varphi - \frac{2U_{,\varphi}}{3\mathcal{H}}\delta\varphi' \,. \tag{3.25}$$

This can also be written as

$$\delta P_{\rm nad} = -\frac{2U_{,\varphi}}{3\mathcal{H}}\left[\delta\varphi' + \left(\frac{a^2 U_{,\varphi}}{\varphi_0'} + \frac{6\mathcal{H}Ua^2}{{\varphi_0'}^2 + 2Ua^2}\right)\delta\varphi\right] \,. \tag{3.26}$$

3.2.3 Observables

As mentioned above the conserved quantities can be used to set initial conditions for Boltzmann codes. The results of these codes then allow us to make predictions for the perturbations we see in the CMB. In order to be able to compare our theoretical results more easily with observations, it is often beneficial to present them in terms of power spectra. The power spectrum for ζ, $P_\zeta^2(k_1)$, is defined as [35],

$$\langle\zeta(\mathbf{k}_1)\zeta(\mathbf{k}_2)\rangle \equiv (2\pi)^3\delta(\mathbf{k}_1 + \mathbf{k}_2)P_\zeta^2(k_1) \,, \tag{3.27}$$

where $\langle ...\rangle$ denotes the ensemble average. It is also useful to define a dimensionless power spectrum as,

$$\mathcal{P}_\zeta^2(k) \equiv \frac{k^3}{2\pi^2}P_\zeta^2(k) \,. \tag{3.28}$$

Similarly for $\mathcal{R}$ we can define the power spectrum $P_\mathcal{R}^2(k_1)$ and the dimensionless power spectrum $\mathcal{P}_\mathcal{R}^2(k)$ as,

$$\langle\mathcal{R}(\mathbf{k}_1)\mathcal{R}(\mathbf{k}_2)\rangle \equiv (2\pi)^3\delta(\mathbf{k}_1 + \mathbf{k}_2)P_\mathcal{R}^2(k_1) \,, \tag{3.29}$$

and

$$\mathcal{P}_\mathcal{R}^2(k) \equiv \frac{k^3}{2\pi^2}P_\mathcal{R}^2(k) \,. \tag{3.30}$$

Both types of curvature perturbation can be used to describe the scalar field perturbation, however, we potentially also have tensor perturbations being produced in the early universe. In the same way as above we can define a tensor power spectrum given by $\mathcal{P}_T^2(k)$ and then define another observational parameter (r) to

describe the ratio between the scalar and tensor power spectra,

$$r \equiv \frac{\mathcal{P}_T^2(k)}{\mathcal{P}_\mathcal{R}^2(k)} \,. \tag{3.31}$$

We expect the power to be dominated by the scalar perturbations and therefore we expect r to be small. The current upper limit provided by PLANCK is $r < 0.11$ [8] whereas BICEP find $r = 0.20^{+0.07}_{-0.05}$ with $r = 0$ disfavored at 7.0σ. However, it is likely that when the contribution of foreground dust is accounted for this value for r will decrease by an amount yet to be determined, possibly bringing this in line with the PLANCK result [61].

One of the predictions of inflation is a near scale invariant spectrum. In order to parametrise how close to scale invariance our observations are we define the spectral index, n_s, as

$$n_s - 1 = \frac{d}{d\mathrm{lnk}} \ln\left(\mathcal{P}_\mathcal{R}^2(\mathrm{k})\right) \,, \tag{3.32}$$

such that $n_s = 1$ implies scale invariance. This allows us to write the dimensionless power spectra as

$$\mathcal{P}_\mathcal{R}^2(k) = \Delta_\mathcal{R}(k_0)^2 \left(\frac{k}{k_0}\right)^{n_s - 1} \,, \tag{3.33}$$

where $\Delta_\mathcal{R}(k_0)^2$ is the amplitude of the power spectrum evaluated at an arbitrary pivot scale (k_0). Current observations from WMAP give $\Delta_\mathcal{R}(k_0)^2 = 2.38 \times 10^{-9}$ [7] with a pivot scale of $k_0 = 0.002\mathrm{Mpc}^{-1}$, and observations from PLANCK gives $n_s = 0.9616 \pm 0.00094$ (68%) [8].

If the dependence on k is more complicated than just a simple power law, we can introduce a second parameter to explain this dependence, the running (α_s),

$$\alpha_s = \frac{d}{d\ln k} n_s \,. \tag{3.34}$$

The current best observations from PLANCK suggest that $\alpha_s = -0.013 \pm 0.009$ (68%) [8]

3.3 Around Horizon crossing

3.3.1 Motivation

In Section 3.2.1 we only considered the two limiting cases $k \ll aH$ and $k \gg aH$. As outlined above it is well known that for adiabatic perturbations the curvature perturbations on both uniform density hypersurfaces, ζ, and on comoving hypersurfaces, $\mathcal{R}$, are conserved on large scales where gradient terms can be neglected (i.e. in the limiting case where $k \ll aH$ and $k \to 0$) [56, 57]. This result follows from the conservation of energy [58] and the evolution equation for the curvature perturbation given in Eq. (3.22).

The standard approach used to calculate the power spectrum of perturbations after horizon crossing assumes that the limit $k \to 0$ has been reached, see Ref. [62]. However, immediately after horizon crossing, the wavenumber will not yet have become sufficiently small for this limit to be accurate and gradient terms may still play a role. In fact, in single field inflation there will still be some residual non-adiabatic pressure perturbation, $\delta P_{\rm nad}$, present [63]. Then, even in the absence of other sources of $\delta P_{\rm nad}$, the curvature perturbation will continue to evolve for some number of e-folds before settling down to its value at the end of inflation. Although it is known that this evolution continues for a short time after horizon crossing, the exact amount of evolution has not been quantified. Exactly how long the evolution will last and how much the magnitude of the power spectrum of ζ may vary in that time are issues which are yet to be addressed in the literature.

This is particularly important as observational cosmology is entering an era in which the data from observations of LSS and the CMB are becoming much more precise. Only eight years ago, the WMAP team were quoting cosmological parameters to an accuracy of about 10% [64]. Now, as data sets are improving both in quality and size, the WMAP seven year observations (hereafter WMAP7) can constrain these parameters to within a couple of percent [6] and PLANCK can do even better. Hence it is essential that the quantities we wish to study in the early universe are understood theoretically to this same level of precision.

Much work has been done calculating the power spectra for the curvature perturbations, ζ and $\mathcal{R}$, during inflation (see for example Refs. [65–70] and the reviews,

Refs. [71, 72]). Analytic studies have to rely on either the slow roll limit, or large scale approximations, to make the calculations viable. In these limits, and without anisotropic stress, the two definitions for the curvature perturbations are equal up to a sign difference, see e.g. Ref. [9].

In the rest of this chapter we will be looking at these conserved quantities in greater detail. Specifically we will quantify the evolution of the curvature perturbation shortly before, during and after horizon crossing by considering the following questions:

- How do ζ and $\mathcal{R}$ differ around horizon crossing?
- How much do the instantaneous horizon crossing values differ from the values at the end of inflation?
- How long does it take for the quantities to reach these final values?

As we do not want to rely on the slow roll approximation or the large scale limit, we will be solving the Klein-Gordon equations numerically. However, first we will consider some of the analytic approximations which are used.

3.3.2 Analytic Solutions

Using numerical techniques we can evaluate the expressions for the curvature perturbation at any time whereas analytically this is not possible. To deduce an analytic expression for the curvature perturbation, such as that used in the popular δN formalism, we start from the definition [35]

$$\mathcal{P}_{\mathcal{R}}(k) = \frac{k^3}{2\pi^2} \left|\mathcal{R}\right|^2 . \tag{3.35}$$

By obtaining an exact solution for power-law inflation and taking the $k \to 0$ limit, and then making an expansion about this solution, we arrive at the following expression [71],

$$\mathcal{P}_{\mathcal{R}}(k)_{\text{est2}*} = [1 - (2C+1)\epsilon_{SR} + C\eta_{\text{SR}}]^2 \frac{a^2 H^4}{(2\pi)^2 {\varphi_0'}^2}\Big|_{k=aH} , \tag{3.36}$$

where $C = -2 + \ln 2 + \gamma$ and γ is the Euler constant and ϵ_{SR} and η_{SR} are slow roll parameters defined in Eq. (1.53) and Eq. (1.55).

The expression given in Eq. (3.36) is only valid in the large scale limit, or equivalently a long time after horizon exit. However, it must be evaluated exactly when the corresponding mode crosses the horizon. In order to arrive at an expression which is valid at all times, we would need to consider the full analytic solution, including logarithmic corrections, as considered to some extent in Ref. [73]. We shall return to this subject in Section 3.4.4.

The above result holds, to the lowest order in slow roll, for any general potential and if the slow roll parameters are assumed to be very small this simplifies to

$$\mathcal{P}_{\mathcal{R}}(k)_{\mathrm{est1}*} = \left.\frac{a^2H^4}{(2\pi)^2{\varphi_0'}^2}\right|_{k=aH}. \tag{3.37}$$

In Eq. (3.37) and Eq. (3.36) above we have used subscript est$*$ to denote that the power spectrum has been calculated analytically, using horizon crossing values. The subscript est2$*$ denotes the full solution to lowest order in slow roll, whilst subscript est1$*$ denotes an approximation to this solution which holds when the slow roll parameters are very small.

It is important to recognise that the analytic solution is derived using the $k \to 0$ limit but is evaluated using quantities at horizon crossing. Although this has been known in the literature for many years it is not often made clear when this mixing of late time solution and horizon crossing values is being used. Here we highlight the large magnitude of the inaccuracies which would result if a naïve calculation of the power spectrum at horizon crossing is performed using horizon crossing values.

For further discussions on the analytic treatment of curvature perturbations close to Horizon crossing, we refer to Ref. [74, 75]

3.3.3 Numerical Setup

As mentioned above instead of relying on the analytic approximations we can solve the system numerically and in doing so we are following the work done by Salopek et al. [50], and use a Runge-Kutta code written in Fortran. Following Ref. [50] we set the initial conditions for each k mode a few e-folds before horizon crossing when

the initial time $\mathcal{N}_{\rm init}(k)$ is such that

$$\frac{k}{aH|_{\rm init}} = 50\,. \tag{3.38}$$

This allows us to assume the Bunch-Davies vacuum (see Section 3.1.1) and therefore have initial conditions described by Eq. (3.11) for modes well inside the horizon. The linear scalar field perturbations are evolved from this initial state well inside the horizon until the inflationary expansion ends.

Most of the results we present here use single field chaotic inflation, the simplest single field inflation model which is in agreement with WMAP7 and Planck. In order to ensure that our results are representative beyond this simplest model, we also study a set of more complicated cannonical single field models, $U = U_0 + \frac{1}{2}m^2\varphi^2$, $U = \frac{1}{4}\lambda\varphi^4$ and $U = \sigma\varphi^{2/3}$. The parameters for the background system are selected depending on the choice of potential:

- $U = \frac{1}{2}m^2\varphi^2$, $m = 6.32$ x $10^{-6}M_{\rm PL}$
- $U = \frac{1}{4}\lambda\varphi^4$, $\lambda = 1.55 \times 10^{-13}$
- $U = U_0 + \frac{1}{2}m^2\varphi^2$, $m_0 = 1.74 \times 10^{-6}M_{\rm PL}$. $U_0 = 5 \times 10^{-10}M_{\rm PL}^4$
- $U = \sigma\varphi^{2/3}$, $\sigma = 3.82 \times 10^{-10}M_{\rm PL}^{10/3}$

The mass values have been chosen such that $\mathcal{P}_{\mathcal{R}}(k) = 2.45$ x 10^{-9} at the end of inflation for the Wmap pivot scale. The initial conditions for ϕ_0 and $\phi_0^\dagger$ are again chosen depending on the choice of potential, so that the k modes which will be calculated begin well inside the horizon, for instance the initial conditions for chaotic inflation are set as $\varphi_0 = 18M_{\rm PL}$ and $\varphi_{0,\mathcal{N}} = -0.1M_{\rm PL}$. We are using parameters and initial conditions specified in Ref. [51, 52].

We select a finite range of k modes which cover all the modes which have been observed in the CMB. The Wmap team have released results corresponding to the range $k \in [3.5\text{x}10^{-4}, 0.12]\text{Mpc}^{-1}$, we will consider a similar range below. We use the number of e-folds, $\mathcal{N} = \log(a/a_{\rm init})$, defined in Eq. (1.44) as our time variable instead of conformal time where $a_{\rm init}$, the value of a at the start of inflation, is evaluated by setting $a = 1$ today and using the background run, assuming instantaneous reheating.

The behaviour of all the modes over the scales we consider are similar, so for clarity only k_1, k_2 and k_3 modes, given below, have been shown in the graphs that follow, where:

$$k_1 = 2.77 \text{ x } 10^{-5}\text{Mpc}^{-1} = 7.28 \text{ x } 10^{-62} M_{\rm PL} \tag{3.39}$$

$$k_2 = 2.00 \text{ x } 10^{-3}\text{Mpc}^{-1} = 5.25 \text{ x } 10^{-60} M_{\rm PL} \quad (\text{WMAP pivot}) \tag{3.40}$$

$$k_3 = 1.45 \text{ x } 10^{-1}\text{Mpc}^{-1} = 3.80 \text{ x } 10^{-58} M_{\rm PL}\,. \tag{3.41}$$

It is worth noting that k_2 is the WMAP pivot scale. We compare these numerical results with the standard analytic solutions for single field inflation. All the numerical results presented below have been verified with a second independent numerical program to ensure their accuracy, see Ref. [76].

3.4 Results

In this section we present our results which attempt to answer the questions presented above. We quantify the difference between ζ and $\mathcal{R}$, the magnitude of error incurred if we would use Eq. (3.35) evaluated at horizon crossing instead of Eq. (3.36), and the length of time taken for the power spectra to settle to their values at the end of inflation. The results presented in the graphs below are for the potential $U = \frac{1}{2}m^2\varphi^2$.

To start we consider the evolution of the power spectra in general. The evolution, and indeed conservation, of the curvature perturbations has been studied in detail in the past, see Ref. [56–58, 77] and, as expected, we find that some time shortly after horizon crossing there is no longer any appreciable evolution in either the power spectrum of ζ, $\mathcal{P}_\zeta(k)$ or the power spectrum of $\mathcal{R}$, $\mathcal{P}_\mathcal{R}(k)$, see Fig. 3.1. The values of these power spectra converge very quickly onto the same conserved value. This behaviour is also supported by the graph in Fig. 3.2 which shows the non-adiabatic pressure perturbation, $\delta P_{\rm nad}$. We find, again as expected, that during and after horizon crossing the size of $\delta P_{\rm nad}$ drops sharply towards zero. The non-adiabatic pressure perturbation is directly related to the curvature perturbation (on large scales), see Ref. [58, 77],

$$\zeta' \propto \delta P_{\rm nad}\,, \tag{3.42}$$

and hence the rapid decrease in the non-adiabatic pressure perturbation causes the curvature perturbations to settle onto a conserved value.

However, it can also be seen from Fig. 3.1 that there is some evolution of the power spectra immediately after horizon crossing. As already stated this is well known in the literature where the phrase 'soon after horizon crossing' is commonly used to refer to the time at which the power spectra have settled down. In the sections that follow we will be looking at this evolution in more detail and in particular quantifying exactly how soon after horizon crossing the power spectra reach their final value and how different this is to the horizon crossing values.

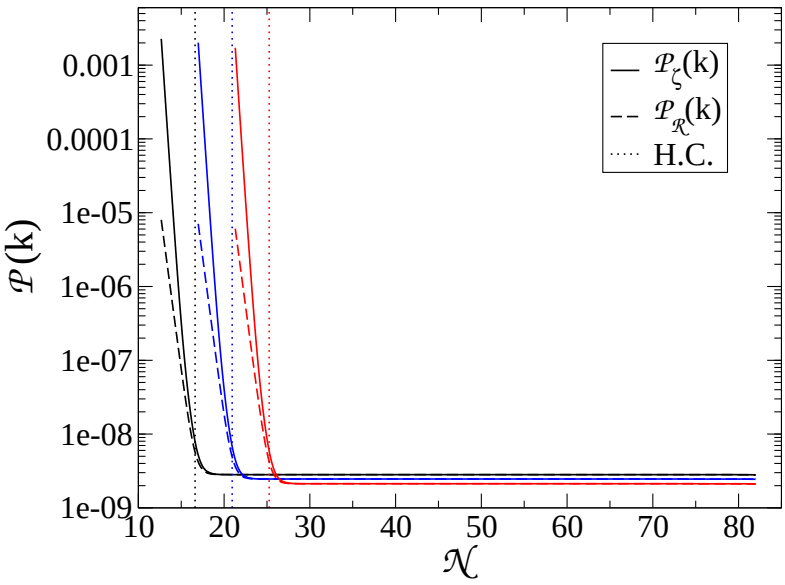

Figure 3.1: The evolution of the power spectrum of ζ, $\mathcal{P}_\zeta(k)$ and $\mathcal{R}$, $\mathcal{P}_\mathcal{R}(k)$ is plotted against the number of e-folds, $\mathcal{N}$. Both power spectra stop evolving shortly after horizon crossing (H.C.), however a short period of evolution immediately after horizon crossing is visible as is a difference between $\mathcal{P}_\zeta(k)$ and $\mathcal{P}_\mathcal{R}(k)$. The line H.C. marks the point at which each scale will cross the Horizon, i.e. when $k = aH$. (Black line, left: k_1, Blue line, middle: k_2, Red line, right: k_3)

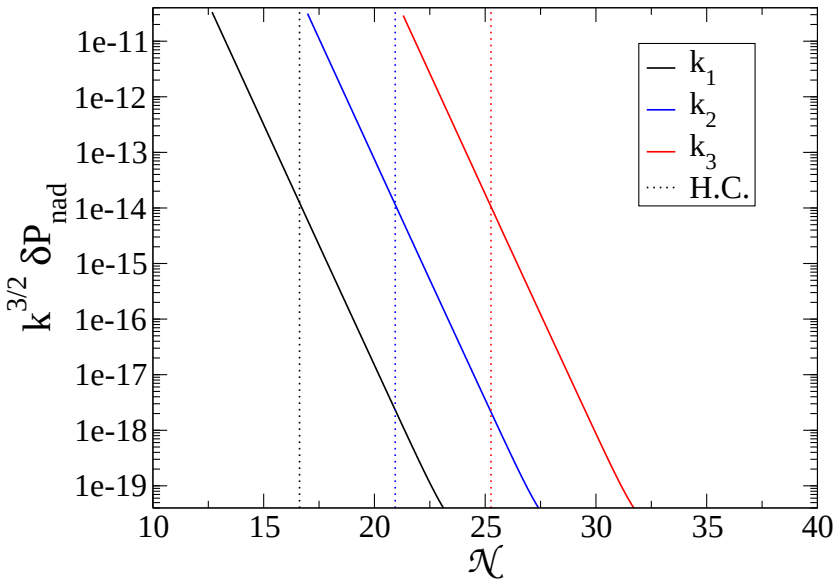

Figure 3.2: The evolution of $\delta P_{\rm nad}$ is plotted against the number of e-folds, $\mathcal{N}$. $\delta P_{\rm nad}$ rapidly drops towards zero after horizon crossing. We apply a cut off to the graph at 10^{-20}, beneath which numerical noise dominates. (Black line, left: k_1, Blue line, middle: k_2, Red line, right: k_3)

3.4.1 How do ζ and $\mathcal{R}$ differ?

ζ and $\mathcal{R}$ are often used interchangeably. Although they have different definitions, see Eq. (3.18) and Eq. (3.20), it is well known that on large scales they are equivalent, as can be seen from Eq. (3.21). This equivalence is however only strictly true in the large scale limit, and on smaller, finite scales this is not the case. In Fig. 3.1 we see that there is a difference between the two curvature perturbations near to horizon crossing. Three different k-modes are plotted throughout their evolution, from deep within the horizon through horizon crossing (indicated by the dotted lines), until the end of inflation.

Fig. 3.3 shows that ζ is as much as 20% larger than $\mathcal{R}$ at horizon crossing and remains significantly larger for at least a couple of e-folds. This highlights the importance of making explicit the choice of curvature perturbation when carrying out calculations close to horizon crossing. We also note that ζ and $\mathcal{R}$ take slightly dif-

ferent amounts of time to settle down after horizon exit, as detailed in Section 3.4.3.

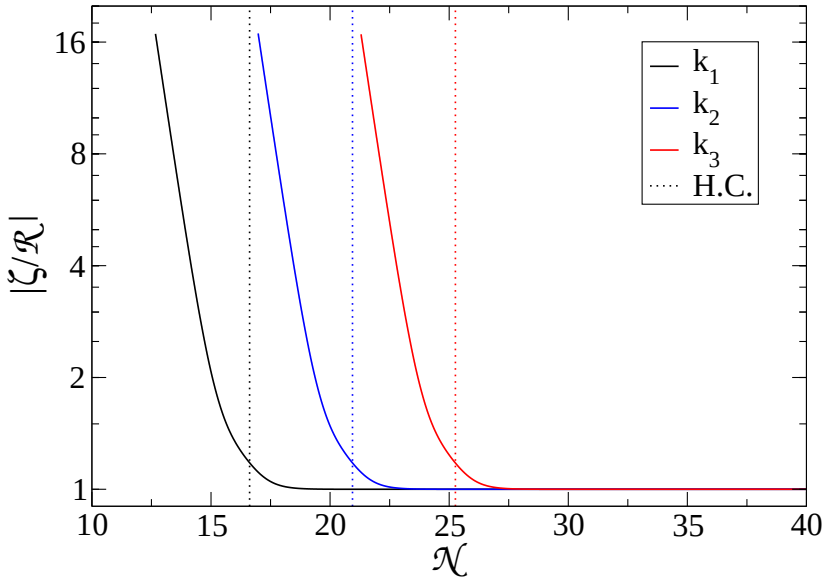

Figure 3.3: The ratio of ζ and $\mathcal{R}$ is plotted against the number of e-folds, $\mathcal{N}$. Evolution is visible for a short period after horizon crossing, during which time ζ is noticeably larger than $\mathcal{R}$.(Black line, left: k_1, Blue line, middle: k_2, Red line, right: k_3)

3.4.2 What is the difference between instantaneous horizon crossing values and values at the end of inflation?

As mentioned above it is well known that the values of the curvature perturbation power spectra are not the same at horizon crossing as they are at the end of inflation. However, it is not clear exactly how much of an error would be incurred if one would use the horizon crossing values instead of the correct values at the end of inflation. In Fig. 3.4 we can see exactly how different the power spectra are at horizon crossing compared to the values they take at the end of inflation. In Fig. 3.4(a) $\mathcal{P}_{\mathcal{R}}(k)$ is 100% larger at horizon crossing and in Fig. 3.4(b) $\mathcal{P}_{\zeta}(k)$ is 180% larger. In fact if we use an analytic approximation that does take into account this behaviour we can

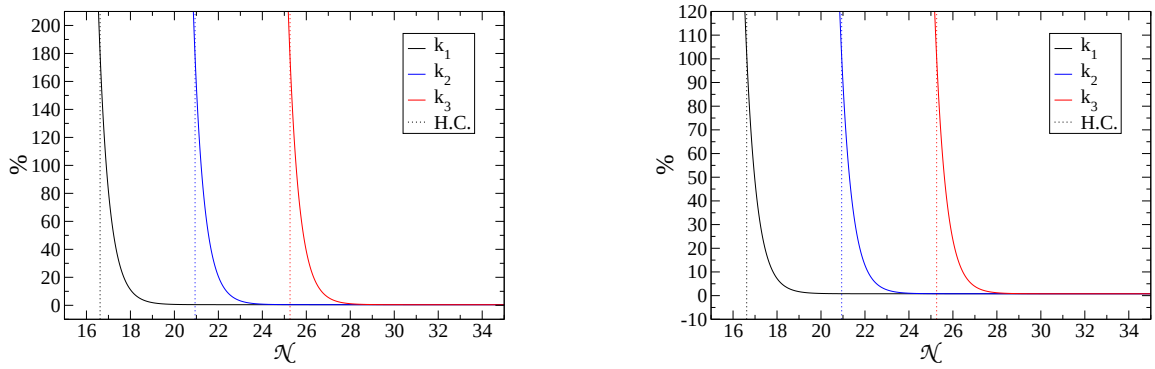

(a) $\mathcal{P}_\zeta(k)$ (b) $\mathcal{P}_\mathcal{R}(k)$

Figure 3.4: The percentage difference between $\mathcal{P}(k)$ evaluated, numerically, at the end of inflation and the $\mathcal{P}(k)$ obtained at each time step. There is as much as 180% difference in the values of $\mathcal{P}_\zeta(k)$ and 100% difference in the values of $\mathcal{P}_\mathcal{R}(k)$. Both the graphs above are plotted for three different k modes. The black line (left) is k_1, the blue line (middle) is k_2, the WMAP pivot scale, and the red line (right) is k_3.

see the 100% difference in the power spectra. Near horizon crossing the scalar field's wavefunction (ψ) is approximately proportional to $(1-ik\eta)e^{ik\eta}$. At horizon crossing $|k\eta| = 1$ and $|\psi|^2 \propto |1 - ik\eta| = 2$. A few e-folds later, $|k\eta| \approx 0$ and $|\psi|^2 \propto |1| = 1$. This is a drop of 1. Hence the power spectra at horizon crossing is expected to be roughly 100% larger than that at late times. The factor of two difference in $\mathcal{P}_\mathcal{R}(k)$, has previously been found analytically, see for example Ref. [53, 75] This is, however, a large difference and might impact on calculations if $\mathcal{P}(k)_{k=aH}$ is used to approximate the value of the power spectra at the end of inflation.

3.4.3 How quickly does the power spectra reach its final value at the end of inflation?

The expressions "soon after horizon crossing" and "a few e-folds after horizon crossing" are often used in the literature to determine when it is reasonable to evaluate the power spectra, so that one can be confident that they have the same value as at the end of inflation. Now that we have established that the values at horizon

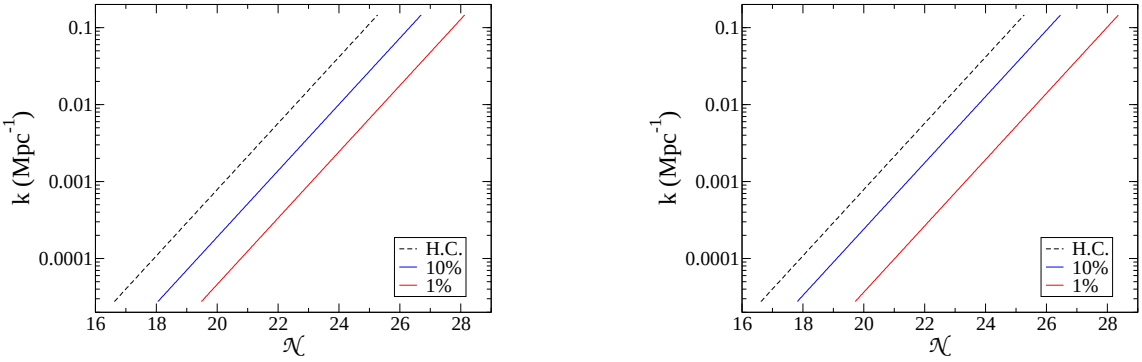

(a) $\mathcal{P}_\zeta(k)$ (b) $\mathcal{P}_\mathcal{R}(k)$

Figure 3.5: These graphs show how many e-folds one needs to wait for $\mathcal{P}(k)$ to be within 10% and 1% of $\mathcal{P}(k)$ at the end of inflation for a given value of k (measured in Mpc^{-1}). Note that this is independent of k. Table 3.1 gives the exact number of e-folds for various potentials.

crossing can be as much as 180% greater than those at the end of inflation we can study exactly how long after horizon crossing we must wait until the power spectra converge onto these final values. Fig. 3.5 shows how many e-folds one needs to wait for the power spectra to be within 10% and 1% of the value they have at the end of inflation. It is clear from these graphs that this is independent of k and is in the region of "a few e-folds". Table 3.1 shows the number of e-folds it takes to be within a fixed percentage of the final value, and also shows data for the three additional potentials we investigated. The choice of potential makes little difference to the result. For every potential considered it took 1.40 – 1.44 e-folds for $\mathcal{P}_\zeta(k)$ to be within 10% and 2.56 – 2.86 to be within 1%. It took 1.14 – 1.20 e-folds for $\mathcal{P}_\mathcal{R}(k)$ to be within 10% and 2.30 – 3.21 e-folds to be within 1%. As we highlighted in Section 3.1 observational data will soon be constraining observables to within a percent, so this is at least the accuracy we would like to be able to evaluate quantities to. Our results show that to be within 1% of the correct power spectra value at the end of inflation, evaluating $\mathcal{P}_\mathcal{R}(k)$ approximately 3.2 e-folds after horizon crossing and evaluating $\mathcal{P}_\zeta$ 2.9 e-folds after horizon crossing, would be sufficient, for all the potentials we studied.

	ζ				$\mathcal{R}$			
	10%	5%	3%	1%	10%	5%	3%	1%
$\frac{1}{2}m^2\varphi^2$	1.43	1.80	2.09	2.86	1.20	1.59	1.91	3.10
$U_0 + \frac{1}{2}m^2\varphi^2$	1.40	1.75	2.01	2.56	1.14	1.49	1.75	2.30
$\frac{1}{4}\lambda\varphi^4$	1.44	1.80	2.08	2.77	1.18	1.55	1.84	2.59
$\sigma\varphi^{2/3}$	1.41	1.77	2.05	2.74	1.20	1.61	1.98	3.21

Table 3.1: The values in this table represent how many e-folds after horizon crossing it takes for the power spectrum to be within a fixed percentage of the power spectrum at the end of inflation.

3.4.4 Comparing analytic and numeric results

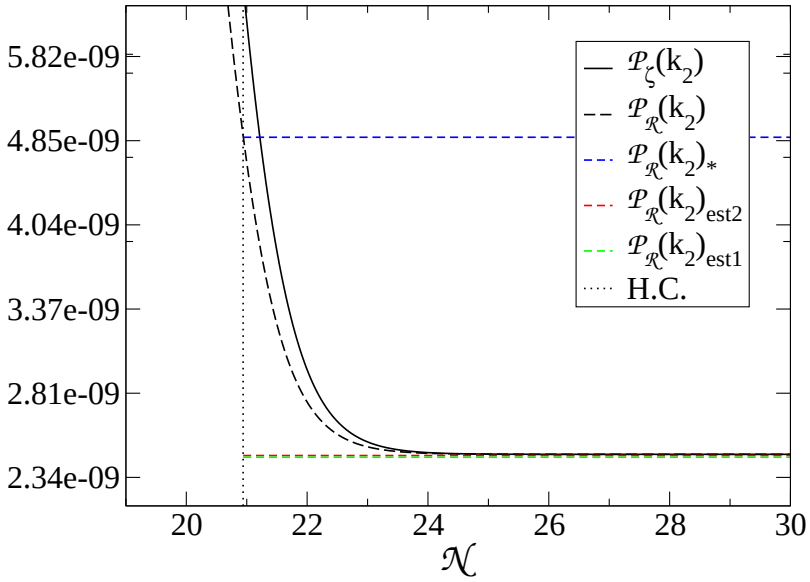

Figure 3.6: The evolution of the power spectrum of ζ, $\mathcal{P}_\zeta(k)$ and $\mathcal{R}$, $\mathcal{P}_\mathcal{R}(k)$ is plotted against the number of e-folds, $\mathcal{N}$ for the mode k_2. The dotted lines show the correct analytic solution with and without slow roll corrections, defined in Eq. (3.36) and Eq. (3.37), and the naïve approximation of evaluating the power spectra at horizon crossing.

In Fig. 3.6 and Fig. 3.7 the evolution of the two types of curvature perturbation,

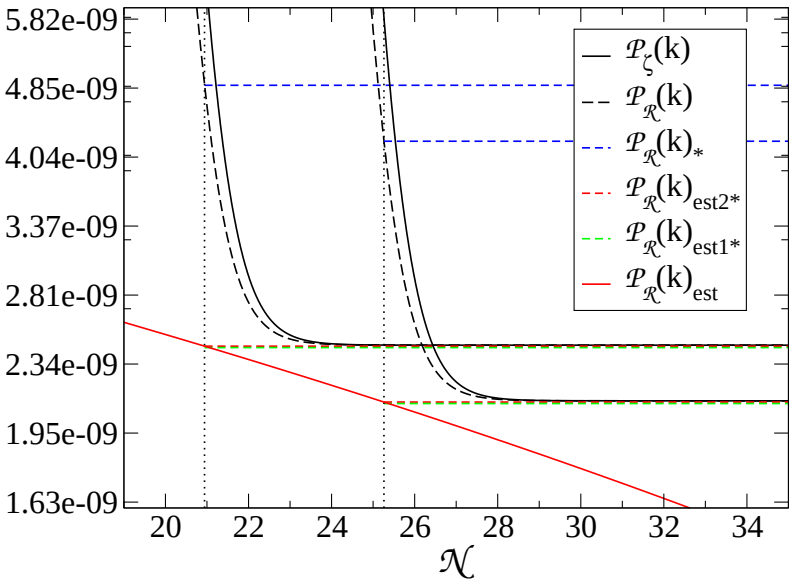

Figure 3.7: The graph shows the same information as Fig. 3.6 but this time for the mode k_2 which is the WMAP pivot scale (left hand lines) and the mode k_3 (right hand lines).

$\mathcal{P}_\mathcal{R}(k)$ and $\mathcal{P}_\zeta(k)$ are plotted against the number of e-folds, $\mathcal{N}$. These numerical solutions are compared to the correct analytic solution with and without slow roll corrections, Eq. (3.36) and Eq. (3.37), and the naïve approximation of evaluating the power spectra at horizon crossing.

In most analytic calculations an expression for the power spectrum is derived using the $k \to 0$ limit but is evaluated using quantities at horizon crossing, as given in Eq. (3.36). As we mentioned in Section 3.3.1, it is often not made explicitly clear in the literature when the mixing of late time solution and horizon crossing values is being used, even when this is well understood by the authors. In Fig. 3.6 we compare both this correct analytic solution and the naïve calculation of the power spectrum at horizon crossing performed using horizon crossing values with the numerical solutions. In Fig. 3.6, as expected, the correct analytic solution gives a very good estimate to the full numerical solution. Even the analytic solution without the slow roll correction, given in Eq. (3.37), is a very good estimate to

the full solution. In fact the error in not including the slow roll corrections for the WMAP scale is only a slight underestimate of -0.38%. However, when we compare the numerical solution to $\mathcal{P}_{\mathcal{R}}(k)$ evaluated at horizon crossing we find, as shown in Fig. 3.4(a), that there is a 100% error in our answer. As we have shown earlier in Fig. 3.4(b), if we evaluated the $\mathcal{P}_{\zeta}(k)$ at horizon crossing the error would be even higher at 180%. This difference in the two power spectra can be seen clearly in Fig. 3.6. This again highlights the importance of establishing that the correct analytic expression is used in calculations, and also when different calculations and results are compared.

Another possible source of error would be to use the analytic expression given in Eq. (3.36) above, but not to evaluate it at horizon crossing. If one were to evaluate this expression 'some e-folds after horizon crossing', one would underestimate the amplitude of the power spectrum. This corresponds to following the red line in Fig. 3.7. For example, evaluating Eq. (3.36) four e-folds after horizon crossing would incur an error of 15%. Furthermore, evaluating the power spectrum at later and later times will increase the error. Lastly, it is worth noting that although the analytic and numerical expressions agree in the large scale limit, they do not agree with each other shortly after horizon crossing. As shown in the section above one must wait at least 3.2 e-folds for these two values to agree. This is particularly important if there is a second phase of evolution caused for example by a second scalar field which starts to dominate during these three e-folds, see for instance Ref. [74].

3.4.5 The Spectral Index

Using observations we can gain information about the power spectrum of curvature perturbations, which in turn allows us to constrain cosmological theories. Many observational results are given in terms of a few observables which can then be compared directly with predictions given by theories. One such observable is the spectral index. This describes the scale dependence of the power spectrum of the curvature perturbation. The spectral index for ζ and $\mathcal{R}$ are defined by [35]

$$n_{\zeta} - 1 \equiv \frac{d\ln\mathcal{P}_{\zeta}(\mathrm{k})}{d\ln\mathrm{k}}\,, \qquad n_{\mathcal{R}} - 1 \equiv \frac{d\ln\mathcal{P}_{\mathcal{R}}(\mathrm{k})}{d\ln\mathrm{k}}\,. \tag{3.43}$$

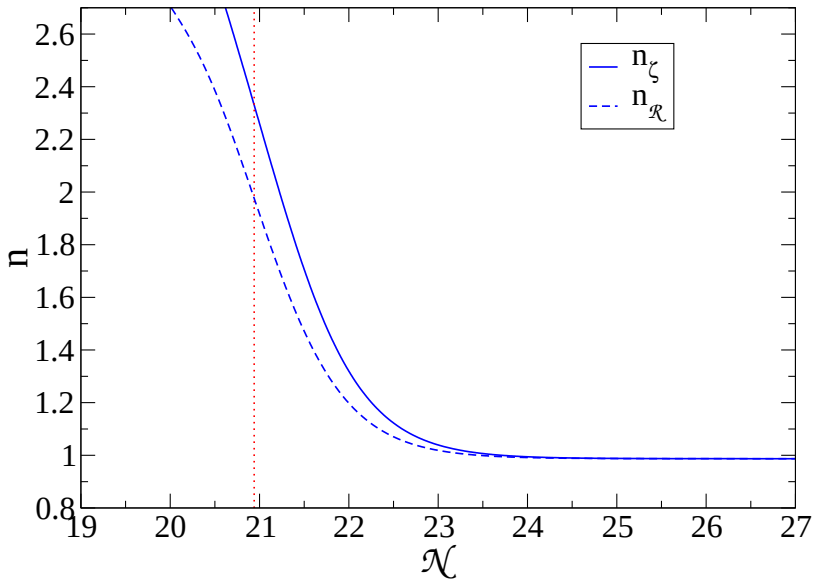

Figure 3.8: The evolution of the spectral index for the two curvature perturbations, $n_{\mathcal{R}}$ and n_ζ, are plotted against the number of e-folds, $\mathcal{N}$. The lines in this graph are shown for the mode k_2 which is the WMAP pivot scale.

As an example of how the results presented in this paper will impact on particular observables we consider the spectral index in more detail presenting results using chaotic inflation. Figure 3.8 shows, as expected, that just like the curvature perturbation the spectral index continues to evolve for a few e-folds after the mode has crossed outside the horizon. Evaluating the spectral index naively at horizon crossing gives a results of $n_{\mathcal{R}} \approx 2$ and $n_\zeta \approx 2.3$, which is an error in both cases of more than 100%. We find that in order for n_ζ and $n_{\mathcal{R}}$ to be within 1% of their values at the end of inflation, we should evaluate them at least 2.91 and 2.66 e-folds after horizon crossing, respectively. These values are similar but slightly less than the number of e-folds it takes for the power spectrum to be within 1% of it's final value, (see Table 1).

3.5 Discussion

In this chapter we have studied the evolution of the curvature perturbations after inflation in detail and highlighted where possible errors may arise. As we are entering an era where we can hope to constrain cosmological parameters to within a percent using the observational data from e.g. PLANCK, it is of particular importance that these errors are both quantified and minimised.

After presenting the evolution equations for the scalar field, we gave the expressions for the curvature perturbations we consider. We then outlined the numerical methods used to solve these equations and gave details of the various models and the initial conditions used. In presenting our results, we found that despite ζ and $\mathcal{R}$ being equivalent very far outside the horizon, the difference between $|\mathcal{R}|$ and $|\zeta|$ at horizon crossing can be as much as 20%. We also found the error in evaluating the power spectra numerically at horizon crossing instead of either using the correct analytic expression or the full numerical solution at late times can be as much as 180% for $\mathcal{P}_\zeta(k)$ and 100% for $\mathcal{P}_\mathcal{R}$. Lastly, we showed that if one wanted to evaluate the power spectra without the use of the analytic expression Eq. (3.36), one would need to wait at least 3.2 e-folds to ensure the answer for $\mathcal{P}_\mathcal{R}(k)$ is correct to within 1% of the value at the end of inflation, and one would need to wait at least 2.9 e-folds to ensure the answer for P_ζ is correct to within 1%. There was no significant difference to these results when we considered the three additional single field models presented at the end of Section 3.3.3.

We emphasise that there is a difference between analytic and numerical expressions close to the horizon. The numerical results are the instantaneous values of the power spectrum and spectral index at horizon crossing, not the expected late time values. These instantaneous results, while not of observational significance, are useful in many ways, including providing initial conditions for other analytical or numerical schemes which operate purely outside the horizon. Firstly, if we are interested in the late time values we should not take the 'naïve' numerical approach of evaluating these at horizon crossing. Unlike the case when using the analytic expressions these results will not be close to the correct answer. Secondly, if we are interested in the instantaneous values at or close to horizon crossing, for instance when developing codes which rely on this information, the normal analytic expres-

sions will not give the correct answers as they are no longer valid and one needs to use numerical methods.

In this chapter we have only studied single field inflation models, in which the non-adiabatic pressure decays rapidly, see Fig. 3.2. This is no longer the case in multi-field systems, as a recent work, Ref. [78] has detailed. It will be interesting to repeat our analysis for more complicated models where superhorizon evolution of the curvature perturbation is expected. This would include, multi-field inflation or "ultra slow roll inflation", see for instance Ref. [68, 74]. Since in this thesis we focus on the single field case, we postpone a study of these cases to future work.

We have chosen the end of inflation as a natural end point of our calculations. After the end of inflation the inflaton is assumed to decay into the standard matter fields during reheating, the detailed mechanism of which is as yet unclear. Also, after reheating we have a multi-fluid system, and hence automatically $\delta P_{\rm nad} \neq 0$ [79], which means that the curvature perturbations are no longer conserved (on any scale). Consequently the values at the end of reheating may no longer be the same as those at the end of inflation.

In conclusion, we have highlighted the fact that the different curvature perturbations do evolve differently immediately after horizon exit. Confusion between the different curvature perturbations can introduce additional errors when comparing theoretical results with observations, which however can easily be avoided, if the correct choice of curvature perturbation is made.

Chapter 4

Multi-fluid perturbation theory

In the first part of this thesis we have been concentrating on single fluid linear perturbation theory. In this chapter we will be looking in detail at the more realistic scenario where we have more than one type of matter in the universe, whilst still working at linear order. This is an area which has been covered in detail in previous literature, see for instance Ref. [80] and references therein. We start by revisiting the formalism needed and then look at a three fluid system of protons, electron and photons, moving in a background electromagnetic fields in the radiation era. This allows us to review the background to the derivation of Eqs. **??**, which appear in one form or another in many papers concerned with primordial magnetogenesis. We will then be analytically solving the system of equations to find an approximation for the electric field strength we can expect in such a scenario.

4.1 Multi-species equations

We start by repeating the derivation of the conservation equations from Section 2.4.2 but this time with multiple matter species present, in addition to the terms we had before we will now have some interaction terms between the species. We treat each species as a fluid and each fluid (α) has stress-energy tensor [80],

$$T_{(\alpha)\mu\nu} = (\rho_{(\alpha)} + P_{(\alpha)})u_{(\alpha)\mu}u_{(\alpha)\nu} + P_{(\alpha)}g_{\mu\nu} + \pi_{(\alpha)\mu\nu}\,, \tag{4.1}$$

where the anisotropic stress tensor, $\pi_{(\alpha)\mu\nu}$, has again no time component and can be separated into scalar, vector and tensor parts as follows [80],

$$\pi^i_j = \Pi_{,}{}^{i}{}_{j} - \frac{1}{3}\nabla^2\Pi\delta^i_j + \frac{1}{2}(\pi^i{}_{,j} + \pi_{j,}{}^{i}) + \pi^i{}_{j}\,. \tag{4.2}$$

Note that the total energy density, pressure and anisotropic stress of the system are given by the sum of the relative quantities for the individual species, i.e.

$$\rho = \sum_\alpha \rho_\alpha\,, \quad P = \sum_\alpha P_\alpha\,, \quad \pi_{\mu\nu} = \sum_\alpha \pi_{(\alpha)\mu\nu}\,, \tag{4.3}$$

and the overall velocity is given by,

$$(\rho + P)V_{1i} = \sum_\alpha (\rho_{(\alpha)} + P_{(\alpha)})V_{1i(\alpha)}\,. \tag{4.4}$$

Here and for the rest of this chapter, to simplify our equations, we have dropped the subscript 0 for background quantities, from this point on any quantity without a subscript should be considered a background quantity. Although the energy and momentum for the system as a whole is conserved this is no longer true for the individual species, which can exchange energy and momentum with one another. We therefore equate the covariant derivative of the stress-energy tensor of the individual fluids to the stress-energy transfer vector,

$$T_{(\alpha)}{}^{\mu}{}_{\nu;\mu} = Q_{(\alpha)\nu}\,, \tag{4.5}$$

where the sum of the stress-energy transfer vector over all species in the system is zero,

$$\sum_\alpha Q_{(\alpha)\nu} = 0\,, \tag{4.6}$$

and the individual stress-energy transfer vector for each species is given by,

$$Q_{(\alpha)0} = -aQ_{(\alpha)}(1+\phi_1) - a\delta Q_{1(\alpha)}\,, \tag{4.7}$$

$$Q_{(\alpha)i} = af_{1(\alpha)i} + aQ_{(\alpha)}(v_{1i} + B_{1i})\,. \tag{4.8}$$

$Q_{(\alpha)} + \delta Q_{1(\alpha)}$ represents the energy transfer to species α and $f_{1(\alpha)i}$ represents the momentum transfer to the species α. The energy transfer to species α, i.e. $Q_{(\alpha)}$, can be split up into a sum of the energy transfer to species α from each other species in the system,

$$Q_{1(\alpha)} = \sum_{(\gamma)} Q_{1(\alpha r)} \,, \tag{4.9}$$

where $Q_{1(\alpha r)}$ is the energy transfer from species r to species α. In the same way the momentum transfer to species α can also be split into a sum over the momentum transfer to species α from each other species in the system,

$$f_{1(\alpha)i} = \sum_{(\gamma)} f_{1(\alpha r)i} \,, \tag{4.10}$$

where $f_{1(\alpha r)i}$ is the momentum transfer from species r to species α.

Substituting the stress-energy tensor into Eq. (4.5) and expanding order by order gives the background continuity equation for the individual species, α,

$$\rho'_{(\alpha)} + 3\mathcal{H}(\rho_{(\alpha)} + P_{(\alpha)}) = aQ_{(\alpha)} \,. \tag{4.11}$$

As we saw in Section 2.4.2 the first order energy-momentum conservation equations lead us to two scalar equations,

$$\delta\rho'_{1(\alpha)} + 3\mathcal{H}(\delta\rho_{1(\alpha)} + \delta P_{1(\alpha)}) = (\rho_{(\alpha)} + P_{(\alpha)})(3\psi'_1 - \nabla^2(E'_1 + v_{1(\alpha)})) + a\phi_1 Q_{(\alpha)} + a\delta Q_{1(\alpha)} \,, \tag{4.12}$$

$$\begin{aligned} & (v_{1(\alpha)} + B_1)' + \left[\frac{aQ_{(\alpha)}}{\rho_{(\alpha)} + P_{(\alpha)}}(1 + c_s^2) + \mathcal{H}(1 - 3c_s^2)\right]((v_{1(\alpha)} + B_1) + \phi_1 \\ + \quad & \frac{1}{\rho_{(\alpha)} + P_{(\alpha)}}\left[\delta P_{1(\alpha)} + \frac{2}{3}\nabla^2\Pi_{1(\alpha)} - aQ_{(\alpha)}(v_1 + B_1) - af_{1(\alpha)}\right] = 0 \,, \end{aligned} \tag{4.13}$$

where $c_s^2 = P'/\rho'$, and one vector equation,

$$\begin{aligned} & (v_{1(\alpha)i} - S_{1i})' + \left[\frac{aQ_{(\alpha)}}{\rho_{(\alpha)} + P_{(\alpha)}}(1 + c_s^2) + \mathcal{H}(1 - 3c_s^2)\right](v_{1(\alpha)i} - S_{1i}) \\ + \quad & \frac{1}{\rho_{(\alpha)} + P_{(\alpha)}}\left[\frac{1}{2}\nabla^2\pi_{1(\alpha)i} - aQ_{(\alpha)}(v_{1i} - S_{1i}) - af_{1(\alpha)i}\right] = 0 \,. \end{aligned} \tag{4.14}$$

For full details of the perturbative equations in the multi-field case see Malik & Wands, Ref. [80], and references therein.

The overall conservation equations can be found by summing the equations above. We find, as expected, that the energy and momentum conservation equations given in Section 2.4.2 still hold, but now the pressure and densities refer to the total pressure and density of the system, defined above. For convenience, we will give the overall conservation equations again here,

$$\rho' + 3\mathcal{H}(\rho + P) = 0\,, \tag{4.15}$$

$$\delta\rho_1' + 3\mathcal{H}(\delta\rho_1 + \delta P_1) = (\rho + P)(3\psi_1' - \nabla^2(E_1' + v_1))\,, \tag{4.16}$$

$$(v_1 + B_1)' + \mathcal{H}(1 - 3c_s^2)((v_1 + B_1) + \phi_1 + \frac{1}{\rho + P}\left[\delta P_1 + \frac{2}{3}\nabla^2\Pi_1\right] = 0\,, \tag{4.17}$$

$$(v_{1i} - S_{1i})' + \mathcal{H}(1 - 3c_s^2)(v_{1i} - S_{1i}) + \frac{1}{2(\rho + P)}\nabla^2\pi_{1i} = 0\,. \tag{4.18}$$

Note that the Einstein equations in the multi fluid case are now given by,

$$G^{\mu\nu} = 8\pi G \sum_\alpha T_{(\alpha)}{}^{\mu\nu}\,. \tag{4.19}$$

This leads to the same Einstein equations we had in Section 2.4.1 but as above, the densities and pressures will now refer to the total densities and pressures of the whole system.

4.2 Interactions of charged species

Now that we have outlined the general theory in dealing with multi-fluid systems we move on to a particularly relevant example. In the early universe cold dark matter and neutrinos are decoupled leaving just baryonic matter and radiation to interact. Considering the positively and negatively charged baryonic matter separately we have three interacting species: negatively charged electrons (e), positively charged ions and protons (p), and photons (γ) and a background electromagnetic field. We assume these three species can be regarded as fluids and will satisfy the individual conservation equations above. To write down a system of equations for the proton,

electron and photon fluids we need to determine the momentum and energy transfer rates. To this end we look in more detail at the interactions between these three species and their energy and momentum transfer rates.

4.2.1 Proton-Electron collisions

When we have two charged species they interact through Coulomb collisions. Here we look at the case of electrons interacting with positively charged ions. In order to arrive at an expression for the energy and momentum transfer from one of the charged species by the other we consider a Maxwellian distribution of electrons moving through a background distribution of ions. We will not go through the full derivation here, but will only highlight the results of considering such interactions. For further details see Ref. [81].

The net momentum loss on the distribution of electrons is

$$m_e n_e \frac{dV_e}{dt} = -m_e n_e \nu_e (V_e - V_i)\,, \tag{4.20}$$

where ν_e is the collision frequency defined by [81]

$$\nu_e = \frac{4\sqrt{2\pi} n_i Z_i^2 e^4 k_B^{3/2} \ln\Lambda}{3(4\pi\epsilon_0)^2 \sqrt{m_e} T_e^{3/2}}\,, \tag{4.21}$$

$\ln\Lambda$ is the Coulomb logarithm and is typically between ten and twenty [82]. n_i and Z_i are the number density and atomic number of the ions and the factors $(4\pi\epsilon_0)^2$ and $k_B^{3/2}$ are included as we are working in SI units. Assuming the ions in question are protons, and the electrons have a temperature equal to the photon temperature, the momentum transfer, defined in section 4.1, is given by,

$$\begin{aligned} f_{pe} &= -n_e n_p e^2 \frac{4\sqrt{2\pi}\sqrt{m_e} e^2 k_B^{3/2} \ln\Lambda}{3(4\pi\epsilon_0)^2 T^{3/2}} (V_p - V_e) \\ &= -n_e n_p e^2 \eta_e (V_p - V_e)\,, \end{aligned} \tag{4.22}$$

where $\eta_e = \frac{4\sqrt{2\pi}\sqrt{m_e} e^2 k_B^{3/2} \ln\Lambda}{3(4\pi\epsilon_0)^2 T^{3/2}}$ is the plasma resistivity. The plasma resistivity is not constant but inherits time dependence from the temperature of the photon fluid on which it depends. This temperature satisfies the constraint $T = T_b a^{-1}$, where T_b is

the temperature of the CMB radiation today. This allows us to write the plasma resistivity in terms of the scale factor as,

$$\eta_e = \hat{\eta}_e a^{3/2} = \frac{4\sqrt{2\pi}\sqrt{m_e}e^2 k_B^{3/2} \ln\Lambda}{3(4\pi\epsilon_0)^2 T_b^{3/2}} a^{3/2} \,. \tag{4.23}$$

The energy transfer of the same distribution of electrons is given by [81]

$$Q_{pe} = 3\beta\nu_e n_e (T_e - T_p) \,. \tag{4.24}$$

As expected, if the protons and electrons are in thermal equilibrium there is no net energy transfer. In the background, this can be assumed to be true and therefore we will be assuming $Q_{pe} = 0$ below.

4.2.2 Radiation-matter collisions

Radiation interacts with charged particles via Thomson interactions. The momentum transfer is given by [35],

$$f_{s\gamma} = \frac{4\rho_\gamma}{3} n_s \sigma_{Ts} (v_s - v_\gamma) \,, \tag{4.25}$$

where σ_{Ts} is the Thompson cross section for species s. In this expression we have neglected any contribution from polarization, this is a higher order effect and only contributes a few percent to the overall result [35]. We also note that the Thompson cross section for protons and electrons are related by, $\sigma_{Tp} = \beta^2 \sigma_{Te}$ and have the form,

$$\sigma_{Ts} = \frac{8\pi}{3} \left(\frac{e^2}{m_s c^2} \right)^2 \,. \tag{4.26}$$

Combining all these results gives us the following expressions for the momentum transfer between photons and charged particles,

$$f_{p\gamma} = -\frac{4}{3}\rho_\gamma n_p \beta^2 \sigma_{Te} (v_p - v_\gamma) = -\frac{4}{3}\rho_\gamma n_p \beta^2 \sigma_{Te} (V_p - V_\gamma) \,, \tag{4.27}$$

$$f_{e\gamma} = -\frac{4}{3}\rho_\gamma n_e \sigma_{Te} (v_e - v_\gamma) = -\frac{4}{3}\rho_\gamma n_e \sigma_{Te} (V_e - V_\gamma) \,, \tag{4.28}$$

Hence, as in the case above the momentum transfer is proportional to the velocity difference between the two species. Note that in the final step above we have substituted v_s for V_s, since when considering a velocity difference the two are the same. Thomson scattering doesn't alter the photon energy and so the energy transfer at the background level will again be zero, i.e. $Q_{s\gamma} = 0$ [39].

4.2.3 Interactions with the electromagnetic sector

We can also allow for a background electromagnetic field which interacts with both the charged ions and the electrons. The momentum transfer from a charged species (s) into the electromagnetic field (F) is given by,

$$f^{\mu}_{sF} = q_s n_s (\mathcal{E}^{\mu} + \epsilon_{\mu\nu\tau} v_s^{\nu} \mathcal{M}^{\tau}) \,. \tag{4.29}$$

where q_s, n_s and v_s are the charge, number density and velocity of species s, $\mathcal{E}$ is the electric field strength and $\mathcal{M}$ is the magnetic field strength. We will discuss the equations that govern the magnetic and electric fields in more detail in Chapter 5.

As we know that both the velocity and magnetic field are at least first order quantities (see Chapter 6), at linear order this momentum transfer rate is given by,

$$f^{\mu}_{sF} = q_s n_s \mathcal{E}^{\mu} \,. \tag{4.30}$$

4.3 Governing Equations for a three fluid system

As mentioned above our aim in this chapter is to study the species that are present in the early universe, in the time after the first protons and electrons form until matter-radiation equality. During this time we are considering a system of three fluids: radiation, electrons and protons, moving within a background electromagnetic field. In this section we will derive a system of equations for the velocities and electric field strength which we will then go on to solve. Hence, starting from the momentum conservation equation, Eq. (4.13), and substituting $P_{(\gamma)} = \frac{1}{3}\rho_{(\gamma)}$ and $P_{(e)} = P_{(p)} = 0$

we have momentum equations for each species,

$$\begin{aligned}
V'_{1(p)} + \left[\frac{aQ_{(p)}}{\rho_{(p)}} + \mathcal{H}\right] V_{1(p)} + \phi_1 + \frac{1}{\rho_{(p)}}\left[\frac{2}{3}\nabla^2\Pi_{1(p)} - aQ_{(p)}V_1 - af_{1(p)}\right] &= 0\,, \\
V'_{1(e)} + \left[\frac{aQ_{(e)}}{\rho_{(e)}} + \mathcal{H}\right] V_{1(e)} + \phi_1 + \frac{1}{\rho_{(e)}}\left[\frac{2}{3}\nabla^2\Pi_{1(e)} - aQ_{(e)}V_1 - af_{1(e)}\right] &= 0\,, \\
V'_{1(\gamma)} + \left[\frac{aQ_{(\gamma)}}{\rho_{(\gamma)}}\right] V_{1(\gamma)} + \phi_1 + \frac{3}{4\rho_{(\gamma)}}\left[\delta P_{1(\gamma)} + \frac{2}{3}\nabla^2\Pi_{1(\gamma)} - aQ_{(\gamma)}V_1 - af_{1(\gamma)}\right] &= 0\,.
\end{aligned}$$

For simplicity, we will assume that the anisotropic stress is zero at first order, we will also assume that the energy transfer is zero in the background, see Section 4.2.1 and Section 4.2.2 for comments on why this is reasonable. We use the Einstein equation,

$$\phi_1 = -\frac{3\mathcal{H}}{2\rho}(\rho + P)V_1\,, \tag{4.31}$$

to substitute for ϕ_1, where ρ and P are the overall density and pressure respectively, for example $\rho = \rho_{(p)} + \rho_{(e)} + \rho_{(\gamma)}$.

This leads us to the following expressions, where we have written the summation of the different momentum transfer rates out explicitly,

$$V'_{1(p)} + \mathcal{H}V_{1(p)} - \frac{3\mathcal{H}}{2\rho}\left(\rho_{(p)}V_{1(p)} + \rho_{(e)}V_{1(e)} + \frac{4}{3}\rho_{(\gamma)}V_{1(\gamma)}\right) - \frac{a}{\rho_{(p)}}(f_{1(pe)} + f_{1(p\gamma)} + f_{1(pF)}) = 0\,, \tag{4.32}$$

$$V'_{1(e)} + \mathcal{H}V_{1(e)} - \frac{3\mathcal{H}}{2\rho}\left(\rho_{(p)}V_{1(p)} + \rho_{(e)}V_{1(e)} + \frac{4}{3}\rho_{(\gamma)}V_{1(\gamma)}\right) - \frac{a}{\rho_{(e)}}(f_{1(ep)} + f_{1(e\gamma)} + f_{1(eF)}) = 0\,, \tag{4.33}$$

$$V'_{1(\gamma)} - \frac{3\mathcal{H}}{2\rho}\left(\rho_{(p)}V_{1(p)} + \rho_{(e)}V_{1(e)} + \frac{4}{3}\rho_{(\gamma)}V_{1(\gamma)}\right) + \frac{1}{4\rho_{(\gamma)}}\delta\rho_{1(\gamma)} - \frac{3a}{4\rho_{(\gamma)}}(f_{1(\gamma p)} + f_{1(\gamma e)}) = 0\,. \tag{4.34}$$

Writing the momentum transfer rates in terms of velocity differences, see Eqs. (4.22) and (4.27), and re-arranging gives the following equations

$$
\begin{aligned}
V'_{1(p)} &+ (\mathcal{H} - \frac{3\mathcal{H}}{2\rho}\rho_{(p)} + \frac{a}{\rho_{(p)}} n_e n_p e^2 \eta_e + \frac{a}{\rho_{(p)}} \frac{4}{3} \rho_\gamma n_p \beta^2 \sigma_{Te}) V_{1(p)} \\
&+ (-\frac{a}{\rho_{(p)}} n_e n_p e^2 \eta_e - \frac{3\mathcal{H}}{2\rho}\rho_{(e)}) V_{1(e)} \\
&+ (-\frac{a}{\rho_{(p)}} \frac{4}{3} \rho_\gamma n_p \beta^2 \sigma_{Te} - \frac{2\mathcal{H}}{\rho}\rho_{(\gamma)}) V_{1(\gamma)} = \frac{a}{\rho_{(p)}} e n_p \mathcal{E}_1 \,, \qquad (4.35) \\
V'_{1(e)} &+ (-\frac{a}{\rho_{(e)}} n_e n_p e^2 \eta_e - \frac{3\mathcal{H}}{2\rho}\rho_{(p)}) V_{1(p)} \\
&+ (\mathcal{H} - \frac{3\mathcal{H}}{2\rho}\rho_{(e)} + \frac{a}{\rho_{(e)}} n_e n_p e^2 \eta_e + \frac{a}{\rho_{(e)}} \frac{4}{3} \rho_\gamma n_e \sigma_{Te}) V_{1(e)} \\
&+ (-\frac{a}{\rho_{(e)}} \frac{4}{3} \rho_\gamma n_e \sigma_{Te} - \frac{2\mathcal{H}}{\rho}\rho_{(\gamma)}) V_{1(\gamma)} = -\frac{a}{\rho_{(e)}} e n_e \mathcal{E}_1 \,, \qquad (4.36) \\
V'_{1(\gamma)} &+ (-\frac{3a}{4\rho_{(\gamma)}} \frac{4}{3} \rho_\gamma n_p \beta^2 \sigma_{Te} - \frac{3\mathcal{H}}{2\rho}\rho_{(p)}) V_{1(p)} + (-\frac{3a}{4\rho_{(\gamma)}} \frac{4}{3} \rho_\gamma n_e \sigma_{Te} - \frac{3\mathcal{H}}{2\rho}\rho_{(e)}) V_{1(e)} \\
&- (\frac{2\mathcal{H}}{\rho}\rho_{(\gamma)} - \frac{3a}{4\rho_{(\gamma)}} \frac{4}{3} \rho_\gamma n_p \beta^2 \sigma_{Te} - \frac{3a}{4\rho_{(\gamma)}} \frac{4}{3} \rho_\gamma n_e \sigma_{Te}) V_{1(\gamma)} = -\frac{1}{4\rho_{(\gamma)}} \delta\rho_{1(\gamma)} \,. \qquad (4.37)
\end{aligned}
$$

We do not yet restrict ourselves to the radiation era, therefore the densities will be written in terms of R_b, the baryon to photon ratio, rather than in terms of η directly.

$$
\begin{aligned}
\rho_e &= m_e n_e = \beta m_p n_b \,, \qquad (4.38) \\
\rho_p &= m_p n_p = m_p n_b \,, \qquad (4.39) \\
\rho_\gamma &= \frac{3 n_b (1+\beta) m_p}{4 R_b} \,, \qquad (4.40)
\end{aligned}
$$

where we have assumed charge neutrality, i.e. $n_p = n_e = n_b$. We know the total number density of nucleons is given by

$$
n_{\rm nuc} = n_p + n_e + n_n = \frac{15}{7} n_b \,, \qquad (4.41)
$$

were we have used both charge neutrality and the fact that the number density of neutrons is approximately seven times smaller than the number density of protons

[39]. We also know the number densities will decay with the spatial volume allowing us to write the proton and electron number density in terms of the number density of nucleons today,

$$n_b = \frac{7}{15} n_{\rm nuc0} a^{-3} \equiv \hat{n}_b a^{-3} \,, \tag{4.42}$$

where we have defined a new constant $\hat{n}_b$, to simplify our expressions, Substituting in the latest value for $n_{\rm nuc0}$, given in Appendix A, we find $\hat{n}_b = 0.117$.

We can also write the baryon to photon ratio in terms of the scale factor,

$$R_b = \frac{3\rho_b}{4\rho_\gamma} = \frac{3\Omega_{b0}}{4\Omega_{\gamma 0}} \equiv \hat{R}_b a \,, \tag{4.43}$$

where once again we have defined the constant $\hat{R}_b$, in order to simplify our equations. Substituting in the latest observational values for Ω_{b0} and $\Omega_{\gamma 0}$ we find that $\hat{R}_b = 757.7$.

Rewriting our equations in terms of the baryon to photon ration and reintroducing the speed of light parameter, c, in order to switch from natural to SI units, we arrive at the following,

$$\begin{aligned} V'_{1(p)} &+ \left(\mathcal{H} - \frac{6\mathcal{H}R_b}{(3+4R_b)(1+\beta)} + \frac{a n_b e^2 \eta_e}{m_p} + \frac{a n_b (1+\beta)\beta^2 \sigma_{Te} c}{R_b} \right) V_{1(p)} \\ &- \left(\frac{a n_b e^2 \eta_e}{m_p} + \frac{6\mathcal{H}\beta R_b}{(3+4R_b)(1+\beta)} \right) V_{1(e)} \\ &- \left(a \frac{(1+\beta) n_b \beta^2 \sigma_{Te} c}{R_b} + \frac{6\mathcal{H}}{(3+4R_b)} \right) V_{1(\gamma)} = \frac{ae\mathcal{E}_1}{c m_p} \,, \end{aligned} \tag{4.44}$$

$$\begin{aligned} V'_{1(e)} &- \left(\frac{a n_b e^2 \eta_e}{m_p \beta} + \frac{6\mathcal{H}R_b}{(3+4R_b)(1+\beta)} \right) V_{1(p)} \\ &+ \left(\mathcal{H} - \frac{6\mathcal{H}R_b\beta}{(3+4R_b)(1+\beta)} + \frac{a n_b e^2 \eta_e}{m_p \beta} + \frac{a n_b (1+\beta)\sigma_{Te} c}{\beta R_b} \right) V_{1(e)} \\ &- \left(\frac{a n_b (1+\beta)\sigma_{Te} c}{\beta R_b} + \frac{6\mathcal{H}}{(3+4R_b)} \right) V_{1(\gamma)} = -\frac{ae\mathcal{E}_1}{c m_p \beta} \,, \end{aligned} \tag{4.45}$$

$$V'_{1(\gamma)} - \left(an_p\beta^2\sigma_{Te}c + \frac{6\mathcal{H}R_b}{(3+4R_b)(1+\beta)}\right)V_{1(p)} - \left(an_e\sigma_{Te}c + \frac{6\mathcal{H}R_b\beta}{(3+4R_b)(1+\beta)}\right)V_{1(e)}$$
$$- \left(\frac{6\mathcal{H}}{(3+4R_b)} - an_p(1+\beta^2)\sigma_{Te}c\right)V_{1(\gamma)} = -\frac{R_bc}{3n_b(1+\beta)m_p}\delta\rho_{1(\gamma)}\,. \tag{4.46}$$

As mentioned at the start our aim in this chapter is not only to determine the scale and time dependence of the velocity of each species but also the electric field strength. With this in mind we subtract Eq. (4.45) from Eq. (4.44) and find an expression for the electric field in terms of velocity differences,

$$\mathcal{E}_1 = \frac{\beta m_pc}{(1+\beta)ae}(V_{1(p)} - V_{1(e)})' + \left(\frac{\mathcal{H}\beta m_pc}{(1+\beta)ae} + n_be\eta_ec\right)(V_{1(p)} - V_{1(e)})$$
$$+\frac{n_b\sigma_{Te}c^2m_p}{R_be}\left(\beta^3(V_{1(p)} - V_{1(\gamma)}) - (V_{1(e)} - V_{1(\gamma)})\right)\,, \tag{4.47}$$

In the next section we will solve this system of equations to find expressions for the velocity of each species and the electric field strength generated. We will be solving the equations in two different scenarios firstly assuming the tight coupling approximation between protons and electrons holds and secondly neglecting this approximation.

4.3.1 Tight Coupling approximation

We start by solving the system of equations above assuming the tight coupling approximation holds. We note that tight coupling can refer to both a tight coupling between baryons and photons and a tight coupling between protons and electrons. In the first case, it is clear that no magnetic fields could be generated [83], so we only consider the second case here, tight coupling between electrons and protons. When no other factors are at play it is natural that the electrons being lighter will follow the motion of the protons, due to electrostatic attraction. Therefore the two charged components will move as one, i.e. $V_p = V_e = V_b$. This approximation is known as the tight coupling approximation and is often applied to plasmas.The tight coupling approximation only holds well before recombination, for realistic cosmological models tight coupling between protons and electrons holds early on in the radiation era when $T \geq 230$eV, therefore while we use tight coupling we may also assume we have

radiation domination. If we assume that we are in radiation domination and tight coupling holds on our system of fluids, then we can rewrite the three differential equations above as,

$$\begin{aligned}
\mathcal{E}_1 &= \frac{n_b m_p(\beta^3-1)(1+\beta)\sigma_{Te}c^2}{2eR_b}(V_{1(b)}-V_{1(\gamma)})\,, && (4.48)\\
V'_{1(b)} &+ \left(\mathcal{H}-2\mathcal{H}R_b+\frac{an_b(\beta^3+1)(1+\beta)\sigma_{Te}c}{2\beta R_b}\right)V_{1(b)}\\
&- \left(2\mathcal{H}+\frac{an_b(\beta^3+1)(1+\beta)\sigma_{Te}c}{2\beta R_b}\right)V_{1(\gamma)}=0\,, && (4.49)\\
V'_{1(\gamma)} &- \left(an_b(\beta^2+1)\sigma_{Te}c+2\mathcal{H}R_b\right)V_{1(b)}-\left(2\mathcal{H}-an_p(1+\beta^2)\sigma_{Te}c\right)V_{1(\gamma)}\\
&= -\frac{R_b c}{3n_b(1+\beta)m_p}\delta\rho_{1(\gamma)}\,. && (4.50)
\end{aligned}$$

Therefore under this approximation the electric field strength will be proportional to the velocity difference between the photon and baryon fluids.

During radiation domination the Hubble parameter is given by $\mathcal{H}=\frac{1}{\eta_0 a}$. Substituting in this expression and the scale factor dependence for R_b and n_b given in Eq. (4.42) and Eq. (4.43) we arrive at,

$$\begin{aligned}
\mathcal{E}_1 &= -\frac{\hat{n}_b m_p(\beta^3-1)(1+\beta)\sigma_{Te}c^2}{2e\hat{R}_b a^4}(V_{1(b)}-V_{1(\gamma)})\,, && (4.51)\\
V'_{1(b)} &+ \left(\frac{1}{\eta_0 a}+\frac{\hat{n}_b(\beta^3+1)(1+\beta)\sigma_{Te}c}{2\beta\hat{R}_b a^3}\right)V_{1(b)}\\
&- \left(\frac{2}{\eta_0 a}+\frac{\hat{n}_b(\beta^3+1)(1+\beta)\sigma_{Te}c}{2\beta\hat{R}_b a^3}\right)V_{1(\gamma)}=0\,, && (4.52)\\
V'_{1(\gamma)} &- \left(\hat{n}_b(\beta^2+1)\sigma_{Te}ca^{-2}+\frac{2\hat{R}_b}{\eta_0}\right)V_{1(b)}-\left(\frac{2}{\eta_0 a}-\hat{n}_p(\beta^2+1)\sigma_{Te}ca^{-2}\right)V_{1(\gamma)}\\
&= -\frac{\hat{R}_b c}{3\hat{n}_b m_p}a^4\delta\rho_{1(\gamma)}\,. && (4.53)
\end{aligned}$$

In order to find solutions in terms of the overall density perturbation rather than the density perturbation of the radiation fluid we need an expression for $\delta\rho_{1(\gamma)}$. Using the conservation equation, Eq. (4.12), and the Einstein equation, Eq. (2.72)

to eliminate B_1 we have,

$$(a^4\delta\rho_{1(\gamma)})' = -\frac{4}{3}a^4\rho_\gamma\left(c\nabla^2 V_{1(\gamma)} - \frac{9\mathcal{H}^2}{2\rho c}(\rho_p V_p + \rho_e V_e + \frac{4}{3}\rho_\gamma V_\gamma) + \frac{3\mathcal{H}}{2\rho}\delta\rho_1\right) . \quad (4.54)$$

Using the fact we are working in the radiation era and under the tight coupling approximation this equation becomes,

$$\begin{aligned}(a^4\delta\rho_{1(\gamma)})' = \quad & 6a^{-1}\eta_0^{-2}c^{-1}\hat{n}_b m_p(1+\beta)V_{1(b)} \\ & + \frac{(1+\beta)\hat{n}_b m_p}{\hat{R}_b}(6c^{-1}\eta_0^{-2}a^{-2} - c\nabla^2)V_{1(\gamma)} - 2\mathcal{H}a^4\delta\rho_1 . \quad (4.55)\end{aligned}$$

By differentiating Eq. (4.53) and eliminating $(a^4\delta\rho_{1(\gamma)})'$ we arrive at a second order differential equation for the evolution of the velocity of the photon fluid in terms of the overall density perturbation. Finally we present this second order equation, now with $\delta\rho_{1\gamma}$, along with the evolution equation for the velocity of the baryon fluid and the equation for the electric field strength,

$$\mathcal{E}_1 = -\frac{\hat{n}_b m_p(\beta^3-1)(1+\beta)\sigma_{Te}c}{2e\hat{R}_b a^4}(V_{1(b)} - V_{1(\gamma)}) , \quad (4.56)$$

$$\begin{aligned}\frac{\partial}{\partial a}V_{1(b)} \quad & + \left(\frac{1}{a} + \frac{\eta_0\hat{n}_b(\beta^3+1)(1+\beta)\sigma_{Te}c}{2\beta\hat{R}_b a^3}\right)V_{1(b)} \\ & - \left(\frac{2}{a} + \frac{\eta_0\hat{n}_b(\beta^3+1)(1+\beta)\sigma_{Te}c}{2\beta\hat{R}_b a^3}\right)V_{1(\gamma)} = 0 , \quad (4.57)\end{aligned}$$

$$\begin{aligned}& \frac{\partial^2}{\partial a^2}V_{1(\gamma)} - \left(\hat{n}_b\eta_0(\beta^2+1)\sigma_{Te}ca^{-2} + 2\hat{R}_b\right)\frac{\partial}{\partial a}V_{1(b)} \\ & + \frac{2}{a^3}(c\eta_0\hat{n}_b(\beta^2+1)\sigma_{Te} + \hat{R}_b a^2(1+\beta))V_{1(b)} \\ & - \left(-\frac{2}{a^2} + 2\eta_0\hat{n}_p(\beta^2+1)\sigma_{Te}ca^{-3} - \frac{1}{3}(1+\beta)(6a^{-2} - \eta_0^2c^2\nabla^2)\right)V_{1(\gamma)} \\ & - \left(\frac{2}{a} - \hat{n}_p(\beta^2+1)\sigma_{Te}\eta_0 ca^{-2}\right)\frac{\partial}{\partial a}V_{1(\gamma)} = \frac{\hat{R}_b c\eta_0^2}{3\hat{n}_b m_p}2\mathcal{H}a^4\delta\rho_1 . \quad (4.58)\end{aligned}$$

where our derivatives are now with respect to the scale factor.

4.3.1.1 Analytical Solution

In this section we would like to better understand which of the effects described in Section 4.2 causes the velocities of the species to evolve and which has the greatest impact on the electric field strength, this would allow us to give predictions for how the velocities might evolve with time. To this end we would like to find an analytic solution and to do so we assume that at leading order in a, for the time period we are interested in the velocities can be described by a power law,

$$V_{1(b)} = V_{1(b)}(\mathbf{x})a^b\,, \tag{4.59}$$

$$V_{1\gamma} = V_{1\gamma}(\mathbf{x})a^g\,. \tag{4.60}$$

Using these expressions will simplify Eq. (4.57) and Eq. (4.58) to give us a set of simultaneous equations to solve,

$$\left(2\beta(1+b)\hat{R}_b a^2 + \eta_0\hat{n}_b\sigma_{Te}c\right)V_{1(b)} = \left(4\beta\hat{R}_b a^2 + \eta_0\hat{n}_b\sigma_{Te}c\right)V_{1(\gamma)}\,, \tag{4.61}$$

$$\begin{aligned}&\left((1-g-g^2-\beta)a^{-2} + (g+2)\hat{n}_b\sigma_{Te}\eta_0 c a^{-3} - c^2(1+\beta)\frac{1}{3}\eta_0^2\nabla^2\right)V_{1(\gamma)}\\ &+\left((2-b)\hat{n}_b\eta_0\sigma_{Te}ca^{-3} + 2\hat{R}_b a^{-1}(\beta-1)\right)V_{1(b)} = \frac{2\hat{R}_b c\eta_0}{3\hat{n}_b m_p}a^3\delta\rho_1\,,\end{aligned} \tag{4.62}$$

where we have also neglected any β contribution which will not have an effect on our final result. On switching to Fourier space, these equations can be solved directly to find the two velocities in terms of $\delta\rho_1$. Firstly eliminating $V_{1(b)}$ to arrive at an expression for $V_{1(\gamma)}$, we get,

$$V_{1(\gamma)} = \frac{(2\beta(1+b)\hat{R}_b a^2 + \eta_0\hat{n}_b\sigma_{Te}c)}{3\mathcal{Q}(a) + \left(2\beta(1+b)\hat{R}_b a^2 + c\eta_0\hat{n}_b\sigma_{Te}\right)k^2\eta_0^2c^2}\frac{2\hat{R}_b c\eta_0}{\hat{n}_b m_p}a^3\delta\rho_1\,, \tag{4.63}$$

where $\mathcal{Q}(a)$ is defined as

$$\begin{aligned}\mathcal{Q}(a) \equiv \quad & 2\beta(1+b)(1-g-g^2)\hat{R}_b + 2(\beta g(1+b)-1)\hat{R}_b\hat{n}_b\sigma_{Te}\eta_0 c a^{-1} - 8\beta\hat{R}_b^2 a\\ & +(1-g-g^2)\eta_0\hat{n}_b\sigma_{Te}ca^{-2} + (g-b+4)\eta_0^2\hat{n}_b^2\sigma_{Te}^2c^2a^{-3}\,.\end{aligned} \tag{4.64}$$

Similarly for $V_{1(b)}$ we arrive at,

$$V_{1(b)} = \frac{(4\beta\hat{R}_b a^2 + \eta_0\hat{n}_b\sigma_{Te}c)}{3\mathcal{Q}(a) + \left(2\beta(1+b)\hat{R}_b a^2 + c\eta_0\hat{n}_b\sigma_{Te}\right)k^2\eta_0^2c^2}\frac{2\hat{R}_b}{\sigma_{Te}\hat{n}_b^2 m_p}a^3\delta\rho_1\,. \tag{4.65}$$

As mentioned above, we are only considering the radiation era in this section of the chapter. This puts a constraint on the size of a. Using this to consider the magnitude of the terms that appear in Eq. (4.63) and Eq. (4.65) above, in particular the terms that make up $\mathcal{Q}(a)$, we can choose to keep only those terms which have the largest contribution. This gives the following simplified expressions for the two velocities,

$$V_{1(\gamma)} = \frac{2\beta(1+b)\hat{R}_b a^2 + \eta_0\hat{n}_b\sigma_{Te}c}{(1-g-g^2)a^{-2} + 4\eta_0\hat{n}_b\sigma_{Te}ca^{-3} + c^2\frac{1}{3}\eta_0^2k^2}\frac{2\hat{R}_b}{3\sigma_{Te}\hat{n}_b^2 m_p}a^3\delta\rho_1\,, \tag{4.66}$$

$$V_{1(b)} = \frac{4\beta\hat{R}_b a^2 + \eta_0\hat{n}_b\sigma_{Te}c}{(1-g-g^2)a^{-2} + 4\eta_0\hat{n}_b\sigma_{Te}ca^{-3} + c^2\frac{1}{3}\eta_0^2k^2}\frac{2\hat{R}_b}{3\sigma_{Te}\hat{n}_b^2 m_p}a^3\delta\rho_1\,. \tag{4.67}$$

We can now use Eq. (4.56) and the velocities above to find an expression for the electric field strength,

$$\mathcal{E}_1 = -\frac{2c(1-b)\beta\hat{R}_b}{3e\hat{n}_b((1-g-g^2)a^{-2} + 4\eta_0\hat{n}_b\sigma_{Te}ca^{-3} + c^2\frac{1}{3}\eta_0^2k^2)}a\delta\rho_1\,. \tag{4.68}$$

The velocities and electric strength in the equations above will have different scale and time dependencies when calculated on small scales compared to large scales. In order to be able to say more about their behaviour we therefore proceed by considering those two cases independently. Firstly, taking a small scale limit ($k^2c^2\eta_0^2a^2 \gg 3$), we see that at leading order in a the baryon fluid and photon fluids have the same velocity,

$$V_{1(\gamma)} = V_{1(b)} = \frac{2(1-b)\hat{R}_b}{c\hat{n}_b m_p\eta_0}k^{-2}a^3\delta\rho_1\,, \tag{4.69}$$

and the electric field strength at leading order in a is given by,

$$\mathcal{E}_1 = \frac{4\hat{R}_b}{e\eta_0^2\hat{n}_b}k^{-2}a\delta\rho_1\,, \tag{4.70}$$

Now we consider taking a large scale limit ($k^2c^2\eta_0^2a^2 \ll 3$). We saw in Section 2.5 that on large scales the density perturbation to leading order in a, is proportional to a^{-4}. We also know from observational data (see Section 6.3.1) that it is approximately scale invariant and therefore the density perturbation is given by Eq. (6.62). Combining this expression for $\delta\rho_1$ with Eq. (4.66) and Eq. (4.67) and taking the large scale limit we see once again that at leading order in a the baryon and photon fluids have the same velocity,

$$V_{1(\gamma)} = V_{1(b)} = \frac{A\hat{R}_b}{6\hat{n}_b^2\sigma_{Te}m_p}a^2\,. \tag{4.71}$$

Finally, to find an expression for the electric field we keep both the leading order term in a and the next to leading order term and arrive at,

$$\begin{aligned}\mathcal{E}_1 &= \frac{Ac\beta\hat{R}_b}{6e\eta_0\sigma_{Te}\hat{n}_b^2}\left(1-\frac{5a}{4\eta_0\hat{n}_b\sigma_{Te}c}\right)^{-1}\,,\\ &= \frac{Ac\beta\hat{R}_b}{6e\eta_0\sigma_{Te}\hat{n}_b^2}\left(1+\frac{5a}{4\eta_0\hat{n}_b\sigma_{Te}c}\right)\,.\end{aligned} \tag{4.72}$$

4.3.2 Breaking the Tight Coupling Approximation

Now we move on to the second scenario, that in which the tight coupling approximation is broken. As mentioned above the tight coupling approximation is a natural one to assume while we are early in the radiation era, however it is not always valid. For instance as we approach recombination in the early universe the turbulent effects mean that we can no longer necessarily assume tight coupling holds, in fact we expect tight coupling to break down as we approach radiation-matter equality. For temperatures below about 0.5eV expansion occurs much more rapidly than Thompson scattering and the photons, baryons and electrons will no longer be tightly coupled. In this next section we will be working out an approximation for the electric field and the velocities in this scenario, i.e. no longer assuming $V_{1(e)} = V_{1(p)}$ and also no longer assuming radiation domination. As we no longer assume $V_{1(p)} = V_{1(e)}$ we will need a further piece of information about the electric field in order to solve this

system, and we will therefore use the Maxwell equation, Eq. (5.37),

$$(a^2\mathcal{E})' = -c^2a^3\mu_0\mathcal{J}\,. \tag{4.73}$$

combined with the definition of current given by,

$$\mathcal{J} = caen_b(V_p - V_e)\,. \tag{4.74}$$

This allows us to eliminate the electric field in terms of velocities. Finally to close the system, as above, we need the expression for $\delta\rho_{1(\gamma)}$, given in Eq. (4.54). We can write down the evolution equation for density perturbation of the photon fluid in terms of baryon to photon ration,

$$\begin{aligned}(a^4\delta\rho_{1(\gamma)})' &= a^4\frac{6n_bm_p}{\eta_0^2a^2c}V_{1(p)} + a^4\frac{6n_bm_p}{\eta_0^2a^2c}\beta V_{1(e)} \\ + \quad a^4&\frac{n_b(1+\beta)m_p}{R_b}(\frac{6}{\eta_0^2a^2c} - c\nabla^2)V_{1(\gamma)} - \frac{2\sqrt{3}}{(3+4R_b)^{1/2}\eta_0 a}a^4\delta\rho_1\,.\end{aligned} \tag{4.75}$$

As mentioned above in this section we are considering time approaching recombination, therefore rather than assuming we are in radiation domination we consider a mixed baryon and photon fluid, with the following Hubble parameter,

$$\mathcal{H} = \frac{(3+4R_b)^{1/2}}{\sqrt{3}\eta_0 a}\,. \tag{4.76}$$

Whilst we do not want to assume we are in the radiation domination here, as we did in the previous section, we are still only interested in the time up to recombination, beyond which other astrophysical effects come into play. Therefore we are still restricting ourselves to $a \leq 10^{-3}$. During this time the factor $(1 + (4/3)\hat{R}_b a)$ which appears in many of our equations is of order 1, it has the range of values

$$1 < (1 + (4/3)\hat{R}_b a) < 2\,. \tag{4.77}$$

In the analytic calculation that follows if we restrict ourselves to obtaining an order of magnitude estimate for our final answers, we can approximate the expression above as a constant, thereby assuming that the leading contribution to the time

dependence of the velocities and electric field strength does not come from this factor. We will set the factor $(1 + (4/3)\hat{R}_b a)$ equal to 1 below, as for most of the period we are interested in $a < 10^{-4}$, and therefore $(1 + (4/3)\hat{R}_b a)$ is within 10% of 1. Making this approximation is equivalent to assuming the Hubble parameter is still behaving as it were in the radiation era. As we have outlined above it is valid approximation to make in this case because firstly, we are not extending the time we are interested in to much beyond matter-radiation equality and secondly, we are only looking for order of magnitude estimate for our final answer. In the rest of this section, to make our equations clearer, we will also be neglecting some β terms, in expressions such as $(1+\beta)$, these are not needed to work out an order of magnitude approximation for the velocities and electric field strength. In all cases it has been checked that this does not induce a cancellation of terms where it should not.

Starting from Eqs. (4.44), (4.45) and (4.46) above we eliminate E and $\delta\rho_\gamma$ by differentiating all three equations. Then we apply the condition $(1+(4/3)\hat{R}_b a) \approx 1$, arriving at a system of three differential equations describing the evolution of the velocity of the proton, electron and photon fluid.

$$
\begin{aligned}
& a\frac{1}{\eta_0^2}\frac{\partial^2}{\partial a^2}V_{1(p)} + \Big(2 - 2\hat{R}_b a + \frac{\hat{n}_b e^2 \hat{\eta}_e a^{1/2}}{m_p} + \frac{\hat{n}_b \beta^2 \sigma_{Te} c}{\hat{R}_b a^2}\Big)\frac{1}{\eta_0}\frac{\partial}{\partial a}V_{1(p)} \\
+ \quad & \Big(-\frac{4\hat{R}_b}{3\eta_0^2} + \frac{4\hat{R}_b^2 a}{3\eta_0^2} - \frac{5\hat{n}_b e^2 \hat{\eta}_e}{2a^{1/2}\eta_0 m_p} - \frac{2\hat{n}_b \beta^2 \sigma_{Te} c}{\hat{R}_b \eta_0 a^3} + \frac{ec^2}{m_p} a\mu_0 e\hat{n}_b\Big)V_{1(p)} \\
& - \left(\frac{\hat{n}_b e^2 \hat{\eta}_e a^{1/2}}{m_p} + \frac{2\beta\hat{R}_b a}{\eta_0}\right)\frac{1}{\eta_0}\frac{\partial}{\partial a}V_{1(e)} \\
- \quad & \left(-\frac{5\hat{n}_b e^2 \hat{\eta}_e}{2\eta_0 m_p a^{1/2}} + \frac{2\beta\hat{R}_b}{\eta_0^2} - \frac{4\beta\hat{R}_b^2 a}{3\eta_0^2} - \frac{ec^2}{m_p} a\mu_0 e\hat{n}_b\right)V_{1(e)} \\
- \quad & \left(\frac{\hat{n}_b \beta^2 \sigma_{Te} c}{\hat{R}_b a^2} + \frac{2}{\eta_0}\right)\frac{1}{\eta_0}\frac{\partial}{\partial a}V_{1(\gamma)} - \left(-\frac{2\hat{n}_b \beta^2 \sigma_{Te} c}{\hat{R}_b a^3 \eta_0} - \frac{4\hat{R}_b}{3\eta_0^2}\right)V_{1(\gamma)} = 0\,, \qquad (4.78)
\end{aligned}
$$

$$
\begin{aligned}
& a\frac{1}{\eta_0^2}\frac{\partial^2}{\partial a^2}V_{1(e)} - \left(\frac{\hat{n}_b e^2 \hat{\eta}_e a^{1/2}}{m_p \beta} + \frac{2\hat{R}_b a}{\eta_0}\right)\frac{1}{\eta_0}\frac{\partial}{\partial a}V_{1(p)} \\
- & \left(-\frac{5\hat{n}_b e^2 \hat{\eta}_e}{2\eta_0 m_p \beta a^{1/2}} + \frac{2\hat{R}_b}{\eta_0^2} - \frac{4\hat{R}_b^2 a}{3\eta_0^2} - \frac{ec^2}{m_p\beta}a\mu_0 e\hat{n}_b\right)V_{1(p)} \\
+ & \left(\frac{2}{\eta_0} - \frac{2\hat{R}_b\beta a}{\eta_0} + \frac{\hat{n}_b e^2\hat{\eta}_e a^{1/2}}{m_p\beta} + \frac{\hat{n}_b\sigma_{Te}c}{\beta\hat{R}_b a^2}\right)\frac{1}{\eta_0}\frac{\partial}{\partial a}V_{1(e)} \\
+ & \Big(-\frac{4\hat{R}_b\beta}{3\eta_0^2} - \frac{4\hat{R}_b^2\beta a}{3\eta_0^2} - \frac{5\hat{n}_b e^2\hat{\eta}_e}{2m_p\beta\eta_0 a^{1/2}} - \frac{2\hat{n}_b\sigma_{Te}c}{\beta\eta_0\hat{R}_b a^3} + \frac{ec^2}{m_p\beta}a\mu_0 e\hat{n}_b\Big)V_{1(e)} \\
& - \left(\frac{\hat{n}_b\sigma_{Te}c}{\beta\hat{R}_b a^2} + \frac{2}{\eta_0}\right)\frac{1}{\eta_0}\frac{\partial}{\partial a}V_{1(\gamma)} - \left(-\frac{2\hat{n}_b\sigma_{Te}c}{\beta\eta_0\hat{R}_b a^3} + \frac{4\hat{R}_b}{3\eta_0^2}\right)V_{1(\gamma)} = 0\,,
\end{aligned}
\tag{4.79}
$$

$$
\begin{aligned}
& \frac{1}{\eta_0^2}\frac{\partial^2}{\partial a^2}V_{1(\gamma)} - \left(\hat{n}_p\beta^2\sigma_{Te}ca^{-2} + \frac{2\hat{R}_b}{\eta_0}\right)\frac{1}{\eta_0}\frac{\partial}{\partial a}V_{1(p)} \\
- & \left(-\frac{2}{\eta_0}\hat{n}_p\beta^2\sigma_{Te}ca^{-3} - \frac{4\hat{R}_b^2}{3\eta_0^2} - \frac{2\hat{R}_b}{\eta_0^2 a}\right)V_{1(p)} - \left(\hat{n}_p\sigma_{Te}ca^{-2} + \frac{2\hat{R}_b\beta}{\eta_0}\right)\frac{1}{\eta_0}\frac{\partial}{\partial a}V_{1(e)} \\
- & \left(-\frac{2}{\eta_0}\hat{n}_p\sigma_{Te}ca^{-3} - \frac{4\hat{R}_b^2\beta}{3\eta_0^2 a} - \frac{2\hat{R}_b}{\eta_0^2 a}\beta\right)V_{1(e)} - \left(\frac{2}{\eta_0 a} - \hat{n}_p\sigma_{Te}ca^{-2}\right)\frac{1}{\eta_0}\frac{\partial}{\partial a}V_{1(\gamma)} \\
- & \left(-\frac{2}{\eta_0^2 a^2} - \frac{4\hat{R}_b}{3\eta_0^2 a} + \frac{2}{\eta_0}\hat{n}_p\sigma_{Te}ca^{-3} - (1+\beta)c^2\left(\frac{2}{\eta_0^2 a^2 c^2} + \frac{1}{3}k^2\right)\right)V_{1(\gamma)} \\
& = \frac{2\hat{R}_b c}{3\hat{n}_b m_p \eta_0 a}a^4\delta\rho_1\,.
\end{aligned}
\tag{4.80}
$$

where once more we have changed the time variable from η to a.

4.3.2.1 Analytically Calculation

As we did in the case of the tight-coupling approximation result above, to solve this system analytically, we assume that the three velocities can be described by a power law in a,

$$V_\gamma = \hat{V}_\gamma a^g\,, \tag{4.81}$$

$$V_p = \hat{V}_p a^p\,, \tag{4.82}$$

$$V_e = \hat{V}_e a^\epsilon\,. \tag{4.83}$$

Following the method we used above we can use the above expressions to eliminate the derivatives in Eqs. (4.78), (4.79) and (4.80)

$$\left(\frac{p(p+1)}{a}+\frac{(p-2)\hat{n}_b\beta^2\sigma_{Te}\eta_0 c}{\hat{R}_b a^3}+\frac{c^2e^2a\mu_0\hat{n}_b\eta_0^2}{m_p}\right)V_{1(p)}+\frac{c^2e^2a\mu_0\eta_0^2\hat{n}_b}{m_p}V_{1(e)}$$
$$-\left(\frac{\hat{n}_b\beta^2\sigma_{Te}c(g-2)\eta_0}{\hat{R}_b a^3}+\frac{2g}{a}-\frac{4\hat{R}_b}{3}\right)V_{1(\gamma)}=0\,, \tag{4.84}$$

$$\frac{c^2e^2a\mu_0\hat{n}_b\eta_0^2}{m_p\beta}V_{1(p)}+\left(\frac{\epsilon(\epsilon+1)}{a}+\frac{\hat{n}_b\sigma_{Te}c(\epsilon-2)\eta_0}{\beta\hat{R}_b a^3}+\frac{c^2e^2a\mu_0\hat{n}_b\eta_0^2}{m_p\beta}\right)V_{1(e)}$$
$$-\left(\frac{\hat{n}_b\sigma_{Te}c(g-2)\eta_0}{\beta\hat{R}_b a^3}+\frac{2g}{a}+\frac{4}{3}\hat{R}_b\right)V_{1(\gamma)}=0\,, \tag{4.85}$$

$$-\left(3(p-2)\hat{n}_b\beta^2\sigma_{Te}\eta_0 c a^{-3}+6\hat{R}_b(p-1)a^{-1}\right)V_{1(p)}-3(\epsilon-2)\hat{n}_p\sigma_{Te}\eta_0 c a^{-3}V_{1(e)}$$
$$-\left(-\frac{3(g-2)\hat{n}_p\eta_0\sigma_{Te}c}{a^3}-(1+\beta)c^2\eta_0^2k^2\right)V_{1(\gamma)}=\frac{2\hat{R}_b\eta_0 c}{\hat{n}_b m_p}a^3\delta\rho_1\,. \tag{4.86}$$

where, following the method we used above, in each bracket in the equations above we have evaluated the magnitude of all terms during the radiation era and around recombination, and have only kept those terms that make the largest contribution. We can now write this system of three linear equations in matrix form and invert the Eqs. (4.84), (4.85) and (4.86) to find expressions for the three velocities.

$$\begin{aligned}V_{1(p)} \;=\; &\Big[-\frac{2c^2(\beta-1)e^2\mu_0\eta_0^2\hat{n}_b g}{m_p\beta}-\frac{4c^2(\beta+1)e^2\mu_0\eta_0^2\hat{n}_b\hat{R}_b a}{3m_p\beta}+\frac{2g\epsilon(\epsilon+1)}{a^2}\\
&-\frac{e^2\mu_0\eta_0^3\hat{n}_b^2\sigma_{Te}c^3(g-2)(1-\beta^2)}{m_p\beta\hat{R}_b a^2}+\frac{\hat{n}_b\beta^2\sigma_{Te}c(g-2)\eta_0\epsilon(\epsilon+1)}{\hat{R}_b a^4}-\frac{4\hat{R}_b\epsilon(\epsilon+1)}{3a}\\
&+\frac{\hat{n}_b^2\beta\sigma_{Te}^2c^2(g-2)\eta_0^2(\epsilon-2)}{\hat{R}_b^2a^6}+\frac{2\hat{n}_b\sigma_{Te}c\eta_0 g(\epsilon-2)}{\beta\hat{R}_b a^4}-\frac{4\hat{n}_b\sigma_{Te}c(\epsilon-2)\eta_0}{3a^3}\Big]\\
&\frac{2\hat{R}_b\eta_0 c}{\hat{n}_b m_p|M|}a^3\delta\rho_1\,,\end{aligned} \tag{4.87}$$

$$
\begin{aligned}
V_{1(e)} \;=\; & \Big[\frac{2c^2(\beta-1)e^2\mu_0\eta_0^2\hat{n}_b g}{m_p\beta} + \frac{4c^2(\beta+1)e^2\mu_0\eta_0^2\hat{n}_b\hat{R}_b a}{3m_p\beta} + \frac{2gp(p+1)}{a^2} \\
& + \frac{e^2\mu_0\eta_0^3\hat{n}_b^2\sigma_{Te}c^3(g-2)(1-\beta^2)}{m_p\beta\hat{R}_b a^2} + \frac{\hat{n}_b\sigma_{Te}c(g-2)\eta_0 p(p+1)}{\beta\hat{R}_b a^4} + \frac{4\hat{R}_b p(p+1)}{3a} \\
& + \frac{\hat{n}_b^2\beta\sigma_{Te}^2c^2(g-2)\eta_0^2(p-2)}{\hat{R}_b^2 a^6} + \frac{2\hat{n}_b\beta^2\sigma_{Te}c\eta_0 g(p-2)}{\hat{R}_b a^4} + \frac{4\hat{n}_b\beta^2\sigma_{Te}c(p-2)\eta_0}{3a^3}\Big] \\
& \frac{2\hat{R}_b\eta_0 c}{\hat{n}_b m_p|M|}a^3\delta\rho_1\,,
\end{aligned}
\tag{4.88}
$$

$$
\begin{aligned}
V_{1(\gamma)} \;=\; & \Big[\frac{p(p+1)\epsilon(\epsilon+1)}{a^2} + (\beta^3(p-2)\epsilon(\epsilon+1) + (\epsilon-2)p(p+1))\frac{\hat{n}_b\sigma_{Te}\eta_0 c}{\beta\hat{R}_b a^4} \\
& + (\epsilon-2)(p-2)\frac{\hat{n}_b^2\sigma_{Te}^2c^2\eta_0^2\beta}{\hat{R}_b^2 a^6} + (p(p+1)+\beta\epsilon(\epsilon+1))\frac{c^2e^2\mu_0\hat{n}_b\eta_0^2}{m_p\beta} \\
& + ((\epsilon-2)+\beta^2(p-2))\frac{e^2\mu_0\hat{n}_b^2\eta_0^3\sigma_{Te}c^3}{\hat{R}_b m_p\beta a^2}\Big]\frac{2\hat{R}_b\eta_0 c}{\hat{n}_b m_p|M|}a^3\delta\rho_1\,,
\end{aligned}
\tag{4.89}
$$

where $|M|$ is the determinant of the system of equations above and to leading order in a is given by,

$$
|M| = \frac{e^2\hat{n}_b^2\eta_0^3\mu_0\sigma_{Te}c^3}{\hat{R}_b\beta m_p a^3}\left(c^2\eta_0^2k^2(\epsilon-2)a + 3((\epsilon-2)2g + (g-2)(p+2)(p-1))\hat{R}_b\right)\,. \tag{4.90}
$$

As we saw in the previous section, these expressions can be greatly simplified by comparing the magnitude of the terms during the era we are interested in (radiation domination and the time around radiation-matter equality) and only keeping those that give the largest effect. This leaves us with the following expressions for the velocities,

$$
V_{1(p)} = \left[\frac{e^2\mu_0\eta_0\hat{n}_b\sigma_{Te}c(2-g)(1-\beta^2)}{\hat{R}_b a^2} - \frac{4}{3}(\beta+1)e^2\mu_0\hat{R}_b a\right]\frac{2\hat{R}_b\eta_0^3c^3}{\beta m_p^2|M|}a^3\delta\rho_1\,, \tag{4.91}
$$

$$
V_{1(e)} = \left[\frac{e^2\mu_0\eta_0\hat{n}_b\sigma_{Te}c(g-2)(1-\beta^2)}{\hat{R}_b a^2} + \frac{4}{3}(\beta+1)e^2\mu_0\hat{R}_b a\right]\frac{2\hat{R}_b\eta_0^3c^3}{\beta m_p^2|M|}a^3\delta\rho_1\,, \tag{4.92}
$$

$$V_{1(\gamma)} = \left[(p-2)\frac{\hat{n}_b^2\sigma_{Te}^2c^2\eta_0^2\beta}{\hat{R}_b^2a^6} + \left(1+\beta^2\frac{(p-2)}{(\epsilon-2)}\right)\frac{e^2\mu_0\hat{n}_b^2\eta_0^3\sigma_{Te}c^3}{\hat{R}_bm_p\beta a^2}\right]\frac{2(\epsilon-2)\hat{R}_b\eta_0c}{\hat{n}_bm_p|M|}a^3\delta\rho_1\,. \tag{4.93}$$

As was the case for the tight coupling results in Section 4.3.1.1, the scale and time dependence of the velocities of the three fluids is different on small and large scales. As we did in that section we will proceed by considering these two cases separately allowing us to find the scale and time dependence in each case.

Firstly, we can consider small scales ($c^2\eta_0^2k^2a \gg \hat{R}_b$) and combine the equations above with our expression for $|M|$ to arrive at the following expressions for the velocities of the species

$$V_{1(p)} = -\frac{2\hat{R}_b(g-2)}{m_p(\epsilon-2)\hat{n}_b\eta_0c}k^{-2}a^3\delta\rho_1\,, \tag{4.94}$$

$$V_{1(e)} = \frac{2\hat{R}_b(g-2)}{m_p(\epsilon-2)\hat{n}_b\eta_0c}k^{-2}a^3\delta\rho_1\,, \tag{4.95}$$

$$V_{1(\gamma)} = \frac{2\hat{R}_b}{m_p\hat{n}_b\eta_0c}k^{-2}a^3\delta\rho_1\,. \tag{4.96}$$

It is clear from these expressions that the scale and time dependence of the velocities on small scales will depend on the bahviour of the density perturbation.

Secondly, we move on to consider large scales ($c^2\eta_0^2k^2a \ll \hat{R}_b$), as in the previous section, as we are considering large scales we can also use use Eq. (6.62) to eliminate $\delta\rho_1$.

$$V_{1(p)} = -\frac{2A\eta_0c(g-2)}{3((\epsilon-2)2g+(g-2)(p+2)(p-1))\hat{n}_bm_p}\,, \tag{4.97}$$

$$V_{1(e)} = \frac{2A\eta_0c(g-2)}{3((\epsilon-2)2g+(g-2)(p+2)(p-1))\hat{n}_bm_p}\,, \tag{4.98}$$

$$V_{1(\gamma)} = \frac{2A((\epsilon-2)+\beta^2(p-2))\eta_0c}{3((\epsilon-2)2g+(g-2)(p+2)(p-1))\hat{n}_bm_p}\,. \tag{4.99}$$

We can read off the exponents in the above equations, $p=\epsilon=g=0$, which imply that to leading order the velocities are constant in time, i.e. slowly varying and are given by,

$$V_{1(e)} = V_{1(\gamma)} = -V_{1(p)} = \frac{A\eta_0c}{3\hat{n}_bm_p}\,. \tag{4.100}$$

As we saw in Eq. (4.47) the electric field can be written in terms of velocity differences and their derivatives,

$$\begin{aligned}\mathcal{E}_1 &= \frac{\beta m_p c}{(1+\beta)ae}(V_{1(p)} - V_{1(e)})' + \left(\frac{\mathcal{H}\beta m_p c}{(1+\beta)ae} + n_b e \eta_e c\right)(V_{1(p)} - V_{1(e)}) \\ &+ \frac{n_b \sigma_{Te} c^2 m_p}{R_b e}\left(\beta^3(V_{1(p)} - V_{1(\gamma)}) - (V_{1(e)} - V_{1(\gamma)})\right) .\end{aligned}$$

This allows us to find an expression for the electric field strength,

$$\mathcal{E}_1 = \frac{2A\beta c^2}{3e\hat{n}_b}a^{-2} + \frac{2A\sigma_{Te}^2 c^2 m_p \beta^2}{3\mu_0 \hat{R}_b e^3}a^{-8} , \tag{4.101}$$

where we have kept the leading order and next to leading order terms in a.

4.4 Electric field strength on large scales

In this chapter we have found expressions for the velocities of a three species system of protons, electrons and photons in both the small and large scale limit, firstly when the tight coupling approximation holds and then when it is broken. In the large scale limit we were able to substitute our large scale solution for the density perturbation to find the scale and time dependencies of the velocities. We found that the velocity differences between the three species can source an electric field and evaluated an approximation for the time dependence and amplitude of such an electric field. When we assumed the tight coupling approximation held we found,

$$\mathcal{E}_1 = \frac{Ac\beta\hat{R}_b}{6e\eta_0\sigma_{Te}\hat{n}_b^2}\left(1 + \frac{5a}{4\eta_0\hat{n}_b\sigma_{Te}c}\right) ,$$

and when tight coupling was broken we found,

$$\mathcal{E}_1 = \frac{2A\beta c^2}{3e\hat{n}_b}a^{-2} + \frac{2A\sigma_{Te}^2 c^2 m_p \beta^2}{3\mu_0 \hat{R}_b e^3}a^{-8} ,$$

where both expressions are given to next to leading order in a. We can also see, both from these results and the expressions for the velocities, that it is the Thompson interactions between the matter and radiation that plays a much more dominant

role in the behaviour of the species than the Coulomb collisions between the charged electrons and protons. It should be noted that each of these expressions are only first order results in a, only accurate to order of magnitude precision and only valid over the range of a considered. In Chapter 6 we will see that a first order electric field such as this generated during the radiation era can itself source a second order magnetic field. In the second half of this thesis we will study the generation of primordial magnetic fields using second order perturbations.

Chapter 5

Magnetic Fields and Cosmology

5.1 Inter-galactic magnetic fields

In the next two chapters we will be looking at an application of second order perturbation theory, namely that of primordial magnetic fields. In this chapter we will review the background to this research area and derive the fully relativistic Maxwell equations to second order in perturbation theory.

5.1.1 Observations

Magnetic fields have been observed in our universe on many scales, from local planetary scales through to intergalactic scales. In fact every time we have been able to probe a new scale we have found magnetic fields there. Magnetic fields were first seen on planetary scales and of course the existence of the Earth's magnetic field has been known for many years. It was in 1962, however, that the first galactic magnetic field was observed, when radio polarization was detected in the Milky Way by Westerhout et al. and Wielebinski et al., Ref. [84]. In the 60's and 70's with the ability to use large radio telescopes, such as the Effelsberg radio telescope and the Very Large Array in New Mexico, the number of galaxies that were known to contain magnetic fields grew and since then our knowledge of galactic magnetic fields has greatly improved. We know that they have typical coherence lengths of a few kpcs and have strengths of approximately a few μG [85–89]. More recently, there have also been observations of magnetic fields, with similar strengths, in higher redshift

galaxies [90]. Following this it was found that magnetic fields are also present in the intra cluster medium between galaxies. In the last couple of decades similar strength magnetic fields (approximately $1\mu G$) have been observed on galaxy cluster scales with coherence lengths of a few Mpcs [90–95] and even in superclusters [96]. However, we are interested here in a more recent discovery; within the last few years there have been observations targeting inter-cluster magnetic fields in voids, far from galaxies. These γ-ray observations give a lower limit for the magnitude of large scale magnetic fields of $10^{-17}G$ (for details of these observations see for instance Refs. [97–101].) Although at present not much is known about these large scale magnetic fields, there are exciting opportunities to learn more about them in the coming years with large radio telescopes such as the Square Kilometre Array on the horizon [102], the possibility of using a cosmic shear survey such as Euclid [103] and polarization data also due from Planck [104]. In the chapters that follow we will be looking at the origin for these inter-galactic magnetic fields which are observed in voids and at higher redshifts. For further information on the history of observed magnetic fields we refer to the reviews, Refs. [105–107].

5.1.2 Astrophysical or cosmological origin?

It is well known that the current observed magnetic fields might be explained by the amplification of small seed fields by either a dynamo mechanism [86, 108–110] or by adiabatic compression of a previously magnetised cloud [110, 111], or indeed both of these mechanisms simultaneously. Galactic dynamos are rotating galaxies containing a seed field. As the galaxy rotates, the field lines wind and rotational kinetic energy is turned into additional magnetic energy, thereby amplifying the magnetic field strength. The magnetic field strength can be amplified by anything between 6 and 24 orders of magnitude, depending on both the efficiency of the dynamo and the cosmological model it operates in (to achieve the largest amplifications of 24 orders is very unlikely as it requires an open universe [112]). Therefore, in order to arrive at magnetic fields with a strength of 1μG, which we currently observe in galaxies, we would need a seed field of between 10^{-12}G and 10^{-30}G. [86]. The adiabatic compression of previously magnetised clouds works in a similar way, the difference being field lines are compressed turning gravitational potential energy into magnetic

energy. This mechanism is not quite as efficient as the dynamo mechanism and only amplifies the field strength by up to 14 orders of magnitude, therefore, we would require a slightly stronger seed field of at least 10^{-20}G [110, 111]. Galactic dynamos and adiabatic compression of magnetised clouds can explain galactic and possibly cluster magnetic fields. However, it is difficult to use these to explain magnetic fields observed at high redshift, and even more so to explain intergalactic fields, since they both require the presence of a galaxy, or a compressing cloud, to work. In addition, the question still remains as to where the seed magnetic fields originated from. There is no definite answer to this question, but much work has been done trying to understand its origin, see for instance the recent reviews, Refs. [113–115]. We outline some of the generation mechanisms below.

The explanations for the seed field can be be split into two categories. Firstly, they could have been created post-recombination from astrophysical processes, for instance, by battery-type effects during structure formation, such as Biermann-battery mechanism [107] or supernova batteries [116]. Secondly, the seed fields could be primordial and have a cosmological origin. The astrophysical processes work on galactic scales and therefore at first it seems they could not source magnetic fields on cluster or intergalactic scales. However, magnetic fields on these scales may have been caused by magnetized outflows from nearby galaxies, for instance galactic winds caused by star formation [117] or relativistic outflows caused by Active Galactic Nuclei [118]. Whilst primordial origins may look more favorable, leading to inter-galactic magnetic fields (IGMFs) occurring even in voids and providing a clearer explanation for the existence of these magnetic fields at higher redshift, they do have their own problems, since sustaining a magnetic field in the early universe is difficult. To study any primordial magnetic field it is best to look at the inter-galactic medium where the effects of amplification are at their lowest. Distinguishing between the primordial and astrophysical origins will need more measurements of both the strength and the coherence length of the IGMF [113]. However, if it were found that these magnetic fields were cosmological in origin and were formed before the formation of the CMB and Big Bang Nucleosynthesis (BBN), this would open up the exciting possibility of using magnetic fields as a new probe for fundamental physics and possibly even physics beyond the Standard Model. It is the cosmological origins of magnetic fields that we will be concentrating on here.

Besides the primordial field needing to be strong enough to act as a seed for the dynamo mechanisms, we also require the early universe magnetic field to satisfy other observational constraints. Strong primordial magnetic fields have implications in the post-recombination universe which limits the potential strength any such seed field can have. The main observational constraints are: Firstly, nucleosynthesis arguments lead to a maximum strength at the time of galaxy formation of $10^{-7}G$ [110]. Secondly, the lack of gravitational wave observations leads to a maximum strength of between $10^{-9}G$ and $10^{-6}G$ depending on the scale of the super cluster they are observed in [119]. Thirdly, various CMB observables such as magnetised Sunyaev-Zeldovich effect, Faraday rotation, non-Gaussianity and the CMB isotropy, lead to a maximum present field strength of $10^{-9}G$ [120, 121]. More recently CMB data has been combined with data from the South Pole Telescope leading to a maximum primordial magnetic field strength of $3.5 \times 10^{-9}G$ [122]. Finally, the constraints coming from ionization data give a maximum comoving field strength of $10^{-9}G$ [123]. All of these observations lead to an upper limit on the strength of any primordial magnetic field observed today of the order of $10^{-9}G$.

5.1.3 Possible cosmological origins

The many explanations for the formation of primordial magnetic fields can be grouped into three main categories: inflation, phase transitions and second order perturbations, which we will outline briefly below. In addition to these three most popular classes of primordial magnetogenesis there are many other generation mechanisms which are possible. For instance magnetogenesis can occur during reheating or during an earlier epoch due to more exotic physics such as string physics and extra dimensions. For further details on all the generation mechanisms mentioned here see for instance Refs. [107, 113, 115, 124] and the references therein.

Firstly, a seed magnetic field could be produced during inflation. The basic premise here is that very long wavelength photons are generated from subhorizon quantum mechanical fluctuations during inflation. Then, at reheating, these electromagnetic waves are converted to large scale magnetic fields when the currents present in the conductive plasma can cause the elimination of the electric part. There are however problems with this mechanism. In order to generate these in-

flationary magnetic fields one must either couple the electromagnetic field to the inflaton, introduce a coupling that breaks conformal or gauge invariance, or both or break conformal symmetry [125–128]. In order to produce magnetic fields strong enough to account for galactic and inter-galactic magnetic fields one has the choice to rely on a very blue spectrum of scalar inflaton fluctuation (which is in tension with current observations), to let the electron charge become very large at early times, or break gauge invariance. Obviously none of these scenarios is ideal. Conventional magnetic fields in a flat FLRW metric are also diluted during inflation, by adiabatic magnetic decay and so are too weak (less than $10^{-50}G$ [125]) to seed and sustain a galactic dynamo. However, there has been much work in this field in trying to come up with a model which will allow the appropriate magnetic field to be generated. For more details see for instance Refs. [115, 129–131].

Secondly, magnetic fields could be produced during phase transitions such as electroweak or QCD symmetry breaking. If the phase transition is first order, bubble nucleation occurs. As the bubbles and horizons grow bubble walls collide and these collisions can produce magnetic fields [132–134]. Whilst the magnetic fields produced can be strong, they often have small coherence lengths. It has been shown though that with an inverse cascade occurring it might be possible to generate a magnetic field of up to $10^{-21}G$ [135]. However in the Standard Model neither of these phase transitions are first order, so the above process would require going beyond the Standard Model. If the phase transition is second order it is still possible to form magnetic fields, however, they have very small coherence lengths and will get damped away [136–138], therefore, we would only expect to generate magnetic fields with a magnitude of approximately $10^{-30}G$ [136]. For more details on magnetic fields generated by phase transitions see for instance Refs. [113, 115].

Lastly, magnetic fields may have been created by second order perturbations between lepton decoupling and recombination. This mechanism was first proposed by Harrison [139], who showed that if we have first order vector perturbations and if electrons and protons are not perfectly coupled, then the difference in the vorticity between the two species can generate a magnetic field. In standard inflation first order vectors are not present, assuming we are not able to directly source them by other means, such as topological defects, the only other way to have first order vectors would be to modify our theory of gravity. For instance, using a vector-tensor

gravity such as Aether theory leads to magnetic fields with strength of approximately $10^{-22}G$ [140]. It is however possible to take this beyond first order and even with no first order vectors, at second order it is possible to generate a magnetic field, although as this is a second order result one would expect the strength of such a magnetic field to be small. There has been some work on this at second order both analytically [83,141–146] and numerically [147–149]. Whilst there is some disagreement between these papers none generate a magnetic field larger than $10^{-24}G$.

There do, however, remain some interesting open questions in this field. In the following two chapters we will be looking at generating magnetic fields using second order perturbations in more detail from an analytic perspective. We will present a more complete analytic calculation than has be done previously, as much of the previous work has concentrated on one or two specific terms rather than the full set of equations. In considering all terms we hope to get a better match to the numerical calculations. We will also look at the scale dependence of the magnetic field and how this varies under different conditions and assumptions and discuss how the result depends on the cut off scale that must be introduced in both analytic and numerical calculations. We will also be presenting an analytic set up that allows us to analyse the difference between the different tight coupling scenarios, what effect that has on the magnetic field produced and what difference it makes if we have non-adiabatic pressure present. In particular, we will look at how the result differs depending on where the non-adiabatic pressure comes from, whether that be isocurvature which is introduced during inflation or non-adiabatic pressure due to a multi-species plasma.

5.2 Relativistic Maxwell Equations

The study of the interaction between plasmas and electromagnetic fields is vast and has many obvious applications. However, if we are to study primordial magnetogenesis in the early universe then we need to also take General Relativity into account. We will need both a relativistic theory of electromagnetism and a formalism for the study of multi-fluid charged systems. As we are interested in magnetogenesis brought about by second order perturbations, both these formalisms will need to be set in cosmological perturbation theory beyond linear order. Multi-fluid charged systems were discussed in detail in Chapter 4 where we derived the multi-species

energy and momentum equations for a multi-fluid system comprising of electrons, protons, photons and a background electric field. There has been much work in the past studying relativistic maxwell equations [150, 151]. Much of the more recent work within cosmology has been using the covariant approach, see for instance Refs [152,153] and the references contained within. In this chapter, whilst the initial equations we present are not new, we do provide a complementary approach by rederiving the fully relativistic maxwell equations using the gauge-invariant Bardeen formalism, which is covered in detail in Chapter 2. We also provide expanded equations, containing all terms in two different gauges, flat and Newtonian and briefly discuss the gauge dependence of the Faraday tensor. We will start by reviewing some of the geometrical quantities we will need and then proceed to review the equations which govern the evolution of electromagnetic fields. Finally, we will derive a self-consistent fully relativistic set of Maxwell Equations, expanded up to second order.

5.2.1 Geometrical Quantities

We will need to decompose the Maxwell equations below with respect to u_μ, the observer's 4-velocity, so that the equations are in a form we can solve perturbatively. With this in mind we consider some geometrical quantities we will need first. The 4-velocity was defined in Eq. (2.53) and Eq. (2.56) and its covariant derivative can be decomposed as follows [9],

$$u_{\mu;\nu} = \sigma_{\mu\nu} + \omega_{\mu\nu} + \frac{1}{3}\theta h_{\mu\nu} - \dot{u_\mu} u_\nu \,, \tag{5.1}$$

where $\dot{u_\mu} = u_{\mu;\nu}u^\nu$ and $\dot{u_\mu}u_\mu = 0$. $\omega_{\mu\nu}$ is the vorticity and is an antisymmetric tensor, $\sigma_{\mu\nu}$ is the shear and is a symmetric and trace free tensor, θ is the expansion rate and $h_{\mu\nu}$ is the symmetric spatial projection tensor. Taking each of these geometrical quantities we can define them in terms of the 4-velocity and therefore write them in terms of the metric perturbations. The projection tensor is defined as,

$$h_{\mu\nu} = g_{\mu\nu} + u_\mu u_\nu \,, \tag{5.2}$$

where $h_{\mu\nu}u^{\nu} = 0$, $h^{\mu}_{\mu} = 3$ and $h^{\mu}_{\nu}h^{\nu}_{\lambda} = h^{\mu}_{\lambda}$. The expansion rate in terms of the 4-velocity is

$$\theta = u^{\mu}_{;\mu}\,. \tag{5.3}$$

Expanding the expansion rate order by order in a series expansion we can write down the background and first order expressions in terms of the metric perturbations [9],

$$\theta_0 = \frac{3}{a}\mathcal{H} \tag{5.4}$$

$$\theta_1 = -\frac{3}{a}\left[\mathcal{H}\phi_1 + \psi_1' - \frac{1}{3}\nabla^2\sigma_1\right], \tag{5.5}$$

where σ_1 is the scalar shear and is defined to be $\sigma_1 \equiv E_1' - B_1$.

The shear in terms of the 4-velocity is

$$\sigma_{\mu\nu} = \frac{1}{2}h^{\alpha}_{\mu}h^{\beta}_{\nu}(u_{\alpha;\beta} + u_{\beta;\alpha}) - \frac{1}{3}\theta h_{\mu\nu}\,. \tag{5.6}$$

Expanding the shear order by order noting that by definition of the FLRW spacetime, the shear is zero in the background, we can write down the first order expressions again in terms of the metric perturbations [9],

$$\sigma_{100} = 0\,, \quad \sigma_{10i} = 0\,, \tag{5.7}$$

$$\sigma_{1ij} = a(\partial_i\partial_j - \frac{1}{3}\delta_{ij}\nabla^2)\sigma_1 + a(F_{1(i,j)}' - B_{1(i,j)}) + \frac{a}{2}h_{1ij}'\,. \tag{5.8}$$

Finally the vorticity in terms of the 4-velocity is

$$\omega_{\mu\nu} = \frac{1}{2}h^{\alpha}_{\mu}h^{\beta}_{\nu}(u_{\alpha;\beta} - u_{\beta;\alpha})\,. \tag{5.9}$$

Again expanding the vorticity order by order and noting that by definition in FLRW spacetime the vorticity is zero in the background, the first order expression in terms of the metric perturbations is,

$$\omega_{100} = 0\,, \quad \omega_{10i} = 0\,, \tag{5.10}$$

$$\omega_{1ij} = \frac{1}{2}(V_{1i,j} - V_{1i,j})\,, \tag{5.11}$$

where $V_1 = v_1 + B_1$.

We can change between the vector and tensor definitions of the vorticity ω using the following relationships.

$$\omega^\mu = \frac{1}{2}\epsilon^{\mu\nu\lambda\gamma}u_\nu\omega_{\lambda\gamma}, \quad \omega_{\mu\nu} = \epsilon_{\mu\nu\lambda\gamma}\omega^\lambda u^\gamma \,. \tag{5.12}$$

5.2.2 Maxwell equations

The main component of the Maxwell equations is the Faraday tensor, which in an inertial frame is defined by

$$F_{\mu\nu} = A_{\nu,\mu} - A_{\mu,\nu} \,, \tag{5.13}$$

where A_μ is the 4-potential, given by

$$A_\mu = (-\phi, \mathbf{A}) \,, \tag{5.14}$$

and ϕ is the scalar electromagnetic potential and $\mathbf{A}$ is the vector electromagnetic potential. The electric ($\mathcal{E}_\mu$) and magnetic ($\mathcal{M}_\mu$) fields are defined in terms of these potentials,

$$\mathcal{M}_\mu = \epsilon_{\mu\nu\lambda}A^{\lambda,\nu}, \quad \mathcal{E}_\mu = -\phi_{,\mu} - \dot{A}_\mu \,. \tag{5.15}$$

The electric and magnetic fields measured by a comoving observer with 4-velocity u^μ can be described using the Faraday tensor,

$$\mathcal{E}^\mu = F^{\mu\nu}u_\nu, \quad \mathcal{M}^\lambda = \frac{1}{2}\epsilon^{\mu\nu\lambda}F_{\mu\nu} = \frac{1}{2}\epsilon^{\mu\nu\lambda\delta}u_\nu F_{\mu\delta} \,, \tag{5.16}$$

where

$$\mathcal{E}_\mu u^\mu = 0, \quad \mathcal{M}_\mu u^\mu = 0 \,. \tag{5.17}$$

Finally, the evolution of these magnetic and electric fields is described by Maxwell's equations,

$$F_{[\mu\nu;\lambda]} = 0, \quad F^{\mu\nu}{}_{;\nu} = \mu_0 j^\mu \,, \tag{5.18}$$

where $j^\mu = a^{-1}(\hat{\rho}, \mathbf{j})$ is the four-current that sources the electromagnetic field, $\hat{\rho}$ is the comoving charge density, $\mathbf{j}$ is the comoving charge current density and μ_0 is the magnetic constant (or vacuum permeability), the value of which is given in

Appendix A. This four-current can be decomposed as follows

$$\hat{\rho} = -j^{\mu}u_{\mu}, \quad \mathcal{J}^{\mu} = h^{\mu}{}_{\nu}j^{\nu}\,. \tag{5.19}$$

where $\mathcal{J}^{\mu}$ is the projected four-current, orthogonal to the 4-velocity.

By projecting the Maxwell equations along and orthogonal to the 4-velocity vector, multiplying by u_{μ} and h^{μ}_{ν} respectively, we can decompose Maxwell's equations with respect to u_{μ}. We present the full details of this projection in Appendix C, and we arrive at the following set of four covariant Maxwell equations,

$$\begin{aligned} \mathcal{E}^{\mu}{}_{,\mu} + \Gamma^{\mu}_{k\mu}\mathcal{E}^{k} - \dot{u_{\mu}}\mathcal{E}^{\mu} &= \hat{\rho} - 2\omega^{\mu}\mathcal{M}_{\mu}\,, \\ \mathcal{M}^{\mu}{}_{,\mu} + \Gamma^{\mu}_{k\mu}\mathcal{M}^{k} - \dot{u_{\mu}}\mathcal{M}^{\mu} &= -\omega^{\mu}\mathcal{E}_{\mu}\,, \end{aligned} \tag{5.20}$$

and

$$\begin{aligned} \dot{\mathcal{E}}^{\lambda\perp} &= (\omega^{\lambda}_{\nu} + \sigma^{\lambda}_{\nu} - \frac{2}{3}\theta h^{\lambda}_{\nu})\mathcal{E}^{\nu} + \epsilon^{\lambda\nu\mu}\dot{u}_{\nu}\mathcal{M}_{\mu} - \epsilon^{\lambda\nu\mu}(\mathcal{M}_{\nu,\mu} - \Gamma^{k}_{\nu\mu}\mathcal{M}_{k}) - \mathcal{J}^{\lambda}\,, \\ \dot{\mathcal{M}}^{\lambda\perp} &= (\omega^{\lambda}_{\nu} + \sigma^{\lambda}_{\nu} - \frac{2}{3}\theta h^{\lambda}_{\nu})\mathcal{M}^{\nu} - \epsilon^{\lambda\nu\mu}\dot{u}_{\nu}\mathcal{E}_{\mu} + \epsilon^{\lambda\nu\mu}(\mathcal{E}_{\nu,\mu} - \Gamma^{k}_{\nu\mu}\mathcal{E}_{k})\,, \end{aligned} \tag{5.21}$$

where $\mathcal{E}^{\lambda\perp}$ and $\mathcal{M}^{\lambda\perp}$ are the projected electric and magnetic field respectively, both orthogonal to the 4-velocity.

Alternatively, the third and fourth equation above can be written as:

$$\begin{aligned} h^{\lambda}_{\mu}u^{\alpha}\mathcal{E}^{\mu}_{,\alpha} &= -(u^{\lambda}u_{\mu}\Gamma^{\mu}_{k\alpha} - \Gamma^{\lambda}_{k\alpha})u^{\alpha}\mathcal{E}^{k} + (\omega^{\lambda}_{\nu} + \sigma^{\lambda}_{\nu} - \frac{2}{3}\theta h^{\lambda}_{\nu})\mathcal{E}^{\nu} + \epsilon^{\lambda\nu\mu}\dot{u}_{\nu}\mathcal{M}_{\mu} \\ &\quad -\epsilon^{\lambda\nu\mu}(\mathcal{M}_{\nu,\mu} - \Gamma^{k}_{\nu\mu}\mathcal{M}_{k}) - \mathcal{J}^{\lambda}\,, \end{aligned} \tag{5.22}$$

$$\begin{aligned} h^{\lambda}_{\mu}u^{\alpha}\mathcal{M}^{\mu}_{,\alpha} &= -(u^{\lambda}u_{\mu}\Gamma^{\mu}_{k\alpha} - \Gamma^{\lambda}_{k\alpha})u^{\alpha}\mathcal{M}^{k} + (\omega^{\lambda}_{\nu} + \sigma^{\lambda}_{\nu} - \frac{2}{3}\theta h^{\lambda}_{\nu})\mathcal{M}^{\nu} - \epsilon^{\lambda\nu\mu}\dot{u}_{\nu}\mathcal{E}_{\mu} \\ &\quad +\epsilon^{\lambda\nu\mu}(\mathcal{E}_{\nu,\mu} - \Gamma^{k}_{\nu\mu}\mathcal{E}_{k})\,. \end{aligned} \tag{5.23}$$

Recalling that we are interested in the second order Maxwell equations we now expand out the Maxwell equations given in Eq. (5.20) and Eq. (5.21). We start by expanding our electric and magnetic components out in a power series as we did

with the density in Eq. (2.3),

$$\mathcal{M} = \mathcal{M}_1 + \frac{1}{2}\mathcal{M}_2 + \frac{1}{6}\mathcal{M}_3 + \dots , \tag{5.24}$$

$$\mathcal{E} = \mathcal{E}_1 + \frac{1}{2}\mathcal{E}_2 + \frac{1}{6}\mathcal{E}_3 + \dots , \tag{5.25}$$

$$\hat{\rho} = \hat{\rho_0} + \hat{\rho_1} + \frac{1}{2}\hat{\rho_2} + \frac{1}{6}\hat{\rho_3} + \dots , \tag{5.26}$$

and similarly for the expansion rate, vorticity and shear. We have set the background electric and magnetic fields to zero in the equations above to satisfy observational constraints on the isotropy of the CMB.

We use CPT, as described in Chapter 2 in order to solve the magnetic field evolution equations order by order. Substituting for the connection terms, (given in Appendix B) into Eq. (5.20) to Eq. (5.21) above and expanding the components to second order we obtain a set of evolution and constraint equations for the magnetic and electric fields. We have used the algebraic computer package Cadabra [154] to assist in simplifying these perturbed equations. We will eliminate the temporal component of the magnetic and electric field by recalling that for a general observer with a 4-velocity given by Eq. (2.56) the time and space components of the magnetic and electric field are related by Eq. (5.17). Expanding these relations order by order it can be shown that the first order temporal components are zero and the second order components satisfy the following constraints,

$$\mathcal{M}_{20} = -2\mathcal{M}_{1i}{v_1}^i , \tag{5.27}$$

$$\mathcal{E}_{20} = -2\mathcal{E}_{1i}{v_1}^i . \tag{5.28}$$

We will also be eliminating the expansion rates in terms of metric components using the expressions given in Eq. (5.4).

5.2.3 First order Maxwell Equations

The first order Maxwell equations are gauge independent and are given by,

$${\mathcal{M}_1}^i{}_{,i} = 0 , \tag{5.29}$$

$$\mathcal{E}_1{}^i{}_{,i} = \mu_0 \hat{\rho}_1 \,, \tag{5.30}$$

$$\mathcal{M}_1{}^{i\prime} + 2\mathcal{H}\mathcal{M}_1{}^i = -a^2 \epsilon^{0ijk} \mathcal{E}_{1k,j} \,, \tag{5.31}$$

$$\mathcal{E}_1{}^{i\prime} + 2\mathcal{H}\mathcal{E}_1{}^i = a^2 \epsilon^{0ijk} \mathcal{M}_{1k,j} - a\mu_0 \mathcal{J}_1{}^i \,. \tag{5.32}$$

If we assume standard inflation then there are no first order vector perturbations sourced during inflation, and any that did exist would rapidly decay. Using the fact (see Section 2.1.2) that any first order vector quantity can be decomposed into the gradient of a scalar and a divergence-free vector part, we now assume that the divergence-free vector parts of these expressions are zero. For instance, the first order electric field can be written as,

$$\mathcal{E}_{1i} = \mathcal{E}_{1i}^{\text{vec}} + \mathcal{E}_{1,i} = \mathcal{E}_{1,i} \,. \tag{5.33}$$

This allows us to write all our first order equations in terms of scalars rather than vectors,

$$\nabla^2 \mathcal{M}_1 = 0 \,, \tag{5.34}$$

$$\nabla^2 \mathcal{E}_1 = \mu_0 \hat{\rho}_1 \,, \tag{5.35}$$

$$\mathcal{M}_{1,}{}^{i\prime} + 2\mathcal{H}\mathcal{M}_{1,}{}^i = -a^2 \epsilon^{0ijk} \mathcal{E}_{1,kj} = 0 \,, \tag{5.36}$$

$$\mathcal{E}_{1,}{}^{i\prime} + 2\mathcal{H}\mathcal{E}_{1,}{}^i = a^2 \epsilon^{0ijk} \mathcal{M}_{1,kj} - a\mu_0 \mathcal{J}_{1,}{}^i = -a\mu_0 \mathcal{J}_{1,}{}^i \,. \tag{5.37}$$

We have used the fact that taking the curl of a gradient of a scalar i.e. $\epsilon^{0ijk}\mathcal{E}_{1,kj}$ will always be zero. This leads us to conclude that at first order the magnetic evolution equation has no source term, as we would expect. In order to proceed we must move to second order.

5.2.4 Second Order Maxwell Equations

Here we present the equations derived using Cadabra [154] for the second order Maxwell equations. We have kept these equations as general as possible, making no assumptions other than a FLRW background and not yet specifying a gauge.

The constraint equations are given by,

$$\begin{aligned}
\mathcal{M}_2{}^i{}_{,i} &= -2(E_{,ji}{}^j - 3\psi_{,i} + 2\mathcal{H}v_{1i} + 2\phi_{1,i} - B_{1,i}{}' + S_{1i}{}' - 2v_{1i}{}')\mathcal{M}_1{}^i \\
&\quad -2a^2\epsilon^{0ijk}v_{1i}\mathcal{E}_{1k,j} + 2\omega_1{}^i\mathcal{E}_{1i}\,, \qquad (5.38)\\
\mathcal{E}_2{}^i{}_{,i} &= -2(E_{,ji}{}^j - 3\psi_{,i} + 2\phi_{1,i} - 2v_{1i}{}' - B_{1,i}{}' + S_{1i}{}' + 2\mathcal{H}v_{1i})\mathcal{E}_1{}^i \\
&\quad +2a^2v_{1i}\epsilon^{0ijk}\mathcal{M}_{1k,j} + \mu_0\hat{\rho}_2 - 4\omega_1{}^i\mathcal{M}_{1i} - 2a\mu_0 v_{1i}\mathcal{J}_1{}^i\,, \qquad (5.39)
\end{aligned}$$

and the evolution equations by,

$$\begin{aligned}
\mathcal{M}_2{}^{i\prime} &+ 2\mathcal{H}\mathcal{M}_2{}^i \\
&= (S_{1j,}{}^i - S_1{}^i{}_{,j} + 2E_{1,j}{}^{i\prime} + 2F_{1(j,}{}^{i)\prime} + h_{1j}{}^{i\prime} + 2a(\omega_1{}^i{}_j + \sigma_1{}^i{}_j))\mathcal{M}_1{}^j \\
&\quad -\frac{2}{3}(2v_1{}^j{}_{,j} + 2E_{1,j}{}^{j\prime} - 3\psi_1')\mathcal{M}_1{}^i - 2v_1{}^j\mathcal{M}_1{}^i{}_{,j} \\
&\quad -2a^4(v_1{}^j + B_{1,}{}^j - S_1{}^j)(\mathcal{M}_{1j,}{}^i - \mathcal{M}_1{}^i\,,j) \\
&\quad -2a^2\epsilon^{0ijk}((v_{1j}{}' + B_{1,j}{}' - S_{1j}{}' - \phi_{1,j} - 2\mathcal{H}(v_{1j} + B_{1,j}) + 2\mathcal{H}S_{1j})\mathcal{E}_{1k} \\
&\quad +\frac{1}{2}\mathcal{E}_{2k,j} - (E_{1,jkl} + F_{1(j,k)l} + \frac{1}{2}h_{1jk,l})\mathcal{E}_1{}^l + 2\phi_1\mathcal{E}_{1k,j} \\
&\quad -v_{1j}a\mu_0\mathcal{J}_{1k} - B_{1,j}a\mu_0\mathcal{J}_{1k} + S_{1j}a\mu_0\mathcal{J}_{1k})\,,
\end{aligned} \qquad (5.40)$$

$$\begin{aligned}
\mathcal{E}_2{}^{i\prime} &+ 2\mathcal{H}\mathcal{E}_2{}^i \\
&= (S_{1j,}{}^i - S_1{}^i{}_{,j} + 2E_{1,j}{}^{i\prime} + 2F_{1(j,}{}^{i)\prime} + h_{1j}{}^{i\prime} + 2a(\omega_1{}^i{}_j + \sigma_1{}^i{}_j))\mathcal{E}_1{}^j \\
&\quad -2v_1{}^j\mathcal{E}_1{}^i{}_{,j} - \frac{2}{3}(2v_1{}^j{}_{,j} + 2E_{1,j}{}^{j\prime} - 3\psi_1')\mathcal{E}_1{}^i \\
&\quad -2a^4(v_1{}^j + B_{1,}{}^j - S_1{}^j)(\mathcal{E}_{1j,}{}^i - \mathcal{E}_1{}^i{}_{,j}) \\
&\quad +2a^2\epsilon^{0ijk}((v_{1j}{}' + B_{1,j}{}' - S_{1j}{}' - \phi_{1,j} - 2\mathcal{H}(v_{1j} + B_{1,j} - S_{1j}))\mathcal{M}_{1k} \\
&\quad +\frac{1}{2}\partial_j\mathcal{M}_{2k} - (E_{1,jkl} + F_{1(j,k)l} + \frac{1}{2}h_{1jk,l})\mathcal{M}_1{}^l + 2\phi_1\mathcal{M}_{1k,j}) \\
&\quad -\mu_0\mathcal{J}_2{}^i - 2\phi_1 a\mu_0\mathcal{J}_1{}^i\,.
\end{aligned} \qquad (5.41)$$

Note that here we do have a source term for the second order Maxwell evolution equation. Again this is as we would expect and there is much work in the literature based on trying to evaluate and explain this source term, see for instance Refs. [146–149]. In Chapter 6 we will be looking at this source term in more detail. In order to make our equations more useful for analytic and numeric calculations we will now

present them in two different gauges. For more information about picking gauges and gauge choices see Section 2.1.

5.2.4.1 Maxwell equations in flat gauge

First we write down the second order Maxwell equations in flat gauge (see Section 2.2.2.1). This is the gauge that we use in Chapter 6 where we study the second order source term. It is a convenient gauge for analytic work.

The constraint equations in flat gauge are given by,

$$\begin{aligned}
{\mathcal{M}_2}^i{}_{,i} &= -2(2\mathcal{H}v_{1i} + 2\phi_{1,i} - {B_{1,i}}' + {S_{1i}}' - 2{v_{1_i}}')\mathcal{M}_1{}^i + 2\omega_1{}^i\mathcal{E}_{1i} \\
&\quad -2a^2\epsilon^{0ijk}v_{1i}\mathcal{E}_{1k,j}\,, \qquad (5.42)\\
{\mathcal{E}_2}^i{}_{,i} &= -2(2\phi_{1,i} - 2{v_{1_i}}' - {B_{1,i}}' + {S_{1i}}' + 2\mathcal{H}v_{1i})\mathcal{E}_1{}^i - 4\omega_1{}^i\mathcal{M}_{1i} \\
&\quad +2a^2v_{1i}\epsilon^{0ijk}\mathcal{M}_{1k,j} + \mu_0\hat{\rho}_2 - 2a\mu_0 v_{1i}\mathcal{J}_1{}^i\,, \qquad (5.43)
\end{aligned}$$

and the evolution equations are,

$$\begin{aligned}
{\mathcal{M}_2}^{i\prime} &+ 2\mathcal{H}{\mathcal{M}_2}^i \\
&= (S_{1j,}{}^i - S_1{}^i{}_{,j} + {h_{1j}}^{i\prime} + 2a({\omega_1}^i{}_j + {\sigma_1}^i{}_j))\mathcal{M}_1{}^j \\
&\quad -\frac{4}{3}{v_1}^j{}_{,j}\mathcal{M}_1{}^i - 2{v_1}^j\mathcal{M}_1{}^i{}_{,j} - 2a^4({v_1}^j + B_{1,}{}^j - S_1{}^j)(\mathcal{M}_{1j,}{}^i - \mathcal{M}_1{}^i{}_{,j}) \\
&\quad -2a^2\epsilon^{0ijk}(({v_{1_j}}' + {B_{1,j}}' - {S_{1j}}' - \phi_{1,j} - 2\mathcal{H}(v_{1j} + B_{1,j}) + 2\mathcal{H}S_{1j})\mathcal{E}_{1k} \\
&\quad +\frac{1}{2}\mathcal{E}_{2k,j} - \frac{1}{2}h_{1jk,l}\mathcal{E}_1{}^l + 2\phi_1\mathcal{E}_{1k,j} - v_{1j}a\mu_0\mathcal{J}_{1k} - B_{1,j}a\mu_0\mathcal{J}_{1k} + S_{1j}a\mu_0\mathcal{J}_{1k})\,, \qquad (5.44)
\end{aligned}$$

$$\begin{aligned}
{\mathcal{E}_2}^{i\prime} &+ 2\mathcal{H}{\mathcal{E}_2}^i \\
&= (S_{1j,}{}^i - S_1{}^i{}_{,j} + {h_{1j}}^{i\prime} + 2a({\omega_1}^i{}_j + {\sigma_1}^i{}_j))\mathcal{E}_1{}^j \\
&\quad -2{v_1}^j\mathcal{E}_1{}^i{}_{,j} - 2a^4({v_1}^j + B_{1,}{}^j - S_1{}^j)(\mathcal{E}_{1j,}{}^i - \mathcal{E}_1{}^i{}_{,j}) - \frac{4}{3}{v_1}^j{}_{,j}\mathcal{E}_1{}^i \\
&\quad +2a^2\epsilon^{0ijk}(({v_{1_j}}' + {B_{1,j}}' - {S_{1j}}' - \phi_{1,j} - 2\mathcal{H}(v_{1j} + B_{1,j} - S_{1j}))\mathcal{M}_{1k} \\
&\quad +\frac{1}{2}\partial_j\mathcal{M}_{2k} - \frac{1}{2}h_{1jk,l}\mathcal{M}_1{}^l + 2\phi_1\mathcal{M}_{1k,j}) - \mu_0\mathcal{J}_2{}^i - 2\phi_1 a\mu_0\mathcal{J}_1{}^i\,. \qquad (5.45)
\end{aligned}$$

5.2.4.2 Maxwell equations in Newtonian Gauge

We also write down our equations in Newtonian gauge (see Section 2.2.2.2). This is a particularly useful gauge to present equations in as it is the gauge used for many of the Boltzmann codes which are needed to evaluate magnetic field numerically, see for instance [155].

The constraint equations in Newtonian gauge are given by,

$$\begin{aligned} {\mathcal{M}_2}^i{}_{,i} &= -2(-3\psi_{,i} + 2\mathcal{H}v_{1i} + 2\phi_{1,i} - 2{v_{1i}}')\mathcal{M}_1{}^i + 2\omega_1{}^i\mathcal{E}_{1i} \\ &\quad -2a^2\epsilon^{0ijk}v_{1i}\mathcal{E}_{1k,j}\,, \qquad (5.46) \\ {\mathcal{E}_2}^i{}_{,i} &\quad -2(-3\psi_{,i} + 2\phi_{1,i} - 2{v_{1i}}' + 2\mathcal{H}v_{1i})\mathcal{E}_1{}^i - 4\omega_1{}^i\mathcal{M}_{1i} \\ &\quad +2a^2v_{1i}\epsilon^{0ijk}\mathcal{M}_{1k,j} + \mu_0\hat{\rho}_2 - 2a\mu_0 v_{1i}\mathcal{J}_1{}^i\,, \qquad (5.47) \end{aligned}$$

and the evolution equations, by,

$$\begin{aligned} {\mathcal{M}_2}^{i'} &+ 2\mathcal{H}{\mathcal{M}_2}^i \\ &= (2{F_{1(j,}}^{i)}{}' + {h_{1j}}^{i'} + 2a({\omega_1}^i{}_j + {\sigma_1}^i{}_j))\mathcal{M}_1{}^j - \frac{2}{3}(2{v_1}^j{}_{,j} - 3\psi_1')\mathcal{M}_1{}^i \\ &\quad -2{v_1}^j\mathcal{M}_1{}^i{}_{,j} - 2a^4{v_1}^j(\mathcal{M}_{1j,}{}^i - \mathcal{M}_1{}^i{}_{,j}) - 2a^2\epsilon^{0ijk}(\frac{1}{2}\mathcal{E}_{2k,j} + 2\phi_1\mathcal{E}_{1k,j} \\ &\quad +({v_{1j}}' - 2\mathcal{H}v_{1j} - \phi_{1,j})\mathcal{E}_{1k} - (F_{1(j,k)l} + \frac{1}{2}h_{1jk,l})\mathcal{E}_1{}^l - v_{1j}a\mu_0\mathcal{J}_{1k})\,, \qquad (5.48) \\ {\mathcal{E}_2}^{i'} &+ 2\mathcal{H}{\mathcal{E}_2}^i \\ &= (2{F_{1(j,}}^{i)}{}' + {h_{1j}}^{i'} + 2a({\omega_1}^i{}_j + {\sigma_1}^i{}_j))\mathcal{E}_1{}^j - 2{v_1}^j\mathcal{E}_1{}^i{}_{,j} - 2a^4{v_1}^j(\mathcal{E}_{1j,}{}^i - \mathcal{E}_1{}^i{}_{,j}) \\ &\quad -\frac{2}{3}(2{v_1}^j{}_{,j} - 3\psi_1')\mathcal{E}_1{}^i + 2a^2\epsilon^{0ijk}(({v_{1j}}' - \phi_{1,j} - 2\mathcal{H}(v_{1j})\mathcal{M}_{1k} + \frac{1}{2}\partial_j\mathcal{M}_{2k} \\ &\quad -(F_{1(j,k)l} + \frac{1}{2}h_{1jk,l})\mathcal{M}_1{}^l + 2\phi_1\mathcal{M}_{1k,j}) - \mu_0\mathcal{J}_2{}^i - 2\phi_1 a\mu_0\mathcal{J}_1{}^i\,. \qquad (5.49) \end{aligned}$$

5.3 Gauge dependence

In this chapter we have combined electromagnetism with CPT. We can now consider the gauge dependence of the magnetic and electric fields by studying how the Faraday tensor transforms.

Splitting the Faraday tensor order by order we have,

$$F_{\mu\nu} = F_{0\mu\nu} + F_{1\mu\nu} + \frac{1}{2}F_{2\mu\nu} + \dots \,. \tag{5.50}$$

where the isotropy of the FLRW metric requires that $F_{0\mu\nu} \equiv 0$. By considering the transformation law for a 2-tensor, which we gave in Eq. (2.28), at first order the Faraday tensor transforms as,

$$\widetilde{F_{1\mu\nu}} = F_{1\mu\nu} \,. \tag{5.51}$$

That is, in the absence of the zeroth order quantity the Faraday tensor is gauge-invariant at first order, (this is known as the Stewart-Walker Lemma).

As introduced in Section 2.2.1 we can give the second order transformation law for a 2-tensor [9],

$$\begin{aligned}\widetilde{\delta T_{2\mu\nu}} \;=\; & \delta T_{2\mu\nu} + + T_{\mu\nu,\ \lambda}\xi_2^\lambda + T_{\lambda\nu}\xi^\lambda_{2,\mu} + T_{\mu\lambda}\xi^\lambda_{2,\nu} + 2\left[\delta T_{\mu\nu,\ \lambda}\xi_1^\lambda + \delta T_{\lambda\nu}\xi^\lambda_{1,\mu} + \delta T_{\mu\lambda}\xi^\lambda_{1,\nu}\right] \\ & + T_{\mu\nu,\ \lambda\alpha}\xi_1^\lambda\xi_1^\alpha + T_{\mu\nu,\ \lambda}\xi^\lambda_{1\ ,\alpha}\xi_1^\alpha + 2\left[T_{\mu\lambda,\ \alpha}\xi_1^\alpha\xi^\lambda_{1\ ,\nu} + T_{\lambda\nu,\ \alpha}\xi_1^\alpha\xi^\lambda_{1\ ,\mu} + T_{\lambda\alpha}\xi^\lambda_{1\ ,\mu}\xi^\alpha_{1\ ,\nu}\right] \\ & + T_{\mu\lambda}\left(\xi^\lambda_{1\ ,\nu\alpha}\xi_1^\alpha + \xi^\lambda_{1\ ,\alpha}\xi^\alpha_{1\ ,\nu}\right) + T_{\lambda\nu}\left(\xi^\lambda_{1\ ,\mu\alpha}\xi_1^\alpha + \xi^\lambda_{1\ ,\alpha}\xi^\alpha_{1\ ,\mu}\right) \,. \end{aligned} \tag{5.52}$$

It is clear that as the Faraday tensor is zero in the background, the above expression will simplify greatly and the second order transformation will only depend on the first order gauge generator, ξ^i,

$$\widetilde{F_{2\mu\nu}} = F_{2\mu\nu} + 2\left[F_{1\mu\nu,\lambda}\xi_1^\lambda + F_{1\mu\lambda}\xi^\lambda_{1,\ \nu} + F_{1\lambda\nu}\xi^\lambda_{1,\ \mu}\right] . \tag{5.53}$$

Thus, at second order the Faraday tensor is gauge dependent.

The magnetic and electric fields inherit the gauge dependence of the Faraday tensor. For example, the magnetic field at linear order is gauge-invariant,

$$\widetilde{\mathcal{M}_{1\mu}} = \mathcal{M}_{1\mu} \,, \tag{5.54}$$

but at second order transforms as

$$\widetilde{\mathcal{M}_{2\mu}} = \mathcal{M}_{2\mu} + 2\left(\mathcal{M}_{1\mu,\lambda}\xi_1^\lambda + \mathcal{M}_{1\lambda}\xi^\lambda_{1,\ \mu}\right) \,, \tag{5.55}$$

which, if we use the expressions given in Section 2.2.2.1, in flat gauge becomes,

$$\widetilde{\mathcal{M}_{2\mu}} = \mathcal{M}_{2\mu} + 2\left(\mathcal{M}_{1\mu}'\frac{\psi}{\mathcal{H}} - \mathcal{M}_{1\mu,i}E_{1,}{}^{i} - \mathcal{M}_{1\mu,i}F_{1}^{i} - \mathcal{M}_{1i}E_{1,\ \mu}{}^{i} - \mathcal{M}_{1i}F_{1,\ \mu}^{i}\right). \tag{5.56}$$

Chapter 6

Magnetic fields generated from perturbations

In Chapter 5 we derived the four relativistic Maxwell equations order by order. In this chapter we will be using the magnetic evolution equation to work out the magnitude and scale dependence of magnetic fields generated during the radiation era. As mentioned in the previous chapter this has been studied in the past [**?**, 83, 141, 142], in particular numerically [144–149]. However, although these previous papers were in very broad agreement, the analytic calculation previously carried out did not address all terms and were not in very close agreement with each other, see Section 6.7.2 for more details. Our aim in this chapter, therefore, is to complete a full analytic calculation of the power spectrum in order to compare to the numerical results. We will be considering all terms, initially, and only then dropping those which are sub-dominant. We hope to gain a deeper understanding of the scale and amplitudes expected and to see how this compares with observations and previous numerical results. We will also be looking at which parts of the source term have the largest effect on the generated magnetic fields, in particular we will be comparing the effect of density perturbation to that of the non-adiabatic pressure perturbation. We will also be looking at the effect of introducing a non-adiabatic term coming from the possible isocurvature remaining at the end of inflation. Throughout this chapter to simplify our equations we will drop the subscript "0" from the background quantities, it should be assumed in this chapter that if a quantity has no subscript

it is a background quantity.

6.1 Solving the magnetic evolution equation

We start this section by considering the first order magnetic evolution equation (Eq. (5.36)),

$$\mathcal{M}_1{}^{i\prime} + 2\mathcal{H}\mathcal{M}_1{}^{i} = -a^2\epsilon^{0ijk}\mathcal{E}_{1k,j}\,. \tag{6.1}$$

As explained in Section 5.2.3, the curl of the first order electric field is zero, which means at first order there is no source term in the equation above. This equation can therefore be rewritten as,

$$(a^2\mathcal{M}_1{}^{i})' = 0\,, \tag{6.2}$$

which implies that $a^2\mathcal{M}_1{}^{i}$ is constant in time. This means if there are no first order magnetic fields present at the end of inflation then there will be no first order magnetic fields throughout this period. We start by assuming that any magnetic fields produced by inflation are negligible, allowing us to concentrate on the magnetic fields generated during this era. We therefore set $\mathcal{M}_1{}^{i} = 0$ in the calculations that follow. We will return to the question of what happens when inflation does produce significant magnetic fields in Chapter 7.

By setting the first order magnetic field to zero in Eqs. (5.42) - (5.45) we obtain the following second order constraint equations,

$$\mathcal{M}_2{}^{i}{}_{,i} = 2\omega_1{}^{i}\mathcal{E}_{1i}\,, \tag{6.3}$$

$$\mathcal{E}_2{}^{i}{}_{,i} = -2(2\phi_{1,i} - 2v_{1i}{}' - B_{1,i}{}' + S_{1i}{}' + 2\mathcal{H}v_{1i})\mathcal{E}_1{}^{i} + \mu_0\rho_2 - 2a\mu_0 v_{1i}\mathcal{J}_1{}^{i}\,, \tag{6.4}$$

and the following second order evolution equations,

$$\begin{aligned}\mathcal{M}_2{}^{i\prime} + 2\mathcal{H}\mathcal{M}_2{}^{i} &= -2a^2\epsilon^{0ijk}((v_{1j}{}' + B_{1,j}{}' - S_{1j}{}' - \phi_{1,j} - 2\mathcal{H}(v_{1j} + B_{1,j} - S_{1j}))\mathcal{E}_{1k} \\ &\quad + \frac{1}{2}\mathcal{E}_{2k,j} - \frac{1}{2}h_{1jk,l}\mathcal{E}_1{}^{l} - (v_{1j} + B_{1,j} - S_{1j})a\mu_0\mathcal{J}_{1k})\,, \end{aligned}\tag{6.5}$$

$$\begin{aligned}\mathcal{E}_2{}^{i\prime} + 2\mathcal{H}\mathcal{E}_2{}^{i} &= ((S_{1j,}{}^{i} - S_1{}^{i}{}_{,j}) + h_{1j}{}^{i\prime} + 2a(\omega_1{}^{i}{}_{j} + \sigma_1{}^{i}{}_{j}))\mathcal{E}_1{}^{j} \\ &\quad - 2a^4(v_1{}^{j} + B_{,}{}^{j} - S_1{}^{j})(\mathcal{E}_{1j,}{}^{i} - \mathcal{E}_1{}^{i}{}_{,j}) - 2v_1{}^{j}\mathcal{E}_1{}^{i}{}_{,j} \\ &\quad - \frac{4}{3}v_1{}^{j}{}_{,j}\mathcal{E}_1{}^{i} + a^2\epsilon^{0ijk}\mathcal{M}_{2k,j} - \mu_0\mathcal{J}_2{}^{i} - 2\phi_1 a\mu_0\mathcal{J}_1{}^{i}\,. \end{aligned}\tag{6.6}$$

In order to simplify these equations and evaluate the power spectrum of any magnetic fields generated we will make a series of approximations which we now justify. Firstly, as mentioned in Section 5.2.3 it is well known that during any period of inflation first order vector perturbations rapidly decay, whilst this is not true for the scalar perturbations. As we did for the first order Maxwell equations in Section 5.2.3 we will therefore set the first order vector metric perturbations to zero. We will also for simplicity drop the tensor contributions; the tensor perturbations are significantly smaller than the scalar perturbations [8] and so we expect them to only make a small contribution to our final result. We will be returning to the case where we have a tensor contribution in Chapter 7. Having no first order vector or tensor contribution also means that the first order vorticity, given in Eq. (5.11), will be zero and that the first order shear given in Eq. (5.8) will simplify, in flat gauge, to

$$\sigma_{1ij} = a(\frac{1}{3}\delta_{ij}\nabla^2 - \partial_i\partial_j)B_1\,. \tag{6.7}$$

Taking all these simplifications into account the four Maxwell equations become,

$$\mathcal{M}_2{}^i{}_{,i} = 0\,, \tag{6.8}$$

$$\mathcal{E}_2{}^i{}_{,i} = -2(2\phi_{1,i} - 2v_{1i}{}' - B_{1,i}{}' + 2\mathcal{H}v_{1i})\mathcal{E}_1{}^i + \mu_0\rho_2 - 2a\mu_0 v_{1i}\mathcal{J}_1{}^i\,, \tag{6.9}$$

$$\mathcal{M}_2{}^{i\prime} + 2\mathcal{H}\mathcal{M}_2{}^i = -2a^2\epsilon^{0ijk}((V_{1j}{}' - \phi_{1,j} - 2\mathcal{H}V_{1j})\mathcal{E}_{1k} + \frac{1}{2}\mathcal{E}_{2k,j} - V_{1j}a\mu_0\mathcal{J}_{1k})\,, \tag{6.10}$$

$$\begin{aligned}\mathcal{E}_2{}^{i\prime} + 2\mathcal{H}\mathcal{E}_2{}^i = {} & 2a\sigma_1{}^i{}_j\mathcal{E}_1{}^j - 4a^4V_1{}^j\mathcal{E}_{1[j,}{}^{i]} - 2v_1{}^j\mathcal{E}_1{}^i{}_{,j} - \frac{4}{3}v_1{}^j{}_{,j}\mathcal{E}_1{}^i \\ & + a^2\epsilon^{0ijk}\mathcal{M}_{2k,j} - \mu_0\mathcal{J}_2{}^i - 2\phi_1 a\mu_0\mathcal{J}_1{}^i\,.\end{aligned} \tag{6.11}$$

where V_i is given by $V_i = v_i + B_i$.

We now concentrate on the magnetic evolution equation and the source term for second order magnetic fields. We may use the conservation equations, Eq. (2.83) and Eq. (2.85), and the Einstein equations, Eqs. (2.72) - (2.75), to eliminate V' and ϕ and write our source term in terms of the density and pressure of the matter

components and the electric field and current.

$$\begin{aligned}\mathcal{M}_2{}^{i\prime} + 2\mathcal{H}\mathcal{M}_2{}^{i} &= S^i \\ &= -2a^2\epsilon^{0ijk}\left(\frac{\mathcal{H}}{2}(1-6c_{\rm s}^2+3\omega)V_{1,j} - \frac{\delta P_{1,j}}{(1+\omega)\rho} - \frac{2\nabla^2\Pi_1}{3(1+\omega)\rho}\right)\mathcal{E}_{1,k} \\ &\quad -a^2\epsilon^{0ijk}\mathcal{E}_{2k,j} + 2a^3\epsilon^{0ijk}\mu_0 V_{1,j}\mathcal{J}_{1,k}\,, \end{aligned} \tag{6.12}$$

where $c_{\rm s}^2 = P'/\rho'$ and $\omega = P/\rho$. Once again, as there are no first order vectors we have also neglected the first order vector part of the fluid velocity, keeping only the scalar contribution.

Switching to Fourier space we can write the source term as the sum of convolution terms,

$$\begin{aligned} S^i(\mathbf{k}) &= -a^2\epsilon^{0ijk}k_j\mathcal{E}_{2k}(\mathbf{k}) - \frac{2a^2\epsilon^{0ijk}}{(2\pi)^{3/2}}\times \\ &\int k_k\tilde{k}_j\left[\left(\frac{\mathcal{H}(1-6c_s^2+3\omega)}{2}V_1(\tilde{\mathbf{k}}) - \frac{\delta P_1(\tilde{\mathbf{k}})}{(1+\omega)\rho}\right)\mathcal{E}_1(\mathbf{k}-\tilde{\mathbf{k}}) - a\mu_0 V_1(\tilde{\mathbf{k}})\mathcal{J}_1(\mathbf{k}-\tilde{\mathbf{k}})\right]d^3\tilde{\mathbf{k}}\,, \end{aligned} \tag{6.13}$$

where for simplicity we have neglected the anisotropic stress (Π). In order to include anisotropic stress we would need to use a Boltzmann code. This is beyond the scope of this thesis but will be included in the numeric follow-up to this work (see Chapter 7). This allows us to substitute for V using the perturbed energy conservation equation, Eq. (2.83), which in Fourier space becomes,

$$V_1(\mathbf{k}) = \frac{2\delta\rho_1'(\mathbf{k}) + 3\mathcal{H}\left[(3+\omega)\delta\rho_1(\mathbf{k}) + 2\delta P_1(\mathbf{k})\right]}{(1+\omega)\rho\left(9\mathcal{H}^2(1+\omega)+2k^2\right)}\,. \tag{6.14}$$

Substituting this into Eq. (6.13) we arrive at an expression for the source terms, in terms of the fluid pressure and densities and the electric field and current,

$$\begin{aligned} S^i(\mathbf{k}) &= -a^2\epsilon^{0ijk}k_j\mathcal{E}_{2k}(\mathbf{k}) + \frac{a^2\epsilon^{0ijk}k_k}{(1+\omega)\rho}\frac{1}{(2\pi)^{3/2}}\int\frac{\tilde{k}_j}{(9\mathcal{H}^2(1+\omega)+2c^2\tilde{k}^2)}\times \\ &\Big[2ac^2\mu_0(2\delta\rho_1'(\tilde{\mathbf{k}}) + 3\mathcal{H}(3+\omega)\delta\rho_1(\tilde{\mathbf{k}}) + 6\mathcal{H}\delta P_1(\tilde{\mathbf{k}})/c^2)\mathcal{J}_1(\mathbf{k}-\tilde{\mathbf{k}}) \\ &-(\mathcal{H}(1-6c_s^2+3\omega)(2\delta\rho_1'(\tilde{\mathbf{k}}) + 3\mathcal{H}(3+\omega)\delta\rho_1(\tilde{\mathbf{k}})) \\ &-4(3\mathcal{H}^2(3c_s^2+1)+c^2\tilde{k}^2)\delta P_1(\tilde{\mathbf{k}})/c^2)\mathcal{E}_1(\mathbf{k}-\tilde{\mathbf{k}})\Big]d^3\tilde{\mathbf{k}}\,. \end{aligned} \tag{6.15}$$

In the above equation we have re-inserted factors of c in order to switch to SI units. For the rest of this chapter we will be working in SI units, making it easier to use order of magnitude arguments and to give our final results in physical units, and thus compare with observations.

We note that the density perturbation to leading order in a has the form,

$$\delta\rho_1(\mathbf{k},\eta) = A(\mathbf{k})a^{-4}\,, \tag{6.16}$$

as found in Section 2.5. Therefore the derivative of the density perturbation can be substituted for the density perturbation itself using the following expression,

$$\delta\rho_1' = -4\mathcal{H}\delta\rho_1\,. \tag{6.17}$$

Finally this allows us to simplify our expression for the source term above to,

$$\begin{aligned} S^i(\mathbf{k}) \;=\; & -a^2\epsilon^{0ijk}k_j\mathcal{E}_{2k}(\mathbf{k}) + \frac{a^2\epsilon^{0ijk}k_k}{(1+\omega)\rho}\frac{1}{(2\pi)^{3/2}}\times \\ & \int\frac{\tilde{k}_j}{(9\mathcal{H}^2(1+\omega)+2c^2\tilde{k}^2)}\Big[2ac^2\mu_0(\mathcal{H}(1+3\omega)\delta\rho_1(\tilde{\mathbf{k}})+6\mathcal{H}\delta P_1(\tilde{\mathbf{k}})/c^2)\mathcal{J}_1(\mathbf{k}-\tilde{\mathbf{k}}) \\ & -(\mathcal{H}(1-6c_s^2+3\omega)(2\delta\rho_1'(\tilde{\mathbf{k}})+3\mathcal{H}(3+\omega)\delta\rho_1(\tilde{\mathbf{k}})) \\ & -4(3\mathcal{H}^2(3c_s^2+1)+c^2\tilde{k}^2)\delta P_1(\tilde{\mathbf{k}})/c^2)\mathcal{E}_1(\mathbf{k}-\tilde{\mathbf{k}})\Big]d^3\tilde{\mathbf{k}}\,. \end{aligned} \tag{6.18}$$

We can see that most of the second order source terms are made up of couplings between first order quantities. However, the first term does contain the second order electric field strength. Therefore, before we go on to use this source term to evaluate the power spectrum of the magnetic fields we will briefly discuss this second order electric field.

6.1.1 Second order electric field

We wish to eliminate the second order electric field in the source term above in favour of first order quantities. To find an expression for the second order electric field we can use the second order constraint equation, Eq. (6.9),

$$\mathcal{E}_2{}^i{}_{,i} = -2(2\phi_{1,i} - V_{1i}{}' - v_{1i}{}' + 2\mathcal{H}v_{1i})\mathcal{E}_1{}^i + c^2\mu_0\hat{\rho}_2 - 2a\mu_0 v_{1i}\mathcal{J}_1{}^i\,. \tag{6.19}$$

Once again we can eliminate V'_{1i} and v'_{1i} using the Einstein equation, Eq. (2.75) and the conservation equation, Eq. (2.85) and as we did above we can neglect the vector part of the fluid velocity, leading to,

$$\begin{aligned}\mathcal{E}_2{}^i{}_{,i} = \quad & c^2\mu_0\hat{\rho}_2 - 2ac\mu_0 v_{1,i}\mathcal{J}^{1i} \\ & +2\left(2(3c_s^2-1)V_{1,i}\mathcal{H} + 2\mathcal{H}B_{1,i} + c\phi_{1,i} + \frac{2\delta P_{1,i}}{c(\rho + P/c^2)}\right)\mathcal{E}_1{}^i\,. \quad (6.20)\end{aligned}$$

For compactify notation we define a new variable,

$$T_1 \equiv 2(3c_s^2-1)V_1\mathcal{H} + 2\mathcal{H}B_1 + c\phi_1 + \frac{2\delta P_1}{c(\rho + P/c^2)}\,, \quad (6.21)$$

and write the constraint equation in terms of this new variable, noting that the current and electric field will also have no first order vector part,

$$\mathcal{E}_2{}^i{}_{,i} = c^2\mu_0\hat{\rho}_2 - 2ac\mu_0 v_{1,i}\mathcal{J}_1{}^i + 2T_{1,i}\mathcal{E}_1{}^i\,. \quad (6.22)$$

Now using convolutions we can write down the constraint equation in Fourier space, and solve for the second order electric field, to find,

$$\begin{aligned}\mathcal{E}_2{}^i(\mathbf{k},\eta) = & -\frac{ik^i}{k^2}c^2\mu_0\hat{\rho}_2(\mathbf{k},\eta) \\ & +\frac{2ik^ik^j}{k^2}\int \tilde{\mathbf{k}}_j\left[ac\mu_0 v_1(\tilde{\mathbf{k}},\eta)\mathcal{J}_1(\mathbf{k}-\tilde{\mathbf{k}},\eta) - 2T_1(\tilde{\mathbf{k}},\eta)\mathcal{E}_1(\mathbf{k}-\tilde{\mathbf{k}},\eta)\right]d^3\tilde{\mathbf{k}}\,(6.23)\end{aligned}$$

We see from this equation that $\mathcal{E}_2{}^i(\mathbf{k},\eta)$ is proportional to k^i. This will be important when we consider the polarizations of the source term in the next section.

6.1.2 Polarization of the source term

Returning to consider our full source term, our aim is to find the two-point correlator of the source term and so evaluate the power spectrum. In order to achieve this we will be calculating the polarizations of the source term. To start we now write the source term in Fourier space,

$$S_i(\mathbf{x},\eta) = \frac{1}{(2\pi)^{3/2}}\int S_i(\mathbf{k},\eta)e^{i\mathbf{kx}}d^3\mathbf{k}\,. \quad (6.24)$$

We can choose any basis to write the source term in, so for simplicity we will consider the following basis vectors, with one basis vector taken to be in the direction of k_i and the other two orthonormal to this,

$$\left(e_i(\mathbf{k}), \bar{e}_i(\mathbf{k}), \hat{k}_i \equiv \frac{k_i}{|\mathbf{k}|}\right) . \tag{6.25}$$

These basis vectors must be right-handed and orthonormal which means they must satisfy three conditions:

- right-handed under sign reversal of $\mathbf{k}$, i.e. $e_i(-\mathbf{k}) = e_i(\mathbf{k})$ and $\bar{e}_i(-\mathbf{k}) = -\bar{e}_i(\mathbf{k})$,
- cyclic, i.e. $\epsilon_{ijk} e^i(\mathbf{k}) \bar{e}^j(\mathbf{k}) = \hat{k}_k$,
- orthonormal, $e_{Ai} e^i_B = 0$, for all combinations of basis vectors.

This gives us the following source term expanded out using the basis vectors above and written in Fourier space,

$$S_i(\mathbf{k}, \eta) = S_A(\mathbf{k}, \eta) e_i(\mathbf{k}) + S_B(\mathbf{k}, \eta) \bar{e}_i(\mathbf{k}) + S_C(\mathbf{k}, \eta) \hat{k}_i \,, \tag{6.26}$$

or in physical space,

$$S_i(\mathbf{x}, \eta) = \frac{1}{(2\pi)^{3/2}} \int d^3\mathbf{k} \left[S_A(\mathbf{k}, \eta) e_i(\mathbf{k}) + S_B(\mathbf{k}, \eta) \bar{e}_i(\mathbf{k}) + S_C(\mathbf{k}, \eta) \hat{k}_i \right] e^{i\mathbf{kx}} \,. \tag{6.27}$$

We can use our expression for S_i in Eq. (6.1) to write out expressions for the amplitudes of the three polarizations

$$\begin{aligned}
S_A(\mathbf{k},\eta) &= -\frac{a^2 k\bar{e}^j}{(2\pi)^{3/2}(1+\omega)\rho}\int \frac{\tilde{k}_j}{(9\mathcal{H}^2(1+\omega)+2c^2\tilde{k}^2)} \\
&\quad [2ac^2\mu_0(\mathcal{H}(1+3\omega)\delta\rho_1(\tilde{\mathbf{k}})+6\mathcal{H}\delta P_1(\tilde{\mathbf{k}})/c^2)\mathcal{J}_1(\mathbf{k}-\tilde{\mathbf{k}}) \\
&\quad -(\mathcal{H}(1-6c_s^2+3\omega)(\mathcal{H}(1+3\omega)\delta\rho_1(\tilde{\mathbf{k}}) \\
&\quad -4(3\mathcal{H}^2(3c_s^2+1)+c^2\tilde{k}^2)\delta P_1(\tilde{\mathbf{k}})/c^2)\mathcal{E}_1(\mathbf{k}-\tilde{\mathbf{k}})]d^3\tilde{\mathbf{k}}\,, \qquad (6.28) \\
S_B(\mathbf{k},\eta) &= \frac{a^2 ke^j}{(2\pi)^{3/2}(1+\omega)\rho}\int \frac{\tilde{k}_j}{(9\mathcal{H}^2(1+\omega)+2c^2\tilde{k}^2)} \\
&\quad [2ac^2\mu_0(\mathcal{H}(1+3\omega)\delta\rho_1(\tilde{\mathbf{k}})+6\mathcal{H}\delta P_1(\tilde{\mathbf{k}})/c^2)\mathcal{J}_1(\mathbf{k}-\tilde{\mathbf{k}}) \\
&\quad -(\mathcal{H}(1-6c_s^2+3\omega)(\mathcal{H}(1+3\omega)\delta\rho_1(\tilde{\mathbf{k}}) \\
&\quad -4(3\mathcal{H}^2(3c_s^2+1)+c^2\tilde{k}^2)\delta P_1(\tilde{\mathbf{k}})/c^2)\mathcal{E}_1(\mathbf{k}-\tilde{\mathbf{k}})]d^3\tilde{\mathbf{k}}\,, \qquad (6.29) \\
S_C(\mathbf{k},\eta) &= 0\,. \qquad (6.30)
\end{aligned}$$

Note that in the first two equations the second order electric field term vanishes as $\bar{e}^k\mathcal{E}_{2k}(\mathbf{k})=0$ and $e^k\mathcal{E}_{2k}(\mathbf{k})=0$, and the third equation is zero because $\epsilon^{0ijk}\hat{k}_i\hat{k}_j\tilde{k}_k = 0$.

In order to calculate the power spectrum below we also need the complex conjugate of this source term. The magnetic field is an axial vector so under the transformation of $\mathbf{x}\to-\mathbf{x}$ the magnetic field will transform as $\mathcal{M}_{2i}\to-\mathcal{M}_{2i}$ and similarly for the source term S_i. Taking the complex conjugate of the source term we arrive at,

$$\begin{aligned}
&S_i(\mathbf{x},\eta) = \\
&\frac{1}{(2\pi)^{3/2}}\int d^3\mathbf{k}\left[S_A^*(\mathbf{k},\eta)e_i(\mathbf{k})+S_B^*(\mathbf{k},\eta)\bar{e}_i(\mathbf{k})+S_C^*(\mathbf{k},\eta)\hat{k}_i\right]e^{-i\mathbf{kx}}\,. \qquad (6.31)
\end{aligned}$$

Writing the source term under the change $\mathbf{k}\to-\mathbf{k}$ we have

$$\begin{aligned}
&S_i(\mathbf{x},\eta) = -\frac{1}{(2\pi)^{3/2}}\times \\
&\int d^3\mathbf{k}\left[S_A(-\mathbf{k},\eta)e_i(-\mathbf{k})+S_B(-\mathbf{k},\eta)\bar{e}_i(-\mathbf{k})+S_C(-\mathbf{k},\eta)(-\hat{k}_i)\right]e^{-i\mathbf{kx}} \qquad (6.32)
\end{aligned}$$

Comparing the two equations above we can find relationships between the fourier amplitudes of each polarization and their complex conjugates,

$$S_A^*(\mathbf{k},\eta) = -S_A(-\mathbf{k},\eta)\,, \tag{6.33}$$

$$S_B^*(\mathbf{k},\eta) = S_B(-\mathbf{k},\eta)\,, \tag{6.34}$$

$$S_C^*(\mathbf{k},\eta) = S_C(-\mathbf{k},\eta)\,. \tag{6.35}$$

This in turn allows us to write down the complex conjugate of each amplitude,

$$\begin{aligned} S_A^*(\mathbf{k},\eta) &= \frac{a^2 k\bar{e}^j}{(2\pi)^{3/2}(1+\omega)\rho}\int \frac{\tilde{k}_j}{(9\mathcal{H}^2(1+\omega)+2c^2\tilde{k}^2)} \\ &\quad [2ac^2\mu_0(\mathcal{H}(1+3\omega)\delta\rho_1(\tilde{\mathbf{k}})+6\mathcal{H}\delta P_1(\tilde{\mathbf{k}})/c^2)\mathcal{J}_1(-\mathbf{k}-\tilde{\mathbf{k}}) \\ &\quad -(\mathcal{H}(1-6c_s^2+3\omega)(\mathcal{H}(1+3\omega)\delta\rho_1(\tilde{\mathbf{k}}) \\ &\quad -4(3\mathcal{H}^2(3c_s^2+1)+c^2\tilde{k}^2)\delta P_1(\tilde{\mathbf{k}})/c^2)\mathcal{E}_1(-\mathbf{k}-\tilde{\mathbf{k}})]d^3\tilde{\mathbf{k}}\,, \end{aligned} \tag{6.36}$$

$$\begin{aligned} S_B^*(\mathbf{k},\eta) &= \frac{a^2 ke^j}{(2\pi)^{3/2}(1+\omega)\rho}\int \frac{\tilde{k}_j}{(9\mathcal{H}^2(1+\omega)+2c^2\tilde{k}^2)} \\ &\quad [2ac^2\mu_0(\mathcal{H}(1+3\omega)\delta\rho_1(\tilde{\mathbf{k}})+6\mathcal{H}\delta P_1(\tilde{\mathbf{k}})/c^2)\mathcal{J}_1(-\mathbf{k}-\tilde{\mathbf{k}}) \\ &\quad -(\mathcal{H}(1-6c_s^2+3\omega)(\mathcal{H}(1+3\omega)\delta\rho_1(\tilde{\mathbf{k}}) \\ &\quad -4(3\mathcal{H}^2(3c_s^2+1)+c^2\tilde{k}^2)\delta P_1(\tilde{\mathbf{k}})/c^2)\mathcal{E}_1(-\mathbf{k}-\tilde{\mathbf{k}})]d^3\tilde{\mathbf{k}}\,. \end{aligned} \tag{6.37}$$

The amplitude of the two non-zero polarizations above are identical up to the basis vector, so for now we need only consider one and we will drop the subscript.

In order to simplify our expressions for the next part of the calculation we now look in more detail at the current and electric field strength. Assuming that the time and scale dependence of the current and electric field are separable, and that they both have the same scale dependence (we discuss this assumption in Section 6.3.3), we can rewrite,

$$\mathcal{J}_1(\mathbf{k},\eta) = J(\eta)\mathcal{E}_1(\mathbf{k})\,, \tag{6.38}$$

$$\mathcal{E}_1(\mathbf{k},\eta) = E(\eta)\mathcal{E}_1(\mathbf{k})\,. \tag{6.39}$$

Hence, the source term and its complex conjugate can be given by

$$S(\mathbf{k},\eta) = \frac{a^2 k\bar{e}^j}{(2\pi)^{3/2}(1+\omega)\rho}\int \frac{\tilde{k}_j}{(9\mathcal{H}^2(1+\omega)+2c^2\tilde{k}^2)}\mathcal{E}_1(\mathbf{k}-\tilde{\mathbf{k}})\times$$
$$[\mathcal{H}(2ac^2\mu_0(1+3\omega)J(\eta)-\mathcal{H}(1-6c_s^2+3\omega)(1+3\omega)E(\eta))\delta\rho_1(\tilde{\mathbf{k}}))$$
$$+4(3ac^2\mu_0\mathcal{H}J(\eta)+(3\mathcal{H}^2(3c_s^2+1)+c^2\tilde{k}^2)E(\eta))\delta P_1(\tilde{\mathbf{k}})/c^2]d^3\tilde{\mathbf{k}}\,, \quad (6.40)$$
$$S^*(\mathbf{k},\eta) = \frac{a^2 k\bar{e}^j}{(2\pi)^{3/2}(1+\omega)\rho}\int \frac{\tilde{k}_j}{(9\mathcal{H}^2(1+\omega)+2c^2\tilde{k}^2)}\mathcal{E}_1(-\mathbf{k}-\tilde{\mathbf{k}})\times$$
$$[\mathcal{H}(2ac^2\mu_0(1+3\omega)J(\eta)-\mathcal{H}(1-6c_s^2+3\omega)(1+3\omega)E(\eta))\delta\rho_1(\tilde{\mathbf{k}}))$$
$$+4(3ac^2\mu_0\mathcal{H}J(\eta)+(3\mathcal{H}^2(3c_s^2+1)+c^2\tilde{k}^2)E(\eta))\delta P_1(\tilde{\mathbf{k}})/c^2]d^3\tilde{\mathbf{k}}\,. \quad (6.41)$$

The source term above depends on both the pressure perturbation and the density perturbation, however, the pressure perturbation itself depends on the density perturbation. As we saw in Eq. (3.24) the pressure perturbation can be written as,

$$\delta P_1(\mathbf{k}) = \frac{c_s^2}{c^2}\delta\rho_1(\mathbf{k}) + \delta P_{1\mathrm{nad}}(\mathbf{k})\,, \quad (6.42)$$

substituting this into the source term above we eliminate the pressure perturbation in favour of the non-adiabatic pressure perturbation,

$$\begin{aligned} S(\mathbf{k},\eta) \;=\; & \frac{a^2 k\bar{e}^j}{(2\pi)^{3/2}(1+\omega)\rho}\int \frac{\tilde{k}_j}{(9\mathcal{H}^2(1+\omega)+2c^2\tilde{k}^2)}\mathcal{E}_1(\mathbf{k}-\tilde{\mathbf{k}})\times \\ & \Big[\Big(2\mathcal{H}ac^2\mu_0(1+3\omega+6c_s^2)J(\eta) \\ & -[\mathcal{H}^2(1-6c_s^2+3\omega)(1+3\omega)-3\mathcal{H}^2c_s^2(3c_s^2+1)-c^2c_s^2\tilde{k}^2]E(\eta)\Big)\delta\rho_1(\tilde{\mathbf{k}}) \\ & +4\Big(3ac^2\mu_0\mathcal{H}J(\eta)+(3\mathcal{H}^2(3c_s^2+1)+c^2\tilde{k}^2)E(\eta)\Big)\delta P_{1\mathrm{nad}}(\tilde{\mathbf{k}})/c^2\Big]d^3\tilde{\mathbf{k}}\,. \end{aligned}$$

Finally compactifying our notation once more, we define two new variables,

$$f(\tilde{k},\eta) \equiv 2\mathcal{H}ac^2\mu_0(1+3\omega+6c_s^2)J(\eta)\,,$$
$$-\left[\mathcal{H}^2(1-6c_s^2+3\omega)(1+3\omega)-3\mathcal{H}^2c_s^2(3c_s^2+1)-c^2c_s^2\tilde{k}^2\right]E(\eta) \quad (6.43)$$
$$g(\tilde{k},\eta) \equiv 4\left[3\mathcal{H}ac^2\mu_0 J(\eta)+\left(3\mathcal{H}^2(3c_s^2+1)+c^2\tilde{k}^2\right)E(\eta)\right]/c^2\,, \quad (6.44)$$

which in radiation domination take the form

$$f(\tilde{k},\eta) = 8\mathcal{H}ac^2\mu_0 J(\eta) + \frac{1}{3}(6\mathcal{H}^2 + c^2\tilde{k}^2)E(\eta)\,, \tag{6.45}$$

$$g(\tilde{k},\eta) = \frac{4}{c^2}\left(3\mathcal{H}ac^2\mu_0 J(\eta) + (6\mathcal{H}^2 + c^2\tilde{k}^2)E(\eta)\right)\,. \tag{6.46}$$

Using these two new variables leaves us with the following simplifed expressions for the source terms,

$$S(\mathbf{k},\eta) = \frac{a^2 k\bar{e}^j}{(2\pi)^{3/2}(1+\omega)\rho} \times \int \frac{\tilde{k}_j \mathcal{E}_1(\mathbf{k}-\tilde{\mathbf{k}})}{(9\mathcal{H}^2(1+\omega)+2c^2\tilde{k}^2)}\left[f(\eta)\delta\rho_1(\tilde{\mathbf{k}}) + g(\tilde{k},\eta)\delta P_{1\mathrm{nad}}(\tilde{\mathbf{k}})\right] d^3\tilde{\mathbf{k}}\,, \tag{6.47}$$

$$S^*(\mathbf{k},\eta) = \frac{a^2 k\bar{e}^j}{(2\pi)^{3/2}(1+\omega)\rho} \times \int \frac{\tilde{k}_j \mathcal{E}_1(-\mathbf{k}-\tilde{\mathbf{k}})}{(9\mathcal{H}^2(1+\omega)+2c^2\tilde{k}^2)}\left[f(\eta)\delta\rho_1(\tilde{\mathbf{k}}) + g(\tilde{k},\eta)\delta P_{1\mathrm{nad}}(\tilde{\mathbf{k}})\right] d^3\tilde{\mathbf{k}}\,. \tag{6.48}$$

Now that we have a more compact form for the source term for the magnetic field we can look at calculating the power spectrum.

6.2 The magnetic field power spectrum

Returning to our second order evolution equation for the magnetic field and writing it in Fourier space we have for each polarization direction,

$$\mathcal{M}_{2A}'(\mathbf{k},\eta) + 2\mathcal{H}\mathcal{M}_{2A}(\mathbf{k},\eta) = S_A(\mathbf{k},\eta)\,. \tag{6.49}$$

Dropping the subscript, as the equations that follow are identical for each polarization, (see Section 6.1.2) and rewriting the left hand side we get,

$$(a^2\mathcal{M}_2(\mathbf{k},\eta))' = a^2 S(\mathbf{k},\eta)\,. \tag{6.50}$$

In radiation domination this can be written as,

$$\mathcal{M}_2(\mathbf{k},\eta) = \frac{1}{\eta^2}\int_{\eta_0}^{\eta} \tilde{\eta}^2 S(\mathbf{k},\tilde{\eta}) d\tilde{\eta}\,. \tag{6.51}$$

We aim to find the power spectrum of the magnetic field, defined by

$$\langle \mathcal{M}_2(\mathbf{k}_1,\eta)\mathcal{M}_2{}^*(\mathbf{k}_2,\eta)\rangle = \frac{2\pi}{k^3}\delta(\mathbf{k}_1-\mathbf{k}_2)\mathcal{P}_{\mathcal{M}}(\mathbf{k},\eta)\,, \tag{6.52}$$

and to this end we use Eq. (6.51) to relate the two-point correlator of the magnetic field to the two-point correlator of the source term,

$$\langle \mathcal{M}_2(\mathbf{k}_1,\eta)\mathcal{M}_2{}^*(\mathbf{k}_2,\eta)\rangle = \frac{1}{\eta^4}\int_{\eta_0}^{\eta}\tilde{\eta}_1^2\int_{\eta_0}^{\eta}\tilde{\eta}_2^2\langle S(\mathbf{k}_1,\tilde{\eta}_1)S^*(\mathbf{k}_2,\tilde{\eta}_2)\rangle d\tilde{\eta}_1 d\tilde{\eta}_2\,. \tag{6.53}$$

Our first step will be calculating the two-point correlator of the source term using the expressions for the source term and its complex conjugate in Eq. (6.47) and Eq. (6.48),

$$\begin{aligned}
&\langle S(\mathbf{k}_1,\eta_1)S^*(\mathbf{k}_2,\eta_2)\rangle = \frac{a_1^2 a_2^2 k_1 k_2 \bar{e}^i \bar{e}^j}{(2\pi)^3(1+\omega)^2\rho(\eta_1)\rho(\eta_2)} \\
&\int d^3\tilde{\mathbf{k}_1}\frac{\tilde{k_{1i}}}{9\mathcal{H}_1^2(1+\omega)+2c^2\tilde{k_1}^2}\int d^3\tilde{\mathbf{k}_2}\frac{\tilde{k_{2j}}}{9\mathcal{H}_2^2(1+\omega)+2c^2\tilde{k_2}^2} \\
&\langle [f(\eta_1)\delta\rho_1(\tilde{\mathbf{k}}_1,\eta_1)+g(\tilde{k}_1,\eta_1)\delta P_{1\mathrm{nad}}(\tilde{\mathbf{k}}_1,\eta_1)]\mathcal{E}_1(\mathbf{k}_1-\tilde{\mathbf{k}}_1,\eta_1) \\
&[f(\eta_2)\delta\rho_1(\tilde{\mathbf{k}}_2,\eta_2)+g(\tilde{k}_2,\eta_2)\delta P_{1\mathrm{nad}}(\tilde{\mathbf{k}}_2,\eta_2)]\mathcal{E}_1(-(\tilde{\mathbf{k}}_2+\mathbf{k}_2),\eta_2)\rangle\,.
\end{aligned} \tag{6.54}$$

Rewriting the terms inside the angled brackets as a sum of correlators and assuming that the fluctuations $\delta\rho_1$ and δP_1 and the electric field are Gaussian, and therefore that their directional dependency can be put into Gaussian random variables $\hat{E}(\mathbf{k})$, allows us to express the terms inside the angles brackets as the sum of four-point correlators. We can then apply Wick's theorem [156] on the four-point correlators of the Gaussian variables and rewrite the resulting two-point functions in terms of delta functions. The details of this step in the calculation are given in Appendix D and lead to the following expression for the two-point correlator of the

source term,

$$\langle S(\mathbf{k}_1,\eta_1)S^*(\mathbf{k}_2,\eta_2)\rangle = \frac{a_1^2a_2^2k_1k_2\bar{e}^i\bar{e}^j}{(2\pi)^3(1+\omega)^2\rho(\eta_1)\rho(\eta_2)}$$
$$\int d^3\tilde{\mathbf{k}_1}\frac{\tilde{k_{1i}}\mathcal{E}_1(|\tilde{\mathbf{k}}_1-\mathbf{k}_1|,\eta_1)}{9\mathcal{H}_1^2(1+\omega)+2c^2\tilde{k_1}^2}\int d^3\tilde{\mathbf{k}_2}\frac{\tilde{k_{2j}}\mathcal{E}_1(|\tilde{\mathbf{k}}_2+\mathbf{k}_2|,\eta_2)}{9\mathcal{H}_2^2(1+\omega)+2c^2\tilde{k_2}^2}$$
$$(f(\eta_1)f(\eta_2)\delta\rho_1(\tilde{k}_1,\eta_1)\delta\rho_1(\tilde{k}_2,\eta_2)$$
$$+f(\eta_1)g(\tilde{k}_2,\eta_2)\delta\rho_1(\tilde{k}_1,\eta_1)\delta P_{1\mathrm{nad}}(\tilde{k}_2,\eta_2)$$
$$+g(\tilde{k}_1,\eta_1)f(\eta_2)\delta P_{1\mathrm{nad}}(\tilde{k}_1,\eta_1)\delta\rho_1(\tilde{k}_2,\eta_2)$$
$$+g(\tilde{k}_1,\eta_1)g(\tilde{k}_2,\eta_2)\delta P_{1\mathrm{nad}}(\tilde{k}_1,\eta_1)\delta P_{1\mathrm{nad}}(\tilde{k}_2,\eta_2))$$
$$(\delta(\tilde{\mathbf{k}}_1+\tilde{\mathbf{k}}_2)\delta(\mathbf{k}_1-\tilde{\mathbf{k}}_2-\tilde{\mathbf{k}}_1-\mathbf{k}_2)+\delta(\tilde{\mathbf{k}}_1-\tilde{\mathbf{k}}_2-\mathbf{k}_2)\delta(\mathbf{k}_1+\tilde{\mathbf{k}}_2-\tilde{\mathbf{k}}_1))\,. \quad (6.55)$$

We finish this section by carrying out the $\tilde{k}_2$ integral over one of the delta functions to find the following expression for the two-point correlator in terms of the density perturbation, pressure perturbation and electric field,

$$\langle S(\mathbf{k}_1,\eta_1)S^*(\mathbf{k}_2,\eta_2)\rangle = \frac{a_1^2a_2^2}{(2\pi)^3(1+\omega)^2\rho(\eta_1)\rho(\eta_2)}k^2\bar{e}^i\bar{e}^j\delta(\mathbf{k}_1-\mathbf{k}_2)$$
$$\int d^3\tilde{\mathbf{k}}\frac{\tilde{k}_i}{9\mathcal{H}_1^2(1+\omega)+2c^2\tilde{k}^2}\mathcal{E}_1(|\tilde{\mathbf{k}}-\mathbf{k}|,\eta_1)$$
$$\Big[\frac{\tilde{k}_j}{9\mathcal{H}_2^2(1+\omega)+2c^2\tilde{k}^2}\mathcal{E}_1(|\tilde{\mathbf{k}}+\mathbf{k}|,\eta_2)\times$$
$$\Big(f(\eta_1)f(\eta_2)\delta\rho_1(\tilde{k},\eta_1)\delta\rho_1(\tilde{k},\eta_2)+f(\eta_1)g(\tilde{k},\eta_2)\delta\rho_1(\tilde{k},\eta_1)\delta P_{1\mathrm{nad}}(\tilde{k},\eta_2)$$
$$+g(\tilde{k},\eta_1)f(\eta_2)\delta P_{1\mathrm{nad}}(\tilde{k},\eta_1)\delta\rho_1(\tilde{k},\eta_2)$$
$$+g(\tilde{k},\eta_1)g(\tilde{k},\eta_2)\delta P_{1\mathrm{nad}}(\tilde{k},\eta_1)\delta P_{1\mathrm{nad}}(\tilde{k},\eta_2)\Big)$$
$$+\frac{|\tilde{\mathbf{k}}-\mathbf{k}|_j}{9\mathcal{H}_2^2(1+\omega)+2c^2|\tilde{\mathbf{k}}-\mathbf{k}|^2}\mathcal{E}_1(\tilde{k},\eta_2)\times$$
$$\Big(f(\eta_1)f(\eta_2)\delta\rho_1(\tilde{k},\eta_1)\delta\rho_1(|\tilde{\mathbf{k}}-\mathbf{k}|,\eta_2)$$
$$+f(\eta_1)g(|\tilde{\mathbf{k}}-\mathbf{k}|,\eta_2)\delta\rho_1(\tilde{k},\eta_1)\delta P_{1\mathrm{nad}}(|\tilde{\mathbf{k}}-\mathbf{k}|,\eta_2)$$
$$+g(\tilde{k},\eta_1)f(\eta_2)\delta P_{1\mathrm{nad}}(\tilde{k},\eta_1)\delta\rho_1(|\tilde{\mathbf{k}}-\mathbf{k}|,\eta_2)$$
$$+g(\tilde{k},\eta_1)g(|\tilde{\mathbf{k}}-\mathbf{k}|,\eta_2)\delta P_{1\mathrm{nad}}(\tilde{k},\eta_1)\delta P_{1\mathrm{nad}}(|\tilde{\mathbf{k}}-\mathbf{k}|,\eta_2)\Big)\Big]\,. \quad (6.56)$$

6.3 Elements of the source term

We will now look at each of the three functions, $\delta\rho_1$, δP_1 and $\mathcal{E}_1$ that the two-point correlator depends on in more detail. We are interested in the time and scale dependence of each of these, so that we can evaluate the power spectrum of the magnetic field.

6.3.1 Density Perturbation

In Section 2.5, we showed that in radiation domination on large scales the density perturbation has the following time dependence,

$$\delta\rho_1(\mathbf{k},\eta) = A(\mathbf{k})\eta^{-4} + B(\mathbf{k})\eta^{-5}\,, \tag{6.57}$$

so to lowest order in η we have,

$$\delta\rho_1(\mathbf{k},\eta) = A(\mathbf{k})\eta^{-4}\,. \tag{6.58}$$

We can use observational data, by relating the density perturbation to the curvature perturbation, ζ, to determine the scale dependence. As we saw in Eq. (3.18), in flat gauge the curvature perturbation on uniform density hypersurfaces is related to the density perturbation by

$$\zeta_1 = -\frac{\mathcal{H}}{\rho_0'}\delta\rho_1 = \frac{1}{3(\rho_0+P_0)}\delta\rho_1\,. \tag{6.59}$$

As the background quantities are not scale dependent this means ζ and $\delta\rho$ will have the same scale dependence, that is, in radiation domination

$$\langle\delta\rho_{1\mathrm{init}}\delta\rho_{1\mathrm{init}}\rangle = 16\rho_{0\mathrm{init}}^2\langle\zeta_{1\mathrm{init}}\zeta_{1\mathrm{init}}\rangle\,. \tag{6.60}$$

We gave the scale dependence of the curvature perturbation in terms of the running in Section 3.2.3 and noting as we did above that the density perturbation has the

same scale dependence we find,

$$\delta\rho_{1\text{init}} \propto \zeta_{1\text{init}} \propto \left(\frac{k}{k_0}\right)^{(n_s-1)} . \tag{6.61}$$

Note that the current best fit value for the spectral index, n_s, given by PLANCK is very close to 1 [8], which implies that the density perturbation is very close to being scale invariant. Hence we have,

$$\delta\rho_1 = A\left(\frac{\eta}{\eta_0}\right)^{-4} , \tag{6.62}$$

where we have rescaled the constant by a factor η_0^4, such that $A = \delta\rho(k_0, \eta_0)$.

To find A we use the observed value for the power spectrum of ζ found by WMAP and given in the equation below by $\Delta^2_\zeta(k_0)$,

$$\langle\zeta_{1\text{init}}\zeta_{1\text{init}}\rangle = \frac{2\pi}{k^3}\mathcal{P}_\zeta(k, \eta_{\text{init}}) = \frac{2\pi}{k^3}\Delta^2_\zeta(k_0) = \frac{2\pi^2}{k^3}\Delta^2_\zeta(k_0)\left(\frac{k}{k_0}\right)^{n_s-1} . \tag{6.63}$$

Recalling the relationship between ζ_1 and $\delta\rho_1$ in Eq. (6.60) we have,

$$A^2 = \delta\rho_1(k_0, \eta_{\text{init}})^2 = 32\pi^2\rho^2_{0\text{init}}L^3k_0^{-3}\Delta^2_{\mathcal{R}}(k_0) . \tag{6.64}$$

In the analysis above we have so far been working in radiation domination and on large scales, however, to complete this picture we should also consider what is happening on smaller scales. Throughout radiation domination the evolution of density perturbations behaves differently on small scales compared to large scales.The boundary between these two types of behavior is given by Jeans length, which leads to a turnover in the powers spectrum at this scale. This turnover length increases in size as the universe evolves. We find that by matter-radiation equality this turnover occurs at $k \approx 0.02h\text{Mpc}^{-1}$ [40]. For scales larger than this the power spectrum of the density contrast has scale dependence $\mathcal{P}_\delta(k) \propto k$, whereas for scales smaller than this the power spectrum has scale dependence $\mathcal{P}_\delta(k) \propto k^{-3}$. If we are interested in smaller scales, in particularly towards the end of the radiation era, this is something we would have to include in our analysis. See Section 6.7.3 for further discussion on this.

6.3.2 Pressure perturbation

We start by splitting the pressure into the adiabatic and the non-adiabatic part, using Eq. (6.42). We know how $\delta\rho(\mathbf{k})$ behaves, see Section 6.3.1, so we now turn our attention to the non-adiabatic pressure perturbation. This non-adiabatic pressure perturbation can once more be split into an intrinsic part, $\delta P_{\rm int}$, and a part caused by the interaction between the different fluids $\delta P_{\rm Rel}$,

$$\delta P_{\rm nad} = \delta P_{\rm int} + \delta P_{\rm Rel}\,. \tag{6.65}$$

As we are treating each fluid individually as a perfect fluid there will be no intrinsic non-adiabatic pressure perturbation, so we need only consider the relative non-adiabatic pressure perturbation. This type of non-adiabatic pressure perturbation is due to the relative entropy perturbation $S_{\alpha\beta}$ between individual fluids, defined as,

$$S_{\alpha\beta} \equiv -3H\left(\frac{\delta\rho_\alpha}{\dot{\rho_\alpha}} - \frac{\delta\rho_\beta}{\dot{\rho_\beta}}\right)\,, \tag{6.66}$$

and is given by,

$$\delta P_{\rm Rel} = -\frac{1}{6H\dot{\rho}}\sum_{\alpha,\beta}\dot{\rho_\alpha}\dot{\rho_\beta}(c_\alpha^2 - c_\beta^2)S_{\alpha\beta}\,. \tag{6.67}$$

There are two origins for this type of non-adiabatic pressure perturbation which we consider here. The first is caused by the interaction between the different fluids during the radiation era ($\delta P_{\rm rel}$) and the second is caused in the same way during inflation ($\delta P_{\rm inf}$) [9, 15].

Up until this point we have been neglecting cold dark matter in our calculations as it does not interact directly with the fluids we are considering and only enters the equations through the background values. However, the non-adiabatic pressure-perturbation will be affected by the presence of cold dark matter, in fact it is one of the largest contributing factors. Therefore, in this section we will be taking the cold dark matter into account. We do this as the effect of cold dark matter on the conservation equations will not be as dominant an effect as the interaction between the charged species. To treat this problem fully we would wish to incorporate dark matter throughout all parts of our calculation, this is left for further work when we solve the equations numerically.

We start by considering what the time evolution of such a non-adiabatic pressure perturbation would be during the radiation era, the period we are interested in. To do this we follow the analytic explanation given in Ref. [79]. We consider a 5-fluid system of baryonic matter (b), cold dark matter (c), photons (γ), neutrinos (ν) and dark energy (Λ). Using the individual density contrast evolution equations for each fluid and defining the scaled entropy difference between two fluids as,

$$\Delta_{\alpha\beta} = (1+\omega_\beta)\delta_\alpha - (1+\omega_\alpha)\delta_\beta \,, \tag{6.68}$$

the evolution equations for the scaled entropy differences are given by,

$$\begin{aligned} \dot{\Delta}_{\gamma b} &= \frac{4}{3}k^2(v_b - v_\gamma)\,, \quad \dot{\Delta}_{\gamma c} = -\frac{4}{3}k^2 v_\gamma \,, \\ \dot{\Delta}_{\nu b} &= \frac{4}{3}k^2(v_b - v_\nu)\,, \quad \dot{\Delta}_{\nu c} = -\frac{4}{3}k^2 v_\nu \,. \end{aligned} \tag{6.69}$$

Integrating these evolution equations for baryons, radiation and cold dark matter under the assumption that we are working on superhorizon scales, in the early universe and neglecting the sub-dominant $\Delta_{\gamma b}$, the non adiabatic pressure perturbation is given by [79],

$$\delta P_{\rm Rel} \approx \frac{3/216 \times H_0^2 \Omega_c (15 + 12R_\nu)}{8\pi G (1 + \frac{3}{4} a \frac{\Omega_M}{\Omega R})(15 + 4R_\nu)} C k^4 \eta^4 a^{-3} \,, \tag{6.70}$$

which during radiation domination is proportional to conformal time.

The non-adiabatic pressure perturbation, therefore, can be written as,

$$\delta P_{\rm 1nad} = P \left(\frac{k}{k_0}\right)^\delta \left(\frac{\eta}{\eta_0}\right) \,, \tag{6.71}$$

where the values of the amplitude, P, and the scale dependence, δ, will depend on which of the two type of non-adiabatic pressure we have ($\delta P_{\rm rel}$ or $\delta P_{\rm inf}$), i.e. when the non-adiabatic pressure is originally sourced.

Inflationary non-adiabatic pressure perturbation

Considering the inflationary non-adiabatic pressure perturbation, we note that the scale dependence is the same as that of the density perturbation, i.e. it is close to being scale invariant [39]. Therefore $\delta = 0$ in our description above and hence,

$$\delta P_{\rm 1inf} = D\left(\frac{\eta}{\eta_0}\right) , \tag{6.72}$$

where $D = \delta P_{\rm inf}(k_0, \eta_0)$.

In order to find an expression for D, the amplitude of the inflationary non-adiabatic pressure perturbation, we will be relating the non-adiabatic pressure to the comoving entropy perturbation, defined in Eq. (6.66). There has been no direct observation of an entropy perturbation from inflation so unlike the power spectrum of the curvature perturbation, observationally we only have an upper bound on the power spectrum of the entropy perturbation. We will therefore be considering what the largest possible magnitude of the non-adiabatic pressure perturbation from inflation would be. The leading contribution for the entropy perturbation is $S_{c\gamma}$, i.e. that due to the entropy difference between the cold dark matter and the radiation and it is the limit on this that we will be using below. The relative amplitude in power spectrum of the entropy and curvature perturbations is given by,

$$\frac{\alpha}{1-\alpha} = \frac{\mathcal{P}_S(k_0)}{\mathcal{P}_{\mathcal{R}}(k_0)} . \tag{6.73}$$

There are two types of entropy modes those which are uncorrelated with the curvature modes and those which are anti-correlated with the curvature modes. As we are interested in the biggest possible effect that entropy modes could have we will be considering the type with the largest magnitude here - that is the uncorrelated modes. The upper bound (95% limit) to the relative amplitude in power of the uncorrelated entropy modes is given by WMAP [7] to be $\alpha < 0.15$.

We can relate this entropy perturbation to the non-adiabatic pressure perturbation by,

$$S_1 = \frac{\mathcal{H}}{c^2 P'} \delta P_{\rm 1nad} . \tag{6.74}$$

During the radiation era, this implies,

$$\delta P_{\rm 1nad} = -\frac{4}{3}c^2\rho S_1\,, \tag{6.75}$$

Recalling that from Section 3.2.3 we know that

$$\mathcal{P}_{\mathcal{R}}(k_0) = \frac{k^3}{2\pi} < |\mathcal{R}_1(k,\eta)|^2 >= \pi\Delta^2_{\mathcal{R}}(k_0)\left(\frac{k}{k_0}\right)^{n_s-1}\,. \tag{6.76}$$

This allows us to write an expression for the power spectrum of the entropy perturbation by relating it to the power spectrum of the curvature perturbation,

$$\begin{aligned}\mathcal{P}_S(k,\eta) &= \frac{k^3}{2\pi} < |S_1(k,\eta)|^2 > \\ &\leq \frac{\alpha(k_0)}{1-\alpha(k_0)}\pi L^3\Delta^2_{\mathcal{R}}(k_0)\left(\frac{k}{k_0}\right)^{n_s-1}\,.\end{aligned} \tag{6.77}$$

Evaluating this at $k = k_0$ and $\eta = \eta_0$ and using Eq. (6.75) we arrive at,

$$\begin{aligned}D^2 &= \delta P^2_{\rm 1nad}(k_0,\eta_0) \\ &\leq c^4\rho^2_{\rm 0init}\frac{32\pi^2}{9k_0^3}\frac{\alpha(k_0)}{1-\alpha(k_0)}\Delta^2_{\mathcal{R}}(k_0) \\ &\leq \frac{c^4}{9}\hat{\alpha}^2A^2\,,\end{aligned} \tag{6.78}$$

where we have defined $\hat{\alpha}^2 \equiv \frac{\alpha(k_0)}{1-\alpha(k_0)}$ and $\alpha(k_0) = 0.15$ is the upper limit given by WMAP [7].

Non-adiabatic pressure perturbation during the radiation era

We now consider the relative non-adiabatic pressure perturbation due to the interaction between the different fluid types which is generated during the radiation era. This non-adiabatic pressure is not scale invariant. We determine the amplitude and scale dependence by considering the numerical calculation performed in Ref. [79] This paper considers a 5-fluid model made up of baryonic matter, cold dark matter, photons, neutrinos and dark energy within a ΛCDM cosmology. The system of equations, which is presented in Ref. [157], is solved to find the velocity perturbations

for the full system using a modified version of CMBFast [158,159]. Initial conditions are set such that it is assumed radiation domination and tight-coupling hold. The non-adiabatic pressure perturbation is then found by integrating the scaled entropy difference evolution equations (see Eq. 6.69). At early times and on large scales the resulting non-adiabatic pressure perturbation is found to scale as k^4, i.e. $\delta = 4$ in our description above, and so has the form,

$$\delta P_{1\mathrm{rel}} = B \left(\frac{k}{k_0}\right)^4 \left(\frac{\eta}{\eta_0}\right) . \tag{6.79}$$

To find the amplitude B we first note that from the expression above we have,

$$\delta P_{1\mathrm{rel}}(k_0, \eta_{\mathrm{eq}}) = B \left(\frac{\eta_{\mathrm{eq}}}{\eta_0}\right) , \tag{6.80}$$

and also from the definition of the power spectrum,

$$\frac{2\pi}{k_0^3} \mathcal{P}_{\delta P_{1\mathrm{rel}}}(k_0, \eta_{\mathrm{eq}}) = \langle |\delta P_{1\mathrm{rel}}(k_0, \eta_{\mathrm{eq}})|^2 \rangle . \tag{6.81}$$

This tells us that the constant B is given by

$$B = \left(\frac{2\pi}{k_0^3}\right)^{1/2} \mathcal{P}_{\delta P_{1\mathrm{rel}}}(k_0, \eta_{\mathrm{eq}})^{1/2} \left(\frac{\eta_0}{\eta_{\mathrm{eq}}}\right) . \tag{6.82}$$

From Ref. [79] we can read off the amplitude of the power spectrum when $k = k_0$ and $\eta = \eta_{\mathrm{eq}}$ to be roughly 10^{-6} and use this to find a value for B. In the calculation that follows we will be using a scaled version of B given by, Setting

$$\hat{B} = \frac{1}{c^2} B . \tag{6.83}$$

6.3.3 The electric field

In order to calculate the power spectrum of the magnetic field the time and scale dependency of the electric field and current are also needed. We have already assumed that the scale and time dependencies of the current and electric field are separable

and that they have the same scale dependence, namely,

$$\begin{aligned}\mathcal{E}_1(\mathbf{k},\eta) &= E(\eta)\mathcal{E}_1(\mathbf{k})\,,\\ \mathcal{J}_1(\mathbf{k},\eta) &= J(\eta)\mathcal{E}_1(\mathbf{k})\,.\end{aligned}$$

In the calculation that follows we will only be considering large scales and we showed in Section 4.3 that on large scales the electric field is scale invariant. By considering the Maxwell equation (Eq. (5.37)), we can see that the current will have the same scale dependence, therefore on large scales the assumption that the current and electric field are separable and have the same scale dependence is valid. As in the large scale case both $\mathcal{E}_1$ and $\mathcal{J}_1$ are scale invariant we only need find expressions for $E(\eta)$ and $J(\eta)$. The specific expressions of which will depend on whether we are considering the tight coupling approximation or not (see Section 4.3.1).

In the non-tight coupling scenario we have the following expression for the electric field (see Eq. (4.101))

$$\mathcal{E}_1 = \frac{2A\beta c^2}{3e\hat{n}_b}a^{-2} + \frac{2A\sigma_{Te}^2 c^2 m_p \beta^2}{3\mu_0 \hat{R}_b e^3}a^{-8}\,, \tag{6.84}$$

which, if we only include the most dominant term is given by,

$$\mathcal{E}_1 = E(\eta) = -\frac{2Ac^2\beta}{3\hat{n}_b a^2 e}\,. \tag{6.85}$$

To find the current we use the Maxwell equation, Eq. (5.37), and differentiate the electric field given in Eq. (6.84),

$$\mathcal{J}_1 = J(\eta) = -\frac{1}{c^2 a^3 \mu_0}(a^2\mathcal{E}_1)' = \frac{4A\sigma_{Te}^2 m_p \beta^2}{\mu_0^2 \hat{R}_b e^3 \eta_0}a^{-10}\,. \tag{6.86}$$

This allows us to find expressions for our functions $f(\eta)$ and $g(\eta)$, which appear in the integral describing the power spectrum and were defined in Eq. (6.44). Using

the above approximations for the electric field and current they are found to be,

$$f(\eta) = \frac{4Ac^2\beta}{3\eta_0^2\hat{n}_b e}\left(\frac{24\hat{n}_b\sigma_{Te}^2 m_p\beta}{\mu_0\hat{R}_b e^2} - a^6\right)a^{-10} = \bar{E}(\bar{J}\eta_0^8\eta^{-10} - \eta_0^2\eta^{-4})\,, \quad (6.87)$$

$$g(\eta) = \frac{48A\beta}{3\eta_0^2\hat{n}_b e}\left(\frac{3\hat{n}_b\sigma_{Te}^2 m_p\beta}{\mu_0\hat{R}_b e^2} - a^6\right)a^{-10} = \frac{12\bar{E}}{c^2}(\frac{\bar{J}}{8}\eta_0^8\eta^{-10} - \eta_0^2\eta^{-4})\,, \quad (6.88)$$

where we have introduced the two constants,

$$\bar{E} \equiv \frac{4Ac^2\beta}{3\hat{n}_b e}\,, \quad (6.89)$$

$$\bar{J} \equiv \frac{24\hat{n}_b\sigma_{Te}^2 m_p\beta}{\mu_0\hat{R}_b e^2} = 1.1\times 10^{-45}\,. \quad (6.90)$$

Secondly, in the tight coupling scenario (see Eq. (4.72)), we have,

$$\mathcal{E}_1 = \frac{Ac\beta\hat{R}_b}{6e\eta_0\sigma_{Te}\hat{n}_b^2}(1 + \frac{5a}{4\eta_0\hat{n}_b\sigma_{Te}c})\,. \quad (6.91)$$

Once again using the Maxwell equation and differentiating the electric field strength we arrive at an expression for the current,

$$\mathcal{J}_1 = J(\eta) = -\frac{1}{c^2a^3\mu_0}(a^2\mathcal{E}_1)' = -\frac{A\beta\hat{R}_b}{6e\eta_0^2\sigma_{Te}\hat{n}_b^2 c\mu_0}a^{-2}(2 + \frac{15a}{4\eta_0\hat{n}_b\sigma_{Te}c})\,. \quad (6.92)$$

This gives the following expressions for the functions $f(\eta)$ and $g(\eta)$,

$$f(\eta) = -\frac{7A\beta\hat{R}_b c}{3e\eta_0\sigma_{Te}\hat{n}_b^2}\eta^{-2} = \bar{F}\eta^{-2}\,, \quad (6.93)$$

$$g(\eta) = -\frac{5A\beta\hat{R}_b}{2e\eta_0^3c^2\sigma_{Te}^2\hat{n}_b^3}\eta^{-1} = \frac{\bar{G}}{c^2\eta_0}\eta^{-1}\,, \quad (6.94)$$

where we have again introduced two constants,

$$\bar{F} \equiv -\frac{7A\beta\hat{R}_b c}{3e\eta_0\sigma_{Te}\hat{n}_b^2}\,, \quad (6.95)$$

$$\bar{G} \equiv -\frac{5A\beta\hat{R}_b}{2e\eta_0^2\sigma_{Te}^2\hat{n}_b^3}\,. \quad (6.96)$$

6.4 Evaluating the Power Spectrum

In this section we will combine everything we have calculated so far, to evaluate the power spectrum. To proceed, we will only be interested in large scales. On sufficiently small scales, strongly non-linear astrophysical effects would dominate the calculation we present here and CPT will break down, and therefore a cut-off scale must be introduced. We can also use this large scale approximation to simplify our equations by considering scales satisfying $k^2c^2 \ll 6\mathcal{H}^2$, see the discussion in Section 6.7.3 for further details on small scales. We start by using our descriptions for the electric field strength, density perturbation and pressure perturbation, given in Eq. (6.84), Eq. (6.71) and Eq. (6.62) to substitute the scale and time dependence for $\delta\rho_1$, δP_1 and $\mathcal{E}_1$ into the Eq. (6.56) above. At present, we do not need to specify which of the two types of non-adiabatic pressure we have or whether we consider tight coupling or not, instead we substitute the general expressions which hold generally for all these scenarios. Finally we use the fact that we are working with a radiation background to simplify the two-point correlator, resulting in the following expression for the two-point correlator of the source term,

$$\begin{aligned}
&\langle S(\mathbf{k}_1,\eta_1)S^*(\mathbf{k}_2,\eta_2)\rangle = \frac{\eta_1^8\eta_2^8}{(2\pi)^3 4^4\rho_0^2\eta_0^{12}}k^2\bar{e}^j\bar{e}^i\delta(\mathbf{k}_1-\mathbf{k}_2)\int d^3\tilde{\mathbf{k}}\ \tilde{k}_i \\
&\Big[\tilde{k}_j\Big(f(\eta_1)f(\eta_2)A^2\eta_0^8\eta_1^{-4}\eta_2^{-4}+f(\eta_1)g(\eta_2)AP\eta_0^3k_0^{-\delta}\eta_1^{-4}\eta_2\tilde{k}^\delta \\
&+g(\eta_1)f(\eta_2)AP\eta_0^3k_0^{-\delta}\eta_1\eta_2^{-4}\tilde{k}^\delta+g(\eta_1)g(\eta_2)P^2\eta_0^{-2}k_0^{-2\delta}\eta_1\eta_2\tilde{k}^{2\delta}\Big) \\
&+|\tilde{\mathbf{k}}-\mathbf{k}|_j\Big(f(\eta_1)f(\eta_2)A^2\eta_0^8\eta_1^{-4}\eta_2^{-4}+f(\eta_1)g(\eta_2)AP\eta_0^3k_0^{-\delta}\eta_1^{-4}\eta_2\ |\tilde{\mathbf{k}}-\mathbf{k}|^\delta \\
&+g(\eta_1)f(\eta_2)AP\eta_0^3k_0^{-\delta}\eta_1\eta_2^{-4}\tilde{k}^\delta+g(\eta_1)g(\eta_2)P^2\eta_0^{-2}k_0^{-2\delta}\eta_1\eta_2\tilde{k}^\delta|\tilde{\mathbf{k}}-\mathbf{k}|^\delta\Big)\Big]\,,
\end{aligned} \tag{6.97}$$

We now outline the steps taken in order to carry out the k space integral above. Firstly, we switch to spherical coordinates, oriented with k in the direction of the axis and the angle between k and $\tilde{k}$ as θ, such that we have $\tilde{k}_i\bar{e^i} = \tilde{k}\sin\theta$. The integral then becomes,

$$\int d^3\tilde{\mathbf{k}} \to \int_0^{k_c}\tilde{k}^2d\tilde{k}\int_0^{\pi}\sin\theta d\theta\int_0^{2\pi}d\phi\,, \tag{6.98}$$

where we have introduced a small scale cut-off k_c as mentioned above. This move to spherical coordinates gives us the following expression for the two-point correlator of the source term,

$$\begin{aligned}
\langle S(\mathbf{k}_1,\eta_1)S^*(\mathbf{k}_2,\eta_2)\rangle \quad &= \frac{\eta_1^8\eta_2^8}{(2\pi)^2 4^4\rho_0^2\eta_0^{12}}k^2\delta(\mathbf{k}_1-\mathbf{k}_2)\int_0^{k_c}d\tilde{k}\int_0^{\pi}\sin^3\theta d\theta \\
&\Big[f(\eta_1)f(\eta_2)A^2\eta_0^8\eta_1^{-4}\eta_2^{-4}k^4\times \\
&\left((\tilde{k}/k)^4+\left(1+(\tilde{k}/k)^2-2(\tilde{k}/k)\cos\theta\right)^{1/2}(\tilde{k}/k)^3\right) \\
&+f(\eta_1)g(\eta_2)AP\eta_0^3k_0^{-\delta}\eta_1^{-4}\eta_2k^{\delta+4}\times \qquad (6.99)\\
&\left((\tilde{k}/k)^{\delta+4}+\left(1+(\tilde{k}/k)^2-2(\tilde{k}/k)\cos\theta\right)^{(\delta+1)/2}(\tilde{k}/k)^3\right) \\
&+g(\eta_1)f(\eta_2)AP\eta_0^3k_0^{-\delta}\eta_1\eta_2^{-4}k^{\delta+4}\times \qquad (6.100)\\
&\left((\tilde{k}/k)^{\delta+4}+(\tilde{k}/k)^{\delta+3}\left(1+(\tilde{k}/k)^2-2(\tilde{k}/k)\cos\theta\right)^{1/2}\right) \\
&+g(\eta_1)g(\eta_2)P^2\eta_0^{-2}k_0^{-2\delta}\eta_1\eta_2k^{2\delta+4}\times \qquad (6.101)\\
&\left((\tilde{k}/k)^{2\delta+4}+(\tilde{k}/k)^{\delta+3}\left(1+(\tilde{k}/k)^2-2(\tilde{k}/k)\cos\theta\right)^{(\delta+1)/2}\right)\Big]. \\
&\qquad (6.102)
\end{aligned}$$

We then carry out a change of variables to u and v defined as,

$$v=\tilde{k}/k\,,\quad u=\left(1+(\tilde{k}/k)^2-2(\tilde{k}/k)\cos\theta\right)^{1/2}\,, \qquad (6.103)$$

and the two-point correlator simplifies to,

$$\begin{aligned}
&\langle S(\mathbf{k}_1,\eta_1)S^*(\mathbf{k}_2,\eta_2)\rangle=\frac{\pi\eta_1^8\eta_2^8}{(2\pi)^3 4^5\rho_0^2\eta_0^{12}}k^3\delta(\mathbf{k}_1-\mathbf{k}_2) \\
&\int_0^{k_c/k}\int_{|1-v|}^{|1+v|}u\left(4v^2-(1+v^2-u^2)^2\right) \\
&\Big[f(\eta_1)f(\eta_2)A^2\eta_0^8\eta_1^{-4}\eta_2^{-4}k^4(v+u) \\
&+f(\eta_1)g(\eta_2)AP\eta_0^3k_0^{-\delta}\eta_1^{-4}\eta_2k^{\delta+4}(v^{\delta+1}+u^{\delta+1}) \\
&+g(\eta_1)f(\eta_2)AP\eta_0^3k_0^{-\delta}\eta_1\eta_2^{-4}k^{\delta+4}(v^{\delta+1}+v^{\delta}u) \\
&+g(\eta_1)g(\eta_2)P^2\eta_0^{-2}k_0^{-2\delta}\eta_1\eta_2k^{2\delta+4}(v^{2\delta+1}+v^{\delta}u^{\delta+1})\Big]dudv\,. \qquad (6.104)
\end{aligned}$$

To solve the integral above we split our calculation into four parts. We define the four integrals I_1, I_2, I_3 and I_4 as,

$$I_1 = k^7 \int_0^{k_c/k} \int_{|1-v|}^{|1+v|} (v+u)u\left(4v^2-(1+v^2-u^2)^2\right) dudv\,, \tag{6.105}$$

$$I_2 = k^{\delta+7}k_0^{-\delta} \int_0^{k_c/k} \int_{|1-v|}^{|1+v|} (v^{\delta+1}+u^{\delta+1})u\left(4v^2-(1+v^2-u^2)^2\right) dudv\,, \tag{6.106}$$

$$I_3 = k^{\delta+7}k_0^{-\delta} \int_0^{k_c/k} \int_{|1-v|}^{|1+v|} (v^{\delta+1}+v^{\delta}u)u\left(4v^2-(1+v^2-u^2)^2\right) dudv\,, \tag{6.107}$$

$$I_4 = k^{2\delta+7}k_0^{-2\delta} \int_0^{k_c/k} \int_{|1-v|}^{|1+v|} (v^{2\delta+1}+v^{\delta}u^{\delta+1})u\left(4v^2-(1+v^2-u^2)^2\right) dudv\,, \tag{6.108}$$

which enables us to write the two-point correlator of the source term as,

$$\begin{aligned}\langle S(\mathbf{k}_1,\eta_1)S^*(\mathbf{k}_2,\eta_2)\rangle \quad &= \frac{\pi\eta_1^8\eta_2^8}{(2\pi)^3 4^5\rho_0^2\eta_0^{12}}\delta(\mathbf{k}_1-\mathbf{k}_2)\times \\ &\Big[f(\eta_1)f(\eta_2)A^2\eta_0^8\eta_1^{-4}\eta_2^{-4}I_1 + f(\eta_1)g(\eta_2)AP\eta_0^3\eta_1^{-4}\eta_2 I_2 \\ &+g(\eta_1)f(\eta_2)AP\eta_0^3\eta_1\eta_2^{-4}I_3 + g(\eta_1)g(\eta_2)P^2\eta_0^{-2}\eta_1\eta_2 I_4\Big]\,.\end{aligned} \tag{6.109}$$

Recalling that we are looking to find the two-point correlator for the magnetic field, we use Eq. (6.53) to arrive at,

$$\begin{aligned}&\langle \mathcal{M}(\mathbf{k}_1,\eta)\mathcal{M}^*(\mathbf{k}_2,\eta)\rangle = \frac{\pi}{(2\pi)^3 4^5\rho_0^2\eta_4\eta_0^{12}}\delta(\mathbf{k}_1-\mathbf{k}_2)\times \\ &\int_{\eta_0}^{\eta}\int_{\eta_0}^{\eta}\Big[f(\tilde\eta_1)f(\tilde\eta_2)A^2\eta_0^8\tilde\eta_1^6\tilde\eta_2^6 I_1 + f(\tilde\eta_1)g(\tilde\eta_2)AP\eta_0^3\tilde\eta_1^6\tilde\eta_2^{11}I_2 \\ &+g(\tilde\eta_1)f(\tilde\eta_2)AP\eta_0^3\tilde\eta_1^{11}\tilde\eta_2^6 I_3 + g(\tilde\eta_1)g(\tilde\eta_2)P^2\eta_0^{-2}\tilde\eta_1^{11}\tilde\eta_2^{11}I_4\Big]d\tilde\eta_1 d\tilde\eta_2\,.\end{aligned} \tag{6.110}$$

In a similar way to above, in order to solve this integral we will split it in to four

parts again. We define four integrals over η, J_1, J_2, J_3 and J_4 as,

$$J_1 = \eta^{-4}\eta_0^{-4}\int_{\eta_0}^{\eta}\int_{\eta_0}^{\eta} f(\tilde{\eta}_1)f(\tilde{\eta}_2)\tilde{\eta}_1^6\tilde{\eta}_2^6 d\tilde{\eta}_1 d\tilde{\eta}_2\,, \tag{6.111}$$

$$J_2 = \eta^{-4}\eta_0^{-9}\int_{\eta_0}^{\eta}\int_{\eta_0}^{\eta} f(\tilde{\eta}_1)g(\tilde{\eta}_2)\tilde{\eta}_1^6\tilde{\eta}_2^{11} d\tilde{\eta}_1 d\tilde{\eta}_2\,, \tag{6.112}$$

$$J_3 = \eta^{-4}\eta_0^{-9}\int_{\eta_0}^{\eta}\int_{\eta_0}^{\eta} g(\tilde{\eta}_1)f(\tilde{\eta}_2)\tilde{\eta}_1^{11}\tilde{\eta}_2^6 d\tilde{\eta}_1 d\tilde{\eta}_2\,, \tag{6.113}$$

$$J_4 = \eta^{-4}\eta_0^{-14}\int_{\eta_0}^{\eta}\int_{\eta_0}^{\eta} g(\tilde{\eta}_1)g(\tilde{\eta}_2)\tilde{\eta}_1^{11}\tilde{\eta}_2^{11} d\tilde{\eta}_1 d\tilde{\eta}_2\,. \tag{6.114}$$

We are now able to write down a much simplified expression for the two point correlator of the magnetic field,

$$\langle \mathcal{M}(\mathbf{k}_1,\eta)\mathcal{M}^*(\mathbf{k}_2,\eta)\rangle = \frac{\delta(\mathbf{k}_1-\mathbf{k}_2)}{2(2\pi)^2 4^5\rho_0^2}\left[A^2 I_1 J_1 + APJ_2 I_2 + APJ_3 I_3 + P^2 J_4 I_4\right]\,. \tag{6.115}$$

Finally to extract the power spectrum we use the relation between the power spectrum and the two-point correlator to find,

$$k^3\mathcal{P}_{\mathcal{M}}(k) = \frac{k^6}{2\times 4^5(2\pi)^3\rho_0^2}\left[A^2 I_1 J_1 + APJ_2 I_2 + APJ_3 I_3 + P^2 J_4 I_4\right]\,. \tag{6.116}$$

In the next sections we will solve the eight integrals defined above, to find a solution of the power spectrum of the magnetic field.

6.4.1 Solving the I integrals

There are two different scenarios for the I integrals, depending on which description we have for the non-adiabatic pressure and we will consider both cases here.

6.4.1.1 Inflationary non-adiabatic pressure perturbation

Firstly, we consider the scenario where we have non-adiabatic pressure arising from inflation. As we saw in Section 6.3.2, in this scenario the non-adiabatic pressure will be described by Eq. (6.72) and hence the exponent is given by $\delta = 1$, and the amplitude is given by $P = D \leq \frac{c^2}{3}\hat{\alpha}A$, where $\hat{\alpha} = \left(\frac{\alpha(k_0)}{1-\alpha(k_0)}\right)^{1/2}$. In the following

sections we evaluate the maximum possible strength of the magnetic field generated due to non-adiabatic pressure perturbations by taking the upper limit for D, i.e. $D = \frac{c^2}{3}\hat{\alpha}A$. Substituting these constants into our expressions for the four I integrals we arrive at,

$$I_1 = k^7 \int_0^{k_c/k} \int_{|1-v|}^{|1+v|} (vu + u^2)\left(4v^2 - (1+v^2-u^2)^2\right) dudv\,, \tag{6.117}$$

$$I_2 = k^8 k_0^{-1} \int_0^{k_c/k} \int_{|1-v|}^{|1+v|} (v^2u + u^3)\left(4v^2 - (1+v^2-u^2)^2\right) dudv\,, \tag{6.118}$$

$$I_3 = k^8 k_0^{-1} \int_0^{k_c/k} \int_{|1-v|}^{|1+v|} (v^2u + u^2v)\left(4v^2 - (1+v^2-u^2)^2\right) dudv\,, \tag{6.119}$$

$$I_4 = k^9 k_0^{-2} \int_0^{k_c/k} \int_{|1-v|}^{|1+v|} (v^3u + vu^3)\left(4v^2 - (1+v^2-u^2)^2\right) dudv\,. \tag{6.120}$$

Carrying out these four integrals gives

$$I_1 = k^7 \left(\frac{2}{45} - \frac{16}{105}\left(\frac{k_c}{k}\right) + \frac{32}{45}\left(\frac{k_c}{k}\right)^3 + \frac{32}{15}\left(\frac{k_c}{k}\right)^5\right), \tag{6.121}$$

$$I_2 = k^8 k_0^{-1} \left(\frac{4}{3}\left(\frac{k_c}{k}\right)^4 + \frac{16}{9}\left(\frac{k_c}{k}\right)^6\right), \tag{6.122}$$

$$I_3 = k^8 k_0^{-1} \left(\frac{8}{945} - \frac{8}{105}\left(\frac{k_c}{k}\right)^2 + \frac{8}{15}\left(\frac{k_c}{k}\right)^4 + \frac{16}{9}\left(\frac{k_c}{k}\right)^6\right), \tag{6.123}$$

$$I_4 = k^9 k_0^{-2} \left(\frac{32}{21}\left(\frac{k_c}{k}\right)^7 + \frac{16}{15}\left(\frac{k_c}{k}\right)^5\right). \tag{6.124}$$

As all scales of interest in this calculation will be larger than the cut-off scale, i.e. $k < k_c$, it is clear that it is the highest power of $\frac{k_c}{k}$ that dominates these integral solutions. If we expand out the brackets above, all four have the same leading order behaviour, that is $I_i \propto \left(\frac{k}{k_c}\right)^2$.

6.4.1.2 Relative non-adiabatic pressure perturbation

Next we consider the scenario where we have non-adiabatic pressure arising from the interaction between different fluid species. In Section 6.3.2, we saw that in this

scenario the non-adiabatic pressure will be described by Eq. (6.79) and hence the exponent is given by $\delta = 4$, and the amplitude is given by $P = B = c^2\hat{B}$, where $\hat{\alpha} = \left(\frac{\alpha(k_0)}{1-\alpha(k_0)}\right)^{1/2}$. Substituting these constants into our expressions for the four I integrals we arrive at,

$$I_1 = k^7 \int_0^{k_c/k} \int_{|1-v|}^{|1+v|} (vu+u^2)\left(4v^2-(1+v^2-u^2)^2\right) dudv\,, \tag{6.125}$$

$$I_5 = k^{13}k_0^{-4} \int_0^{k_c/k} \int_{|1-v|}^{|1+v|} (v^5u+u^6)\left(4v^2-(1+v^2-u^2)^2\right) dudv\,, \tag{6.126}$$

$$I_6 = k^{13}k_0^{-4} \int_0^{k_c/k} \int_{|1-v|}^{|1+v|} (v^5u+u^2v^4)\left(4v^2-(1+v^2-u^2)^2\right) dudv\,, \tag{6.127}$$

$$I_7 = k^{15}k_0^{-8} \int_0^{k_c/k} \int_{|1-v|}^{|1+v|} (v^9u+v^4u^6)\left(4v^2-(1+v^2-u^2)^2\right) dudv\,, \tag{6.128}$$

where we have renamed the last three integrals to avoid confusion below. Carrying out these four integrals leads to

$$I_1 = k^7\left(\frac{2}{45}-\frac{16}{105}\left(\frac{k_c}{k}\right)+\frac{32}{45}\left(\frac{k_c}{k}\right)^3+\frac{32}{15}\left(\frac{k_c}{k}\right)^5\right), \tag{6.129}$$

$$I_5 = k^{11}k_0^{-4}\Big(\frac{4}{945}-\frac{16}{693}\left(\frac{k_c}{k}\right)+\frac{64}{189}\left(\frac{k_c}{k}\right)^3+\frac{96}{35}\left(\frac{k_c}{k}\right)^5 + \frac{64}{21}\left(\frac{k_c}{k}\right)^7+\frac{32}{27}\left(\frac{k_c}{k}\right)^9\Big), \tag{6.130}$$

$$I_6 = k^{11}k_0^{-4}\left(\frac{2}{4725}-\frac{16}{525}\left(\frac{k_c}{k}\right)^5+\frac{32}{105}\left(\frac{k_c}{k}\right)^7+\frac{32}{27}\left(\frac{k_c}{k}\right)^9\right), \tag{6.131}$$

$$I_7 = k^{15}k_0^{-8}\Big(\frac{1}{105105}-\frac{16}{3465}\left(\frac{k_c}{k}\right)^5+\frac{64}{441}\left(\frac{k_c}{k}\right)^7+\frac{32}{21}\left(\frac{k_c}{k}\right)^9 + \frac{64}{33}\left(\frac{k_c}{k}\right)^{11}+\frac{32}{39}\left(\frac{k_c}{k}\right)^{13}\Big). \tag{6.132}$$

These four integrals again have the same leading order behaviour as did the four integrals I_1 to I_4, that is, at leading order in k/k_c we have $I_i \propto \left(\frac{k}{k_c}\right)^2$.

6.4.2 Solving the J integrals

For the η integrals we also have two cases, this time depending on whether we have used the tight coupling approximation or not, when evaluating the electric field and the current.

6.4.2.1 Tight Coupling

Let us first look into the case where we have assumed the tight coupling approximation. The definitions for the functions $f(\eta)$ and $g(\eta)$ were given in Section 6.3.3 as,

$$f(\eta) = \bar{F}\eta^{-2}\,, \tag{6.133}$$

$$g(\eta) = \frac{\bar{G}}{c^2\eta_0}\eta^{-1}\,, \tag{6.134}$$

where $\bar{F}$ and $\bar{G}$ were defined in Eq. (6.95) and Eq. (6.96). Substituting the expressions for $f(\eta)$ and $g(\eta)$ into the four J integrals gives us,

$$J_1 = \bar{F}^2\eta^{-4}\eta_0^{-4}\int_{\eta_0}^{\eta}\int_{\eta_0}^{\eta}\tilde{\eta}_1^4\tilde{\eta}_2^4 d\tilde{\eta}_1 d\tilde{\eta}_2\,, \tag{6.135}$$

$$J_2 = \frac{\bar{F}\bar{G}}{c^2}\eta^{-4}\eta_0^{-10}\int_{\eta_0}^{\eta}\int_{\eta_0}^{\eta}\tilde{\eta}_1^4\tilde{\eta}_2^{10} d\tilde{\eta}_1 d\tilde{\eta}_2\,, \tag{6.136}$$

$$J_3 = \frac{\bar{F}\bar{G}}{c^2}\eta^{-4}\eta_0^{-10}\int_{\eta_0}^{\eta}\int_{\eta_0}^{\eta}\tilde{\eta}_1^{10}\tilde{\eta}_2^4 d\tilde{\eta}_1 d\tilde{\eta}_2\,, \tag{6.137}$$

$$J_4 = \frac{\bar{G}^2}{c^4}\eta^{-4}\eta_0^{-16}\int_{\eta_0}^{\eta}\int_{\eta_0}^{\eta}\tilde{\eta}_1^{10}\tilde{\eta}_2^{10} d\tilde{\eta}_1 d\tilde{\eta}_2\,. \tag{6.138}$$

Performing the integrations we obtain,

$$J_1 = \frac{\bar{F}^2}{25}\eta^{-4}\eta_0^{-4}\left(\eta^5-\eta_0^5\right)^2\,, \tag{6.139}$$

$$J_2 = J_3 = \frac{\bar{F}\bar{G}}{55c^2}\eta^{-4}\eta_0^{-10}\left(\eta^5-\eta_0^5\right)\left(\eta^{11}-\eta_0^{11}\right)\,, \tag{6.140}$$

$$J_4 = \frac{\bar{G}^2}{121c^4}\eta^{-4}\eta_0^{-16}\left(\eta^{11}-\eta_c^{11}\right)^2\,. \tag{6.141}$$

and expanding, using the fact that $\eta \ll \eta_0$ we end up with at first order,

$$J_1 = \frac{\bar{F}^2}{25}\eta^{-4}\eta_0^6\,, \quad J_2 = J_3 = \frac{\bar{F}\bar{G}}{55c^2}\eta^{-4}\eta_0^6\,, \quad J_4 = \frac{\bar{G}^2}{121c^4}\eta^{-4}\eta_0^6\,. \tag{6.142}$$

We can see from the above expressions that all the integrals have the same η dependence, that is $J_i \propto \left(\frac{\eta_0}{\eta}\right)^4$.

6.4.2.2 Non-tight coupling

We can now study the case where we have not assumed the tight coupling approximation. Once again our descriptions for the functions $f(\eta)$ and $g(\eta)$ were given above in Section 6.3.3,

$$f(\eta) = \bar{E}(\bar{J}\eta_0^8\eta^{-10} - \eta_0^2\eta^{-4})\,, \tag{6.143}$$

$$g(\eta) = \frac{12\bar{E}}{c^2}(\frac{\bar{J}}{8}\eta_0^8\eta^{-10} - \eta_0^2\eta^{-4})\,, \tag{6.144}$$

where $\bar{E}$ and $\bar{J}$ were defined in Eq. (6.89) and Eq. (6.90). Substituting these into our four J integrals gives us,

$$J_1 = \bar{E}^2\eta^{-4}\eta_0^{-4}\int_{\eta_0}^{\eta}\int_{\eta_0}^{\eta}(\bar{J}\eta_0^8\tilde{\eta}_1^{-4} - \eta_0^2\tilde{\eta}_1^2)(\bar{J}\eta_0^8\tilde{\eta}_2^{-4} - \eta_0^2\tilde{\eta}_2^2)d\tilde{\eta}_1 d\tilde{\eta}_2\,, \tag{6.145}$$

$$J_2 = \frac{12\bar{E}^2}{c^2}\eta^{-4}\eta_0^{-9}\int_{\eta_0}^{\eta}\int_{\eta_0}^{\eta}(\bar{J}\eta_0^8\tilde{\eta}_1^{-4} - \eta_0^2\tilde{\eta}_1^2)(\frac{\bar{J}}{8}\eta_0^8\tilde{\eta}_2 - \eta_0^2\tilde{\eta}_2^7)d\tilde{\eta}_1 d\tilde{\eta}_2\,, \tag{6.146}$$

$$J_3 = \frac{12\bar{E}^2}{c^2}\eta^{-4}\eta_0^{-9}\int_{\eta_0}^{\eta}\int_{\eta_0}^{\eta}(\frac{\bar{J}}{8}\eta_0^8\tilde{\eta}_1 - \eta_0^2\tilde{\eta}_1^7)(\bar{J}\eta_0^8\tilde{\eta}_2^{-4} - \eta_0^2\tilde{\eta}_2^2)d\tilde{\eta}_1 d\tilde{\eta}_2\,, \tag{6.147}$$

$$J_4 = \frac{144\bar{E}^2}{c^4}\eta^{-4}\eta_0^{-14}\int_{\eta_0}^{\eta}\int_{\eta_0}^{\eta}(\frac{\bar{J}}{8}\eta_0^8\tilde{\eta}_1 - \eta_0^2\tilde{\eta}_1^7)(\frac{\bar{J}}{8}\eta_0^8\tilde{\eta}_2 - \eta_0^2\tilde{\eta}_2^7)d\tilde{\eta}_1 d\tilde{\eta}_2\,. \tag{6.148}$$

Once again carrying out the η integrals gives us

$$J_1 = \bar{E}^2\eta^{-4}\eta_0^{-4}\left(-\frac{\bar{J}}{3}\eta_0^8(\eta^{-3}-\eta_0^{-3})-\frac{1}{3}\eta_0^2(\eta^3-\eta_0^3)\right)^2, \quad (6.149)$$

$$J_2 = J_3 = \frac{\bar{E}^2}{2c^2}\eta^{-4}\eta_0^{-9}\left(-\bar{J}\eta_0^8(\eta^{-3}-\eta_0^{-3})-\eta_0^2(\eta^3-\eta_0^3)\right)\times \left(\frac{\bar{J}}{2}\eta_0^8(\eta^2-\eta_0^2)-\eta_0^2(\eta^8-\eta_0^8)\right), \quad (6.150)$$

$$J_4 = \frac{144\bar{E}^2}{c^4}\eta^{-4}\eta_0^{-14}\left(\frac{\bar{J}}{16}\eta_0^8(\eta^2-\eta_0^2)-\frac{1}{8}\eta_0^2(\eta^8-\eta_0^8)\right)^2. \quad (6.151)$$

Noting once more that $\eta \ll \eta_0$ and expanding the expressions to first order in η,

$$J_1 = \frac{\bar{E}^2}{9}\eta^{-4}\eta_0^6(\bar{J}+1)^2, \quad (6.152)$$

$$J_2 = J_3 = \frac{\bar{E}^2}{2c^2}\eta^{-4}\eta_0^6(\bar{J}+1)(1-\frac{\bar{J}}{2}), \quad (6.153)$$

$$J_4 = \frac{9\bar{E}^2}{4c^4}\eta^{-4}\eta_0^6(1-\frac{\bar{J}}{2})^2, \quad (6.154)$$

and finally, since Eq. (6.90) implies that $\bar{J} \ll 1$, we can neglect the $\bar{J}$ to obtain,

$$J_1 = \frac{\bar{E}^2}{9}\eta^{-4}\eta_0^6, \quad J_2 = J_3 = \frac{\bar{E}^2}{2c^2}\eta^{-4}\eta_0^6, \quad J_4 = \frac{9\bar{E}^2}{4c^4}\eta^{-4}\eta_0^6. \quad (6.155)$$

The η dependence is the same in these four integrals as it was in the previous four. Thus all eight η integrals are proportional to $\left(\frac{\eta_0}{\eta}\right)^4$, with just different constants in the front.only differing through the constants of proportionality.

6.5 Results

Now that we have expressions for all the J and I integrals we can put everything together, using Eq. (6.116), for all four cases and find expressions for the power spectrum. We will consider the four cases one at a time below.

6.5.1 Inflationary non-adiabatic pressure and tight coupling

Firstly we will calculate the power spectrum of the magnetic field when we have an inflationary non-adiabatic pressure. Substituting for the J integrals, using Eq. (6.142), and the constants leads to the following expression for the upper limit of the power spectrum of the magnetic field in the tight coupling case,

$$k^3\mathcal{P}_{\mathcal{M}}(k,\eta) = \frac{A^2k^6\eta_0^2}{2\times 4^5(2\pi)^3\rho_0^2}\left(\frac{\eta_0}{\eta}\right)^4\left[\frac{\bar{F}^2}{25}I_1 + \frac{\hat{\alpha}}{3}\frac{\bar{F}\bar{G}}{55}I_2 + \frac{\hat{\alpha}}{3}\frac{\bar{F}\bar{G}}{55}I_3 + +\frac{\hat{\alpha}^2}{9}\frac{\bar{G}^2}{121}I_4\right]. \tag{6.156}$$

On substituting the four I integrals, defined in Eqs. (6.121), (6.122), (6.123) and (6.124) and in each case working to leading order in k, we find,

$$\begin{aligned}\sqrt{k^3\mathcal{P}_{\mathcal{M}}(k,\eta)} &= \frac{A\bar{F}\eta_0}{32\sqrt{2}(2\pi)^{3/2}\rho_0}\left(\frac{k_c}{\mathrm{Mpc}^{-1}}\right)^{13/2}\left(\frac{\eta_0}{\eta}\right)^2\times \\ &\left[\frac{32}{375}+\frac{\bar{G}}{\bar{F}}\frac{32\hat{\alpha}}{1485}\frac{k_c}{k_0}+\frac{\bar{G}^2}{\bar{F}^2}\frac{32\hat{\alpha}^2}{22869}\left(\frac{k_c}{k_0}\right)^2\right]^{1/2}\left(\frac{k}{k_c}\right)^4,\end{aligned} \tag{6.157}$$

where we have taken the square root of the expression to arrive at an approximation for the magnetic field strength. Finally putting in all the constants we find,

$$\sqrt{k^3\mathcal{P}_{\mathcal{M}}(k,\eta)} = 1.34\times 10^{-23}G\left(\frac{k_c}{\mathrm{Mpc}^{-1}}\right)^{15/2}\left(\frac{\eta_0}{\eta}\right)^2\left(\frac{k}{k_c}\right)^4. \tag{6.158}$$

For illustrative purposes we now choose a cut-off scale of 10 Mpc^{-1} in order to get an approximation for the strength of the magnetic field today. For more discussion on this choice of cut-off see Section 6.7.3 Evaluated today with $k_c = 10$ Mpc^{-1} on cluster scales $k = 1$ Mpc^{-1} this gives

$$\sqrt{k^3\mathcal{P}_{\mathcal{M}}(k,\eta)} = 4.24\times 10^{-20}G\,. \tag{6.159}$$

6.5.2 Inflationary non-adiabatic pressure & non- tight coupling

Keeping the inflationary non-adiabatic pressure contribution, we now look at the case where we do not assume the tight coupling approximation. Substituting for

the J integrals and constants (noting that this time we use the J integrals from Eq. (6.155)) we arrive at the following expression for the upper limit of the power spectrum,

$$k^3\mathcal{P}_{\mathcal{M}}(k,\eta) = \frac{A^2\bar{E}^2k^6\eta_0^2}{2\times 4^5(2\pi)^3\rho_0^2}\left(\frac{\eta_0}{\eta}\right)^4\left[\frac{1}{9}I_1+\frac{\hat{\alpha}}{3}\frac{1}{2}I_2+\frac{\hat{\alpha}}{3}\frac{1}{2}I_3++\frac{\hat{\alpha}^2}{9}\frac{9}{4}I_4\right]. \quad (6.160)$$

Following the steps as in the previous section and substituting for the I integrals gives the following expression,

$$\begin{aligned}\sqrt{k^3\mathcal{P}_{\mathcal{M}}(k,\eta)} &= \frac{A\bar{E}\eta_0}{32\sqrt{2}(2\pi)^{3/2}\rho_0}\left(\frac{k_c}{\mathrm{Mpc}^{-1}}\right)^{13/2}\left(\frac{\eta_0}{\eta}\right)^2\times \\ &\quad\left[\frac{32}{135}+\hat{\alpha}\frac{16}{27}\frac{k_c}{k_0}+\hat{\alpha}^2\frac{8}{21}\left(\frac{k_c}{k_0}\right)^2\right]^{1/2}\left(\frac{k}{k_c}\right)^4,\end{aligned} \quad (6.161)$$

where once more we only substitute the leading term for the four I integrals and take the square root to get an approximation for the magnetic field strength. Finally putting in all the constants we find,

$$\sqrt{k^3\mathcal{P}_{\mathcal{M}}(k,\eta)} = 2.4\times 10^{-30}G\left(\frac{k_c}{\mathrm{Mpc}^{-1}}\right)^{15/2}\left(\frac{\eta_0}{\eta}\right)^2\left(\frac{k}{k_c}\right)^4. \quad (6.162)$$

Evaluated today with $k_c = 10$ Mpc^{-1} on cluster scales $k = 1$ Mpc^{-1}, this gives

$$\sqrt{k^3\mathcal{P}_{\mathcal{M}}(k,\eta)} = 8\times 10^{-27}G\,. \quad (6.163)$$

6.5.3 Relative non-adiabatic pressure & tight coupling

We now consider the second case for non-adiabatic pressure that arises due to the interaction between species during the radiation era itself. We will start by calculating the power spectrum of the magnetic field in this case when we additionally assume the tight coupling approximation. We substitute for the J integrals using Eq. (6.142) and the constants and obtain the following expression for the power

spectrum of the magnetic field,

$$k^3\mathcal{P}_{\mathcal{M}}(k,\eta) = \frac{k^6\eta_0^2}{2\times 4^5(2\pi)^3\rho_0^2}\left(\frac{\eta_0}{\eta}\right)^4\left[A^2\frac{\bar{F}^2}{25}I_1 + A\hat{B}\frac{\bar{F}\bar{G}}{55}I_5 + A\hat{B}\frac{\bar{F}\bar{G}}{55}I_6 + +\hat{B}^2\frac{\bar{G}^2}{121}I_7\right]. \tag{6.164}$$

On substituting the four I integrals, this time defined in Eqs. (6.129), (6.130), (6.131) and (6.132), in each case working to leading order in k, we find,

$$\begin{aligned}\sqrt{k^3\mathcal{P}_{\mathcal{M}}(k,\eta)} &= \frac{A\bar{F}\eta_0}{32\sqrt{2}(2\pi)^{3/2}\rho_0}\left(\frac{k_c}{\mathrm{Mpc}^{-1}}\right)^{13/2}\left(\frac{\eta_0}{\eta}\right)^2\times \\ &\left[\frac{32}{375}+\frac{64}{1485}\frac{\hat{B}}{A}\frac{\bar{G}}{\bar{F}}\left(\frac{k_c}{k_0}\right)^4+\frac{32}{4719}\frac{\hat{B}^2}{A^2}\frac{\bar{G}^2}{\bar{F}^2}\left(\frac{k_c}{k_0}\right)^8\right]^{1/2}\left(\frac{k}{k_c}\right)^4,\end{aligned} \tag{6.165}$$

again having taken the square root of our power spectrum. Once more putting in all the constants we find,

$$\sqrt{k^3\mathcal{P}_{\mathcal{M}}(k,\eta)} = 1.9\times 10^{-29}G\left(\frac{k_c}{\mathrm{Mpc}^{-1}}\right)^{13/2}\left(\frac{\eta_0}{\eta}\right)^2\left(\frac{k}{k_c}\right)^4. \tag{6.166}$$

Evaluated today with $k_c = 10$ Mpc^{-1} on cluster scales $k = 1$ Mpc^{-1},

$$\sqrt{k^3\mathcal{P}_{\mathcal{M}}(k,\eta)} = 5.9\times 10^{-27}G\,. \tag{6.167}$$

6.5.4 Relative non-adiabatic pressure & non- tight coupling

Lastly, we move on to the final of the four cases, keeping the non-adiabatic pressure contribution, and relaxing the assumption of tight coupling. Once again we substitute the J integrals (from Eq. (6.155)) and the constants, to obtain,

$$k^3\mathcal{P}_{\mathcal{M}}(k,\eta) = \frac{\bar{E}^2k^6\eta_0^2}{2\times 4^5(2\pi)^3\rho_0^2}\left(\frac{\eta_0}{\eta}\right)^4\left[A^2\frac{1}{9}I_1 + A\hat{B}\frac{1}{2}I_5 + A\hat{B}\frac{1}{2}I_6 + +\hat{B}^2\frac{9}{4}I_7\right]. \tag{6.168}$$

Following the steps as in the previous section and substituting for the four I integrals and then taking the square root we get the following expression,

$$\sqrt{k^3\mathcal{P}_{\mathcal{M}}(k,\eta)} = \frac{\bar{E}A\eta_0}{32\sqrt{2}(2\pi)^{3/2}\rho_0}\left(\frac{k_c}{\mathrm{Mpc}^{-1}}\right)^{13/2}\left(\frac{\eta_0}{\eta}\right)^2 \times \left[\frac{32}{135}+\frac{32}{27}\frac{\hat{B}}{A}\left(\frac{k_c}{k_0}\right)^4+\frac{24}{13}\frac{\hat{B}^2}{A^2}\left(\frac{k_c}{k_0}\right)^8\right]^{1/2}\left(\frac{k}{k_c}\right)^4. \tag{6.169}$$

Substituting in all the constants we find,

$$\sqrt{k^3\mathcal{P}_{\mathcal{M}}(k,\eta)} = 6.5\times10^{-33}G\left(\frac{k_c}{\mathrm{Mpc}^{-1}}\right)^{13/2}\left(\frac{\eta_0}{\eta}\right)^2\left(\frac{k}{k_c}\right)^4. \tag{6.170}$$

Evaluated today with $k_c = 10$ Mpc^{-1} on cluster scales $k = 1$ Mpc^{-1}, we finally get,

$$\sqrt{k^3\mathcal{P}_{\mathcal{M}}(k,\eta)} = 2\times10^{-30}G\,. \tag{6.171}$$

6.6 Silk Damping

Around recombination photon diffusion will increase as the photon mean path becomes larger, leading to the damping of small length scale fluctuations, an effect that was first highlighted by Silk and is therefore referred to as Silk damping [160]. Photons are still only able to travel a comoving distance of k_D^{-1}, due to some Thompson scattering still occurring. The length the photon can travel is related to the opacity, and is given by $ak_D^{-1} \approx \left(\frac{t}{n_e\sigma_T}\right)^{1/2}$, at matter-radiation equality this gives $k_D \approx 0.5\mathrm{Mpc}^{-1}$. The effect of the increase in photon diffusion efficiency is to reduce the amplitude of fluctuations by a factor of $\exp\left[-\left(\frac{k}{k_D}\right)^2\right]$ [39]. We can incorporate Silk Damping into our results by multiplying our amplitudes by this exponential factor and we do this in the results we present below.

6.7 Discussion

One can first observe that in all four scenarios on large scales the magnetic field has the same scale and time dependence, namely

$$\mathcal{M}(k,\eta) \propto k^4\eta^{-2}\,. \tag{6.172}$$

This is as we would expect and matches the numerical results see for instance, Ref [149]. The amplitudes we get for all four results are also in agreement with previous numerical calculations (which are in the range $10^{-20} - 10^{-29}G$ [147–149]) and are in agreement with current observational limits ($\mathcal{M} \leq 10^{-9}G$ [120, 123]).

In order to make comparisons with previous results more easily we have evaluated the magnetic field strength at cluster scales ($k = 1$ Mpc^{-1}) that would be observed today if generated by this mechanism, we have also included silk damping. We can summarise the findings as:

- Inflationary non-adiabatic pressure & no tight coupling: $1.5 \times 10^{-28}G$
- Inflationary non-adiabatic pressure & tight coupling: $7.8 \times 10^{-22}G$
- Relative non-adiabatic pressure & no tight coupling: $3.7 \times 10^{-32}G$
- Relative non-adiabatic pressure & tight coupling: $1.1 \times 10^{-28}G$.

Tight coupling vs no tight coupling

Let us firstly compare the results we get considering tight coupling with the result we get if we do not assume this limit. At this point it is worth reiterating that we have considered two scenarios which are realized at different points in the early universe. The tight coupling of proton and electrons that we have assumed in our tight coupling scenario, occurs at the very start of the radiation era when $T \geq 230$eV. The complete breaking of all tight coupling between any species, which we allow in our non-tight coupling scenario, occurs as we approach decoupling at $T < 0.5$eV. In between these two extremes there is a period of the radiation era in which tight coupling holds between baryons and photons, to generate magnetic fields during

this era one needs to go to higher orders in tight coupling expansions. This is the scenario that has already been widely studied in the literature, see Section 6.7.2.

We find that when tight coupling is completely broken (see Eq. (6.163) and Eq. (6.171)), which, as mentioned above, is what we expect to happen as we approach matter-radiation equality, a stronger magnetic field is not generated, compared to when tight coupling is not broken (see Eq. (6.159) and Eq. (6.167)). This implies that well before recombination it is the interactions between the photons and baryons which have the dominant effect on the generation of the magnetic fields, rather than the interactions between protons and electrons. Although it should be stressed that we expect the proton-electron interaction to be stronger around recombination.

Finding a true approximation for the magnetic field close to recombination requires a full Boltzmann analysis, in our calculation we do not take into account additional physical effects which come into play close to recombination. For instance, we assume the number densities for our protons and electrons will only vary with the volume expansion, rather than decrease as they combine to form Hydrogen and we do not include the interactions with Hydrogen atoms at all. This decrease in free electrons will obviously effect the momentum transfer due to interactions between charged matter and radiation, which we defined in Section 4.2.2. During the recombination regime our baryon and photon fluids will also no longer behave as perfect fluids meaning the system of equations we have here will break down. In addition there are a host of more complicated physics processes which play a part during the production of both Hydrogen and Helium, for more details on these see Ref. [161].

The result we implement close to recombination, which we refer to as the non-tight coupling result, will not be the full result for magnetic generation during recombination, due to the reasons listed in the previous paragraph. It is merely an indication of what amplitude magnetic field we would expect to be produced solely from the interaction of the three species at this time without taking into account the physics of recombination. We should therefore keeping this in mind when considering the amplitude of the magnetic field produced during this regime. In order to find the full magnetic field generated during recombination we would need to incorporate the effects listed above. This is something that we will look at in more detail when we combine our equations with a Boltzmann code, see Section (7.2). However, it

should be noted that both our results which use the relative non-adiabatic pressure (as the previous numerical and analytical studies do) do not differ greatly between the tight coupling and non-tight coupling scenarios and are both in broad agreement with previous work.

Origin of the non-adiabatic pressure

Secondly, let us look at the full expression for the power spectrum of the magnetic field for the two different types of pressure perturbation i.e. Eq. (6.157), Eq. (6.161), Eq. (6.165) and Eq. (6.169). In both the cases where we considered the relative non-adiabatic pressure perturbation, it is the first of the three terms in (Eq. (6.165) and Eq. (6.169)) which makes the largest contribution (i.e. the term containing the I_1 integral). Looking back to Section 6.4 and in particular Eq. (6.116), we can see that this first source term contains the density perturbation, an electromagnetic component but no non-adiabatic pressure contribution. Thus in the case of non-adiabatic pressure originating from the interaction of different species, we can say that it is the density perturbation rather than the non-adiabatic pressure perturbation which has the dominant effect on the strength of the magnetic field generated and we would get the same result here if we considered no non-adiabatic pressure at all.

However, this is not the case when we use the inflationary non-adiabatic pressure perturbation. In both the cases in which we considered the inflationary non-adiabatic pressure perturbation, i.e. Eq. (6.157) and Eq. (6.161), it is the final term (the term containing the I_4 integral) which makes the largest contribution. Once again looking back at Section 6.4 and in particular Eq. (6.116), it is clear that the final source term contains the non-adiabatic pressure perturbation, an electromagnetic component, but no density perturbation contribution. Therefore, in this case the non-adiabatic pressure does play a role and leads to a larger amplitude for the generated magnetic field than we would expect from assuming no non-adiabatic pressure at all. In fact, in the case of the tight coupling result the amplitude of $10^{-20}G$ (see Eq. (6.157)) is significantly larger than most papers have previously predicted, the only numerical result which produces a similar result is Maeda et al. [148], who also consider non-adiabatic initial conditions. It is worth noting at this point that the amplitude we have used for the non-adiabatic pressure perturba-

tion from inflation is an upper bound on the allowed values and hence this numerical value for the magnetic field strength may not actually be attained and should also be considered an upper bound. From our results we can conclude that we expect a magnetic field with an amplitude of $10^{-30} - 10^{-20}G$, depending on the amount of isocurvature remaining after the end of inflation. This range of amplitudes is within the allowed observational bounds. Interestingly, if the isocurvature was close to the upper limit, then a magnetic field of close to $10^{-20}G$ may be generated, which is potentially large enough to act as a seed field.

6.7.1 Results in detail

Since we have seen that the possible presence of non-adiabatic pressure perturbation from inflation can generate a large amplitude for the magnetic field we will discuss these two cases in more detail. Firstly, we present the results here again, but this time substituting the full expressions for the I integrals rather than just the leading order term. For the non-tight coupling result we arrive at,

$$\sqrt{k^3\mathcal{P}_{\mathcal{M}}(k,\eta)} = 2.8\times10^{-31}G\left(\frac{k_c}{\mathrm{Mpc}^{-1}}\right)^7\left(\frac{\eta_0}{\eta}\right)^2\exp\left[-\left(\frac{\mathrm{k}}{\mathrm{k_D}}\right)^2\right]\times \left[\frac{8\hat{\alpha}}{21}\frac{k_c}{k_0}\left(\frac{k}{k_c}\right)^8+\frac{4\hat{\alpha}}{15}\frac{k_c}{k_0}\left(\frac{k}{k_c}\right)^{10}-\frac{4}{315}\left(\frac{k}{k_c}\right)^{12}+\frac{4}{2835}\left(\frac{k}{k_c}\right)^{14}\right]^{1/2}, \tag{6.173}$$

and when we set $k_c = 10\ \mathrm{Mpc}^{-1}$ and evaluate at matter-radiation equality this becomes,

$$\begin{aligned}\sqrt{k^3\mathcal{P}_{\mathcal{M}}} &= 3.2\times10^{-17}e^{-4k^2}\Big[736.3\left(\frac{k}{10}\right)^8+515.4\left(\frac{k}{10}\right)^{10} \\ &\quad -\frac{4}{315}\left(\frac{k}{10}\right)^{12}+\frac{4}{2835}\left(\frac{k}{10}\right)^{14}\Big]^{1/2}.\end{aligned} \tag{6.174}$$

Similarly for the tight-coupling result we have,

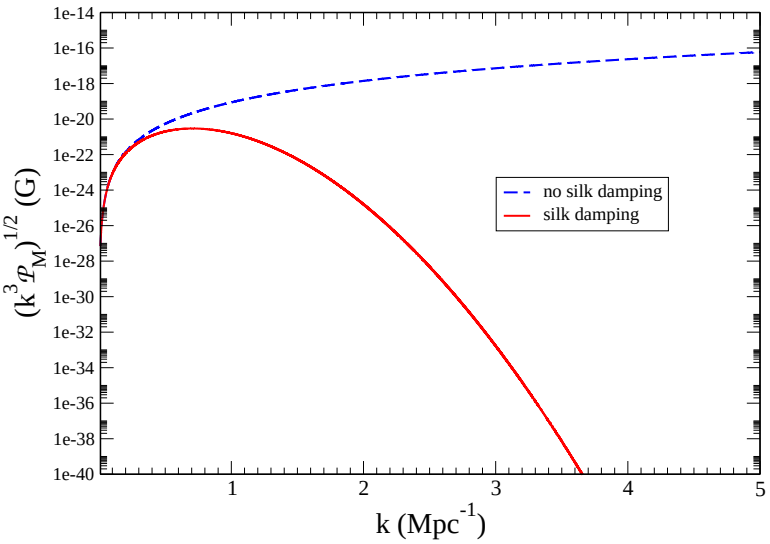

Figure 6.1: Plot showing $\sqrt{k^3\mathcal{P}_\mathcal{M}}$ in the scenario where we have an inflationary non-adiabatic pressure perturbation and no tight coupling. We have used the choice of $k_c = 10$ Mpc^{-1} evaluated at $\eta = \eta_{\rm eq}$. The graph compares the results including and not including silk damping.

$$\sqrt{k^3\mathcal{P}_\mathcal{M}(k,\eta)} = 6.66\times10^{-25}G\left(\frac{k_c}{\mathrm{Mpc}^{-1}}\right)^7\left(\frac{\eta_0}{\eta}\right)^2\exp\left[-\left(\frac{\mathrm{k}}{\mathrm{k_D}}\right)^2\right]\times$$
$$\left[0.9327\frac{k_c}{k_0}\left(\frac{k}{k_c}\right)^8+0.5668\frac{k_c}{k_0}\left(\frac{k}{k_c}\right)^{10}-\frac{8}{5775}\left(\frac{k}{k_c}\right)^{12}+\frac{8}{51975}\left(\frac{k}{k_c}\right)^{14}\right]^{1/2}, \tag{6.175}$$

and when we set $k_c = 10Mpc^{-1}$ and evaluate at matter-radiation equality this becomes,

$$\begin{aligned}\sqrt{k^3\mathcal{P}_\mathcal{M}} &= 7.7\times10^{-11}e^{-4k^2}\Big[4664\left(\frac{k}{10}\right)^8+2834\left(\frac{k}{10}\right)^{10}\\ &\quad-\frac{8}{5775}\left(\frac{k}{10}\right)^{12}+\frac{8}{51975}\left(\frac{k}{10}\right)^{14}\Big]^{1/2}.\end{aligned} \tag{6.176}$$

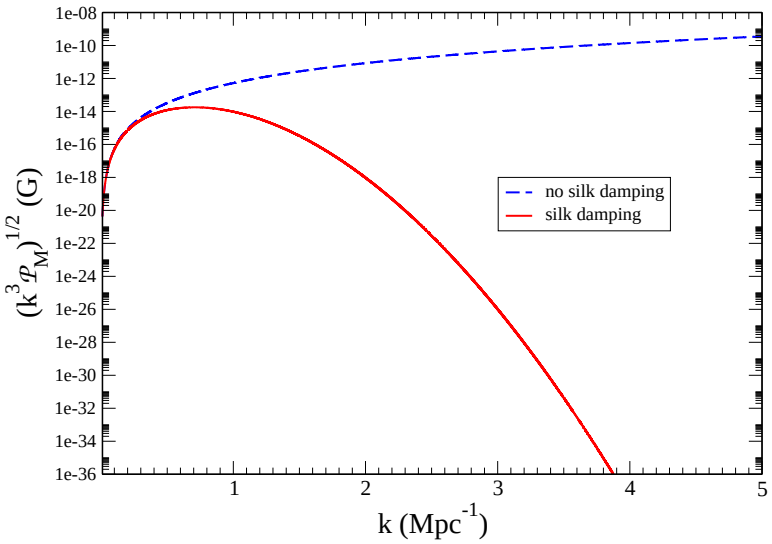

Figure 6.2: Plot showing $\sqrt{k^3\mathcal{P}_\mathcal{M}}$ in the scenario where we have an inflationary non-adiabatic pressure perturbation and we do have tight coupling. We have used the choice of $k_c = 10$ Mpc^{-1} evaluated at $\eta = \eta_{\rm eq}$. The graph compares the results including and not including silk damping.

In Fig. 6.1 and Fig. 6.2 we have plotted the results given in Eq. (6.174) and Eq. (6.176), that is, $\sqrt{k^3\mathcal{P}_\mathcal{M}}$ in the scenario where we have an inflationary non-adiabatic pressure, for the case where we do not assume tight-coupling and the case where we do, respectively. These illustrate that in both scenarios, if we ignore silk damping, the spectrum is rising towards small scales, which is something that has also been noted in previous numerical work, for instance Ref [149]. It is possible our magnitudes could be enhanced by considering small scale contributions, (see the discussion below for more details).

Order of magnitude estimate of our final result

We can see where the amplitude of our result comes from by considering the dominant terms in, for example, the inflationary tight coupling situation (our largest

result above). We recall that the source term is related to the magnetic field by,

$$\mathcal{M}(\mathbf{k},\eta) = \frac{1}{\eta^2}\int_{\eta_0}^{\eta} \tilde{\eta}^2 S(\mathbf{k},\tilde{\eta}) d\tilde{\eta}\,, \tag{6.177}$$

and, as highlighted above, the dominant source term is the one containing the non-adiabatic pressure, that is,

$$S \approx \frac{3\mathcal{H}k\bar{e}^j}{4(2\pi)^{3/2}c^2\rho\mathcal{H}^2}\int \tilde{k}_j \left(2a^2\mathcal{H}\mathcal{E}(\eta) - (a^2\mathcal{E}(\eta))'\right)\delta P_{\rm inf}(\tilde{\mathbf{k}},\eta) d^3\tilde{\mathbf{k}}\,, \tag{6.178}$$

So we find our dominant term comes from a coupling between the non-adiabatic pressure and the first order electric field. The first order electric field can be found from the momentum conservation equations and is given by

$$\mathcal{E}(\eta) = \frac{n_b m_p \sigma_{Te} c^2}{2eR_b}(V_{1(b)} - V_{1(\gamma)})\,, \tag{6.179}$$

where the velocity difference is

$$(V_{1(b)} - V_{1(\gamma)}) \approx \frac{\beta\mathcal{H}R_b}{c\sigma_{Te}^2 n_b^2 a^2}\frac{\delta\rho_\gamma}{4\rho_\gamma}\,. \tag{6.180}$$

The non-adiabatic pressure is given by

$$\delta P_{\rm inf}(\tilde{\mathbf{k}},\eta) = \frac{c^2}{3}\hat{\alpha}A\left(\frac{\eta}{\eta_0}\right)\,, \tag{6.181}$$

where the constant A satisfies,

$$A^2 = \delta\rho_1(k_0,\eta_{\rm init})^2 = 32\pi^2\rho_{0\rm init}^2 L^3 k_0^{-3}\Delta_{\mathcal{R}}^2(k_0)\,. \tag{6.182}$$

Combining these expressions above we find an order of magnitude estimate for the magnetic field, evaluated today at cluster scales

$$\mathcal{M}_1 \approx \frac{8\pi^2\rho_{0\rm init}k_0^{-3}\Delta_{\mathcal{R}}^2(k_0)\beta R_b\hat{\alpha}}{3e\eta_0\sigma_{Te}n_b^2(2\pi)^{3/2}} \approx 10^{-23}G\,. \tag{6.183}$$

This is line with the result we find above.

6.7.2 Comparison with previous analytic work

In the previous sections we have outlined the magnitude of the magnetic field that is generated by second order perturbations. There have been a few attempts previously to evaluate analytically the magnitude of such a magnetic field.

Paper	Assumptions	Amplitude of magnetic field (Gauss)
Betschart et al. [141]	no scattering & thermal effects	
	no 2nd order effects	$< 10^{-28} - 10^{-29}$ (rec)
	no anisotropic stress	$< 10^{-30} - 10^{-31}$ (now)
	no tensors	(oscillatory & on large scales)
	only adiabatic fluctuations	
Matarrese et al. [142]	no tensors	10^{-23} (rec)
	no anisotropic stress	10^{-29} (now)
	only adiabatic fluctuations	$(k = 1Mpc^{-1})$
Gopal et al. [143]	only adiabatic fluctuations	$<= 10^{-30}$ (now)
	no tensors	$(kpc^{-1} < k < 100Mpc^{-1})$
	no metric vector terms	
Siegel et al. [162]	no tensors	
	no anisotropic stress	10^{-24} (rec)
	only adiabatic fluctuations	$(k = 0.1Mpc^{-1})$
	no metric vector terms	
Kobayashi et al. [83]	no anisotropic stress	
	no tensors	10^{-27} (rec)
	only adiabatic fluctuations	(horizon scale)
Maeda et al. [146]	only adiabatic fluctuations	
	no anisotropic stress	10^{-29} (rec)
	no tensors	(horizon scale)

Table 6.1: A table summarising the analytic predictions for primordial magnetic fields in some current literature

All analytic calculations require that we make some assumptions in order to

simplify the calculations, in Table 6.1 we summarise the assumptions that have been taken and the resulting amplitudes of the magnetic fields produced in some of the previous literature. While we use similar methods to many of these papers we also consider non adiabatic fluctuations in our initial conditions, which is something none of the above papers look at. Like most of the papers above we neglect both the anisotropic stress and the tensors in our calculation. There is also yet to be a detailed analysis of the effect of tensor perturbation on the generation magnetic fields, which is something we plan to work on in the future. The results in Table 6.1 are in line with the magnitude of the magnetic field that we generate in our calculation.

6.7.3 Cut-off dependence

The final results we have presented here carry a dependence on the cut-off scale that we choose. There are various mathematical and physical reasons that a cut-off has had to be introduced here. Firstly, to simplify the calculation presented here we took the limit $c^2k^2 \ll 6\mathcal{H}^2$. This is equivalent to the limit that during the radiation era the wave number satisfies $ak \ll 7630$ Mpc^{-1}. Therefore whilst using that simplification we must have a cut-off that is no bigger than this. To increase the k cut-off more than this we would need to repeat the calculation without making the large scale assumptions. However, this is not necessary here due to other physical cut-off scales coming into play which are themselves smaller than this.

Secondly, as mentioned in Section 6.3.1, there is a turnover in the power spectrum of the density contrast at $k \approx 0.02$Mpc^{-1}. Therefore, on scales smaller than this we should be using a different scale dependence for the density perturbation in our calculation. Whilst close to this turnover we would not expect the results to greatly change, this would effect both results at scales much smaller than the turnover and the overall dependence on the cut-off scale. This is especially important as we approach matter-radiation equality. Prior to this the scale at which this turn over happens is smaller and will impact less on the results presented here.

Finally, it is also worth noting that we will need a cut-off scale in the calculation as on very small scales the calculation we focus on here will become dominated by strongly nonlinear astrophysical effects. These non-linear effects will eventually lead to a break down of CPT and give us an absolute cut-off scale, we can work

out this cut-off using effective field theory. The cut-off below which CPT does not apply is $k_{PT} = \frac{M_P^2}{H}$, where M_P is the reduced Planck mass [163]. At this point CPT will break down and although it may be possible that power could be moved from short scales into the large scale magnetic fields, to study this would need a different approach, such as effective field theory. This is outside the scope of this thesis and we leave further discussion of this for future work.

We need to choose a cut-off that is larger than the scales we are interested in, namely cluster scales ($k \approx 1$ Mpc^{-1}). In the approximations above we have therefore chosen a cut-off of 10 Mpc^{-1} in order to get a typical result. However, as the result is cut-off dependent we will now look at how picking a different cut-off would effect our values. If we vary our cut-off scale between 1 Mpc^{-1} and 1000 Mpc^{-1}, we will obtain different results. For instance, taking the inflationary non-tight coupling result we get the following approximations for the magnetic field strength evaluated on cluster scales today,

$$\begin{aligned} k_c &= 1Mpc^{-1} \qquad \sqrt{k^3\mathcal{P}_\mathcal{M}} \approx 4.4 \times 10^{-32}G \\ k_c &= 10Mpc^{-1} \qquad \sqrt{k^3\mathcal{P}_\mathcal{M}} \approx 1.5 \times 10^{-28}G \\ k_c &= 100Mpc^{-1} \qquad \sqrt{k^3\mathcal{P}_\mathcal{M}} \approx 4.4 \times 10^{-25}G \end{aligned} \tag{6.184}$$

Broadly speaking what ever cut-off scale we choose we still expect the magnitude of the generated magnetic field to lie in the range $10^{-32} - 10^{-24}G$.

To get a better understanding of our results on smaller scales a full small scale calculation is needed. As a first step we could repeat the calculation presented here taking the small rather than large scale limit and incorporate the turnover of the matter power spectrum into our results. This would lead to a different calculation than we have presented here in a number of ways. Firstly there would be further terms containing k which are currently neglected in our limit. Secondly the spectral index of the matter power spectrum is negative and is only valid up to a certain scale, so when carrying out the small scale calculation we would need to use both a small and large scale cut-off (a small scale cut-off corresponding to the break down of CPT and a large scale cut-off corresponding to the turnover scale in the matter power spectrum). Finally the k and η integrals would no longer be separable as

they are here, due to the turnover scale for the matter power spectrum evolving in time. Despite these three differences leading to equations with quite different k dependence the calculation could be completed as before, once the various cut-off scales have been incorporated. As the amplitude of the density power spectrum over most of the scales and times we are interested in would not be greatly different, we would expect to arrive at a similar amplitude to those given above. However the dependence on the small scale cut-off would be entirely determined by this new small scale calculation and therefore, incorporating it into our results would affect how our results depend on the cut-off scale. Whilst beyond the scope of the work in this thesis, this would be an obvious next step to take to extend these results. To go even further and fully investigate the very small scale result we would need to move from using CPT to an effective field theory approach.

Chapter 7

Outlook and Conclusions

Here we will summarise the work contained in this thesis and the conclusions made, before moving on to look at future directions in which this work may be taken. We finish with an outlook to the field of cosmological perturbation theory and magnetogenesis more generally.

7.1 Summary

Cosmological perturbation theory (CPT) is an important tool to studying the inhomogeneities in our universe. Since the first studies using CPT in the mid 1900's many have used CPT to study a variety of problems. Whilst linear-order perturbation theory has been well understood for many decades, it is only more recently that cosmologists have started using higher order perturbation theory to study many interesting applications such as non-Gaussianity or vorticity generation [45]. In this thesis we have focused on applications of CPT both at linear and second order.

At linear order we looked in detail at two applications to CPT. In Chapter 3 we used CPT to study the evolution of the curvature perturbation close to horizon crossing. In particular we looked at how much evolution occurred after horizon crossing. We found that ζ evaluated at horizon crossing can differ by up to 180% from its late time value and that to be within 1% of this value we must wait 2.9 e-folds. We finished this chapter by discussing the differences between the magnitude of ζ at horizon crossing, compared to at the end of inflation and using this to discuss

the analytic results and when these are valid.

Chapter 4 contained our second application of linear CTP where we moved on to present the formalism needed to study a multi-fluid system. After briefly summarising the equations needed we considered the specific example of a system of proton, electron and photon fluids in the early universe. We set up the governing equations and then solved them analytically by considering a small time period over which the velocities can be considered to evolve by a power law. We examined the difference in results when using the tight coupling approximation both to how the velocities of the species and the electric field strength would evolve. The time and scale dependence for the velocity of the three fluids and the strength of the electric field on large scales was also determined.

We then went on to look at the application of second order CPT to cosmological magnetogenesis in Chapter 5 and Chapter 6. Here we presented the fully relativistic Maxwell equations up to second order, giving these equations in flat gauge, and in Newtonian gauge, (which is very popular for numerical applications). Then we briefly discussed the gauge dependence of the Faraday tensor. We then used this formalism to study how primordial magnetic fields could be generated during the radiation era. We showed that at second order a magnetic field is sourced by various couplings between first order quantities, such as the density perturbation, non-adiabatic pressure perturbations, the current and the electric field strength. We discussed how we expected each of these first order quantities to behave during the time period we are interested in and then went on to calculate the generated magnetic fields' spectrum. We found that assuming only adiabatic initial conditions we could generate a magnetic field with strength approximately $10^{-27}G$ and that, as expected, on large scales $\sqrt{k^3\mathcal{P}_{\mathcal{M}}} \propto k^4\eta^{-2}$, in agreement with previous numerical work. However, we find, that upon including non-adiabatic initial conditions or isocurvature perturbations from inflation it may be possible to generate magnetic fields with magnitude up to $10^{-20}G$.

7.2 Future Directions

Whilst significant progress has been made in Chapter 5 and Chapter 6, there is clearly still much work to be done in the field of cosmological magnetogenesis, in

particular using perturbation theory. In Chapter 6 we made several assumptions in order to carry out our calculation, namely, we assumed that there were no first order magnetic fields generated from inflation, that the tensor perturbation does not affect our overall results and that anisotropic stress was negligible. The most obvious extension to our work would be to relax one or more of these assumptions.

As a first step we could include inflationary magnetic fields. Although we know that vector perturbations decay during inflation, there is still the possibility of magnetic fields being generated during this era and there is currently much research dedicated to inflationary magnetogenesis [115, 129–131]. If some first order inflationary magnetic fields do remain at the start of the radiation era then, even if they are decaying, this magnetic field could act as an initial condition to the generation of magnetic fields in the radiation era and possibly amplify our result. To proceed we would need to keep the first order vector perturbations in our equations and consider the presence of a decaying first order magnetic field. This would give us the following evolution equation for magnetic fields at second order,

$$\begin{aligned}
{\mathcal{M}_2}^{i\prime} &+ 2\mathcal{H}{\mathcal{M}_2}^{i} \\
&= (2{S_{1[j,}}^{i]} + 2a({\omega_1}^{i}{}_{j} + {\sigma_1}^{i}{}_{j}))\mathcal{M}_1{}^{j} \\
&\quad -\frac{4}{3}{v_1}^{j}{}_{,j}{\mathcal{M}_1}^{i} - 2{v_1}^{j}{\mathcal{M}_1}^{i}{}_{,j} - 2a^4({v_1}^{j} + {B_{1,}}^{j} - {S_1}^{j})({\mathcal{M}_{1j,}}^{i} - {\mathcal{M}_1}^{i}, j) \\
&\quad -2a^2\epsilon^{0ijk}((v_{1j}{}' + B_{1,j}{}' - S_{1j}{}' - \phi_{1,j} - 2\mathcal{H}(v_{1j} + B_{1,j}) + 2\mathcal{H}S_{1j})\mathcal{E}_{1k} \\
&\quad +\frac{1}{2}\mathcal{E}_{2k,j} + 2\phi_1\mathcal{E}_{1k,j} - v_{1j}a\mu_0\mathcal{J}_{1k} - B_{1,j}a\mu_0\mathcal{J}_{1k} + S_{1j}a\mu_0\mathcal{J}_{1k}),
\end{aligned}$$

where we now have additional source terms due to the initial magnetic field from inflation.

An alternative extension would be to include the tensor contribution to our source term. This is particularly relevant as the recent detection of a B-mode signal by BICEP [61], which is yet to be confirmed raises the possibility of a tensor contribution large enough to effect our results. If we once again assume that there are no magnetic fields generated from inflation but this time relax the condition that the tensors are

negligible, we arrive at the following evolution equation for the magnetic field,

$$\mathcal{M}_2{}^{i\prime} + 2\mathcal{H}\mathcal{M}_2{}^i = -2a^2\epsilon^{0ijk}\Big((V_{1j}{}' \;-\; \phi_{1,j} - 2\mathcal{H}V_{1j})\mathcal{E}_{1k} + \frac{1}{2}\mathcal{E}_{2k,j} \\ -\; \frac{1}{2}h_{1jk,l}\mathcal{E}_1{}^l + 2\phi_1\mathcal{E}_{1k,j} - V_{1j}a\mu_0\mathcal{J}_{1k}\Big)\,, \quad (7.1)$$

where the source term now contains an additional tensor term S_t^i,

$$S_t^i = a^2\epsilon^{0ijk}h_{1jk,l}\mathcal{E}_1{}^l\,. \quad (7.2)$$

Thirdly, we could include a small first order contribution to the anisotropic stress, which we neglected in our calculation. Along with including the tensor contribution, this would mean we were neglecting none of the source term contributions.

Lastly, as we include more contributions to the source term it makes sense to move to a fully rigorous numerical analysis of the problem. Although some numerical work has already been completed [146–149] in order to consider the extensions above we would wish to include some of the vector and tensor contributions which are currently neglected in many numerical models. This would allow a more detailed look at how the inflationary magnetic fields would impact the second order predictions and what effect gravitational waves would have. The relativistic Maxwell equations in Newtonian gauge (Eqs. (5.46)-(5.49)) are written in a form such that they can easily be combined with an existing second order Boltzmann code, such as SONG [155], to achieve this aim.

7.3 Outlook

We started this thesis by commenting on the vast improvement of data and observations that we currently have access to as cosmologists, over the next years this is likely to get even better. Whilst Planck has released some of its first data recently, we have yet to hear of the polarization results which are due to be released soon and there are other exciting telescopes and satellites in the pipeline. As mentioned in Section 7.2 Bicep at the South Pole, has recently detected a signal for B-mode polarization [61], and this could potentially be confirmed by the Planck polarization data. Observations from other ground-based telescopes such as the Atacama

Cosmology Telescope could also provide additional information which would help cosmologists towards a B-mode detection. It is possible that a B-mode signal can be explained be the presence of primordial magnetic fields, and therefore any detections of such a signal could give us further information about the possible generation mechanisms and scale dependence of such a magnetic field. As the type, amount and precision of data improves we can expect not only more accurate values for current observables but also the possiblity of new observables. For instance, if primordial magnetic fields are observed, then there is the possibility they could be used as a probe to deepen our understanding of early universe physics. With this in mind, and given that the precision at which we work analytically will need to match the level of precision reached in the observations, higher order perturbation theory will become an even more useful tool in the coming years.

A: Constants and Parameters

In this appendix we will list all the constants and parameter used throughout the thesis. We also include a useful check list of dimensions of various cosmological quantities.

Constants given in SI units

$$
\begin{aligned}
G &= 6.67300 \times 10^{-11} m^3 kg^{-1} s^{-2} \\
c &= 2.99792458 \times 10^{8} m s^{-1} \\
m_e &= 9.10938188 \times 10^{-31} kg \\
m_p &= 1.67262158 \times 10^{-27} kg \\
\sigma_{Te} &= 6.65245854533 \times 10^{-29} m^2 \\
\zeta(3) &= 1.202056903159594 \\
\sigma_{SB} &= 5.670373 \times 10^{-8} kg s^{-3} K^{-4} \\
e &= 1.60217646 \times 10^{-19} C \\
\epsilon_0 &= 8.854187817620 \times 10^{-12} C^2 kg^{-1} m^{-3} s^2 \\
\mu_0 &= 1.256637 \times 10^{-6} C^{-2} kgm \\
k_B &= 1.3806503 \times 10^{-23} m^2 kg s^{-2} K^{-1} \\
\beta &= 5.446170245 \times 10^{-4}
\end{aligned}
$$

Cosmological Parameters

We use a value for the CMB temperature based on the WMAP data and given in Ref. [164].

$$T_b = 2.72548 \pm 0.00057K$$

The following parameters have been taken from the PLANCK results combined with the WMAP polarization [8].

$$\begin{aligned} H_0 &= 67.3 \pm 1.2 kms^{-1}Mpc^{-1} \text{ (68\% CL)} \\ \Omega_k &= -0.037^{+0.043}_{-0.049} \text{ (95\% CL)} \\ z_{\rm eq} &= 3391 \pm 60 \text{ (68\% CL)} \\ h^2\Omega_{b0} &= 0.02205 \pm 0.00028 \text{ (68\% CL)} \end{aligned}$$

The following parameters have been taken from the WMAP results [6, 7].

$$\begin{aligned} \alpha_0(k_0) &= 0.15 \text{ (95\% CL)} \\ 10^9\Delta^2_{\mathcal{R}}(k_0) &= 2.41 \pm 0.10 \text{ (95\% CL)} \\ k_0 &= 0.002Mpc^{-1} \end{aligned}$$

We can calculate the following parameters based on the information given above

$$\begin{aligned} a_{\rm eq} &= (1 + z_{\rm eq})^{-1} = 2.94 \times 10^{-4} \\ \eta_0 &= \frac{2}{H_0} \\ \rho_c &= 8.508 \times 10^{-27} kgm^{-3} \\ \rho_{0\rm init} &= 8.823 \times 10^{-27} kgm^{-3} \\ \Omega_{\gamma 0} &= 3.78 \times 10^{-5} \\ n_{\gamma 0} &= 4.08 \times 10^8 m^{-3} \\ \eta_{B0} &= 6.160956522 \times 10^{-10} \\ n_{n0} &= 0.251 m^{-3} \end{aligned}$$

Dimensions and Units

We note that when we take the scalar part of a vector perturbation the dimension of the quantity changes by one length factor (L) i.e.

$$[V] = L\,[V_i]\ . \tag{3}$$

We also not that when moving to Fourier space quantities will have three extra length dimension units, i.e.

$$[V(k)] = L^3\,[V(x)]\ . \tag{4}$$

Finally we list some of the quantities we work with and their dimensions, where L represents a length dimension, m, a mass dimension, t a time dimension and B a magnetic dimension, such as Tesla or Gauss. Note that the magnetic units are related to the charge units by, $T = kgC^{-1}s^{-1}$.

$$\begin{aligned}
[B_i] &= [v_i] = [V_i] = 1 \\
[\phi_1] &= 1 \\
[u_i] &= mt^{-1} \\
[\eta] &= t \\
[\mathcal{M}_i(x,\eta)] &= B \\
[\mathcal{E}_i(x,\eta)] &= MLt^{-1} \\
[\mu_0\mathcal{J}(x,\eta)] &= B \\
[\rho(x,\eta)] &= [\delta\rho(x,\eta)] = mL^{-3} \\
[P(x,\eta)] &= [\delta P(x,\eta)] = mL^{-1}t^{-2}
\end{aligned}$$

B: Second Order Metric & Connection

In this appendix we will provide some of the useful geometrical quantities at second order [9].

Metric

$$
\begin{aligned}
g_{00} &= -a^2\left[1+2\phi_1+\phi_2\right] && (5)\\
g_{0i} &= a^2\left[B_{1i}+\frac{1}{2}B_{2i}\right] && (6)\\
g_{ij} &= a^2\left[\delta_{ij}+2C_{1ij}+C_{2ij}\right] && (7)
\end{aligned}
$$

$$
\begin{aligned}
g^{00} &= -a^{-2}\left[1-2\phi_1-\phi_2+4\phi_1^2-B_{1k}B_1^k\right] && (8)\\
g^{0i} &= a^{-2}\left[B_1^i+\frac{1}{2}B_2^i-2\phi_1B_1^i-2B_{1k}C_1^{ki}\right] && (9)\\
g^{ij} &= a^{-2}\left[\delta^{ij}-2C_1^{ij}-C_2^{ij}+4C_1^{ik}C_{1k}^j-B_1^iB_1^j\right] && (10)
\end{aligned}
$$

4-velocity

$$
\begin{aligned}
u_0 &= -a\left[1+\phi_1+\frac{1}{2}\phi_2-\frac{1}{2}\phi_1^2+v_{1k}v_1^k\right] && (11)\\
u_i &= a\left[v_{1i}+B_{1i}+\frac{1}{2}(v_{2i}+B_{2i})-\phi_1 B_{1i}+2C_{1ik}v_1^k\right] && (12)\\
u^0 &= a^{-1}\left[1-\phi_1-\frac{1}{2}\phi_2+\frac{3}{2}\phi_1^2+v_{1k}(v_1^k+2B_1^k)\right] && (13)\\
u^i &= a^{-1}\left[v_1^i+\frac{1}{2}v_2^i\right] && (14)
\end{aligned}
$$

Connections

$$
\begin{aligned}
\Gamma^0_{00} &= \mathcal{H}(1+B_1^iB_{1i})+\phi_1{}'+\frac{1}{2}\phi_2{}'-2\phi_1\phi_1{}'+B_1^iB_{1i}{}'+B_1^i\phi_{1,i} && (15)\\
\Gamma^0_{0i}=\Gamma^0_{i0} &= \phi_{1,i}+\frac{1}{2}\phi_{2,i}-2\phi_1\phi_{1,i}+\frac{1}{2}B_1^j(B_{1j,i}-B_{1i,j}+2\dot{C}_{1ij})\\
&\quad +\mathcal{H}(\frac{1}{2}B_{2i}+B_{1i}-2\phi_1B_{1i}) && (16)\\
\Gamma^i_{00} &= \mathcal{H}(B_1^i+\frac{1}{2}B_2^i-2B_{1k}C_1^{ki})-\phi_1{}'B_1^i+B_1^{i\prime}+\frac{1}{2}B_2^{i\prime}+\phi^i_{1,}+\frac{1}{2}\phi^i_{2,}\\
&\quad -C_1^{ij}(2B_{ij}{}'+2\phi_{1,j}) && (17)\\
\Gamma^0_{ij} &= \mathcal{H}\left[(\delta_{ij}+2C_{1ij}+C_{2ij})-\delta_{ij}(\phi_2-4\phi_1^2+B_{1k}B_1^k)-2\phi_1(\delta_{ij}+2C_{1ij})\right]\\
&\quad +C_{1ij}{}'+\frac{1}{2}C_{2ij}{}'-\frac{1}{4}(2B_{1i,j}+B_{2i,j}+2B_{1j,i}+B_{2j,i})-\phi_1(2C_{1ij}{}'-B_{1i,j}-B_{1j,i})\\
&\quad +B_1^k(C_{1ki,j}+C_{1jk,i}-C_{1ij,k})\\
\Gamma^i_{0j}=\Gamma^i_{j0} &= \mathcal{H}\left[\delta^i_j-B_{1j}B_1^i\right]-B_1^i\phi_{1,j}+\frac{1}{4}(2B^i_{1,j}+B^i_{2,j}-2B^i_{1j,}-B^i_{2j,})\\
&\quad +C^i_{1j}{}'+\frac{1}{2}C^i_{2j}{}'-C_1^{ki}B_{1k,j}+C_1^{ki}B_{1j,k}-2C_1^kiC_{1jk}{}' && (18)\\
\Gamma^i_{jk} &= -\mathcal{H}\left[(B_1^i+\frac{1}{2}B_2^i+2\phi_1B_1^i+2B_{1l}C_1^{li})\delta_{jk}+2B_1^iC_{1jk}\right]\\
&\quad +\frac{1}{2}B_1^i(B_{1j,k}+B_{1k,j}-2C_{1jk}{}')\\
&\quad +\frac{1}{2}(2C^i_{1j,k}+C^i_{2j,k}+2C^i_{1k,j}+C^i_{2k,j}-2C^i_{1jk,}-C^i_{2jk,})\\
&\quad -2C_1^{li}(C_{1lj,k}+C_{1kl,j}-C_{1jk,l}) && (19)
\end{aligned}
$$

C: Maxwell Equations

In this appendix we present the details of the projection of the Maxwell equations. Starting from the Maxwell's equations themselves,

$$F_{[\mu\nu;\lambda]} = 0, \quad F^{\mu\nu}{}_{;\nu} = \mu_0 j^\mu \,, \tag{20}$$

where $j^\mu = a^{-1}(\hat{\rho}, \mathbf{j})$ is the four-current that sources the electromagnetic field, $\hat{\rho}$ is the comoving charge density, $\mathbf{j}$ is the comoving charge current density and μ_0 is the magnetic constant and the four-current can be decomposed as follows

$$\hat{\rho} = -j^\mu u_\mu, \quad \mathcal{J}^\mu = h^\mu{}_\nu j^\nu \,. \tag{21}$$

where $\mathcal{J}^\mu$ is the projected four-current, orthogonal to the 4-velocity. We project the Maxwell equations along and orthogonal to the 4-velocity vector, multiplying by u_μ and h^μ_ν respectively, to decompose Maxwell's equations with respect to u_μ. This will give us the following four equations,

$$u_\mu F^{\mu\nu}{}_{;\nu} = \mu_0 u_\mu j^\mu \,, \tag{22}$$

$$u_\mu F_{[\mu\nu;\lambda]} = 0 \,, \tag{23}$$

$$h^\lambda_\mu F^{\mu\nu}{}_{;\nu} = h^\lambda_\mu \mu_0 j^\mu \,, \tag{24}$$

$$h^\lambda_\mu F_{[\mu\nu;\lambda]} = 0 \,. \tag{25}$$

We study each equation in turn and expand out both sides using the expressions we wrote down in Section 5.2.1. Firstly we consider the projection along the 4-velocity vector of the equation $F^{\mu\nu}{}_{;\nu} = j^\mu$ by multiplying by u_μ, i.e. Eq. (22) above. We work through this calculation below, using the decomposition of the 4-velocity,

Eq. (5.1), and the definition of the electric and magnetic field, Eq. (5.16), given above.

$$\begin{aligned}
u_\mu F^{\mu\nu}{}_{;\nu} &= \mu_0 u_\mu j^\mu\,, \\
(u_\mu F^{\mu\nu})_{;\nu} - F^{\mu\nu}u_{\mu;\nu} &= \mu_0 u_\mu j^\mu\,, \\
-\mathcal{E}^\mu{}_{;\mu} - F^{\mu\nu}(\sigma_{\mu\nu} + \frac{1}{3}\theta h_{\mu\nu} + \omega_{\mu\nu} - \dot{u_\mu}u_\nu) &= -\mu_0\hat{\rho}\,, \\
\mathcal{E}^\mu{}_{;\mu} + F^{\mu\nu}(\omega_{\mu\nu} - \dot{u_\mu}u_\nu) &= \mu_0\hat{\rho}\,, \\
\mathcal{E}^\mu{}_{;\mu} + F^{\mu\nu}\epsilon_{\mu\nu\lambda\delta}\omega^\lambda u^\delta - \mathcal{E}^\mu\dot{u_\mu} &= \mu_0\hat{\rho}\,, \\
\mathcal{E}^\mu{}_{;\mu} + 2\omega^\lambda\mathcal{M}_\lambda - \mathcal{E}^\mu\dot{u_\mu} &= \mu_0\hat{\rho}\,, \\
\mathcal{E}^\mu{}_{;\mu} - \mathcal{E}^\mu\dot{u_\mu} &= \mu_0\hat{\rho} - 2\omega^\lambda\mathcal{M}_\lambda\,. \qquad (26)
\end{aligned}$$

In the same way we can obtain the projection along the 4-velocity of the equation $F_{[\mu\nu;\lambda]} = 0$ i.e. by expanding out Eq. (23).

$$\begin{aligned}
u_\mu\epsilon^{\mu\nu\lambda\delta}F_{\nu\lambda;\delta} &= 0\,, \\
(u_\mu\epsilon^{\mu\nu\lambda\delta}F_{\nu\lambda})_{;\delta} - \epsilon^{\mu\nu\lambda\delta}F_{\nu\lambda}u_{\mu;\delta} &= 0\,, \\
2\mathcal{M}^\delta{}_{;\delta} - \epsilon^{\mu\nu\lambda\delta}F_{\nu\lambda}(\sigma_{\mu\delta} + \frac{1}{3}\theta h_{\mu\delta} + \omega_{\mu\delta} - \dot{u_\mu}u_\delta) &= 0\,, \\
2\mathcal{M}^\mu{}_{;\mu} - 2\dot{u_\mu}\mathcal{M}^\mu - \omega_{\mu\delta}\epsilon^{\mu\nu\lambda\delta}F_{\nu\lambda} &= 0\,, \\
\mathcal{M}^\mu{}_{;\mu} - \dot{u_\mu}\mathcal{M}^\mu - \omega^\mu\mathcal{E}_\mu &= 0\,. \qquad (27)
\end{aligned}$$

Now we repeat the process above to find the projection of the Maxwell equations orthogonal to the 4-velocity by multiplying the equations by the projection tensor $h^\lambda{}_\mu$, i.e. we expand out Eq. (24) and Eq. (25). This give us two further decomposed Maxwell equations.

$$\begin{aligned}
h^\lambda{}_\mu F^{\mu\nu}{}_{;\nu} &= \mu_0 h^\lambda{}_\mu j^\mu\,, \\
h^\lambda{}_\mu\dot{\mathcal{E}^\mu} &= (\omega^\lambda{}_\nu + \sigma^\lambda{}_\nu - \frac{2}{3}\theta h^\lambda{}_\nu)\mathcal{E}^\nu + \epsilon^{\lambda\mu\nu\alpha}u_\mu\dot{u_\nu}\mathcal{M}_\alpha - \epsilon^{\lambda\mu\nu\alpha}u_\mu\mathcal{M}_{\nu;\alpha} - \mu_0\mathcal{J}^\lambda\,, \qquad (28)
\end{aligned}$$

and

$$\begin{aligned} h^{\lambda}{}_{\mu}\epsilon^{\mu\nu\delta\beta}F_{\nu\delta;\beta} &= 0\,, \\ h^{\lambda}{}_{\mu}\dot{\mathcal{M}}^{\mu} &= (\omega^{\lambda}{}_{\nu}+\sigma^{\lambda}{}_{\nu}-\frac{2}{3}\theta h^{\lambda}{}_{\nu})\mathcal{M}^{\nu}-\epsilon^{\lambda\mu\nu\alpha}u_{\mu}\dot{u}_{\nu}\mathcal{E}_{\alpha}+\epsilon^{\lambda\mu\nu\alpha}u_{\mu}\mathcal{E}_{\nu;\alpha}\,. \end{aligned} \tag{29}$$

Recalling that the covariant derivative of a vector quantity is given by $\mathcal{E}^{\mu}{}_{;\nu} = \mathcal{E}^{\mu}{}_{,\nu}+\Gamma^{\mu}_{k\nu}\mathcal{E}^{k}$

we have the following set of four covariant Maxwell equations,

$$\begin{aligned} \mathcal{E}^{\mu}{}_{,\mu}+\Gamma^{\mu}_{k\mu}\mathcal{E}^{k}-\dot{u}_{\mu}\mathcal{E}^{\mu} &= \hat{\rho}-2\omega^{\mu}\mathcal{M}_{\mu}\,, \\ \mathcal{M}^{\mu}{}_{,\mu}+\Gamma^{\mu}_{k\mu}\mathcal{M}^{k}-\dot{u}_{\mu}\mathcal{M}^{\mu} &= -\omega^{\mu}\mathcal{E}_{\mu}\,, \end{aligned} \tag{30}$$

and

$$\begin{aligned} \dot{\mathcal{E}}^{\lambda\perp} &= (\omega^{\lambda}_{\nu}+\sigma^{\lambda}_{\nu}-\frac{2}{3}\theta h^{\lambda}_{\nu})\mathcal{E}^{\nu}+\epsilon^{\lambda\nu\mu}\dot{u}_{\nu}\mathcal{M}_{\mu}-\epsilon^{\lambda\nu\mu}(\mathcal{M}_{\nu,\mu}-\Gamma^{k}_{\nu\mu}\mathcal{M}_{k})-\mathcal{J}^{\lambda}\,, \\ \dot{\mathcal{M}}^{\lambda\perp} &= (\omega^{\lambda}_{\nu}+\sigma^{\lambda}_{\nu}-\frac{2}{3}\theta h^{\lambda}_{\nu})\mathcal{M}^{\nu}-\epsilon^{\lambda\nu\mu}\dot{u}_{\nu}\mathcal{E}_{\mu}+\epsilon^{\lambda\nu\mu}(\mathcal{E}_{\nu,\mu}-\Gamma^{k}_{\nu\mu}\mathcal{E}_{k})\,, \end{aligned} \tag{31}$$

where $\mathcal{E}^{\lambda\perp}$ and $\mathcal{M}^{\lambda\perp}$ are the projected electric and magnetic field respectively, both orthogonal to the 4-velocity.

D: Writing correlators as delta functions

In this appendix we show the full details of the calculation in Chapter 6 in which we rewrite a long correlator in terms of delta functions.

We start from our expression for the two-point correlator of the source term,

$$\begin{aligned}
&\langle S(\mathbf{k}_1,\eta_1)S^*(\mathbf{k}_2,\eta_2)\rangle = \frac{a_1^2 a_2^2 k_1 k_2 \bar{e}^i \bar{e}^j}{(2\pi)^3(1+\omega)^2\rho(\eta_1)\rho(\eta_2)} \\
&\int d^3\tilde{\mathbf{k}_1}\frac{\tilde{k_{1i}}}{9\mathcal{H}_1^2(1+\omega)+2c^2\tilde{k_1}^2}\int d^3\tilde{\mathbf{k}_2}\frac{\tilde{k_{2j}}}{9\mathcal{H}_2^2(1+\omega)+2c^2\tilde{k_2}^2} \\
&\langle [f(\eta_1)\delta\rho_1(\tilde{\mathbf{k}_1},\eta_1)+g(\tilde{k}_1,\eta_1)\delta P_{1\mathrm{nad}}(\tilde{\mathbf{k}_1},\eta_1)]\mathcal{E}_1(\mathbf{k}_1-\tilde{\mathbf{k}_1},\eta_1) \\
&[f(\eta_2)\delta\rho_1(\tilde{\mathbf{k}_2},\eta_2)+g(\tilde{k}_2,\eta_2)\delta P_{1\mathrm{nad}}(\tilde{\mathbf{k}_2},\eta_2)]\mathcal{E}_1(-(\tilde{\mathbf{k}_2}+\mathbf{k}_2),\eta_2)\rangle\,. \qquad (32)
\end{aligned}$$

As correlators are simply averages over probability distributions, we may expand out the terms inside the angled brackets and rewrite them as a sum of correlators,

$$\begin{aligned}
&\langle\rangle \equiv \langle [f(\eta_1)\delta\rho_1(\tilde{\mathbf{k}_1},\eta_1)+g(\tilde{k}_1,\eta_1)\delta P_{1\mathrm{nad}}(\tilde{\mathbf{k}_1},\eta_1)]\mathcal{E}_1(\mathbf{k}_1-\tilde{\mathbf{k}_1},\eta_1) \\
&[f(\eta_2)\delta\rho_1(\tilde{\mathbf{k}_2},\eta_2)+g(\tilde{k}_2,\eta_2)\delta P_{1\mathrm{nad}}(\tilde{\mathbf{k}_2},\eta_2)]\mathcal{E}_1(-(\tilde{\mathbf{k}_2}+\mathbf{k}_2),\eta_2)\rangle = \\
&f(\eta_1)f(\eta_2)\langle\delta\rho_1(\tilde{\mathbf{k}_1},\eta_1)\mathcal{E}_1(\mathbf{k}_1-\tilde{\mathbf{k}_1},\eta_1)\delta\rho_1(\tilde{\mathbf{k}_2},\eta_2)\mathcal{E}_1(-(\tilde{\mathbf{k}_2}+\mathbf{k}_2),\eta_2)\rangle \\
&+f(\eta_1)g(\tilde{k}_2,\eta_2)\langle\delta\rho_1(\tilde{\mathbf{k}_1},\eta_1)\mathcal{E}_1(\mathbf{k}_1-\tilde{\mathbf{k}_1},\eta_1)\delta P_{1\mathrm{nad}}(\tilde{\mathbf{k}_2},\eta_2)\mathcal{E}_1(-(\tilde{\mathbf{k}_2}+\mathbf{k}_2),\eta_2)\rangle \\
&+g(\tilde{k}_1,\eta_1)f(\eta_2)\langle\delta P_{1\mathrm{nad}}(\tilde{\mathbf{k}_1},\eta_1)\mathcal{E}_1(\mathbf{k}_1-\tilde{\mathbf{k}_1},\eta_1)\delta\rho_1(\tilde{\mathbf{k}_2},\eta_2)\mathcal{E}_1(-(\tilde{\mathbf{k}_2}+\mathbf{k}_2),\eta_2)\rangle \\
&+g(\tilde{k}_1,\eta_1)g(\tilde{k}_2,\eta_2)\langle\delta P_{1\mathrm{nad}}(\tilde{\mathbf{k}_1},\eta_1)\mathcal{E}_1(\mathbf{k}_1-\tilde{\mathbf{k}_1},\eta_1)\delta P_{1\mathrm{nad}}(\tilde{\mathbf{k}_2},\eta_2)\mathcal{E}_1(-(\tilde{\mathbf{k}_2}+\mathbf{k}_2),\eta_2)\rangle\,, \qquad (33)
\end{aligned}$$

where we have introduced the notation $\langle\rangle$ to correspond to the full four-point correlator.

We assume that the fluctuations $\delta\rho_1$ and δP_1 and the electric field are Gaussian (note that we showed in Chapter 4 that the electric field was related to $\delta\rho$, therefore if $\delta\rho$ is Gaussian this will imply that the electric field is too). We therefore proceed by putting the directional dependency of these three into Gaussian random variables $\hat{E}(\mathbf{k})$ as follows,

$$\delta\rho_1(\mathbf{k},\eta) = \delta\rho_1(k,\eta)\hat{E}(\mathbf{k})\,, \tag{34}$$

$$\delta P_{1\mathrm{nad}}(\mathbf{k},\eta) = \delta P_{1\mathrm{nad}}(k,\eta)\hat{E}(\mathbf{k})\,, \tag{35}$$

$$\mathcal{E}_1(\mathbf{k},\eta) = \mathcal{E}_1(k,\eta)\hat{E}(\mathbf{k})\,. \tag{36}$$

Gaussian variables obey the relationships

$$\langle\hat{E}^*(\mathbf{k}_1)\hat{E}(\mathbf{k}_2)\rangle = \delta(\mathbf{k}_1-\mathbf{k}_2)\,, \quad \langle\hat{E}(\mathbf{k}_1)\hat{E}(\mathbf{k}_2)\rangle = \delta(\mathbf{k}_1+\mathbf{k}_2)\,. \tag{37}$$

We can now write our four-point correlators, from Eq. (33) in terms of Gaussian random variables as,

$$\begin{aligned} &f(\eta_1)f(\eta_2)\langle\delta\rho_1(\tilde{\mathbf{k}}_1,\eta_1)\mathcal{E}_1(\mathbf{k}_1-\tilde{\mathbf{k}}_1,\eta_1)\delta\rho_1(\tilde{\mathbf{k}}_2,\eta_2)\mathcal{E}_1(-(\tilde{\mathbf{k}}_2+\mathbf{k}_2),\eta_2)\rangle \\ &\quad = f(\eta_1)f(\eta_2)\delta\rho_1(\tilde{k}_1,\eta_1)\mathcal{E}_1(|\tilde{\mathbf{k}}_1-\mathbf{k}_1|,\eta_1)\delta\rho_1(\tilde{k}_2,\eta_2)\mathcal{E}_1(|\tilde{\mathbf{k}}_2+\mathbf{k}_2|,\eta_2) \\ &\quad \langle\hat{E}(\tilde{\mathbf{k}}_1)\hat{E}(\mathbf{k}_1-\tilde{\mathbf{k}}_1)\hat{E}(\tilde{\mathbf{k}}_2)\hat{E}(-(\tilde{\mathbf{k}}_2+\mathbf{k}_2))\rangle\,, \end{aligned} \tag{38}$$

$$\begin{aligned} &f(\eta_1)g(\tilde{k}_2,\eta_2)\langle\delta\rho_1(\tilde{\mathbf{k}}_1,\eta_1)\mathcal{E}_1(\mathbf{k}_1-\tilde{\mathbf{k}}_1,\eta_1)\delta P_{1\mathrm{nad}}(\tilde{\mathbf{k}}_2,\eta_2)\mathcal{E}_1(-(\tilde{\mathbf{k}}_2+\mathbf{k}_2),\eta_2)\rangle \\ &\quad = f(\eta_1)g(\tilde{k}_2,\eta_2)\delta\rho_1(\tilde{k}_1,\eta_1)\mathcal{E}_1(|\tilde{\mathbf{k}}_1-\mathbf{k}_1|,\eta_1)\delta P_{1\mathrm{nad}}(\tilde{k}_2,\eta_2)\mathcal{E}_1(|\tilde{\mathbf{k}}_2+\mathbf{k}_2|,\eta_2) \\ &\quad \langle\hat{E}(\tilde{\mathbf{k}}_1)\hat{E}(\mathbf{k}_1-\tilde{\mathbf{k}}_1)\hat{E}(\tilde{\mathbf{k}}_2)\hat{E}(-(\tilde{\mathbf{k}}_2+\mathbf{k}_2))\rangle\,, \end{aligned} \tag{39}$$

$$\begin{aligned} &g(\tilde{k}_1,\eta_1)f(\eta_2)\langle\delta P_{1\mathrm{nad}}(\tilde{\mathbf{k}}_1,\eta_1)\mathcal{E}_1(\mathbf{k}_1-\tilde{\mathbf{k}}_1,\eta_1)\delta\rho_1(\tilde{\mathbf{k}}_2,\eta_2)\mathcal{E}_1(-(\tilde{\mathbf{k}}_2+\mathbf{k}_2),\eta_2)\rangle \\ &\quad = g(\tilde{k}_1,\eta_1)f(\eta_2)\delta P_{1\mathrm{nad}}(\tilde{k}_1,\eta_1)\mathcal{E}_1(|\tilde{\mathbf{k}}_1-\mathbf{k}_1|,\eta_1)\delta\rho_1(\tilde{k}_2,\eta_2)\mathcal{E}_1(|\tilde{\mathbf{k}}_2+\mathbf{k}_2|,\eta_2) \\ &\quad \langle\hat{E}(\tilde{\mathbf{k}}_1)\hat{E}(\mathbf{k}_1-\tilde{\mathbf{k}}_1)\hat{E}(\tilde{\mathbf{k}}_2)\hat{E}(-(\tilde{\mathbf{k}}_2+\mathbf{k}_2))\rangle\,, \end{aligned} \tag{40}$$

$$g(\tilde{k}_1,\eta_1)g(\tilde{k}_2,\eta_2)\langle\delta P_{\rm 1nad}(\tilde{\mathbf{k}}_1,\eta_1)\mathcal{E}_1(\mathbf{k}_1-\tilde{\mathbf{k}}_1,\eta_1)\delta P_{\rm 1nad}(\tilde{\mathbf{k}}_2,\eta_2)\mathcal{E}_1(-(\tilde{\mathbf{k}}_2+\mathbf{k}_2),\eta_2)\rangle$$
$$= g(\tilde{k}_1,\eta_1)g(\tilde{k}_2,\eta_2)\delta P_{\rm 1nad}(\tilde{k}_1,\eta_1)\mathcal{E}_1(|\tilde{\mathbf{k}}_1-\mathbf{k}_1|,\eta_1)\delta P_{\rm 1nad}(\tilde{k}_2,\eta_2)\mathcal{E}_1(|\tilde{\mathbf{k}}_2+\mathbf{k}_2|,\eta_2)$$
$$\langle\hat{E}(\tilde{\mathbf{k}}_1)\hat{E}(\mathbf{k}_1-\tilde{\mathbf{k}}_1)\hat{E}(\tilde{\mathbf{k}}_2)\hat{E}(-(\tilde{\mathbf{k}}_2+\mathbf{k}_2))\rangle\,. \tag{41}$$

The four-point correlator in all the above expressions is the same so summing all the above terms leads to the following expression for the overall correlator in Eq. (33),

$$\begin{aligned}\langle\rangle \;=\;& \mathcal{E}_1(|\tilde{\mathbf{k}}_1-\mathbf{k}_1|,\eta_1)\mathcal{E}_1(|\tilde{\mathbf{k}}_2+\mathbf{k}_2|,\eta_2)\times\\ & (f(\eta_1)f(\eta_2)\delta\rho_1(\tilde{k}_1,\eta_1)\delta\rho_1(\tilde{k}_2,\eta_2)\\ & +f(\eta_1)g(\tilde{k}_2,\eta_2)\delta\rho_1(\tilde{k}_1,\eta_1)\delta P_{\rm 1nad}(\tilde{k}_2,\eta_2)\\ & +g(\tilde{k}_1,\eta_1)f(\eta_2)\delta P_{\rm 1nad}(\tilde{k}_1,\eta_1)\delta\rho_1(\tilde{k}_2,\eta_2)\\ & +g(\tilde{k}_1,\eta_1)g(\tilde{k}_2,\eta_2)\delta P_{\rm 1nad}(\tilde{k}_1,\eta_1)\delta P_{\rm 1nad}(\tilde{k}_2,\eta_2))\\ & \langle\hat{E}(\tilde{\mathbf{k}}_1)\hat{E}(\mathbf{k}_1-\tilde{\mathbf{k}}_1)\hat{E}(\tilde{\mathbf{k}}_2)\hat{E}(-(\tilde{\mathbf{k}}_2+\mathbf{k}_2))\rangle\,.\end{aligned} \tag{42}$$

In order to expand out our four-point correlator above we make use of Wick's theorem [156],

$$\begin{aligned}&\langle\hat{E}(\tilde{\mathbf{k}}_1)\hat{E}(\mathbf{k}_1-\tilde{\mathbf{k}}_1)\hat{E}(\tilde{\mathbf{k}}_2)\hat{E}(-(\tilde{\mathbf{k}}_2+\mathbf{k}_2))\rangle =\\ &\quad\langle\hat{E}(\tilde{\mathbf{k}}_1)\hat{E}(\mathbf{k}_1-\tilde{\mathbf{k}}_1)\rangle\langle\hat{E}(\tilde{\mathbf{k}}_2)\hat{E}(-\tilde{\mathbf{k}}_2-\mathbf{k}_2)\rangle\\ &\quad+\langle\hat{E}(\tilde{\mathbf{k}}_1)\hat{E}(\tilde{\mathbf{k}}_2)\rangle\langle\hat{E}(\mathbf{k}_1-\tilde{\mathbf{k}}_1)\hat{E}(-\tilde{\mathbf{k}}_2-\mathbf{k}_2)\rangle\\ &\quad+\langle\hat{E}(\tilde{\mathbf{k}}_1)\hat{E}(-\tilde{\mathbf{k}}_2-\mathbf{k}_2)\rangle\langle\hat{E}(\mathbf{k}_1-\tilde{\mathbf{k}}_1)\hat{E}(\tilde{\mathbf{k}}_2)\rangle\,,\end{aligned} \tag{43}$$

and then substituting in delta functions in place of the two-point correlators, we find

$$\begin{aligned}&\langle\hat{E}(\tilde{\mathbf{k}}_1)\hat{E}(\mathbf{k}_1-\tilde{\mathbf{k}}_1)\hat{E}(\tilde{\mathbf{k}}_2)\hat{E}(-(\tilde{\mathbf{k}}_2+\mathbf{k}_2))\rangle\\ &=\delta(\tilde{\mathbf{k}}_1+\tilde{\mathbf{k}}_2)\delta(\mathbf{k}_1-\tilde{\mathbf{k}}_2-\tilde{\mathbf{k}}_1-\mathbf{k}_2)+\delta(\tilde{\mathbf{k}}_1-\tilde{\mathbf{k}}_2-\mathbf{k}_2)\delta(\mathbf{k}_1+\tilde{\mathbf{k}}_2-\tilde{\mathbf{k}}_1)\,.\end{aligned} \tag{44}$$

Inserting this expression for the four-point correlator into Eq. (32), we arrive at,

$$\begin{aligned}
&\langle S(\mathbf{k}_1,\eta_1)S^*(\mathbf{k}_2,\eta_2)\rangle = \frac{a_1^2 a_2^2 k_1 k_2 \bar{e}^i \bar{e}^j}{(2\pi)^3(1+\omega)^2\rho(\eta_1)\rho(\eta_2)} \\
&\int d^3\tilde{\mathbf{k}_1}\frac{\tilde{k_{1i}}\mathcal{E}_1(|\tilde{\mathbf{k}}_1-\mathbf{k}_1|,\eta_1)}{9\mathcal{H}_1^2(1+\omega)+2c^2\tilde{k_1}^2}\int d^3\tilde{\mathbf{k}_2}\frac{\tilde{k_{2j}}\mathcal{E}_1(|\tilde{\mathbf{k}}_2+\mathbf{k}_2|,\eta_2)}{9\mathcal{H}_2^2(1+\omega)+2c^2\tilde{k_2}^2} \\
&(f(\eta_1)f(\eta_2)\delta\rho_1(\tilde{k}_1,\eta_1)\delta\rho_1(\tilde{k}_2,\eta_2) \\
&+f(\eta_1)g(\tilde{k}_2,\eta_2)\delta\rho_1(\tilde{k}_1,\eta_1)\delta P_{1\mathrm{nad}}(\tilde{k}_2,\eta_2) \\
&+g(\tilde{k}_1,\eta_1)f(\eta_2)\delta P_{1\mathrm{nad}}(\tilde{k}_1,\eta_1)\delta\rho_1(\tilde{k}_2,\eta_2) \\
&+g(\tilde{k}_1,\eta_1)g(\tilde{k}_2,\eta_2)\delta P_{1\mathrm{nad}}(\tilde{k}_1,\eta_1)\delta P_{1\mathrm{nad}}(\tilde{k}_2,\eta_2)) \\
&(\delta(\tilde{\mathbf{k}}_1+\tilde{\mathbf{k}}_2)\delta(\mathbf{k}_1-\tilde{\mathbf{k}}_2-\tilde{\mathbf{k}}_1-\mathbf{k}_2)+\delta(\tilde{\mathbf{k}}_1-\tilde{\mathbf{k}}_2-\mathbf{k}_2)\delta(\mathbf{k}_1+\tilde{\mathbf{k}}_2-\tilde{\mathbf{k}}_1))\,. \quad (45)
\end{aligned}$$

References

[1] E. Nalson, A. J. Christopherson, I. Huston, and K. A. Malik, "Quantifying the behaviour of curvature perturbations during inflation," *Class.Quant.Grav.*, vol. 30, p. 065008, 2013, 1111.6940. 2, 48

[2] E. Nalson, A. J. Christopherson, I. Huston, and K. A. Malik, "Quantifying the behaviour of curvature perturbations near Horizon Crossing," 2013, 1301.7613. 2, 48

[3] E. Nalson, A. J. Christopherson, and K. A. Malik, "Effects of non-linearities on magnetic field generation," 2013, 1312.6504. 2

[4] A. A. Penzias and R. W. Wilson, "A Measurement of excess antenna temperature at 4080-Mc/s," *Astrophys.J.*, vol. 142, pp. 419–421, 1965. 12

[5] C. Bennett, A. Kogut, G. Hinshaw, A. Banday, E. Wright, *et al.*, "Cosmic temperature fluctuations from two years of COBE differential microwave radiometers observations," *Astrophys.J.*, vol. 436, pp. 423–442, 1994, astro-ph/9401012. 12

[6] E. Komatsu *et al.*, "Seven-Year Wilkinson Microwave Anisotropy Probe (WMAP) Observations: Cosmological Interpretation," *Astrophys.J.Suppl.*, vol. 192, p. 18, 2011, 1001.4538. 12, 14, 22, 57, 166

[7] G. Hinshaw *et al.*, "Nine-Year Wilkinson Microwave Anisotropy Probe (WMAP) Observations: Cosmological Parameter Results," *Astrophys.J.Suppl.*, vol. 208, p. 19, 2013, 1212.5226. 12, 22, 56, 131, 132, 166

[8] P. Ade *et al.*, "Planck 2013 results. XVI. Cosmological parameters," 2013, 1303.5076. 12, 14, 20, 21, 22, 26, 56, 116, 128, 166

[9] K. A. Malik and D. Wands, "Cosmological perturbations," *Phys.Rept.*, vol. 475, pp. 1–51, 2009, 0809.4944. 12, 29, 37, 40, 58, 103, 104, 112, 129, 168

[10] E. Lifshitz, "On the Gravitational stability of the expanding universe," *J.Phys.(USSR)*, vol. 10, p. 116, 1946. 13

[11] E. Lifshitz and I. Khalatnikov, "Investigations in relativistic cosmology," *Adv.Phys.*, vol. 12, pp. 185–249, 1963. 13

[12] S. Hawking, "Perturbations of an expanding universe," *Astrophys.J.*, vol. 145, pp. 544–554, 1966. 13

[13] D. Olson, "Density Perturbations on Cosmological Models," *Phys.Rev.*, vol. D14, pp. 327–331, 1976. 13

[14] J. M. Bardeen, "Gauge Invariant Cosmological Perturbations," *Phys. Rev.*, vol. D22, pp. 1882–1905, 1980. 13, 30, 37

[15] H. Kodama and M. Sasaki, "Cosmological Perturbation Theory," *Prog.Theor.Phys.Suppl.*, vol. 78, pp. 1–166, 1984. 13, 129

[16] R. H. Brandenberger, H. Feldman, and V. F. Mukhanov, "Gauge invariant cosmological perturbations," 1992. 13

[17] G. Ellis and M. Bruni, "Covariant and Gauge Invariant Approach to Cosmological Density Fluctuations," *Phys.Rev.*, vol. D40, pp. 1804–1818, 1989. 13

[18] G. Ellis, J. Hwang, and M. Bruni, "Covariant and Gauge Independent Perfect Fluid Robertson-Walker Perturbations," *Phys.Rev.*, vol. D40, pp. 1819–1826, 1989. 13

[19] G. Ellis, M. Bruni, and J. Hwang, "Density Gradient - Vorticity Relation in Perfect Fluid Robertson-Walker Perturbations," *Phys.Rev.*, vol. D42, pp. 1035–1046, 1990. 13

[20] M. Bruni, P. K. Dunsby, and G. F. Ellis, "Cosmological perturbations and the physical meaning of gauge invariant variables," *Astrophys.J.*, vol. 395, pp. 34–53, 1992. 13

[21] V. Acquaviva, N. Bartolo, S. Matarrese, and A. Riotto, "Second order cosmological perturbations from inflation," *Nucl.Phys.*, vol. B667, pp. 119–148, 2003, astro-ph/0209156. 13

[22] N. Bartolo, E. Komatsu, S. Matarrese, and A. Riotto, "Non-Gaussianity from inflation: Theory and observations," *Phys.Rept.*, vol. 402, pp. 103–266, 2004, astro-ph/0406398. 13

[23] M. Bruni, S. Matarrese, S. Mollerach, and S. Sonego, "Perturbations of spacetime: Gauge transformations and gauge invariance at second order and beyond," *Class.Quant.Grav.*, vol. 14, pp. 2585–2606, 1997, gr-qc/9609040. 13

[24] A. J. Christopherson, K. A. Malik, D. R. Matravers, and K. Nakamura, "Comparing different formulations of non-linear cosmological perturbation theory," *Class.Quant.Grav.*, vol. 28, p. 225024, 2011, 1101.3525. 13

[25] K. A. Malik, "Gauge-invariant perturbations at second order: Multiple scalar fields on large scales," *JCAP*, vol. 0511, p. 005, 2005, astro-ph/0506532. 13

[26] K. A. Malik and D. Wands, "Evolution of second-order cosmological perturbations," *Class.Quant.Grav.*, vol. 21, pp. L65–L72, 2004, astro-ph/0307055. 13

[27] V. F. Mukhanov, L. R. W. Abramo, and R. H. Brandenberger, "On the Back reaction problem for gravitational perturbations," *Phys.Rev.Lett.*, vol. 78, pp. 1624–1627, 1997, gr-qc/9609026. 13, 35

[28] K. Nakamura, "Gauge invariant variables in two parameter nonlinear perturbations," *Prog.Theor.Phys.*, vol. 110, pp. 723–755, 2003, gr-qc/0303090. 13

[29] K. Nakamura, "Second-order Gauge-Invariant Cosmological Perturbation Theory: Current Status," *Adv.Astron.*, vol. 2010, p. 576273, 2010, 1001.2621. 13

[30] H. Noh and J. chan Hwang, "Second-order perturbations of the Friedmann world model," *Phys.Rev.*, vol. D69, p. 104011, 2004. 13

[31] A. J. Christopherson and K. A. Malik, "Practical tools for third order cosmological perturbations," *JCAP*, vol. 0911, p. 012, 2009, 0909.0942. 13

[32] P. Ade *et al.*, "Planck 2013 results. XXIII. Isotropy and statistics of the CMB," 2013, 1303.5083. 14

[33] P. Ade *et al.*, "Planck 2013 results. XXVI. Background geometry and topology of the Universe," 2013, 1303.5086. 14

[34] C. W. Misner, K. Thorne, and J. Wheeler, "Gravitation," 1974. 16

[35] A. R. Liddle and D. Lyth, "Cosmological inflation and large scale structure," 2000. 21, 25, 26, 55, 58, 69, 78

[36] A. H. Guth, "The Inflationary Universe: A Possible Solution to the Horizon and Flatness Problems," *Phys.Rev.*, vol. D23, pp. 347–356, 1981. 22

[37] R. Allahverdi, R. Brandenberger, F.-Y. Cyr-Racine, and A. Mazumdar, "Reheating in Inflationary Cosmology: Theory and Applications," *Ann.Rev.Nucl.Part.Sci.*, vol. 60, pp. 27–51, 2010, 1001.2600. 24, 52

[38] B. A. Bassett, S. Tsujikawa, and D. Wands, "Inflation dynamics and reheating," *Rev.Mod.Phys.*, vol. 78, pp. 537–589, 2006, astro-ph/0507632. 24, 52

[39] D. H. Lyth and A. R. Liddle, "The primordial density perturbation: Cosmology, inflation and the origin of structure," 2009. 24, 79, 82, 131, 148

[40] S. Weinberg, "Cosmology," 2008. 24, 128

[41] D. Baumann, "TASI Lectures on Inflation," 2009, 0907.5424. 26

[42] A. Leithes and K. A. Malik, "Conserved Quantities in Lemaitre-Tolman-Bondi Cosmology," 2014, 1403.7661. 29

[43] M. Sasaki, "Large Scale Quantum Fluctuations in the Inflationary Universe," *Prog.Theor.Phys.*, vol. 76, p. 1036, 1986. 38

[44] V. F. Mukhanov, "Quantum Theory of Gauge Invariant Cosmological Perturbations," *Sov.Phys.JETP*, vol. 67, pp. 1297–1302, 1988. 38

[45] A. J. Christopherson, K. A. Malik, and D. R. Matravers, "Estimating the amount of vorticity generated by cosmological perturbations in the early universe," *Phys.Rev.*, vol. D83, p. 123512, 2011, 1008.4866. 46, 160

[46] V. Mukhanov, "Physical foundations of cosmology," 2005. 49

[47] N. Birrell and P. Davies, "Quantum Fields in Curved Space," *Cambridge Monogr.Math.Phys.*, 1982. 49

[48] W. Unruh, "Notes on black hole evaporation," *Phys.Rev.*, vol. D14, p. 870, 1976. 49

[49] W. H. Kinney, "TASI Lectures on Inflation," 2009, 0902.1529. 49

[50] D. Salopek, J. Bond, and J. M. Bardeen, "Designing Density Fluctuation Spectra in Inflation," *Phys.Rev.*, vol. D40, p. 1753, 1989. 50, 59

[51] I. Huston and K. A. Malik, "Numerical calculation of second order perturbations," *JCAP*, vol. 0909, p. 019, 2009, 0907.2917. 50, 60

[52] I. Huston, "Constraining Inflationary Scenarios with Braneworld Models and Second Order Cosmological Perturbations," 1006.5321. 50, 60

[53] D. Polarski and A. A. Starobinsky, "Semiclassicality and decoherence of cosmological perturbations," *Class.Quant.Grav.*, vol. 13, pp. 377–392, 1996, gr-qc/9504030. 51, 65

[54] D. H. Lyth and D. Seery, "Classicality of the primordial perturbations," *Phys.Lett.*, vol. B662, pp. 309–313, 2008, astro-ph/0607647. 51

[55] A. Lewis and A. Challinor, "camb." 53

[56] J. M. Bardeen, P. J. Steinhardt, and M. S. Turner, "Spontaneous Creation of Almost Scale - Free Density Perturbations in an Inflationary Universe," *Phys.Rev.*, vol. D28, p. 679, 1983. 53, 57, 61

[57] D. Lyth, "Large Scale Energy Density Perturbations and Inflation," *Phys.Rev.*, vol. D31, pp. 1792–1798, 1985. 53, 57, 61

[58] D. Wands, K. A. Malik, D. H. Lyth, and A. R. Liddle, "A New approach to the evolution of cosmological perturbations on large scales," *Phys.Rev.*, vol. D62, p. 043527, 2000, astro-ph/0003278. 54, 57, 61

[59] H. Kodama and M. Sasaki, "Cosmological Perturbation Theory," *Prog. Theor. Phys. Suppl.*, vol. 78, pp. 1–166, 1984. 54

[60] A. J. Christopherson and K. A. Malik, "The non-adiabatic pressure in general scalar field systems," *Phys.Lett.*, vol. B675, pp. 159–163, 2009, 0809.3518. 55

[61] P. Ade *et al.*, "Detection of B-Mode Polarization at Degree Angular Scales by BICEP2," *Phys.Rev.Lett.*, vol. 112, p. 241101, 2014, 1403.3985. 56, 162, 163

[62] E. J. Copeland, E. W. Kolb, A. R. Liddle, and J. E. Lidsey, "Reconstructing the inflation potential, in principle and in practice," *Phys.Rev.*, vol. D48, pp. 2529–2547, 1993, hep-ph/9303288. 57

[63] S. Mollerach, "Isocurvature Baryon Perturbations and Inflation," *Phys.Rev.*, vol. D42, pp. 313–325, 1990. 57

[64] E. Komatsu *et al.*, "First year Wilkinson Microwave Anisotropy Probe (WMAP) observations: tests of gaussianity," *Astrophys.J.Suppl.*, vol. 148, pp. 119–134, 2003, astro-ph/0302223. 57

[65] E. D. Stewart and D. H. Lyth, "A More accurate analytic calculation of the spectrum of cosmological perturbations produced during inflation," *Phys.Lett.*, vol. B302, pp. 171–175, 1993, gr-qc/9302019. 57

[66] I. J. Grivell and A. R. Liddle, "Accurate determination of inflationary perturbations," *Phys.Rev.*, vol. D54, pp. 7191–7198, 1996, astro-ph/9607096. 57

[67] D. Huang, W. Lin, and X. Zhang, "Remark on approximation in the calculation of the primordial spectrum generated during inflation," *Phys.Rev.*, vol. D62, p. 087302, 2000, hep-ph/0007064. 57

[68] S. M. Leach, M. Sasaki, D. Wands, and A. R. Liddle, "Enhancement of superhorizon scale inflationary curvature perturbations," *Phys.Rev.*, vol. D64, p. 023512, 2001, astro-ph/0101406. 57, 72

[69] S. M. Leach and A. R. Liddle, "Inflationary perturbations near horizon crossing," *Phys.Rev.*, vol. D63, p. 043508, 2001, astro-ph/0010082. 57

[70] E. D. Stewart, "The Spectrum of density perturbations produced during inflation to leading order in a general slow roll approximation," *Phys.Rev.*, vol. D65, p. 103508, 2002, astro-ph/0110322. 57

[71] J. E. Lidsey, A. R. Liddle, E. W. Kolb, E. J. Copeland, T. Barreiro, *et al.*, "Reconstructing the inflation potential : An overview," *Rev.Mod.Phys.*, vol. 69, pp. 373–410, 1997, astro-ph/9508078. 58

[72] D. H. Lyth and A. Riotto, "Particle physics models of inflation and the cosmological density perturbation," *Phys.Rept.*, vol. 314, pp. 1–146, 1999, hep-ph/9807278. 58

[73] C. Burrage, R. H. Ribeiro, and D. Seery, "Large slow-roll corrections to the bispectrum of noncanonical inflation," *JCAP*, vol. 1107, p. 032, 2011, 1103.4126. 59

[74] W. H. Kinney, "Horizon crossing and inflation with large eta," *Phys.Rev.*, vol. D72, p. 023515, 2005, gr-qc/0503017. 59, 69, 72

[75] C. T. Byrnes, S. Nurmi, G. Tasinato, and D. Wands, "Scale dependence of local f_NL," *JCAP*, vol. 1002, p. 034, 2010, 0911.2780. 59, 65

[76] I. Huston and K. A. Malik, "Second Order Perturbations During Inflation Beyond Slow-roll," *JCAP*, vol. 1110, p. 029, 2011, 1103.0912. 61

[77] J. Garcia-Bellido and D. Wands, "Metric perturbations in two field inflation," *Phys.Rev.*, vol. D53, pp. 5437–5445, 1996, astro-ph/9511029. 61

[78] I. Huston and A. J. Christopherson, "Calculating Non-adiabatic Pressure Perturbations during Multi-field Inflation," *Phys.Rev.*, vol. D85, p. 063507, 2012, 1111.6919. 72

[79] I. A. Brown, A. J. Christopherson, and K. A. Malik, "The magnitude of the non-adiabatic pressure in the cosmic fluid," *Mon.Not.Roy.Astron.Soc.*, vol. 423, p. 1411, 2012, 1108.0639. 72, 130, 132, 133

[80] K. A. Malik and D. Wands, "Adiabatic and entropy perturbations with interacting fluids and fields," *JCAP*, vol. 0502, p. 007, 2005, astro-ph/0411703. 73, 74, 76

[81] J. D. Callen, "Fundamentals of Plasma Physics," 2006. 77, 78

[82] G. A. P. Mulser and M. Murakami, "Revision of the Coulomb logarithm in the ideal plasma," 2013, 1312.3896. 77

[83] T. Kobayashi, R. Maartens, T. Shiromizu, and K. Takahashi, "Cosmological magnetic fields from nonlinear effects," *Phys.Rev.*, vol. D75, p. 103501, 2007, astro-ph/0701596. 83, 102, 114, 156

[84] W. R. and B. R., *Magnetic Fields in the Milky Way, Derived from Radio Sontinuum Observations and Faraday Rotation Studies. In: Cosmic Magnetic Fields, Lecture Notes in Physics, Berlin Springer Verlag*, vol. 664. 2005. 97

[85] L. M. Widrow, "Origin of galactic and extragalactic magnetic fields," *Rev.Mod.Phys.*, vol. 74, pp. 775–823, 2002, astro-ph/0207240. 97

[86] R. M. Kulsrud and E. G. Zweibel, "The Origin of Astrophysical Magnetic Fields," *Rept.Prog.Phys.*, vol. 71, p. 0046091, 2008, 0707.2783. 97, 98

[87] P. P. Kronberg, "Extragalactic magnetic fields," *Rept.Prog.Phys.*, vol. 57, pp. 325–382, 1994. 97

[88] C. Carilli and G. Taylor, "Cluster magnetic fields," *Ann.Rev.Astron.Astrophys.*, vol. 40, pp. 319–348, 2002, astro-ph/0110655. 97

[89] A. Fletcher, "Magnetic fields in nearby galaxies," 2011, 1104.2427. 97

[90] M. L. Bernet, F. Miniati, S. J. Lilly, P. P. Kronberg, and M. Dessauges-Zavadsky, "Strong magnetic fields in normal galaxies at high redshifts," *Nature*, vol. 454, pp. 302–304, 2008, 0807.3347. 98

[91] K. Kim, P. Tribble, and P. Kronberg, "Detection of excess rotation measure due to intracluster magnetic fields in clusters of galaxies," *Astrophys.J.*, vol. 379, pp. 80–88, 1991. 98

[92] B. Deiss, W. Reich, H. Lesch, and R. Wielebinski, "The large scale structure of the diffuse radio halo of the coma cluster at 1.4 ghz," 1996, astro-ph/9609189. 98

[93] P. Kronberg, M. Bernet, F. Miniati, S. Lilly, M. Short, *et al.*, "A Global Probe of Cosmic Magnetic Fields to High Redshifts," *Astrophys.J.*, vol. 676, p. 7079, 2008, 0712.0435. 98

[94] A. M. Wolfe, R. A. Jorgenson, T. Robishaw, C. Heiles, and J. X. Prochaska, "An 84 microGauss Magnetic Field in a Galaxy at Redshift z=0.692," *Nature*, vol. 455, p. 638, 2008, 0811.2408. 98

[95] T. Clarke, P. Kronberg, and H. Boehringer, "A New radio - X-ray probe of galaxy cluster magnetic fields," *Astrophys.J.*, vol. 547, pp. L111–L114, 2001, astro-ph/0011281. 98

[96] Y. Xu, P. P. Kronberg, S. Habib, and Q. W. Dufton, "A faraday rotation search for magnetic fields in large scale structure," *Astrophys.J.*, vol. 637, pp. 19–26, 2006, astro-ph/0509826. 98

[97] F. Tavecchio, G. Ghisellini, L. Foschini, G. Bonnoli, G. Ghirlanda, *et al.*, "The intergalactic magnetic field constrained by Fermi/LAT observations of the TeV blazar 1ES 0229+200," *Mon.Not.Roy.Astron.Soc.*, vol. 406, pp. L70–L74, 2010, 1004.1329. 98

[98] S. Ando and A. Kusenko, "Evidence for Gamma-Ray Halos Around Active Galactic Nuclei and the First Measurement of Intergalactic Magnetic Fields," *Astrophys.J.*, vol. 722, p. L39, 2010, 1005.1924. 98

[99] A. Neronov and I. Vovk, "Evidence for strong extragalactic magnetic fields from Fermi observations of TeV blazars," *Science*, vol. 328, pp. 73–75, 2010, 1006.3504. 98

[100] F. Tavecchio, G. Ghisellini, G. Bonnoli, and L. Foschini, "Extreme TeV blazars and the intergalactic magnetic field," 2010, 1009.1048. 98

[101] W. Essey, S. Ando, and A. Kusenko, "Determination of intergalactic magnetic fields from gamma ray data," *Astropart.Phys.*, vol. 35, pp. 135–139, 2011, 1012.5313. 98

[102] R. Beck, "Future Observations of Cosmic Magnetic Fields with the SKA and its Precursors," 2011, 1111.5802. 98

[103] C. Fedeli and L. Moscardini, "Constraining Primordial Magnetic Fields with Future Cosmic Shear Surveys," *JCAP*, vol. 1211, p. 055, 2012, 1209.6332. 98

[104] M. Shiraishi, "Polarization bispectrum for measuring primordial magnetic fields," *JCAP*, vol. 1311, p. 006, 2013, 1308.2531. 98

[105] J.-L. Han and R. Wielebinski, "Milestones in the observations of cosmic magnetic fields," *Chin.J.Astron.Astrophys.*, vol. 2, pp. 293–324, 2002, astro-ph/0209090. 98

[106] P. Kronberg, "Intergalactic magnetic fields, and some connections with cosmic rays," *Space Sci.Rev.*, vol. 75, pp. 387–399, 1996. 98

[107] M. Giovannini, "The Magnetized universe," *Int.J.Mod.Phys.*, vol. D13, pp. 391–502, 2004, astro-ph/0312614. 98, 99, 100

[108] R. M. Kulsrud, R. Cen, J. P. Ostriker, and D. Ryu, "The Protogalactic origin for cosmic magnetic fields," *Astrophys.J.*, vol. 480, p. 481, 1997, astro-ph/9607141. 98

[109] A. Brandenburg and K. Subramanian, "Astrophysical magnetic fields and nonlinear dynamo theory," *Phys.Rept.*, vol. 417, pp. 1–209, 2005, astro-ph/0405052. 98

[110] D. Grasso and H. R. Rubinstein, "Magnetic fields in the early universe," *Phys.Rept.*, vol. 348, pp. 163–266, 2001, astro-ph/0009061. 98, 99, 100

[111] E. J. King and P. Coles, "Amplification of primordial magnetic fields by anisotropic gravitational collapse," *Mon.Not.Roy.Astron.Soc.*, vol. 365, pp. 1288–1294, 2006, astro-ph/0508370. 98, 99

[112] J. D. Barrow, C. G. Tsagas, and K. Yamamoto, "Do Intergalactic Magnetic Fields Imply An Open Universe?," *Phys.Rev.*, vol. D86, p. 107302, 2012, 1210.1183. 98

[113] R. Durrer and A. Neronov, "Cosmological Magnetic Fields: Their Generation, Evolution and Observation," 2013, 1303.7121. 99, 100, 101

[114] L. M. Widrow, D. Ryu, D. R. Schleicher, K. Subramanian, C. G. Tsagas, *et al.*, "The First Magnetic Fields," *Space Sci.Rev.*, vol. 166, pp. 37–70, 2012, 1109.4052. 99

[115] A. Kandus, K. E. Kunze, and C. G. Tsagas, "Primordial magnetogenesis," *Phys.Rept.*, vol. 505, pp. 1–58, 2011, 1007.3891. 99, 100, 101, 162

[116] H. Hanayama, K. Takahashi, K. Kotake, M. Oguri, K. Ichiki, *et al.*, "Biermann mechanism in primordial supernova remnant and seed magnetic fields," *Astrophys.J.*, vol. 633, p. 941, 2005, astro-ph/0501538. 99

[117] S. Bertone, C. Vogt, and T. Ensslin, "Magnetic Field Seeding by Galactic Winds," *Mon.Not.Roy.Astron.Soc.*, vol. 370, pp. 319–330, 2006, astro-ph/0604462. 99

[118] T. A. Ensslin, P. L. Biermann, P. P. Kronberg, and X.-P. Wu, "Cosmic ray protons and magnetic fields in clusters of galaxies and their cosmological consequences," *Astrophys.J.*, vol. 477, p. 560, 1997, astro-ph/9609190. 99

[119] S. Wang, "New primordial-magnetic-field limit from the latest LIGO S-5 data," *Phys.Rev.*, vol. D81, p. 023002, 2010, 0810.5620. 100

[120] J. D. Barrow, P. G. Ferreira, and J. Silk, "Constraints on a primordial magnetic field," *Phys.Rev.Lett.*, vol. 78, pp. 3610–3613, 1997, astro-ph/9701063. 100, 149

[121] A. Lewis, "CMB anisotropies from primordial inhomogeneous magnetic fields," *Phys.Rev.*, vol. D70, p. 043011, 2004, astro-ph/0406096. 100

[122] D. Paoletti and F. Finelli, "Constraints on a Stochastic Background of Primordial Magnetic Fields with WMAP and South Pole Telescope data," *Phys.Lett.*, vol. B726, pp. 45–49, 2013, 1208.2625. 100

[123] D. R. Schleicher, R. Banerjee, and R. S. Klesser, "Reionization - A probe for the stellar population and the physics of the early universe," *Phys.Rev.*, vol. D78, p. 083005, 2008, 0807.3802. 100, 149

[124] A. Dolgov, "Magnetic fields in cosmology," 2003, astro-ph/0306443. 100

[125] M. S. Turner and L. M. Widrow, "Inflation Produced, Large Scale Magnetic Fields," *Phys.Rev.*, vol. D37, p. 2743, 1988. 101

[126] B. Ratra, "Cosmological 'seed' magnetic field from inflation," *Astrophys.J.*, vol. 391, pp. L1–L4, 1992. 101

[127] J. Martin and J. Yokoyama, "Generation of Large-Scale Magnetic Fields in Single-Field Inflation," *JCAP*, vol. 0801, p. 025, 2008, 0711.4307. 101

[128] K. Enqvist, A. Jokinen, and A. Mazumdar, "Seed perturbations for primordial magnetic fields from MSSM flat directions," *JCAP*, vol. 0411, p. 001, 2004, hep-ph/0404269. 101

[129] R. K. Jain and M. S. Sloth, "Consistency relation for cosmic magnetic fields," *Phys.Rev.*, vol. D86, p. 123528, 2012, 1207.4187. 101, 162

[130] L. Motta and R. R. Caldwell, "Non-Gaussian features of primordial magnetic fields in power-law inflation," *Phys.Rev.*, vol. D85, p. 103532, 2012, 1203.1033. 101, 162

[131] K. E. Kunze, "Large scale magnetic fields from gravitationally coupled electrodynamics," *Phys.Rev.*, vol. D81, p. 043526, 2010, 0911.1101. 101, 162

[132] C. J. Hogan, "Magnetohydrodynamic Effects of a First-Order Cosmological Phase Transition," *Phys.Rev.Lett.*, vol. 51, pp. 1488–1491, 1983. 101

[133] G. Baym, D. Bodeker, and L. D. McLerran, "Magnetic fields produced by phase transition bubbles in the electroweak phase transition," *Phys.Rev.*, vol. D53, pp. 662–667, 1996, hep-ph/9507429. 101

[134] K. Enqvist, J. Ignatius, K. Kajantie, and K. Rummukainen, "Nucleation and bubble growth in a first order cosmological electroweak phase transition," *Phys.Rev.*, vol. D45, pp. 3415–3428, 1992.

[135] J. Ahonen and K. Enqvist, "Magnetic field generation in first order phase transition bubble collisions," *Phys.Rev.*, vol. D57, pp. 664–673, 1998, hep-ph/9704334. 101

[136] T. Vachaspati, "Magnetic fields from cosmological phase transitions," *Phys.Lett.*, vol. B265, pp. 258–261, 1991. 101

[137] S. Davidson, "Ingredients and equations for making a magnetic field in the early universe," *Phys.Lett.*, vol. B380, pp. 253–256, 1996, astro-ph/9605086. 101

[138] D. Grasso and A. Riotto, "On the nature of the magnetic fields generated during the electroweak phase transition," *Phys.Lett.*, vol. B418, pp. 258–265, 1998, hep-ph/9707265. 101

[139] E. Harrison, "Origin of Magnetic Fields in the Early Universe," *Phys.Rev.Lett.*, vol. 30, pp. 188–190, 1973. 101

[140] S. Saga, M. Shiraishi, K. Ichiki, and N. Sugiyama, "Generation of magnetic fields in Einstein-Aether gravity," *Phys.Rev.*, vol. D87, no. 10, p. 104025, 2013, 1302.4189. 102

[141] G. Betschart, P. K. Dunsby, and M. Marklund, "Cosmic magnetic fields from velocity perturbations in the early universe," *Class.Quant.Grav.*, vol. 21, pp. 2115–2126, 2004, gr-qc/0310085. 102, 114, 156

[142] S. Matarrese, S. Mollerach, A. Notari, and A. Riotto, "Large-scale magnetic fields from density perturbations," *Phys. Rev.*, vol. D71, p. 043502, 2005, astro-ph/0410687. 102, 114, 156

[143] R. Gopal and S. Sethi, "Generation of Magnetic Field in the Pre-recombination Era," *Mon. Not. Roy. Astron. Soc.*, vol. 363, pp. 521–528, 2005, astro-ph/0411170. 102, 156

[144] K. Ichiki, K. Takahashi, H. Ohno, H. Hanayama, and N. Sugiyama, "Cosmological Magnetic Field: a fossil of density perturbations in the early universe," *Science*, vol. 311, pp. 827–829, 2006, astro-ph/0603631. 102, 114

[145] K. Takahashi, K. Ichiki, H. Ohno, and H. Hanayama, "Magnetic field generation from cosmological perturbations," *Phys. Rev. Lett.*, vol. 95, p. 121301, 2005, astro-ph/0502283. 102, 114

[146] S. Maeda, S. Kitagawa, T. Kobayashi, and T. Shiromizu, "Primordial magnetic fields from second-order cosmological perturbations:Tight coupling approximation," *Class.Quant.Grav.*, vol. 26, p. 135014, 2009, 0805.0169. 102, 109, 114, 156, 163

[147] K. Ichiki, K. Takahashi, N. Sugiyama, H. Hanayama, and H. Ohno, "Magnetic Field Spectrum at Cosmological Recombination," 2007, astro-ph/0701329. 102, 109, 114, 149, 163

[148] S. Maeda, K. Takahashi, and K. Ichiki, "Primordial magnetic fields generated by the non-adiabatic fluctuations at pre-recombination era," *JCAP*, vol. 1111, p. 045, 2011, 1109.0691. 102, 109, 114, 149, 151, 163

[149] E. Fenu, C. Pitrou, and R. Maartens, "The seed magnetic field generated during recombination," *Mon.Not.Roy.Astron.Soc.*, vol. 414, pp. 2354–2366, 2011, 1012.2958. 102, 109, 114, 149, 154, 163

[150] D. Papadopoulos and F. Esposito, "ON THE TRANSFORMATION OF GRAVITATIONAL RADIATION INTO ELECTROMAGNETIC RADIATION," *Astrophys.J.*, vol. 248, pp. 783–789, 1981. 103

[151] K. Subramanian and J. D. Barrow, "Magnetohydrodynamics in the early universe and the damping of noninear Alfven waves," *Phys.Rev.*, vol. D58, p. 083502, 1998, astro-ph/9712083. 103

[152] J. D. Barrow, R. Maartens, and C. G. Tsagas, "Cosmology with inhomogeneous magnetic fields," *Phys.Rept.*, vol. 449, pp. 131–171, 2007, astro-ph/0611537. 103

[153] M. Marklund, P. K. Dunsby, and G. Brodin, "Cosmological electromagnetic fields due to gravitational wave perturbations," *Phys.Rev.*, vol. D62, p. 101501, 2000, gr-qc/0007035. 103

[154] K. Peeters, "Introducing Cadabra: A Symbolic computer algebra system for field theory problems," 2007, hep-th/0701238. 107, 108

[155] G. W. Pettinari, C. Fidler, R. Crittenden, K. Koyama, and D. Wands, "The intrinsic bispectrum of the Cosmic Microwave Background," *JCAP*, vol. 1304, p. 003, 2013, 1302.0832. 111, 163

[156] M. E. Peskin and D. V. Schroeder, "An Introduction to quantum field theory," 1995. 125, 175

[157] C.-P. Ma and E. Bertschinger, "Cosmological perturbation theory in the synchronous and conformal Newtonian gauges," *Astrophys.J.*, vol. 455, pp. 7–25, 1995, astro-ph/9506072. 132

[158] E. Bertschinger, "COSMICS: cosmological initial conditions and microwave anisotropy codes," 1995, astro-ph/9506070. 133

[159] U. Seljak and M. Zaldarriaga, "A Line of sight integration approach to cosmic microwave background anisotropies," *Astrophys.J.*, vol. 469, pp. 437–444, 1996, astro-ph/9603033. 133

[160] J. Silk, "Cosmic black body radiation and galaxy formation," *Astrophys.J.*, vol. 151, pp. 459–471, 1968. 148

[161] J. Rubino-Martin, J. Chluba, W. Fendt, and B. Wandelt, "Estimating the impact of recombination uncertainties on the cosmological parameter constraints from cosmic microwave background experiments," 2009, 0910.4383. 150

[162] E. R. Siegel and J. N. Fry, "Cosmological Structure Formation Creates Large-Scale Magnetic Fields," *Astrophys.J.*, vol. 651, pp. 627–635, 2006, astro-ph/0604526. 156

[163] C. Armendariz-Picon, M. Fontanini, R. Penco, and M. Trodden, "Where does Cosmological Perturbation Theory Break Down?," *Class.Quant.Grav.*, vol. 26, p. 185002, 2009, 0805.0114. 158

[164] D. Fixsen, "The Temperature of the Cosmic Microwave Background," *Astrophys.J.*, vol. 707, pp. 916–920, 2009, 0911.1955. 166